TRANSPORT, TURBULENCE AND INSTABILITIES IN COSMIC MAGNETIC FIELDS

by

GIUSEPPE DI BERNARDO

A dissertation presented to the Graduate Faculty of Natural Science, University of Gothenburg, in partial fulfilment of the requirements for the degree of *Doctor of Philosophy* in the subject of ASTRONOMY & ASTROPHYSICS

UNIVERSITY OF GOTHENBURG

Department of Physics
http://www.physics.gu.se/
Göteborg, SE–412 96 SWEDEN
2014

Transport, Turbulence and Instabilities in Cosmic Magnetic Fields.

COLOPHON
Doktorsavhandling vid Göteborgs Universitet
ISBN: 978-91-628-9094-0
Printed by Kompendiet AB
Electronic version available at:
http://hdl.handle.net/2077/35797

WEBSITE:
http://www.physics.gu.se/
E-MAIL:
giuseppe.dibernardo@physics.gu.se

Astronomy & Astrophysics Group
Department of Physics
University of Gothenburg
SE-412 96, Göteborg
Sweden
Telephone + 46 (0)31 768 91 51

The thesis has been typeset in LaTeX, using the ArsClassica package (© Lorenzo Pantieri, 2008-2012), freely provided under the terms of the LaTeX General Public Licence, and distributed from CTAN archives in directory http://www.ctan.org/tex-archive/macros/latex/contrib/arsclassica/.

All figures were created using both free software, e.g., Python (from Python Software Foundation. Python Language Reference, version 2.7. Available at http://www.python.org), and proprietary software, e.g., IDL (version 8.2., from Exelis Visual Information Solutions, Boulder, Colorado). The figures presented in the Thesis are the original work of the author unless otherwise stated.

The cover page reproduces the oil on canvas titled *The Starry Night*, by Vincent van Gogh. "Looking at the stars always makes me dream," he said. The picture was obtained from http://www.wikiart.org/en/vincent-van-gogh/the-starry-night-1889#close).

«Voyager, c'est bien utile, ça fait travailler l'imagination.
Tout le reste n'est que déceptions et fatigues.
Notre voyage à nous est entièrement imaginaire.
Voilà sa force.
Il va de la vie à la mort.
Hommes, bêtes, villes et choses, tout est imaginé.
C'est un roman, rien qu'une histoire fictive.
Littré le dit, qui ne se trompe jamais.
Et puis d'abord tout le monde peut en faire autant.
Il suffit de fermer les yeux.
C'est de l'autre côté de la vie.»
Voyage au bout de la nuit, by Louis Ferdinand Cèline
(Courbevoiz, Seine 1894 - Meudon, Paris 1961).

To my lovely parents, *Antonella & Biagio*, and my syster *Ida*.
For their unconditional patience and encouragement.
And in memory of *Pasquale*, who taught me
how to repair a bicycle, and *Ida*, *Biagio*'s mother.

PREFACE

The present manuscript is an outgrowth of the research carried out during the time of my Ph.D. program. The key science driver of the discussion presented in the present Thesis is the *transport*, in some of most intriguing astrophysical settings, with a special attention to the: (a) transport of Cosmic Rays in the Interstellar Medium, and (b) transport of angular momentum, and material, in Accretion Flows. Both themes are largely characterized by the active role of large-scale magnetic field, and turbulence.

The Manuscript is so divided: (i) *Theoretical Framework*, which is an introduction, a "road map" if you will, to the original research achievements presented in the part (ii) *Scientific Papers*.

ACKNOWLEDGEMENTS

It is a pleasure to express my gratitude to the many professors, colleagues and friends with whom I enjoyed very fruitful discussions on the topics of this manuscript. In particular, I would like to thank my DPhil advisor, Dr. Ulf Torkelsson. Over the last four years, Ulf has granted me the freedom I wanted and given me the guidance I needed, providing the best possible environment for the completion of this thesis. I consider myself lucky having had such a committed, diligent and supportive supervisor.

Then, I want to express my gratitude to the DRAGON team (in alphabetical order): Dr. Evoli Carmelo, Dr. Gaggero Daniele, Dr. Grasso Dario, and Dr. Maccione Luca (with the baby Francesco). They are more than colleagues: over the last years, I have been lucky to share with them the exciting adventure of the *Astrophysics of Cosmic Rays*. In particular I am grateful to Dario, who has been my advisor during my undergraduate program. Without their support, this manuscript would not have been possible.

I would like to acknowledge Prof. Axel Brandenburg, for his hospitality in NORDITA, and Prof. Eliot Quataert, accepting me for an entire academic year c/o the Department of Astronomy in Berkeley (CA). I am so grateful to him for transmitting me his enthusiasm and curiosity in Astrophysics.

Writing this manuscript has taken more time than I planned. My deepest thanks go to my family, my mother Antonia, my father Biagio, and my little sister Ida. Without their continuing encouragement, this Thesis could not have been completed.

Giuseppe Di Bernardo

Göteborg, September 2014

ABSTRACT

THIS DECADE HAS SEEN A LARGE NUMBER of space missions, which, alongside ground-based radio, optical and γ-ray telescopes, have enabled a deep insight into the non-thermal astrophysical environments. Interstellar Medium (ISM), Supernovae Remnants (SNRs) and Black-Hole (BH) accretion discs (ADS) are only a few examples of *natural habitat* of interaction of relativistic particles and magnetic fields, largely mediated by the action of the turbulence. In spite of many efforts, and the recent progress in this field, we are still missing a fully comprehension of the nature of the problem.

Throughout the THESIS, the key science driver concept is the transport in magnetic turbulent fields. The aims of the work here presented are meant to be a step in that direction. They can be precisely grouped into two main themes: (i) understanding the transport of Cosmic Rays (CRs), and their dynamical role in the *Milky Way*; (ii) understanding the physics of ADS, with special attention on the magnetic, turbulent environment around compact objects responsible of driving inflow material through the discs. In this regard, I will firstly give a review intended to cover the main theoretical aspects involved in the astrophysics of CRs. A section will be dedicated to the presentation of preliminary results accomplished in the context of the magnetohydrodynamics (MHD) shearing box numerical simulations of turbulence in ADS.

I will move on by introducing the main achievements of my scientific activity, as reported in the following THESIS. A detailed cosmic ray transport description in the Galaxy has been implemented in the DRAGON code, a numerical tool used to simulate the local interstellar spectra (LIS) of CRs. There is by now compelling evidence of an *anomalous* rise with energy of the cosmic ray positron fraction. Conversely to the *standard picture* of a pure secondary positron production, the data strengthen the evidence for the presence of two distinct electron and positron spectral components. Given the cosmic ray transport model, I will show that nearby pulsars are viable source candidates of the required $e^{\pm}$ extra-component.

In a multichannel analysis of cosmic ray electron and positron spectra, I will present the results of our recent study on the diffuse synchrotron emission of the Galaxy. At low energies - roughly below 4 GeV - we find that the electron primary spectrum is significantly suppressed so that the low-energy total spectrum will turn out to be dominated by secondary particles. Comparing the computed synchrotron emission intensity with the radio data, we placed a constraint on the diffusive magnetic halo scale height, of relevant importance especially for indirect Dark Matter searches.

Fairly poor knowledge is still present about the cosmic ray spectra at low energies, due to the distortion produced by the solar wind on the particle fluxes. Going beyond the standard force-field solar modulation, I will show the results of a self-consistent galactic-plus-solar transport model, where charge-sign dependent motion effects are taken in account.

Lately, I will discuss the impact of a realistic spiral arm distribution of CRs source in the Galaxy, modelling the $e^{\pm}$ spectra measured by PAMELA and AMS-02 by running DRAGON in a full three-dimensional version.

Keywords: Cosmic Rays, ISM, Galactic Magnetic Fields, MHD turbulence, ADS.

LIST OF PAPERS

PUBLICATIONS PRESENTED IN THIS THESIS

PAPER I **Di Bernardo, G.**, Evoli, C., Gaggero, D., Grasso, D., Maccione, L., and Mazziotta, M.N.: "Implications of the Cosmic Ray Electron Spectrum and Anisotropy measured with Fermi-LAT", *Astroparticle Physics 34* (Feb. 2011), 528 - 583.

PAPER II **Di Bernardo, G.**, Evoli, C., Gaggero, D., Grasso, D., Maccione, L.: "Cosmic Ray Electrons, Positrons and the Synchrotron emission of the Galaxy: consistent analysis and implications", *JCAP* 3, (Mar. 2013), 36.

PAPER III Gaggero, D. Maccione, L. **Di Bernardo, G.**, Evoli, C. Grasso, D., "Three-Dimensional Model of Cosmic-Ray Lepton Propagation Reproduces Data from the Alpha Magnetic Spectrometer on the International Space Station", *Physical Review Letters 111*, 2 (Jul. 2013), 021102.

PAPER IV Gaggero, D. Maccione, L., Grasso, D., **Di Bernardo, G.**, Evoli, C. "PAMELA and AMS-02 e^+ and e^- spectra are reproduced by three-dimensional cosmic-ray modeling", *Physical Review D*, (Apr. 2014).

PAPER V **Di Bernardo, G.**, Torkelsson, U., (Feb. 2013):"Wave modes from the magneto-rotational instability in accretion discs." In Zhang, C. M. Belloni, T. Méndez, M. Zhang, S. N. (Eds.) *Feeding Compact Objects : Accretion on All Scales*. Paper presented at the XXVIIIth International Astronomical Union Symposium, Beijing, China Nanjing, 20-31 Aug. 2012.

PUBLICATIONS RELATED TO MY SCIENTIFIC ACTIVITY AND MARGINALLY TOUCHED IN THIS THESIS

- **Di Bernardo, G.**, Evoli, C., Gaggero, D., Grasso,D., and Maccione, L.: "Unified interpretation of cosmic-ray nuclei and antiproton recent measurements", *Astroparticle Physics 34* (Dec. 2010), 274 - 283.
- Ackerman, M., et al., [FERMI Collaboration]: "Searches for cosmic-ray electron anisotropies with the Fermi Large Area Telescope", *Physical Review D 82*, 9 (Nov. 2010), 092003
- Ackerman, M., et al., [FERMI Collaboration]: "Fermi-LAT observations of cosmic-ray electrons from 7 GeV to 1 TeV", *Physical Review D 82*, 9 (Nov. 2010), 092004.
- Grasso, D., **Di Bernardo, G.**, Evoli, C., Gaggero, D., Maccione, L. (Jun. 2013): "Galactic electron and positron properties from cosmic ray and radio observations." Accepted for the presentation in the proceedings of the ICRC Conference on Cosmic Rays for Particle and Astroparticle Physics, Rio de Janeiro, Brazil, Jul. 2013.

- Gaggero, D.,Maccione, L., **Di Bernardo, G.**, Evoli, C., Grasso, D. (Jun. 2013):"Three dimensional modeling of CR propagation." Accepted for the presentation in the proceedings of the ICRC Conference on Cosmic Rays for Particle and Astroparticle Physics, Rio de Janeiro, (Brazil), Jul. 2013.

- **Di Bernardo, G.**, Evoli, C., Gaggero, D., Grasso, D., Maccione, L.,: "Cosmic Ray Electrons, Positrons and the Synchrotron emission of the Galaxy: consistent analysis and implications". Paper presented at the HEAD meeting, Monterey, California (USA), Apr. 2013.

- **Di Bernardo, G.**, Evoli, C., Gaggero, D., Grasso, D., Maccione, L., Mazziotta, M. N.: "A consistent interpretation of recent CR nuclei and electron spectra". Accepted for the presentation in the proceedings of the ICATPP Conference on Cosmic Rays for Particle and Astroparticle Physics, Villa Olmo (Como), Oct. 2010.

- Grasso, D., et al., [Fermi Collaboration]: "Possible Interpretations of High Energy Cosmic Ray Electron Spectrum Measured with the Fermi Space Telescope." Proc. of the 31^{st} International Cosmic Ray Conference (Icrc), Łódź, July 2009. *Nuclear Instruments and Methods in Physics Research A 630, 48-51* (Feb. 2011).

- Grasso, D., Profumo, S., Strong, A. W., Baldini, L.,Bellazzini, R., Bloom, E. D., Bregeon, J., **Di Bernardo, G.**, Gaggero, D., Giglietto, N., Kamae, T., Latronico, L., Longo, F., Mazziotta, M. N., Moiseev, A. A., Morselli, A. and Ormes, J. F., Pesce-Rollins, M.,Pohl, M., Razzano, M., Sgro, C., Spandre, G., and Stephens, T. E.: "Possible Interpretations of High Energy Cosmic Ray Electron Spectrum Measured with the Fermi Space Telescope." Proc. of the 2^{nd} Roma International Conference on Astro-Particle Physics (Ricap). *Nuclear Instruments and Methods in Physics Research A 630, 48-51* (Feb. 2011).

- **Di Bernardo, G.**, Evoli, C., Gaggero, D., Grasso, D., and Maccione, L.: "A Combined Interpretation of Cosmic Ray Light Nuclei and Antiproton Measurements." Proc. of the 2^{nd} Roma International Conference on Astro-Particle Physics (Ricap). *Nuclear Instruments and Methods in Physics Research A 630, 67-69* (Feb. 2011).

CONTENTS

PREFACE IV
ABSTRACT V
LIST OF PAPERS VI

I Theoretical Framework 3

1 PROLOGUE 5
1.1 The Astrophysics of Cosmic Rays 5
1.1.1 The Positron Affair 6
1.1.2 The Solar Modulation 7
1.1.3 Cosmic Rays: a Multichannel Investigation 7
1.1.4 The 3D Model of Cosmic Ray Transport 8
1.1.5 Cosmic Rays: A Viable Path to Catch Dark Matter 8
1.2 Accretion Discs 9
1.2.1 Transport, Turbulence, Mixing and Instabilities in ADs 10

2 TRANSPORT AND TURBULENCE IN ASTROPHYSICAL PLASMAS 11
2.1 On Astrophysical Turbulence 12
2.1.1 Fundamental Ideas in Fluid Turbulence 12
2.1.2 The Picture of Alfvénic Turbulence 15
2.2 Transport of Cosmic Rays in the Interstellar Medium 18
2.2.1 Unperturbed Motion and Wave-Particle Resonance 18
2.2.2 Diffusion Approximation in the Quasi Linear Theory 22
2.3 Angular Momentum Transport in Accretion Discs 29
2.3.1 The α Viscosity Prescription 30
2.3.2 The Magneto-Rotational Instability in Accretion Discs 31

3 COSMIC RAYS AND THEIR GALACTIC ENVIRONMENT 35
3.1 A Hitchhiker's Guide to the Galaxy 35
3.1.1 Overall Picture of the Galaxy 36
3.1.2 Anatomy of the Galaxy 38
3.2 The ISM and its Typical Phases 42
3.3 Cosmic Rays: The Standard Picture 48
3.3.1 The Early Years 48
3.3.2 Cosmic Rays: Energy Spectrum and Composition 50
3.3.3 Cosmic Rays: Energy and Pressure 55
3.4 Transport of CRs at Astrophysical Shocks 57
3.4.1 The Fermi Picture 59
3.4.2 The Test Particle Shock Acceleration 61
3.5 Interstellar Radiation Fields 67
3.5.1 The Magnetic Structure of the Galaxy 68
3.5.2 Interstellar Radiation 69
3.6 Concluding Remarks 70

4 MODELS FOR COSMIC RAY TRANSPORT IN THE INTERSTELLAR MEDIUM 73
4.1 The Leaky-Box Model 74
4.2 The Cosmic Ray Framework in the Dragon Code 77
4.2.1 The Solar Modulation 84
4.3 The Electron Component of Cosmic Rays 85

4.3.1 A General Overview 85
4.3.2 The Main Features of the Transport of Relativistic $e^{\pm}$ 87
4.3.3 The Diffuse Propagation of Electrons in the Galaxy 89

5 e^+ AND e^- COSMIC RAYS AND THE SYNCHROTRON EMISSION 95
5.1 The Fermi-LAT spectrum 96
5.1.1 The case of the mean distribution of GCRE 96
5.1.2 Double component scenario 102
5.2 The Synchrotron Emission of the Galaxy 120
5.3 The AMS-02 result: a More Realistic Distribution 123

6 EPILOGUE 127

BIBLIOGRAPHY 133

«Per aspera sic itur ad astra»

TRANSPORT, TURBULENCE AND INSTABILITIES IN COSMIC MAGNETIC FIELDS

GIUSEPPE DI BERNARDO

Gaetano: «Chell ch'è stato è stato... basta, ricomincio da tre...»
Lello: «Da zero!...»
Gaetano: «Eh?...»
Lello: «Da zero: ricomincio da zero.»
Gaetano: «Nossignore, ricomincio da... cioè... tre cose me so' riuscite dint'a vita, pecché aggia perdere pure chest? Aggia ricomincià da zero? Da tre!»
Massimo Troisi and Lello Arena in *Ricomincio da tre* (*I'm starting from three*, a 1981 Italian comedy film).

Part I

Theoretical Framework

1 PROLOGUE

«The beginning is the most
important part of the work.»
The Republic

by Plato
(Athens, 428/427 BC - 348/347 BC)

PLASMA IS AN UBIQUITOUS FORM OF MATTER in the Universe. That should not really be surprising. According to the Big Bang theory, the cosmos erupted into existence 13.7 billion of years ago and spent most of its first 300000 years as unalloyed expanding plasma until it cooled sufficiently for the first neutral atoms to form.

Remarkably, plasma is nearly always found to be magnetized and turbulent. One must understand this behaviour to interpret a broad spectrum of phenomena, from the way stars and planets coalesce out of plasma discs, to the evolution of galaxies. Examples include turbulence in the Interstellar Medium (ISM), which is stirred by violent events like supernova explosions; turbulence in accretion flows around stars and compact objects; and turbulence in the solar wind streaming outward from our Sun. Common to these turbulent systems is the presence of an inertial range, an extent of scales through which energy cascades from the large scales - at which the turbulence is stirred - to the small scales - at which dissipative mechanisms convert the turbulent energy into heat.

Throughout the present THESIS, the key science driver concept is the transport in magnetic turbulent fields. The aims of the work here presented are meant to be a step in that direction. They can be precisely grouped into two main themes: (i) understanding the transport of Cosmic Rays (CRs), and their dynamical role in the *Milky Way*; (ii) understanding the physics of Accretion discs (ADS), with special attention on the magnetic, turbulent environment around compact objects responsible of driving inflow material through the discs.

1.1 THE ASTROPHYSICS OF COSMIC RAYS

The particles circulating in the cosmos include the so-called *Cosmic Rays* (CRs), intensively studied since their discovery by Hess, in 1912. CRs are relativistic particles (e.g. protons, heavier atomic nuclei and electrons) that propagate through the ISM. Showers of secondary charged particles originate from the interaction of CRs with the upper atmosphere, and reach the Earth's surface at the considerable rate of $10^4 \times \ \mathrm{m}^{-2} \times \ \mathrm{s}^{-1}$. Their energy spectrum covers about 11 orders of magnitude and extends up to extreme energies, above 10^{20} eV!

Since CRs carry an electric charge, these particles can interact with any magnetic fields that are present. It is believed that supernova explosions in

the ISM not only accelerate CRs, but also lead to turbulent flows that drive dynamo action in the Galaxy. It is now well known that dynamo action of this type produces a complex magnetic field distribution, with very specific properties. Cosmic ray research is of interest not only to scientists working in various different subjects areas, including *astro-particle* physics, dynamo theory, radio astronomy and the physics of the ISM, but also particularly well suited to outreach work. For example, Galactic Cosmic Rays (GCRs) may have important consequences for the health of astronauts in future manned space flights. Moreover, the cosmic ray flux depends crucially upon the magnetic fields that are associated with the solar wind.

Much of the research - carried out over the time of my Ph.D. study program - has been centred on the physics of GCRs, with special attention to the charged lepton particles. The studies of the galactic properties of the ISM, taking benefit of both data from the high-energy γ-ray telescope *Fermi Large Area Telescope* (*Fermi*-LAT)*, and the observations from the all-sky surveys by PLANCK mission†, as well as the searches for Dark Matter with neutrino telescopes ICECUBE‡ and DEEPCORE, represent the main reasons motivating the scientific activity outlined in the present manuscript.

CRs represent an unique probe of the ISM properties since they can transverse extended regions in the Galaxy before reaching the Earth's atmosphere, providing us with informations about galactic magnetic fields, gas distributions and stellar rates (Maurin et al., 2002). However, the propagation of CRs in the Galaxy is far from being fully exploited. Therefore, it turns out that understanding the transport of GCRs is a crucial topic in astrophysics (see e.g., Berezinskii et al., 1984; Schlickeiser, 2002; Waxman, 2011).

Nowadays, the study of CRs is a very relevant sector, because there still are several open problems, about the origin and transport of those relativistic particles. The questions raised in this field are strictly connected to some of the most intriguing puzzles of the modern physics, like as the nature of the Dark Matter (for a comprehensive review, see e.g., Bertone et al., 2005). My collaborators and I have succeeded in building a comprehensive model of transport of GCRs, providing a very good fit of the cosmic ray light nuclei and antiprotons spectra (Di Bernardo, Evoli, Gaggero, Grasso, and Maccione, 2010). For these purposes, the new numerical package, named `DRAGON` code§, has been used. It has been designed by our research group to solve the diffusion-loss equation, with the specific attention to the case of GCRs, by taking into account realistic distribution for CRs source, galactic gas and magnetic field distribution, and including all the relevant network of nuclear processes (*spallation*) and radiative energy losses that are involved in transport of CRs.

1.1.1 The Positron Affair

Currently, on the lepton side, one major challenge is represented by the spectrum of the *positron fraction* (PF). Hints of such an *anomalous* cosmic ray spectrum excess were recognized in the older times, but we got confirmation of that - with any doubts - only in the present days, when PAMELA satellite¶ measured, for the first time, the PF with high accuracy at energies

* http://fermi.gsfc.nasa.gov/
† http://www.rssd.esa.int/index.php?project=planck
‡ http://icecube.wisc.edu/
§ http://www.dragonproject.org/Home.html
¶ http://pamela.roma2.infn.it/index.php

ranging from below 1 GeV up to about 100 GeV. The same result was then confirmed by Fermi-Lat and later on by Ams-02[‖]. We found that a simple phenomenological model, in which a nearby cosmic accelerator of electrons and positrons is added to a diffuse conventional emission, predicts a total electron spectrum compatible with all the existing observations (Ackermann et al., 2010a; Di Bernardo, Evoli, Gaggero, Grasso, Maccione, and Mazziotta, 2011; see also Grasso et al., 2009; Hooper et al., 2009; Profumo, 2008).

However, concerning the nature of this extra component, the debate is still open (see e.g., Bergström et al., 2009; Blasi, 2009; Cholis et al., 2009; Delahaye, Lineros, F. Donato, Fornengo, J. Lavalle, et al., 2009; P. Serpico, 2012; Shaviv et al., 2009).

1.1.2 The Solar Modulation

While the positron excess is a fact which has raised the attention of most of the astro-particle physics community, fairly poor knowledge is still present about the cosmic ray spectra at low energies, precisely below 10 GeV. Before they reach the top of the Earth's atmosphere, cosmic ray electrons and positrons must force their way through the outward flowing solar wind which, at those energies, can push them outward and alter their flux (e.g., Davis et al., 2000; Gleeson and Axford, 1968).

As a consequence, relativistic galactic electrons experience extraordinary large *modulation* in the *inner heliosphere*, an effect which depends - via drifts in the large scale gradients of the solar magnetic field (Smf) - on the particle charge, including its sign. Then, it depends upon the polarity of the Smf, which changes periodically every 11 years. In this regard, I remind that the Smf has two opposite polarities, in the northern and southern hemispheres respectively. At the interface between opposite polarity regions, a heliospheric current sheet (Hcs) is formed. The Hcs swings then in a region whose angular extension is described phenomenologically by the tilt angle α, whose magnitude depends upon the solar activity. An extensive review of the solar modulation of Crs in the heliosphere can be found in Potgieter (2013).

A realistic modulation model has been recently implemented in the numerical code named HelioProp (Maccione, 2013), in order to take in account the charge-dependent drifts when Crs transport equations are solved in the context of the solar system. In a theoretical framework based upon the diffusion approximation theory, and combining observations relative to the heliosphere with our propagation model, for the first time we were able to reproduce the observed spectra of cosmic ray particles with a primary electron injection index close to the that used for nuclei, in rough agreement with the radio observations of Snrs (Gaggero, Maccione, Di Bernardo, et al., 2013). A more detailed study of several combinations of solar and galactic parameters is left for future work.

1.1.3 Cosmic Rays: a Multichannel Investigation

Remarkably, it is important to point out that a *multi-messenger approach* is required in order to address all the open problems aforementioned. It is important to look not only at cosmic ray charged particles, but also at the secondary radiation originated from Crs through various mechanisms, like as

‖ http://www.ams02.org/

synchrotron, *bremsstrahlung*, *Inverse Compton*, and decay of pions - produced via interaction with interstellar gas. In particular, γ-rays (e.g., Kachelrieß and Ostapchenko, 2012; Kachelrieß, Ostapchenko, and Tomàs, 2012) and radio waves can help to test the several model predictions.

In the microwave band, *free-free* and dust emission tend to dominate, making more difficult the separation of the two components. Advanced modelling of the different emissions - both total and polarized components - is important for separating synchrotron emission from other components. Synchrotron modelling requires a knowledge of the Galactic magnetic fields and CRs electrons in the Galaxy. Hence, the observed diffuse emission, compared with the theoretical models turns out to be a fundamental tool for studying Galactic magnetic fields, CRs electrons and their transport and distribution in the Galaxy.

For this purposes, we have probed the GCRs electron spectrum - and spatial distribution - by performing a combined analysis of recent cosmic ray (Fermi-Lat and Pamela most importantly) and radio data, aiming to constraint the scale height of the CRs distribution (Di Bernardo, Evoli, Gaggero, Grasso, and Maccione, 2013). For the first time, we have placed a constraint on the CRs diffusive halo scale height, based upon the comparison of the computed synchrotron emission intensity with the observations. The constraint derives from the attempt of fitting the electron spectra measured by the Fermi-Lat, and the expected value of the Galactic magnetic field as measured via Faraday RMs. Limits on the magnetic halo scale height are of great importance for indirect Dark Matter searches.

Moreover, the strategy adopted allowed us to exploit the Galactic diffuse synchrotron emission to measure the low energy local interstellar spectrum (LIS) of cosmic ray electrons and positrons - like exploiting the diffuse γ-ray emission gives us insights into the local interstellar proton spectrum. This is a valuable information for studies of solar modulation.

1.1.4 The Three Dimensional Model of Cosmic Ray Transport

In terms of a novel propagation model, in which the sources are distributed in the spiral arm patterns in agreement with astrophysical observations, we have studied the compatibility of AMS-02 data on the cosmic-ray PF with data on the CRs electron and positron spectra provided by Pamela and *Fermi*-Lat. For this purpose we used a newly developed 3-D propagation code to account for the spiral arm distribution of cosmic ray astrophysical sources (Gaggero, Maccione, Di Bernardo, et al., 2013). We found that, once the propagation models are tuned to reproduce the light nuclei and proton data, the lepton data provide valuable new informations about CRs transport properties and on the nature of the $e^- + e^+$ extra-component, responsible for the famous *positron excess* (Gaggero, Maccione, Grasso, et al., 2014).

1.1.5 Cosmic Rays: A Viable Path to Catch Dark Matter

Unveiling the nature of cosmic *Dark Matter* is an urgent issue in cosmology. Only about five percent of the matter in the Universe is familiar to us. The identity of the remaining 95%, dubbed "dark matter" is unknown. Though scientists have not yet detected it directly in laboratories on Earth, Dark Matter existence has been deduced from its gravitational effects on the stars and gases that make up all of the galaxies known in the Universe (see e.g., Silk,

2004). In addition to its physical effects, dark matter is a crucial component of the cosmological theory because of its key role in defining the structure of the universe and in binding all galaxies, even our own *Milky Way*, together. Modern astrophysics and particle physics theory suggests that dark matter exists in the form of a yet undiscovered elementary particle. Dark matter is pervasive throughout the Universe, so it's no surprise that dark matter is also prevalent on Earth. Based on observations of the motions of nearby stars, theory predicts that one dark matter particle will inhabit a volume the size of your coffee cup. The direct identification of the nature of dark matter will establish a firm connection between physics on the largest astronomical scales and the smallest scales studied in laboratories on Earth.

The nature of dark matter remains a mystery because, so far, we cannot see it directly but only detect its effects indirectly on the large-scale structure of the universe (see e.g., M. Cirelli, 2012; Delahaye, Lineros, F. Donato, Fornengo, and P. Salati, 2008; J. Lavalle and P. Salati, 2012; P. D. Serpico, 2012). Apart from directly detecting the interaction of the dark matter particles (WIMPs, see e.g., Bertone, 2010) passing through matter on Earth, a possible method to obtain information is to look for the secondary particles produced in their annihilation. The most likely form of dark matter is a new class of elementary particles predicted by the so-called "super-symmetric extensions" to the standard model of particle physics. Most of such models predict that the dark matter particle can "self-annihilate". This happens when two dark matter particles collide. When particles strike one another, energy is released in the form of detectable standard model elementary particles such as photons or charged particles such as positrons and electrons.

According to what discussed above, CRs could be the first place where the elusive dark matter component of the universe will be detected.

1.2 ACCRETION DISCS

With masses up to billions of times that of the Sun, Massive Black Holes (MBHs) are now considered to have a major role in the evolution of galaxies. The co-evolution of MBHs and their host galaxies remains one of the main unsolved problems in cosmic structure formation studies. It is now widely recognized that nuclear activity is an important ingredient in shaping the evolution of galaxies (Fabian et al., 2009). Active Galactic Nuclei (AGN) are intimately connected to the hierarchy of galaxies building process. A major focus has become observational and theoretical investigation of nuclear activity in the context of the galactic environment, which can be described in terms of "feeding" and "feedback" (Cattaneo et al., 2009). AGN feeding is tightly correlated with red shift-dependent star formation in the host galaxy. AGN feedback, in the form of relativistic *jets*, massive winds, and intense radiation, has been invoked to solve a broad range of problems that arise in Cold Dark Matter-based (CDM) models of galaxy formation: setting the critical mass scale for galaxies, regulating cooling in clusters, and shutting down star formation. Such feedback, feeding, and their mutual interaction might possibly account for the tight relationship between galactic bulge mass and central black hole mass.

Because of its firm connection to black holes themselves, *black hole accretion disc theory* belongs to the realm of fundamental physics. Studies of black holes, and accretion flows in general, have fundamental importance and are at the frontiers of today's physics and astrophysics. Discs are ubiq-

uitous in astrophysics, but many fundamental questions remain about their behaviour. In both proto-planetary and AGN discs, turbulence, shocks, cooling, and fragmentation play important roles. The details of transport is determined by the turbulence, and the details of heating are determined by the shock physics in the disc.

1.2.1 Transport, Turbulence, Mixing and Instabilities in Accretion Discs

The big challenge in accretion disc theory is to understand the outwards transport of angular momentum, which provides the driving mechanism for the matter inflow through the disc. It is easy to show that ordinary viscosity is unable to drive this inflow, rather it must be a form of *anomalous viscosity*, usually referred to as the "α - prescription", maybe magnetic in origin due to the turbulence in the disc (Shakura and Sunyaev, 1973). In 1991 Balbus and Hawley showed that a Kepler shear flow in the discs is unstable in the presence of a weak magnetic field (Balbus and Hawley, 1991; Hawley and Balbus, 1991). A few years later several research groups, like for example Brandenburg et al. (1995), were able to prove that turbulence can be driven by the Balbus-Hawley (or *magnetorotational*) instability by a magnetic field that in turn is generated by this very same turbulence. Through numerical simulations of magnetohydrodynamics (MHD) in a shearing box, which represents a small fraction of the disc, they pointed out that this instability is a key process for driving efficient angular momentum transport in astrophysical discs.

It is vital to realize that accretion disc theory is still incomplete. The properties of this kind of magnetic turbulence determine the dynamics of the accretion disc, not only the energy production in the disc, but also the response of the disc to external perturbations and the *oscillatory modes* that the disk can support. These other aspects of the turbulence have hardly been explored so far.

The physical origin of high-frequency QPOs in black-hole X-ray binaries remains an enigma despite many years of detailed studies (see e.g., Abramowicz and Fragile, 2013 and references therein). One of the aims pursued over the time of my Ph.D. graduate program, and that will continue over the coming years, has been to explore the connection between the turbulence and the oscillatory modes in the accretion disc. There are in particular two aspects of the turbulence that are of interest, firstly which modes can be excited by the turbulence itself, and secondly how the turbulence is interacting with and damping modes that have been excited in some other way (Di Bernardo and Torkelsson, 2013). These investigations are of interest in understanding the quasi-periodic oscillations that have been observed in the light curves of many sources that are driven by accretion discs. As research tool I used the PENCIL CODE[**], which is a public domain code, originally developed by *Prof. Axel Brandenburg*[††] and *Prof. Wolfgang Dobler*[‡‡] at Nordita, with the aim of solving MHD partial differential equations on massively parallel computers.

** http://pencil-code.nordita.org/
†† http://www.nordita.org/~brandenb/
‡‡ http://www.capca.ucalgary.ca/wdobler/

2 TRANSPORT AND TURBULENCE IN ASTROPHYSICAL PLASMAS

«[...] I've seen things you people wouldn't believe. Attack ships on fire off the shoulder of Orion. I watched c-beams glitter in the dark near the Tannhäuser Gates. All those moments will be lost in time, like tears in rain [...]»
Roy Batty, in Blade Runner

by Ridley Scott (USA, 1982)

MAGNETISM HAS BEEN FUNDAMENTAL FOR TRAVELLING and exploring our planet, with the Earth's magnetic field guiding birds, bees and compass needles. Furthermore, the effect of the Earth's magnetic field on charged particles from the Sun has both shielded us from their harmful affects and entranced us with the beautiful aurorae lighting up the northern and southern polar skies.

Through decades of astrophysical research, we have established that magnetism is ubiquitous in our Universe, with interstellar gas, planets, stars and galaxies all showing the presence of magnetic fields. Generating magnetic fields on such large physical scales cannot be achieved through permanent magnets like those found in school science kits, but instead requires huge densities, volumes or motions of electrically charged material, such as the gas that pervades the Milky Way or the outflows of material from the energetic centres of galaxies.

Cosmic magnetism spans an enormous range in its strength, varying by a factor of a hundred billion billion between the weak magnetic fields in interstellar space and the extreme magnetism found on the surface of collapsed stars. Because these cosmic magnetic fields are all-pervasive, they play a vital role in controlling how celestial sources form, age and evolve.

While there is often a component of the field that is spatially coherent at the scale of the astrophysical object, the field lines are tangled chaotically and there are magnetic fluctuations at scales that range over orders of magnitude. The cause of this disorder is the turbulent state of the plasma in these systems.

In a recent review by Brandenburg and Nordlund (2011), properties of turbulence have been discussed for the solar wind, stellar convection zones, the ISM, accretion discs, galaxy clusters, and the early Universe. One would hope that there are universal properties of magnetic turbulence that hold in all applications. Several important questions for astrophysics arise in the context of turbulent plasmas: How does the turbulence amplify, sustain and shape magnetic fields? What is the spectrum and the structure of this field at large and small scales? How does the turbulent flow and magnetic field enhance or inhibit the transport of heat, angular momentum and CRs?

The aim of the present chapter is to give a general overview of the most basic properties of astrophysical MHD turbulence. I shall touch primarily on

two applications: (i) properties of turbulent transport in the ISM (§ 2.2), and the implications for the propagation of CRs, (ii) causes of the transport of the angular momentum in accretion discs (§ 2.3). The main concepts discussed in the following will turn to be useful for the rest of the manuscript.

2.1 ON ASTROPHYSICAL TURBULENCE

«*Ladies and Gentlemen this is your captain speaking, we seem to be experiencing some turbulence, please return to your seat and fasten your seatbelt, Thank You.*»

If you have at some time experienced a very bumpy ride in an air plane, you have experienced the best (and for that matter the *worst*) practical introduction to the problem of *clear air* turbulence. It is sometimes said that turbulence is the last great unsolved problem of classical physics. On his death bed, Heisenberg is reported to have said, «*When I meet God, I am going to ask him two questions: Why relativity? And why turbulence? I really believe he will have an answer for the first*.» However, this quote is also attributed to Horace Lamb.*

Hydrodynamic turbulence is a long studied but still incompletely addressed fundamental process. It is clearly the first step towards the more complex MHD turbulence, in view of studying the pronounced role that large-scale magnetic fields play in astrophysical plasmas, even in influencing much smaller scale turbulence phenomena. MHD turbulence, or turbulence of conducting fluid, exists in many physical systems: liquid-metal experiments, fusion devices, the Earth's interior and virtually all astrophysical plasmas from stars to galaxies and galaxy clusters. Many observed properties of astrophysical bodies - and, in some cases, their very existence - cannot be explained without recourse to some model of turbulence and turbulent transport in the constituent plasma. Thus, one could view the theory of MHD turbulence as a theory of the fundamental properties of luminous matter that makes up large-scale astrophysical bodies.

MHD turbulence is an area of very active current research, motivated by the recent rapid and simultaneous progress in astrophysical observations (especially of the solar photosphere, interstellar and intra-cluster medium), high-resolution numerical simulations, and liquid-metal laboratory experiments, but to some extent still *a terra incognita*. The goal of the present section is to give an overview of the concepts and ideas underlying the MHD turbulence, with focus more on the energy cascades - due to the large-scale magnetic fields - and the multiple time scales involved in the basic physics of the various astrophysical processes, rather than going into too much detail as for the the computational aspect.

2.1.1 Fundamental Ideas in Fluid Turbulence

I shall start with some basic concepts of incompressible hydrodynamic turbulence, and later generalize to the compressible, magneto hydrodynamic

* British fluid dynamicist who published a classic text entitled *Hydrodynamics*. At a meeting of the British Association in London in 1932, he is reputed to have said, «*I am an old man now, and when I die and go to Heaven there are two matters on which I hope for enlightenment. One is quantum electrodynamics and the other is the turbulent motion of fluids. And about the former I am really rather optimistic*» (Tabor 1989, p. 187).

case. A turbulent flow satisfies the Navier-Stokes equation (Batchelor, 1970) which is the momentum evolution of an element of fluid,

$$\frac{\partial \boldsymbol{u}}{\partial t} + \boldsymbol{u} \cdot \boldsymbol{\nabla} \boldsymbol{u} = -\frac{1}{\rho} \boldsymbol{\nabla} p + \nu \boldsymbol{\nabla}^2 \boldsymbol{u} + \boldsymbol{f}. \tag{2.1}$$

Here $\boldsymbol{u}$ is the velocity field, in general a fluctuating quantity in time t and space $\boldsymbol{x}$, $\boldsymbol{\nabla}$ is the gradient with respect to $\boldsymbol{x}$, ρ and p are the density and the pressure of the medium, respectively, and ν is the kinematic viscosity (molecular viscosity/density), and $\boldsymbol{f}$ is the body force that models large-scale energy input. The incompressibility constraint is guaranteed by the divergence-free condition $\boldsymbol{\nabla} \cdot \boldsymbol{u} = 0$. Turbulent flows are characterized by high Reynolds numbers:

$$\mathcal{R}_e := \frac{\mathcal{U}\mathcal{L}}{\nu}, \tag{2.2}$$

where $\mathcal{U}$ is the typical flow velocity (basically the root mean square of the fluctuating velocity field), and $\mathcal{L}$ is a typical, *large* scale of the (astro)-physical setting. Regardless of how the flow becomes turbulent, once it does, the macroscopic random motions, namely the non-linear convective term $\boldsymbol{u} \cdot \boldsymbol{\nabla} \boldsymbol{u}$, dominate over the molecular viscosity or, in other words, the dissipative term $\nu \boldsymbol{\nabla}^2 \boldsymbol{u}$ of Eq. (2.2). The specific energy injection mechanisms are various: typically in astrophysics, they can be either background gradients, like e.g. the Kepler velocity shear in accretion discs, the temperature gradient $\boldsymbol{\nabla} T$ in stellar convective zones, which mediate the conversion of gravitational energy into kinetic energy of the fluid motion, or direct sources of energy such as the supernovae in the ISM or active galactic nuclei in galaxy clusters. The joint feature of all these injection mechanisms is the scale at which they run, large compared with the size of the system. However, even a small value of the viscosity could be responsible of the energy decay, which evolves - from the largest to the smallest scale - through a *cascade*, described in terms of eddies, reflecting thus the vortical nature of the turbulence.

Kolmogorov Spectrum: The Role of Dissipation

The breakthrough of a proper mathematical description to the nature of the turbulence came with the seminal paper in 1941 by Kolmogorov (hereafter K41), who applied a simple, and genuinely beautiful dimensional argument to get a heuristic theory on the origin of the turbulence spectrum (Kolmogorov, 1941). We can envisage the basic picture of the energy transfer process as follows: at a large-scale $\mathcal{L}$ a force is applied to the fluid, injecting thus energy into the flow. The fluid motion at scale $\mathcal{L}$ becomes unstable and loses its energy to neighbouring smaller scales without directly dissipating energy into heat: the largest eddies produce others that, in turn, collide and further subdivide, and so on. The process repeats itself until one reaches a dissipation scale, or the Kolmogorov scale l_ν, where the energy is finally dispersed into heat by the action of the molecular viscosity.

The phenomenology of the energy-containing eddies gives a reasonable picture of global energy decay and makes clear how the energy reservoir at the large scales controls the process. The Kolmogorov's assumption was that the energy transfer and interacting scales are *local*. While the large-scale dynamics depend on the specific astrophysical context, the cornerstone of all theories of turbulence is the universality of the non-linear dynamics at

small scales ($\ll \mathcal{L}$).[†] Therefore, at *every length scale*, the principle introduced by Kolmogorov holds - the velocity fluctuations created by the driving are precisely those required to transfer the energy "down" the cascade.

Let $\delta u_{\mathcal{L}}$ be the typical fluctuating velocity difference across the scale $\mathcal{L}$. As a consequence, the energy associated with these fluctuations is $\delta u_{\mathcal{L}}^2$, and $\mathcal{L}/\delta u_{\mathcal{L}}$ - sometimes called the *eddy turnover* time scale $\tau_{\rm eddy}$ - is the characteristic time for this energy to cascade to smaller scales via non-linear effects. The energy flux ϵ first injected at the large scales, and then transferred into the turbulent cascade, is then given by

$$\epsilon = \langle \boldsymbol{u} \cdot \boldsymbol{f} \rangle \sim \frac{\delta u_{\mathcal{L}}^3}{\mathcal{L}}. \tag{2.3}$$

The above energy input rate is, on average, equal to the rate of the energy dissipation at the Kolmogorov scale, $\epsilon = \nu \langle |\boldsymbol{\nabla} \times \boldsymbol{u}|^2 \rangle$, and thus so the energy transfer rate across the spectrum at intermediate scales. In the turbulence theory, the range of intermediate scales is commonly called *inertial range*. ϵ is a finite quantity defined by the large-scale energy-injection process, and therefore it cannot depend upon the viscosity ν: the velocity must develop very small scales so that $\nu \langle |\boldsymbol{\nabla} \times \boldsymbol{u}|^2 \rangle$ has a constant limit as $\nu \to 0^+$. The smallest length scale that can be, dimensionally, constructed out of the energy rate ϵ and the (kinetic) viscosity ν is[‡]

$$l_\nu \sim \left(\frac{\nu^3}{\epsilon} \right)^{1/4} \sim \mathcal{R}_e^{-3/4} \mathcal{L}, \tag{2.5}$$

where the Reynolds number, $\mathcal{R}_e \sim \delta u_{\mathcal{L}} \mathcal{L}/\nu$, is typically a very large for several astrophysical settings. Besides the universality of the non-linear processes at all scales belonging to the inertial range, the hydrodynamic turbulence theory assumes:

- homogeneity;
- scale invariance;
- isotropy;
- locality of interactions.

Then, at each length scale l in the inertial range, such that $\mathcal{L} \gg l \gg l_\nu$, the total power injected at large scale and afterwards passed on to smaller scales is given by

$$\epsilon \sim \frac{\delta u_l^2}{\tau_l}, \tag{2.6}$$

where δu_l is the typical velocity of the eddies across the length scale l, and τ_l is the non-linear dynamical time scale, or cascade time. The only possible dimensional combination constructed out of the local quantities is simply $\tau_l \sim l/\delta u_l$. From Eq. (2.6), solving for δu_l, we end up to the scaling for

† Prior to Kolmogorov's ground-breaking work on the smaller-scale inertial range, Taylor (1935, 1938) and von Karman and Howarth (1938) took in consideration the idea of global decay of incompressible homogeneous isotropic turbulence.

‡ Given the Kolmogorov's principle of inertial range, in the turbulent regime the effective (dynamical) viscosity can be thought as

$$\nu = \delta u_l l = \epsilon^{1/3} l^{4/3}, \tag{2.4}$$

δu_l being the velocity fluctuation over the intermediate scale l. From this, Eq. (2.5) derives.

the eddy energy $\delta u_l \sim (\epsilon l)^{1/3}$ or, analogously, to the to well-known $-5/3$ Kolmogorov's spectrum for the kinetic energy $W(k)$,

$$\delta u_l^2 \sim \int_{k=1/l}^{\infty} dk' W(k') \sim \epsilon^{2/3} k^{-2/3} \tag{2.7}$$

$$\hookrightarrow W(k) = C_K \epsilon^{2/3} k^{-5/3}. \tag{2.8}$$

Here, C_K is the Kolmogorov constant, and k is the wave number associated to the inertial range scales: $l \propto 1/k$. The spectrum follows also from purely dimensional considerations on assuming that $W(k)$ depends only on the local value k and the energy transfer rate ϵ,

$$W(k) \sim \epsilon^{\alpha} k^{\beta}. \tag{2.9}$$

The exponents α and β are determined by matching the dimension using $[W(k)] = L^3 T^{-2}$ and $[\epsilon] = L^2 T^{-3}$.

2.1.2 The Picture of Alfvénic Turbulence

The MHD turbulence has been developing over the last half-century, and it can be viewed as a succession of attempts to adapt Kolmogorov's idea to fluids carrying magnetic fields. The pioneering works by Iroshnikov (1963) and Kraichnan (1965) (Iroshnikov, 1963; Kraichnan and Nagarajan, 1967) pointed out the crucial role played by the dynamics of Alfvén waves in the MHD turbulence. According to this picture, small-scale fluctuations, driven by a weak forcing, are not independent of the macro-state but rather are strongly affected by the large-scale magnetic field, which makes the fundamental turbulent excitations behave approximately as Alfvén waves.

The fundamental effect of such perturbations in MHD becomes evident when one writes the (non-linear) MHD equations in terms of the *Elsässer fields*

$$\boldsymbol{z}^{\pm} := \boldsymbol{u} \pm \delta \boldsymbol{B}, \tag{2.10}$$

$\delta \boldsymbol{B}$ being the fluctuating part of the total magnetic field $\boldsymbol{B} = \boldsymbol{B}_0 + \delta \boldsymbol{B}$, with $\boldsymbol{B}_0$ the (large-scale) guide field. The remarkable property of the dynamic equations for the Elsässer fields (Biskamp, 2003)

$$\frac{\partial \boldsymbol{z}^{\pm}}{\partial t} \mp v_A \boldsymbol{\nabla}_{\parallel} \boldsymbol{z}^{\pm} + \boldsymbol{z}^{\mp} \cdot \boldsymbol{\nabla} \boldsymbol{z}^{\pm} = -\boldsymbol{\nabla} p + \frac{1}{2}(\nu + \eta) \boldsymbol{\nabla}^2 \boldsymbol{z}^{\pm} + \frac{1}{2}(\nu - \eta) \boldsymbol{\nabla}^2 \boldsymbol{z}^{\mp} + \boldsymbol{f}, \tag{2.11}$$

is the absence of the self-interactions in the non-linear term, which just couples the variables $\boldsymbol{z}^+$ and $\boldsymbol{z}^-$. Hence, only Alfvén waves propagating in opposite direction along the large-scale field can interact each other, as described by the following equation

$$\frac{\partial \boldsymbol{z}^{\pm}}{\partial t} \mp \boldsymbol{B}_0 \cdot \boldsymbol{\nabla} \boldsymbol{z}^{\pm} = 0. \tag{2.12}$$

Iroshnikov-Kraichnan (hereafter IK) model was thus the extension of K41's turbulence model, with the aforementioned *Alfvén effect* modifying the basic *isotropic* inertial-range scaling, and giving a manifestly anisotropic character to the magnetic turbulence: the cascade dynamics is mainly due to scattering of Alfvén waves.

Iroshnikov-Kraichnan Turbulence Spectrum

Alfvén counter propagating wave packets, δz_l^+ and δz_l^-, interact over an Alfvén time $\tau_A \sim l_\parallel / v_A$. Another characteristic time scale involved in the problem is the non-magnetic strain (or "eddy") time $\tau_s \sim l/\delta z_l^\pm$: it is the distortion time of a wave packet δz_l^+ of scale l by a similar eddy δz_l^+ and vice versa. Here, we can think of $l_\parallel$ as the parallel (to the mean field) extent of the Alfvén-wave packets, and l as that perpendicular. As in the case of K41's turbulence, here the intermediate scales l in the inertial range are smaller than the forcing scale $\mathcal{L}$, and for the time being we do not specify how $l_\parallel$ is related with l. Furthermore, we assume that $\delta z_l^+ \sim \delta z_l^-, \delta u_l, \delta B_l$. In the approximation of *weak turbulence*, the change of amplitude $\Delta\delta u_l$ during a single collision - of duration τ_A - of two wave packets is small

$$\Delta\delta u_l \sim \frac{\delta u_l^2}{l}\tau_A \sim \delta u_l \frac{\tau_A}{\tau_s}. \tag{2.13}$$

Because of the diffusive nature of the process, $N \sim (\delta z_l/\Delta\delta z_l)^2$ elementary interactions are required in order to change δu_l by an amount comparable to itself. Hence, the energy-transfer time or, which is equivalent, the cascade time τ_l can be estimated as

$$\tau_l \sim N\tau_A \sim \frac{\tau_s^2}{\tau_A} \sim \frac{l^2 v_A}{l_\parallel \delta u_l^2}. \tag{2.14}$$

Applying the K41 scenario of energy cascade, from the Eq. 2.6, we get

$$\delta u_l \sim (\epsilon v_A)^{1/4} l_\parallel^{-1/4} l^{1/2}. \tag{2.15}$$

Lastly, under the hypothesis of isotropy, $l_\parallel \sim l$, we end up to the IK turbulence scaling

$$\delta u_l \sim (\epsilon v_A)^{1/4} l^{1/4}, \tag{2.16}$$

which corresponds to the well known $-3/2$ energy spectrum of MHD turbulence in the IK model

$$W(k) = C_{IK}(\epsilon v_A)^{1/2} k^{-3/2}. \tag{2.17}$$

Anisotropy of MHD Turbulence: Goldreich-Shridar Picture

Dissimilarly to the assumption of isotropy made in the preceding paragraph, we suppose that magnetized Alfvénic eddies have a pronounced elongation in the direction of the mean magnetic field, showing thus an anisotropic configuration: the expected small-scale modes are thus primarily excited perpendicularly to the magnetic field, $k_\perp \gg k_\parallel$. Here, I will give a simple phenomenological discussion of the spectral anisotropy of fully developed MHD (weak) turbulence, highlighting the main physical concepts underlying the theory originally proposed by Goldreich and Shridhar in 1995 (hereafter GS95), and now widely accepted as the most suitable model to describe the compressible MHD turbulence (Goldreich and Sridhar, 1995; Sridhar and Goldreich, 1994).

We can imagine eddies mixing magnetic field lines perpendicular to the direction of the mean field. Hence, the spectral cascade takes place mainly in the $k_\perp$ plane, where the original Kolmogorov picture is applicable

$$\epsilon \sim \delta z_{l_\perp}^3 l_\perp \simeq \delta u_{l_\perp}^3 l_\perp, \tag{2.18}$$

$l_\perp$ denoting the eddy scales perpendicular to the magnetic field. These mixing motions induce Alfvénic perturbations that determine the parallel elongation of the eddy. Goldreich & Shridhar conjectured the idea of *critical balance* as the cornerstone for their MHD turbulence theory, i.e. the equality of the eddy turnover time, $l_\perp/v_{l_\perp}$, and the corresponding parallel propagation time of Alfvén waves, $l_\parallel/v_A$,

$$l_\parallel \sim v_A \epsilon^{-1/3} l_\perp^{2/3} \tag{2.19}$$

which reflects the tendency of eddies to become more and more elongated as energy cascades to smaller scales.

The Eq. (2.18) is equivalent to the K41 energy spectrum, perpendicular to the local field direction

$$W(k_\perp) \sim \epsilon^{2/3} k_\perp^{-5/3}. \tag{2.20}$$

From the same equation, the parallel spectrum is easily inferred when considering the Eq. (2.19)

$$W(k_\parallel) \sim \epsilon^{3/2} v_A^{-5/2} k_\parallel^{-5/2}. \tag{2.21}$$

In presence of a mean field B_0, the GS95 model predicts a Kolmogorov spectrum only in the perpendicular direction, while the amplitude of the parallel field fluctuations turns out to be small.

Comments

After nearly 30 years following Kraichnan's paper, the GS95 turbulence theory has now replaced the IK model as the standard accepted description of MHD turbulence. The $k^{-5/3}$ MHD turbulence spectrum, as predicted by the GS95 theory, and seen e.g., in the solar wind (Matthaeus and Goldstein, 1982) and ISM (Armstrong et al., 1995; Elmegreen and Scalo, 2004), is, however, at odd with the consistent failure of recent numerical simulations in reproducing such a spectrum: such numerical experiments obtained a spectral index rather close to the IK's $-3/2$ (e.g. Maron and Goldreich, 2001), and this seems to be the more pronounced the stronger the mean field (e.g. Cho et al., 2002).

Indeed, the issue of the spectral slope is of both theoretical and practical importance. If from one side the differences between spectral slopes of $-5/3$ and $-3/2$ or even -2 do not look large, on the other one they correspond to very different physical pictures. The spectrum of $-5/3$ is representative of a strongly Kolmogorov-type of eddies, $-3/2$ corresponds, instead, to a kind of interactions decreasing with the scale of turbulent motions, while -2 corresponds to a typical spectrum of shocks.

Yan and Lazarian (2004) pointed out the extremely important role played by the anisotropies - as predicted by the different aforementioned MHD turbulence scenarios - in the transport of CRs in the ionized material of the ISM. A K41 ($k^{-5/3}$) and IK ($k^{-3/2}$) can both coexist in the MHD turbulence theory provided by Goldreich and Schridar. However, the fast magnetosonic wave modes associated to the isotropic IK spectrum seem to be to most efficient in scattering CRs in the interstellar plasma, as it has been pointed out by recent numerical MHD simulations (e.g., Cho et al., 2002; Yan and Lazarian, 2004).

2.2 TRANSPORT OF CRS IN THE ISM

The ISM is turbulent on scales ranging from AUs to kpc (Armstrong et al., 1995; Elmegreen and Scalo, 2004; Scalo and Elmegreen, 2004), with an embedded magnetic field that influences almost all of its properties. MHD turbulence is accepted to be of key importance for fundamental astrophysical processes, e.g. star formation, propagation and acceleration of cosmic rays. It is therefore not surprising that attempts to obtain spectra of interstellar turbulence have been numerous since the 1950s (Münch, 1958).

It is generally accepted that the energy of turbulence is most probably due to supernovae explosions and cascaded down to small scales, where resonance with CRs of moderate energies happens. In this section I will review the main aspects of the micro physics involved in the scattering between charged cosmic particles and fluctuating components of the galactic magnetic field.

2.2.1 From the Unperturbed System to the Wave-Particle Scattering

The trajectories of charged particles in a generic electromagnetic field is described by integrating the the Lorentz equation of motion:

$$\frac{d\boldsymbol{p}}{dt} = q\left(\boldsymbol{E} + \frac{\boldsymbol{v}}{c} \times \boldsymbol{B}\right), \tag{2.22}$$

where q is the particle charge, $\boldsymbol{v}$ the particle velocity, $\boldsymbol{p} = m\gamma\boldsymbol{v}$ is the relativistic momentum of the particle with rest mass m, and $\boldsymbol{E}(\boldsymbol{r}, t)$ and $\boldsymbol{B}(\boldsymbol{r}, t)$ are the electric and magnetic fields, respectively. We choose our Cartesian system of coordinates so that the z-axis is aligned parallel to the mean field (or background field) $\boldsymbol{B}_0 = B_0\hat{e}_z$. Furthermore, we approximate the absolute value of the ordered magnetic field B_0 by a constant field. Consequently, we have

$$\langle \boldsymbol{B} \rangle = \boldsymbol{B}_0 = B_0 \boldsymbol{e}_z. \tag{2.23}$$

In the case of galactic particle propagation, the mean field can be identified with the ordered magnetic field disposed along the spiral arms in our Milky Way. Because of the high conductivity of cosmic plasmas, no large-scale electric fields are present

$$\langle \boldsymbol{E} \rangle = \boldsymbol{E}_0 = 0, \tag{2.24}$$

and thus in general we can write

$$\boldsymbol{B} = B_0 \boldsymbol{e}_z + \delta\boldsymbol{B}, \quad \boldsymbol{E} = \delta\boldsymbol{E}, \tag{2.25}$$

with the turbulent electric and magnetic fields $(\delta\boldsymbol{E}, \delta\boldsymbol{B})$. The main reason for using the model of purely magnetic fluctuations is that the electric fields are much smaller than the magnetic fields. As we will see, electric fields are less important for spatial diffusion.

UNIFORM FIELD For the unperturbed system ($\delta\boldsymbol{B} = 0$), the motion of a particle conserves the component of the momentum in the $\boldsymbol{e}_z$ direction and since the magnetic field cannot do work on a charged particle, the modules of the momentum is also conserved. This implies that the particle trajectory

consists of a rotation in the xy plane perpendicular to $\boldsymbol{e}_z$, with a frequency given by

$$\Omega := \frac{qB_0}{mc}\sqrt{1-v^2/c^2}, \tag{2.26}$$

referred to as (relativistic) *gyration frequency*, and a regular motion in the $\boldsymbol{e}_z$-direction with the momentum $p_z = p\mu$, where $\mu \equiv \boldsymbol{p}\cdot\boldsymbol{B}/pB$ is the cosine of the *pitch angle* of the particle, which is the angle between the velocity direction and the uniform magnetic field

$$\theta := \angle(\boldsymbol{v}, \boldsymbol{B}). \tag{2.27}$$

In this case, the equations of motion reduce to

$$\dot{v}_x = \Omega v_y, \tag{2.28}$$
$$\dot{v}_y = -\Omega v_x, \tag{2.29}$$
$$\dot{v}_z = 0. \tag{2.30}$$

These equations can easily be solved by

$$v_x = v_\perp \cos(\Omega t + \Phi_0), \tag{2.31}$$
$$v_y = -v_\perp \sin(\Omega t + \Phi_0), \tag{2.32}$$
$$v_z = v_\parallel = v\mu = \text{constant}, \tag{2.33}$$

where Φ_0 is the (arbitrary) initial gyro-phase, and $v_\parallel$ and $v_\perp$ are the parallel and perpendicular component to the background field B_0, respectively. In terms of the pitch angle they can be written as

$$v_\parallel = v\mu, \quad v_\perp = v\sqrt{1-\mu^2} \tag{2.34}$$

and the *gyro-radius* is

$$r_g(\mu) := \frac{v_\perp}{\Omega} = \frac{v}{\Omega}\sqrt{1-\mu^2} = r_L\sqrt{1-\mu^2}, \tag{2.35}$$

where we used the Larmor radius $r_L = v/\Omega = \text{constant}$. For the particle trajectory, we therefore find

$$x(t) = x(0) + \frac{v_\perp}{\Omega}\sin(\Phi_0) + \frac{v_\perp}{\Omega}\sin(\Omega t + \Phi_0), \tag{2.36}$$
$$y(t) = y(0) + \frac{v_\perp}{\Omega}\cos(\Phi_0) + \frac{v_\perp}{\Omega}\cos(\Omega t + \Phi_0), \tag{2.37}$$
$$z(t) = z(0) + v_\parallel t. \tag{2.38}$$

TURBULENT FIELD More challenging than the unperturbed system is to study particle transport mediated by a turbulent magnetic field. In this case, the particles experience both scattering parallel and perpendicular to the background magnetic field. Let us suppose now that on top of the ordered magnetic field B_0 there is an oscillating magnetic field consisting of the superposition of MHD waves, namely Alfvén waves, and for sake of the simplicity let us consider waves linearly polarized in a plane perpendicular to the z-axis, for example along the x-axis. In the reference of the waves ($v_A \ll c$) the electric field vanishes so that a purely magnetic systems builds up, and one can write the single Fourier modes as

$$\delta\boldsymbol{B} = \delta B \sin(kz - \omega t)\boldsymbol{e}_z \approx \delta B \sin(kz)\boldsymbol{e}_z, \tag{2.39}$$

where the z-coordinate of the particle is $v_{\parallel} t = v\mu t$. Therefore, the equation of motion along z-direction is

$$m\gamma \dot{v}_z = -\frac{q}{c}\delta B_x v_y \tag{2.40}$$

$$\hookrightarrow \frac{d\mu}{dt} = \frac{\delta B}{B_0}\sqrt{1-\mu^2}\sin(\Omega t + \Phi_0)\sin(kv\mu t), \tag{2.41}$$

which can be rewritten, after some trigonometric algebra manipulation, as

$$\frac{d\mu}{dt} = \frac{\Omega}{2}\frac{\delta B}{B_0}\sqrt{1-\mu^2}\big(\cos\big[(\Omega - kv\mu)t + \Phi_0\big] - \cos\big[(\Omega + kv\mu)t + \Phi_0\big]\big). \tag{2.42}$$

Now, we know that according to the Taylor-Green-Kubo (TGK) formalism, the mean square displacement of a generic physical quantity χ is defined as

$$\langle(\Delta\chi)^2\rangle = \langle\big(\chi(t) - \chi(0)\big)^2\rangle, \tag{2.43}$$

where we introduced the averaging operator $\langle ... \rangle$. By assuming the mean square displacement scales with the time like as

$$\langle(\Delta\chi)^2\rangle \propto t^{\sigma}, \tag{2.44}$$

we can characterize the particle motion by accounting for different diffusion regimes, secondly of the value assumed by the parameter σ:

$$0 < \sigma < 1: \quad \text{subdiffusion}, \tag{2.45}$$

$$\sigma = 1: \quad \text{normal (Markovian) diffusion}, \tag{2.46}$$

$$1 < \sigma < 2: \quad \text{super diffusion}, \tag{2.47}$$

$$\sigma = 2: \quad \text{ballistic motion(free streaming)}. \tag{2.48}$$

In most cases, particle transport in astrophysical turbulence behaves diffusively ($\sigma = 1$), and only few cases are known for which particle transport behaves sub- or super diffusively. Finally, cases with $\sigma > 2$ are not known in CRs transport theory, and will be discarded in the present THESIS.

SCATTERING Back to the Eq. (2.42), for particles moving in the positive direction ($\mu > 0$) $\Omega + kv\mu$ is always positive and then the cosine averages to zero on a long time scale. The first cosine of Eq. (2.42) also averages to zero, except at the *resonant wave number*

$$k_{res} = \frac{\Omega}{v\mu}, \tag{2.49}$$

in which case the sign of $\delta\mu$ depends on the random (cosine) phase, $\cos\Phi_0$. Therefore, the average over the phase also vanishes, but not the mean square displacement of the cosine pitch angle, defined as:[§]

$$D_{\mu\mu} := \lim_{t\to\infty}\left\langle\frac{(\Delta\mu)^2}{2\Delta t}\right\rangle_{\Phi_0} = \frac{\pi}{2}\Omega^2\left(\frac{\delta B}{B_0}\right)^2\frac{(1-\mu^2)}{\mu}\delta\left(k - \frac{\Omega}{v\mu}\right). \tag{2.50}$$

According to the Eqs. ((2.45) - (2.48)), the linear scaling of the mean square displacement of the pitch angle cosine with time is indicative of the *diffusive*

§ I used the relationship $\langle\cos^2\Phi_0\rangle = \langle\sin^2\Phi_0\rangle = 1/2$

motion of the particles. In terms of the pitch angle diffusion coefficient $D_{\theta\theta}$, the scattering frequency in pitch angle is given by

$$D_{\theta\theta} := \lim_{t\to\infty}\left\langle \frac{(\Delta\theta)^2}{2\Delta t}\right\rangle_{\Phi_0} = \frac{\pi}{2}\Omega^2\left(\frac{\delta B}{B_0}\right)^2\frac{1}{\mu}\delta\left(k-\frac{\Omega}{v\mu}\right). \tag{2.51}$$

We should note, however, that considering infinitely late times is unrealistic because of the finite size of the system. Then, the condition $t\to\infty$ has to be replaced by $t \gg t_{diff}$, where t_{diff} is a characteristic time-scale that the particle needs in order to reach the diffusive character. Moreover, it is worthy to remind that the Eqs. (2.50) & (2.51) are valid as long as $\delta B/B_0 \ll 1$: CRs are pitch angle scattered by gyro-scale magnetic field fluctuations, which may be hydromagnetic waves in the interstellar turbulence, inducing thus a decorrelation of the particle velocities with respect to the unperturbed trajectories.

SPATIAL DIFFUSION From Eq. (2.51), it is inferred that the total scattering rate in terms of the relativistic gyro-frequency Ω and the relative magnetic perturbation amplitude $\delta B/B_0$ can be written as (R. M. Kulsrud, 2005):

$$\nu = \frac{\pi}{2}\Omega\left(\frac{\delta B}{B_0}\right)^2. \tag{2.52}$$

If $W(k_{res})dk$ is the spectral energy density of the magnetic fluctuations in the wave number range dk at the resonant wave number (2.49), normalized as $\int dk\, W(k) = \delta B^2/4\pi$, the total scattering rate, again after Eq. (2.51), can then be written, as

$$\nu = \frac{\pi}{2}\Omega\frac{k_{res}W(k_{res})}{B_0^2/4\pi}, \tag{2.53}$$

so that the time required for the particle to change direction by $\delta\theta \approx \delta B/B_0 \sim 1$ can be estimated as

$$\tau_{sca} \sim \nu^{-1} \sim \Omega^{-1}\left(\frac{k_{res}W(k_{res})}{B_0^2/4\pi}\right)^{-1}. \tag{2.54}$$

It was shown by R. Kulsrud and Pearce (1969) that pitch angle scattering leads to spatial diffusion as long as it is frequent compared to global dynamical times, or when the mean free path $\lambda_\parallel \equiv v/\nu$ is short compared with global length scales. The parallel diffusion coefficient $D_\parallel$ (i.e. D_{zz} in our simple set up) is defined to be

$$D_\parallel = \left\langle\frac{v_\parallel^2}{\nu}\right\rangle = v^2\frac{\int_{-1}^{1} f(\mu)\frac{\mu^2}{\nu}d\mu}{\int_{-1}^{1}d\mu} = \frac{v^2}{3\nu}, \tag{2.55}$$

where $f(\mu)$ is the pitch angle distribution function at fixed momentum and the last equality holds for an isotropic distribution function in pitch angle and a scattering frequency independent of μ. Therefore, the spatial (parallel) diffusion coefficient can be estimated as

$$D_{zz}(p) = \frac{1}{3}v(v\tau_{sca}) \simeq v^2\Omega^{-1}\left(\frac{k_{res}W(k_{res})}{B_0^2/4\pi}\right)^{-1} = \frac{1}{3}\frac{r_L v}{\mathcal{F}}, \tag{2.56}$$

where $r_L = v/\Omega$ is the Larmor radius, and $\mathcal{F} = \left(\frac{k_{res}W(k_{res})}{B_0^2/4\pi}\right)$.

We may note that the escape time of CRs as inferred from the boron-to-carbon ratio measurement and from unstable elements, namely a time of order 10^7 years in the energy range ~ 1 GeV, corresponds to requiring $H^2/D(p) \sim 10^7$ yr, where $H \sim 3$ kpc is the estimated size of the magnetic galactic halo (Swordy et al., 1990; see also § 4). This implies $D \approx 10^{29}$ cm^2 s^{-1}, i.e. a turbulence level $\delta B/B_0$ of $\mathcal{O}(10^{-4})$ at the resonant wave number. In order to diffuse, and confine CRs in the Galaxy, a very small power in the form of Alfvèn waves is needed; the requirements become even less demanding when higher energy CRs are considered. The perpendicular spatial diffusion coefficient (i.e. D_{xx} in our simple set up) follows from the equation of the motion of the guide centre $\boldsymbol{r}_{gc}$

$$\Delta \boldsymbol{r}_{gc} = \frac{\Delta \boldsymbol{v} \times \boldsymbol{B}}{\Omega B}, \tag{2.57}$$

and is given by Parker (1965) and Forman and Gleeson (1975). When $\lambda_{\parallel}/r_g \gg 1$ (which corresponds to $\delta B/B_0 \ll 1$), we have

$$D_{\perp} = D_{\parallel} \frac{r_g^2}{\lambda_{\parallel}^2} = \frac{r_g^2 \nu}{3}, \tag{2.58}$$

where as in Eq. (2.55) the last equality holds for an isotropic distribution and a μ-independent scattering coefficient. Both coefficients are proportional to vp, the different scale being determined by the turbulence level $\delta B/B_0$. Comparing the Eqs. (2.55) and (2.58), by using Eq. (2.52) we get (for small angle scattering, i.e. $\mu^2 \approx 0$)

$$\frac{D_{\perp}}{D_{\parallel}} = \frac{\pi^2}{4} \left(\frac{\delta B}{B_0}\right)^2 \ll 1. \tag{2.59}$$

The perturbative nature of the formalism introduced here limits its applicability to situations in which $\delta B/B \ll 1$. Moreover, as discussed by Jokipii and Parker (1969), when the $\delta B/B$ becomes closer to unity, the random walk of magnetic field lines may become the most important reason for particle transport perpendicular to the background magnetic field. The combined transport of particles as due to diffusion parallel to the magnetic field and perpendicular to it is not yet fully understood, and in fact it is not completely clear that the overall motion can be described as purely diffusive.

2.2.2 A more rigorous description: diffusion in the Quasi Linear Theory

Now we embark on the problem of understanding the dynamics of charged particles in a *turbulent plasma, far from equilibrium*. We address this topic in plasma turbulence by taking advantage of the *quasi-linear theory* (QLT), following closely the approach proposed in Berezinskii et al. (1984). Plasma turbulence is usually thought to result from the non-linear evolution of a spectrum of unstable collective modes. A collective instability is an excitation and a process whereby some available potential energy stored in the initial distribution function (either in its velocity space structure or in the gradients of the parameters which define the local Maxwellian) is converted to fluctuating electromagnetic fields and kinetic energy.

CRs form a plasma of ionized particles and each particle carries a charge which is responsible for a long range interaction. The collective macroscopic field, generated by the CRs themselves, reduces the free mean path to zero. Thus, if the plasma is dense enough we can neglect collisions. In the case of

a rarefied plasma the Debye length can be used to characterize the interaction range of the macroscopic field. If the Debye length is large compared to the mean distance between particles, collisions can be disregarded. Introducing the Lorentz force $\boldsymbol{F}_L = Ze(\boldsymbol{E} + (\dot{\boldsymbol{r}}/c \times \boldsymbol{B}))$, the magnetic field $\boldsymbol{B}$ and the electric field $\boldsymbol{E}$, we can write the kinetic equation as

$$\frac{\partial f}{\partial t} + (\dot{\boldsymbol{r}} \cdot \boldsymbol{\nabla}) f + Ze\left(\boldsymbol{E} + \frac{\dot{\boldsymbol{r}}}{c} \times \boldsymbol{B}\right) \cdot \frac{\partial f}{\partial \boldsymbol{p}} = 0. \tag{2.60}$$

Here, Ze is the charge of the particle and the function f obeys to the normalization condition

$$N(t, \boldsymbol{r}) = \int_{V_6} d^3\boldsymbol{p}\, f(t, \boldsymbol{r}, \boldsymbol{p}), \tag{2.61}$$

being N the particle density and V_6 the volume of the phase space.

Since the evolution occurs on a time scale which is necessarily longer that the characteristic times of the waves, we may say that $\langle f \rangle = \langle f(\nu, t) \rangle$ so that $\langle f \rangle$ evolves on slow times scales. QLT is concerned with describing the slow evolution of $\langle f \rangle$ and its relaxation back to a marginally stable state. QLT is, in some sense, the simplest possible theory of plasm turbulence and instability saturation, since it is limited solely to determining how $\langle f \rangle$ relaxes.

In the ISM various types of oscillations and waves easily build up. The CRs must interact with these pulsations and waves - they scatter on them, and change their energy. According to the QLT, under the hypothesis of small perturbations to the equilibrium state, the distribution function $f(t, \boldsymbol{r}, \boldsymbol{p})$ reads

$$f(t, \boldsymbol{r}, \boldsymbol{p}) = f_0(t, \boldsymbol{r}, \boldsymbol{p}) + f_1(t, \boldsymbol{r}, \boldsymbol{p}), \tag{2.62}$$

where we separate the average value $f_0(t, \boldsymbol{r}, \boldsymbol{p})$, expressing the slowly evolving background, from the fluctuating part $f_1(t, \boldsymbol{r}, \boldsymbol{p})$, assumed to be small with respect to f_0 as required by the QLT, $f_1 \ll f_0$. Here, we consider a perturbation such that a continuous spectrum of waves is excited. If the wavelength of the perturbation is of the order of a few Debye lengths f_0 can be considered spatially uniform. Averaging over the ensemble of waves the fluctuating part vanishes

$$\langle f_1 \rangle = 0, \tag{2.63}$$

and we are left with the average value

$$\langle f \rangle = f_0. \tag{2.64}$$

The same applies to the magnetic field, so that

$$\boldsymbol{B} = \boldsymbol{B}_0 + \boldsymbol{B}_1, \tag{2.65}$$

where in $\boldsymbol{B}_1$ we recognize the random fluctuating part of $\boldsymbol{B}$, corresponding to an ensemble of waves with random phases, and

$$\langle \boldsymbol{B} \rangle = \boldsymbol{B}_0, \quad \langle \boldsymbol{B}_1 \rangle = 0. \tag{2.66}$$

Since the ISM plasma is a highly conductive medium, the mean value of the electric field averaged on the ensemble of waves vanishes, so that

$$\langle \boldsymbol{E} \rangle = 0. \tag{2.67}$$

Taking the magnetic field $\boldsymbol{B}_0$ uniform and directed e.g., along the z axis, the magnetic perturbations $\boldsymbol{B}_1$ and $\boldsymbol{E}$ can be thought of as a superposition of waves with random continuous phases. Therefore, in a Fourier representation we get:

$$\boldsymbol{B}_1(t,\boldsymbol{r}) = \sum_\alpha \int d^3k\, e^{-i[\omega^\alpha(\boldsymbol{k})t - \boldsymbol{k}\cdot\boldsymbol{r}]} \boldsymbol{B}_1^\alpha(\boldsymbol{k}), \tag{2.68}$$

$$\boldsymbol{E}(t,\boldsymbol{r}) = \sum_\alpha \int d^3k\, e^{-i[\omega^\alpha(\boldsymbol{k})t - \boldsymbol{k}\cdot\boldsymbol{r}]} \boldsymbol{E}_1^\alpha(\boldsymbol{k}), \tag{2.69}$$

where the index α refers to a particular MHD oscillation normal mode, determined by the dispersion relation $\omega = \omega^\alpha(\boldsymbol{k})$. By considering the Maxwell equation

$$\boldsymbol{\nabla}\times\boldsymbol{E} = -\frac{1}{c}\frac{\partial \boldsymbol{B}_1}{\partial t}, \tag{2.70}$$

we may express the electric and magnetic Fourier coefficients in terms of one another by

$$\boldsymbol{B}_1^\alpha(\boldsymbol{k}) = \frac{c}{\omega^\alpha(\boldsymbol{k})}[\boldsymbol{k}\times\boldsymbol{E}^\alpha(\boldsymbol{k})], \tag{2.71}$$

thus enabling us to eliminate one type of coefficient.

First, inserting Eqs. (2.62) and (2.65) in (2.60), yields

$$\begin{aligned}\frac{\partial(f_0+f_1)}{\partial t} + (\dot{\boldsymbol{r}}\cdot\boldsymbol{\nabla})(f_0+f_1) + Ze\left[\boldsymbol{E}+\frac{\dot{\boldsymbol{r}}}{c}\times(\boldsymbol{B}_0+\boldsymbol{B}_1)\right]\cdot\frac{\partial f_0}{\partial \boldsymbol{p}} + \\ Ze\left[\boldsymbol{E}+\frac{\dot{\boldsymbol{r}}}{c}\times(\boldsymbol{B}_0+\boldsymbol{B}_1)\right]\cdot\frac{\partial f_1}{\partial \boldsymbol{p}} = 0.\end{aligned} \tag{2.72}$$

Second, if we average the Vlasov's equation over the ensemble of waves we get

$$\frac{\partial f_0}{\partial t} + (\dot{\boldsymbol{r}}\cdot\boldsymbol{\nabla})f_0 + Ze\left[\frac{\dot{\boldsymbol{r}}}{c}\times\boldsymbol{B}_0\right]\cdot\frac{\partial f_0}{\partial \boldsymbol{p}} = -\left\langle Ze\left[\boldsymbol{E}+\frac{\dot{\boldsymbol{r}}}{c}\times\boldsymbol{B}_1\right]\cdot\frac{\partial f_1}{\partial \boldsymbol{p}}\right\rangle. \tag{2.73}$$

Now, subtracting Eq. (2.73) from Eq. (2.72), and taking care of neglecting all the quadratic terms in $f_1, \boldsymbol{E}$, and $\boldsymbol{B}_1$, we get a closed equation for the fluctuating term f_1:

$$\frac{\partial f_1}{\partial t} + (\dot{\boldsymbol{r}}\cdot\boldsymbol{\nabla})f_1 + Ze\left[\frac{\dot{\boldsymbol{r}}}{c}\times\boldsymbol{B}_0\right]\cdot\frac{\partial f_1}{\partial \boldsymbol{p}} = -Ze\left[\boldsymbol{E}+\frac{\dot{\boldsymbol{r}}}{c}\times\boldsymbol{B}_1\right]\cdot\frac{\partial f_0}{\partial \boldsymbol{p}}, \tag{2.74}$$

which admits a solution of type:

$$f_1 = -\int_{-\infty}^{t} dt'\, Ze\left[\boldsymbol{E}+\frac{\dot{\boldsymbol{r}}}{c}\times\boldsymbol{B}_1\right]\cdot\frac{\partial f_0}{\partial \boldsymbol{p}}, \tag{2.75}$$

which is the 1^{st} order expression for the function f_1. Since we are looking for a closed equation for the average distribution function f_0, we substitute the expression for f_1 in Eq. (2.73), getting

$$\begin{aligned}\frac{\partial f_0}{\partial t} + (\dot{\boldsymbol{r}}\cdot\boldsymbol{\nabla})f_0 + Ze\left[\frac{\dot{\boldsymbol{r}}}{c}\times\boldsymbol{B}_0\right]\cdot\frac{\partial f_0}{\partial \boldsymbol{p}} = \\ Z^2e^2\left\langle\left[\boldsymbol{E}+\frac{\dot{\boldsymbol{r}}}{c}\times\boldsymbol{B}_1\right]\cdot\frac{\partial}{\partial \boldsymbol{p}}\int_{-\infty}^{t} dt'\left[\boldsymbol{E}+\frac{\dot{\boldsymbol{r}}}{c}\times\boldsymbol{B}_1\right]\cdot\frac{\partial f_0}{\partial \boldsymbol{p}}\right\rangle.\end{aligned} \tag{2.76}$$

We can simplify the problem by introducing cylindrical coordinates ($p_\parallel$, $p_\perp$, φ) in momentum space with

$$\boldsymbol{p}\cdot\boldsymbol{B} = p_\parallel B_0. \tag{2.77}$$

In the case of strong turbulence, the time scale of magnetic fluctuations in $\boldsymbol{E}$ and $\boldsymbol{B}_1$ is expected much shorter than the typical time scale given by the (relativistic) gyro-frequency Ω, associated to the circular motion a charged particle induced by the surrounding magnetic field, namely

$$\Delta t^{-1} \sim \Omega = \frac{Z|e|B_0}{E}, \tag{2.78}$$

where E is the particle total energy

$$E^2 = \boldsymbol{p}^2c^2 + m^2c^4. \tag{2.79}$$

Therefore, the transport of CRs is driven by the random field fluctuations. On the opposite limit, when the time scale Δt is much shorter than the time scale associated to the frequency of the random fluctuations of $\boldsymbol{E}$ and $\boldsymbol{B}_1$, the field fluctuations have little influence on the circular motion of fast moving particles. This allow a reasonable average over the angle φ so that in first order $f_0(t,\boldsymbol{r},\boldsymbol{p})$ should not depend on the angle φ, and can be replaced by

$$\bar{f}_0(t,\boldsymbol{r},p_\parallel,p_\perp) = \frac{1}{2}\int_0^{2\pi} d\varphi f_0(t,\boldsymbol{r},p_\parallel,p_\perp). \tag{2.80}$$

With the above approximation, in the pioneering work by Akhiezer (1975) and Kennel & Engelmann (1966) it was demonstrated that the evolution equation for the slowly varying distribution function can be written as

$$\begin{aligned}
&\frac{\partial \bar{f}_0}{\partial t} + v_\parallel \frac{\partial \bar{f}_0}{\partial z} = \pi Z^2 e^2 \times \sum_\alpha \int d^3k \sum_{s=-\infty}^{s=+\infty} \\
&\left\langle \left[E^\alpha_\parallel J_s \hat{\mathcal{P}}^\alpha_\parallel + E^\alpha_\perp \hat{\mathcal{P}}^\alpha_\perp + \frac{E^\alpha_\perp}{p_\perp}\left(1 - \frac{k_\parallel v_\parallel}{\omega^\alpha(\boldsymbol{k})}\right) - \frac{E^\alpha_\parallel}{p_\perp}\frac{v_\parallel}{v_\perp}\frac{s\Omega}{\omega^\alpha(\boldsymbol{k})} J_s \right] \right\rangle \\
&\times \left[E^\alpha J_s \hat{\mathcal{P}}^\alpha_\perp \right] \delta(\omega^\alpha(\boldsymbol{k}) - k_\parallel v_\parallel - s\Omega)\bar{f}_0,
\end{aligned} \tag{2.81}$$

where

$$\hat{\mathcal{P}}^\alpha_\parallel = \frac{\partial}{\partial p_\parallel} - \frac{s\Omega}{\omega^\alpha(\boldsymbol{k})}\frac{1}{v_\perp}\left(v_\perp - v_\parallel \frac{\partial}{\partial p_\perp}\right), \tag{2.82}$$

$$\hat{\mathcal{P}}^\alpha_\perp = \frac{\partial}{\partial p_\perp} + \frac{\boldsymbol{k}_\parallel}{\omega^\alpha(\boldsymbol{k})}\left(v_\perp - v_\parallel \frac{\partial}{\partial p_\perp}\right), \tag{2.83}$$

$$E^\alpha = \frac{1}{2}\left(E^\alpha_R(\boldsymbol{k})e^{i\Psi}J_{s+1} + E^\alpha_L(\boldsymbol{k})e^{-i\Psi}J_{s-1}\right), \tag{2.84}$$

$$E^\alpha_{L,R}(\boldsymbol{k}) = E^\alpha_x(\boldsymbol{k}) \pm iE^\alpha_y(\boldsymbol{k}), \tag{2.85}$$

$$E^\alpha_\parallel(\boldsymbol{k}) = E^\alpha_z(\boldsymbol{k}), \tag{2.86}$$

E^α being the component of the field E^α projected along the uniform magnetic field $\boldsymbol{B}_0$; Ψ is the azimuthal angle of the wave vector $\boldsymbol{k}$, and $J_s = J_s(k_\perp v_\perp/\Omega)$ is a Bessel function of order s.

From the Eq. (2.81) we can easily infer the most important feature of the interaction between ionized plasma and particles, namely the *resonance* character of the wave-particle interaction, recognizable in the δ-function. The

gyro-resonance occurs only for plasma-wave frequencies multiple of the cyclotron frequency of the particle in the regular magnetic field B_0[¶]:

$$\omega^\alpha(\boldsymbol{k}) = k_\parallel v_\parallel + s\Omega, \quad s \in \mathbb{Z}, \tag{2.88}$$

where the $k_\parallel v_\parallel$ term takes into account the Doppler shift.

Comparing the gyro-radius (or the Larmor radius) of the particle and the wavelength of the magnetic wave tells us whether the particle effectively interacts with the wave or, to the contrary, it moves in a straight line. In the first case, the particle is said *magnetized*. There are two limits worthy to address:

- magnetized particle, $k_\perp v_\perp/\Omega \ll 1$: the interactions take place mainly at the following harmonics:
  - for $E^\alpha_\parallel \neq 0 \Rightarrow s = 0$, and $\omega^\alpha = k_\parallel v_\parallel$;
  - for $E^\alpha_\perp \neq 0 \Rightarrow s \pm 1$, and $\omega^\alpha(\boldsymbol{k}) = k_\parallel v_\parallel \pm \Omega$;
- not magnetized particle, $k_\perp v_\perp/\Omega \gg 1$: the harmonics involved (cit. Tsytovich 1977) are characterized by the following values:
  - $s \sim k_\perp v_\perp/\Omega \Rightarrow \omega^\alpha(\boldsymbol{k}) - k_\parallel v_\parallel - s\Omega \sim \omega^\alpha(\boldsymbol{k}) - \boldsymbol{k}\cdot\boldsymbol{v} = 0$.

In the second case, we have e.g., ion-acoustic waves, Langmuir waves, and short MHD waves with $\lambda \ll 2\pi r_L$, where the effective scattering rate of ultra-relativistic particles ($E \geqslant \mathcal{O}(10^2)$ MeV) has an energy dependence E^{-2}. Such an energy dependence is ruled out by the slope of the boron-to-carbon ratio above 1 GeV, which decreases with the energy as $\approx E^{-\delta}$ with $\delta \in [0.3 \div 0.7]$ (e.g., Evoli et al., 2008; Maurin et al., 2002). In correspondence, the escape time is

$$\tau_{esc} \sim D(p)^{-1} \propto E^{-\delta}, \quad \delta \in [0.3 \div 0.7]. \tag{2.89}$$

Therefore, in the ISM the aforementioned second kind of scattering cannot play a large role. On the other side, if the wavelength is comparable to the particle Larmor radius, i.e. $\lambda \sim 2\pi r_L$, each frequency in the spectrum of turbulences interacts with a particle of different energy, leading to an energy dependence of the effective scattering rate and thus the diffusion coefficient. A full discussion would require to consider different types of waves separately. Here we restrict ourselves to the case of supersonic turbulence

$$c_s \ll v_A, \tag{2.90}$$

with

$$c_s = \sqrt{\frac{k_B T_e}{m}}, \tag{2.91}$$

the sound speed of in a medium with T_e being the temperature of thermal electrons and $v_A = B_0/(4\pi\rho)^{1/2}$ the Alfvén speed, and ρ is the density of the ISM.

In the ideal MHD regime (i.e. for $\omega \ll \Omega$), we focus on two types of plasma oscillations:

¶ Some authors introduce the *resonance function* of the QLT as

$$R^{QLT}_\pm = \pi\delta(k_\parallel v_\parallel \pm \Omega). \tag{2.87}$$

- Alfvén waves identified by the dispersion relation

$$\omega^{\alpha}(\boldsymbol{k}) = \pm |k_{\parallel}| v_A, \tag{2.92}$$

and by the following properties

$$\boldsymbol{v} \perp (\boldsymbol{k}, \boldsymbol{B}), \tag{2.93}$$
$$\boldsymbol{E} \in (\boldsymbol{k}, \boldsymbol{B}), \tag{2.94}$$

where $(\boldsymbol{k}, \boldsymbol{B})$ is the plane identified by $\boldsymbol{k}$ and $\boldsymbol{B}$;

- magneto-sonic (fast and slow) waves, identified by

$$\omega^{\alpha}(\boldsymbol{k}) = \pm k v_A \tag{2.95}$$
$$\boldsymbol{v} \in (\boldsymbol{k}, \boldsymbol{B}), \tag{2.96}$$
$$\boldsymbol{E} \perp (\boldsymbol{k}, \boldsymbol{B}). \tag{2.97}$$

Both Alfvén and magneto-sonic are transverse waves, with opposite circular polarization, which propagate along the magnetic field with Alfvén speed.

Limiting ourselves to the approximate case of waves propagating only along the regular magnetic field B_0[‖], so that $k = k_{\parallel}, E^{\alpha}_{\perp} \neq 0$ the resonance condition (2.88), for $s = \pm 1$, reads

$$k_{\parallel} = \pm \frac{\Omega}{\omega^{\alpha}(\boldsymbol{k})/k - v\cos\theta} = \frac{ZeB_0}{pc(\omega^{\alpha}(\boldsymbol{k})/vk - \mu)}, \tag{2.98}$$

where, of course, μ is the cosine of the pitch angle θ. With the above approximation the Eq. (2.74) becomes

$$\begin{aligned} \frac{\partial \bar{f}_0}{\partial t} + \mu v \frac{\partial \bar{f}_0}{\partial z} = \\ \pi^2 Z^2 e^2 \sum_{\alpha} \left(\frac{\omega^{\alpha}(\boldsymbol{k})}{kc}\right)^2 \frac{1}{p^2} \left(\frac{\partial}{\partial p} + \frac{\partial}{\partial \mu}\left(\frac{k_{res} v}{\omega^{\alpha}(k_{res} - \mu)}\right)\right) \times \\ \frac{p(1-\mu^2) W^{\alpha}(k_{res})}{|v\mu - \omega^{\alpha}(k_{res})/k|} \left(\frac{\partial}{\partial p} + \left(\frac{k_{res} v}{\omega^{\alpha}(k_{res} - \mu)}\right) \frac{1}{p} \frac{\partial}{\partial \mu}\right) \bar{f}_0. \end{aligned} \tag{2.99}$$

Here, a change of variables from $p_{\parallel}$ and $p_{\perp}$ to the variables $p = |\boldsymbol{p}|$ and μ has been carried out, so that $\bar{f} = \bar{f}(t, z, p, \mu)$, and the resonant wave number

$$k_{res} = \left|\frac{ZeB_0}{pc\mu}\right| = \frac{\Omega}{c\mu} = \frac{1}{r_L \mu} \tag{2.100}$$

has been introduced. Finally, the quantity $W^{\alpha}(k)$ is, as seen before, the spectral energy density of the MHD waves of type α with random phases and a random polarization distribution, satisfying the normalization condition

$$\int_0^{\infty} dk_{\parallel} W^{\alpha}(k_{\parallel}) = \int_{-\infty}^{\infty} dk_{\parallel} \frac{|B_1^{\alpha}(k_{\parallel})|^2}{4\pi}. \tag{2.101}$$

By looking at Eq. (2.99), we recognize the effective scattering rate term defined like in Eq. (2.53)

$$\nu^{\alpha}_{\mu} := 2\pi^2 \Omega \frac{k_{res} W^{\alpha}(k_{res})}{B_0^2} \left(1 - \frac{\omega^{\alpha}(k_{res})}{k_{res} v} \mu\right)^2 \tag{2.102}$$
$$\approx 2\pi^2 \Omega \frac{k_{res} W^{\alpha}(k_{res})}{B_0^2}. \tag{2.103}$$

‖ Moreover, for $k_{\perp} \neq 0$ the MHD waves are strongly damped

Analogously, the relaxation time required to get an isotropic cosmic ray flux is given by

$$t_{sca} := (\nu_\mu^\alpha)^{-1} \approx \frac{1}{2\pi^2\Omega}\frac{B_0^2}{k_{res}W^\alpha(k_{res})}. \tag{2.104}$$

From Eq. (2.102), the assumption of weak turbulence, i.e. $\nu_\mu^\alpha \ll \Omega$, takes the explicit form

$$W^\alpha(k_{res}) \ll \frac{B_0^2}{2\pi^2 k_{res}}. \tag{2.105}$$

The transport equation (2.99) can be further simplified by introducing two scattering rates, corresponding to waves propagating along and opposite to the uniform field, respectively:

$$\nu^\pm :\approx 2\pi^2\Omega\frac{k_{res}W^\pm(k_{res})}{B_0^2}, \tag{2.106}$$

where $W^\pm(k_{res})$ are the spectral energies associated with the two propagation directions. In the approximation $|\omega^\alpha(k)/kv| = v_A/v \ll 1$, and then

$$\left|\frac{k_{res}v}{\omega^\alpha(k_{res})} - \mu\right| \approx \frac{v}{v_A} \gg 1, \tag{2.107}$$

we can express the Eq. (2.99) as sum of the two transport modes in the following form

$$\begin{aligned}\frac{\partial\bar{f}_0}{\partial t} + \mu v\frac{\partial\bar{f}_0}{\partial z} =& \frac{v_A^2}{p^2}\left(\frac{\partial}{\partial p}p + \frac{\nu}{v_A}\frac{\partial}{\partial\mu}\right)\frac{1-\mu^2}{2}\nu_\mu^+\frac{p^3}{v^2}\left(\frac{\partial}{\partial p} + \frac{\nu}{v_A}\frac{1}{p}\frac{\partial}{\partial\mu}\right)\bar{f}_0 + \\ & \frac{v_A^2}{p^2}\left(\frac{\partial}{\partial p}p - \frac{\nu}{v_A}\frac{\partial}{\partial\mu}\right)\frac{1-\mu^2}{2}\nu_\mu^-\frac{p^3}{v^2}\left(\frac{\partial}{\partial p} - \frac{\nu}{v_A}\frac{1}{p}\frac{\partial}{\partial\mu}\right)\bar{f}_0.\end{aligned} \tag{2.108}$$

Given the weights of the $\partial/\partial\mu$ terms (2.107), from the above equation, we can infer that the scattering changes angles rapidly compared to changes in energy. Under the reasonable hypothesis of an isotropic distribution function,

$$\hat{f}_0 = \frac{1}{2}\int_{-1}^{1} d\mu\bar{f}_0, \tag{2.109}$$

where $\hat{f}_0$ is the mean value of $\bar{f}_0$ over the angles, and in the limit of diffusion approximation

$$\Delta t \gg t_{sca}, \quad \Delta x \gg \lambda_{sca}, \tag{2.110}$$

from the Eq. (2.108) we end up with a *diffusion-convection* equation for the particle transport, given by

$$\frac{\partial\hat{f}_0}{\partial t} - \frac{\partial}{\partial z}D_{zz}\frac{\partial\hat{f}_0}{\partial z} + \frac{1}{3p^2}\frac{(p^3u_w)}{\partial p}\frac{\partial\hat{f}_0}{\partial z} - \frac{\partial u_w}{\partial z}\frac{p}{3}\frac{\partial\hat{f}_0}{\partial p} = \frac{1}{p^2}\frac{\partial}{\partial p}p^2D_{pp}\frac{\partial\hat{f}_0}{\partial p}. \tag{2.111}$$

Here, we introduced the effective velocity of convective particle transport by the waves

$$u_w := v_A\int_0^1 d\mu\frac{3(1-\mu^2)}{2}\frac{\nu_\mu^+ - \nu_\mu^-}{\nu_\mu^+ + \nu_\mu^-}, \tag{2.112}$$

which constitutes a drift due to the different energy density $v_\mu^\pm$ of the waves along the magnetic field. The spatial diffusion coefficient along the regular magnetic field $\boldsymbol{B}_0$ is defined as (compare it with (2.102))

$$D_{zz} := \frac{v^2}{2}\int_0^1 d\mu \frac{1-\mu^2}{v_\mu^+ + v_\mu^-}. \tag{2.113}$$

The stochastic acceleration of CRs is instead expressed in terms of the momentum diffusion coefficient, given by

$$D_{pp} = p^2 \frac{v_A^2}{v^2}\int_0^1 d\mu\, 2(1-\mu^2)\frac{v_\mu^+ v_\mu^-}{v_\mu^+ + v_\mu^-}. \tag{2.114}$$

A few comments about the Eq. (2.111):

- the transport equation (2.111) represents the benchmark for all the diffusion-convection models we need for studying the propagation of CRs in the ISM, but it is still incomplete. In fact, it is missing of the additional terms due to momentum losses in the ISM, particle losses due to spallation and fragmentation and source terms (see § 4);
- if the energy density propagating in opposite directions is the same, $v_\mu^+ = v_\mu^-$ and the convection velocity (2.112) vanishes;
- if the energy density propagates only in one direction, then the diffusion in momentum space disappears, i.e. non stocastic acceleration occurs.

2.3 ANGULAR MOMENTUM TRANSPORT IN ADS

Matter spiralling into a black hole converts a tremendous amount of gravitational binding energy into heat and radiation. This process is called *Accretion*.

Accretion provides radiant energy in a variety of astrophysical sources: stellar binaries, active galactic nuclei, proto-planetary discs, and in some types of gamma ray bursts. Accretion of plasma onto a central black hole or neutron star is responsible for many of the most energetic phenomena observed in astrophysics (see, e.g., Narayan & Quataert 2005 for a review). Black hole accretion in quasars is the most powerful and the most efficient steady energy source known in the Universe. The primary goal of black hole accretion theory is to explain observational properties of quasars, other active galactic nuclei, and micro quasars. These observations contain clues about the most fundamental black hole physics.

However, the clues cannot be fully decoded today. Black hole accretion physics rests on two pillars of a very different quality. The first one is an exact and well understood description of the strong gravity given in terms of the Kerr metric $g_{\mu\nu}$, and its symmetries. The second one is an uncertain description of the matter properties (radiation transport, turbulence and viscosity, convection and magnetic fields, etc.) given by the stress energy tensor $\mathcal{T}_{\mu\nu}$ and several phenomenological, often only approximate, material equations.

The present models assume that (at least a part of) the accreted matter stays (at least temporarily) close to a stationary and axially symmetric equilibrium, in which matter moves on approximately circular orbits, i.e. remains for some time at almost the same distance from the black hole. This

is possible because the high angular momentum of matter provides an effective potential barrier against the black hole gravity. Then, the high angular momentum of matter is gradually removed by "viscous" stresses that operate against the shear in the accretion disc.

The quasi-steady accretion of a particle of mass m through a Kepler disc from a large outer radius, r_{out}, to an inner radius, r_{in}, requires that the particle give up an amount of energy $\sim 0.1mc^2$. To do this, the particle must also give up an amount of angular momentum $\sim (GMr_{out})^{1/2}$. Viscous stresses within the fluid can facilitate this mass transfer in, angular momentum transfer out, and energy dissipation. However, the stresses can not come from ordinary molecular viscosity, as this is much too weak in astrophysical accretion discs. Instead, the stresses likely come from turbulence that acts like an effective viscosity.

2.3.1 The α Viscosity Prescription

Several *ad hoc* phenomenological prescriptions have been routinely used to describe the unknown dissipative processes. The most crucial, and perhaps the most controversial, of these is the "alpha" viscosity prescription,

$$(\text{viscous stress})\ \mathcal{T} = -\alpha\ (\text{pressure } P), \tag{2.115}$$

where $0 < \alpha < 1$ is a phenomenological constant. The α-prescription (Shakura and Sunyaev, 1973) and its variations have been largely used in hydrodynamical models of accretion discs simply because there is no better alternatives.

It is now widely accepted that, in many types of accretion discs, the primary source of such stresses is the turbulence generated by the *magneto-rotational* "Balbus-Hawley" instability (MRI), that occurs in weekly magnetized, non-rigidity rotating fluids (Balbus and Hawley, 1991; Hawley and Balbus, 1991).

Even so, one can still parametrize the stresses within the disk as an effective viscosity and use the normal machinery of standard hydrodynamics without the complication of magnetohydrodynamics (MHD). This is sometimes desirable as analytic treatments of MHD can be very difficult to work with and full numerical treatments can be costly. Shakura and Sunyaev realized that if the source of viscosity in accretion discs is turbulence, then the kinematic viscosity coefficient $\nu_\star$ has the form

$$\nu_\star \approx l_0 v_0, \tag{2.116}$$

where l_0 is the correlation length of turbulence and v_0 is the mean turbulent speed. Assuming subsonic turbulence, $v_0 < c_s$, and that the typical size of the turbulent eddies cannot be greater than the disc thickness, $l_0 < H$, one gets

$$\nu_\star = \alpha H c_s, \tag{2.117}$$

with $0 < \alpha < 1$ is the dimensionless coefficient aforementioned, assumed by Shakura and Sunyaev to be constant. For thin accretion discs, the viscous stress tensor reduces to an internal torque with the following approximate form

$$\mathcal{T}_{r\phi} \approx \nu_\star r \frac{\partial \Omega}{\partial r}, \tag{2.118}$$

where $\Omega(r)$ is the angular velocity of the disc, function of the radial distance r. However, for thin discs, $r(\partial\Omega/\partial r) \approx -\Omega$ and $c_s \approx (P/\rho)^{1/2} \approx \Omega H$, so Shakura and Sunyaev argued that the total stress is proportional to the total pressure, hence the torque must have the form $\mathcal{T}_{r\phi} = -\alpha P$. Nowadays, by using numerical simulations, we know the appropriate pressure to be $P_{\rm Tot} = P_{\rm gas} + P_{\rm rad}$.

For more details than can be given in this manuscript, I recall that there are several excellent textbooks and review articles devoted, partially or fully, to black hole accretion discs. The well known and most authoritative textbook on accretion is *Accretion Power in Astrophysics* by Frank, King and Raine. Two monographs are devoted to black hole accretions discs: *Black-Hole Accretion Disks* by Kato, Fukue and Mineshige, and *Theory of Black Hole Accretions Disks* by Abramowicz, Björnsson, and Pringle. Throughout the rest of the present chapter I will limit to introduce preliminary results achieved in the framework of the MRI by *shearing box*, large-scale, numerical simulations of non-relativistic, gas-dominated accretion flows.

2.3.2 The Magneto-Rotational Instability in Accretion Discs

Theoretical Framework

In the previous section I have pointed out that ordinary molecular viscosity is too weak to provide the necessary level of stress. Another possible source is turbulence. The mean stress from turbulence always has the property that $\mathcal{T}_{r\phi} < 0$, and so it can act as an effective viscosity.

Magnetic fields may play many interesting roles in black hole accretion discs. Large scale magnetic fields threading a disc may exert a torque, thereby extracting angular momentum. Similarly, large scale *poloidal* magnetic fields threading the inner disc, ergo-sphere, or black hole, have been shown to be able to carry energy and angular momentum away from the system, and power jets. Weak magnetic fields can tap the differential rotation of the disc itself to amplify and trigger an instability that leads to turbulence, angular momentum transport, and energy dissipation (exactly the processes that are needed for accretion to happen). This happens through a mechanism known as the magneto-rotational (or "Balbus-Hawley") instability.

Originally discovered by Velikhov (1959), and later on generalized by Chandrasekhar (1960), in the context of vertically magnetized *Couette* flow between differentially rotating cylinders, the application of this instability to accretion discs was initially missed until the rediscovery of the MRI by Balbus and Hawley.

The instability itself can be understood through a simple mechanical analogy. Consider two particles of gas connected by a magnetic field line. Arrange the particles such that they are initially located at the same cylindrical distance from the black hole but with some vertical separation. Give one of the particles (say the upper one) a small amount of extra angular momentum, while simultaneously taking away a small amount of angular momentum from the lower one. The upper particle now has too much angular momentum to stay where it is and moves outward to a new radius. The lower particle experiences the opposite behaviour and moves to a smaller radius. In the usual case where the angular velocity of the flow drops off with radius, the upper particle will now be orbiting slower than the lower one. Since these two particles are connected by a magnetic field line, the differing orbital speeds mean the field line will get stretched. The additional

tension coming from the stretching of the field line provides a torque, which transfers angular momentum from the lower particle to the upper one. This just reinforces the initial perturbation, so the separation grows and angular momentum transfer is enhanced. This is the fundamental nature of the instability.

In most black hole accretion discs, it is reasonable to assume ideal MHD, whereby the conductivity is infinite, and consequently the magnetic diffusivity is zero. Whenever this is true, magnetic field lines are effectively frozen into the fluid. In a more formal description, we can consider a disc threaded with a vertical magnetic field B_z and having an Alfvén speed $v_A^2 = B_z^2/(4\pi\rho)$. The dispersion relation for perturbations of a fluid quantity $\delta X \sim \exp[i(kz - \omega t)]$ is

$$\omega^4 - (2kv_A + \omega_r^2)\omega^2 + kv_A(kv_A + r d\Omega^2/dr) = 0, \tag{2.119}$$

where Ω is the rotational speed of the fluid, and ω_r is the radial epicyclic frequency (Biskamp, 2003). The Eq. (2.119) has an unstable solution ($\omega^2 < 0$), if and only if, $kv_A + r d\Omega^2/dr = 0$. The condition for occurrence of the MRI instability in weakly magnetized discs is, therefore,

$$\frac{\partial \Omega}{\partial r} < 0, \tag{2.120}$$

which is always satisfied, as in accretion discs angular velocity decreases with the radius.

We may note that the MRI exists even for intermediate magnetic field strengths. In terms of the natural length scale of the instability ($\sim v_A/\Omega$), the field strength is constrained at the upper limit by the requirement that the unstable MRI wavelength fit inside the vertical thickness of the disc ($v_A/\Omega \lesssim H$). This corresponds to magnetic field energy densities that are less than the thermal pressure, i.e., $\mathcal{B}^2 < P_{gas}$. Fluid MHD simulations show that the MRI-generated turbulence in discs is subsonic and has $\beta \equiv P_{gas}/P_{mag} \sim [10 \div 100]$. At the lower end, dissipative processes set a floor on the relevant length scales, and hence, field strengths.

Preliminary Results

To conclude the present discussion centred on the role played by magnetic fields and turbulence in the transport of angular momentum, and matter, through an accretion flows, I will schematically show some of the results achieved in this direction, in order to provide, in my opinion, the reader with the necessary background when she or he comes to the reading of PAPER V (Di Bernardo and Torkelsson, 2013), appended to the manuscript. Firstly, briefly I recap the main guidelines of the MRI.

The linear instability of differentially rotating plasmas, i.e. the magneto-rotational instability (MRI), amplifies magnetic fields and gives rise to MHD turbulence in astrophysical discs. Magnetic stresses due to this turbulence transport angular momentum, allowing plasma to accrete. The MRI converts the gravitational potential energy of the inflowing plasma into turbulence at the outer scale that is comparable to the scale height of the disc. This energy is then cascaded to small scales and dissipated into heat-powering the radiation that we see from accretion flows.

3D SHEARING BOX NUMERICAL SET UP In simulating accretion discs around black holes, there are a number of challenging issues. First, there is quite a

lot of physics involved: relativistic gravity, hydrodynamics, magnetic fields, and radiation being the most fundamental. Then there is the issue that accretion discs are inherently multi-dimensional objects. Going to three-dimensions and relaxing all symmetry requirements increases the computational expense yet again by a similar factor. Simulations of this size have only become feasible within the last decade and still only with a subset of the physics one is interested in and usually with a very limited time duration.

Another hindrance in simulating accretion discs is the very large range of scales that can be present. In terms of a grid based code, a disc with a scale height of H/R requiring N_z zones to resolve in the vertical direction at some radius R_{in}, would require something of the order $N_z/(H/R)$ zones to cover each factor of R_{in} that is treated in the radial direction. The azimuthal direction in a full three-dimensional simulation would require a comparable number of zones to what is used in the radial direction.

There are many numerical codes available today that include relativistic hydrodynamics or MHD that are, or can be, used to simulate accretion discs. Along with settling on a numerical scheme, a decision must also be made whether or not to try to treat the disc as a whole or to try to understand it in parts. The latter choice includes "shearing-box" simulations, the name coming from the type of boundary conditions one imposes on the domain to mimic the shear that would be present in a real disc. The obvious advantage of treating the disc in parts is that one circumvents the previously noted problem of the large range in scales in the disc by simply ignoring the large scales. Instead one treats a rectangular volume generally no larger than a few vertical scale heights on a side and in some cases much smaller. In this way, for a moderate number of computational zones, one can get as good, or often much better, resolution over the region being simulated than can be achieved in global simulations.

I use, for these purposes, the PENCIL CODE**, which is a high-order finite-difference code for compressible hydrodynamic flows with magnetic fields. It is highly modular and can easily be adapted to different types of problems. The formal equation solved by the PENCIL CODE, in a shearing-box formalism, are

$$\begin{aligned}\partial_t \boldsymbol{u} + \boldsymbol{u}\cdot\boldsymbol{\nabla}\boldsymbol{u} + u_y^0\partial_y\boldsymbol{u} = {} & 2\Omega u_y \boldsymbol{e}_x - \frac{1}{2}\Omega u_x \boldsymbol{e}_y - \Omega^2 z\boldsymbol{e}_z \\ & + \frac{1}{\rho}\boldsymbol{J}\times\boldsymbol{B} - \frac{1}{\rho}\boldsymbol{\nabla}P + \boldsymbol{f}_\nu(\boldsymbol{u},\rho),\end{aligned} \tag{2.121}$$

$$\partial_t \boldsymbol{A} + u_y^0\partial_y\boldsymbol{A} = \boldsymbol{u}\times\boldsymbol{B} + \frac{3}{2}\Omega A_y\boldsymbol{e}_x + \boldsymbol{f}_\eta(\boldsymbol{A}), \tag{2.122}$$

$$\partial_t \rho + u_y^0\partial_y\rho = -\rho\boldsymbol{\nabla}\cdot\boldsymbol{u} + \boldsymbol{f}_D(\rho), \tag{2.123}$$

$$\boldsymbol{B} = \nabla\times\nabla A. \tag{2.124}$$

To start with, we use an isothermal equation of state, including the gravity, and hence for the density a vertical stratified configuration:

$$\rho(x,y,x) = \rho_0 \exp\left(-\frac{z^2}{H^2}\right) \tag{2.125}$$

$$H = \frac{c_s}{\Omega} = 1 \quad \text{adimensional units} \tag{2.126}$$

** The code runs efficiently under MPI on massively parallel shared- or distributed-memory computers.

MRI: A FULLY TURBULENT GAS If the conditions (2.119) for the instability are met, the fastest-growing mode, which dominates the early evolution, has the form of a "channel flow" involving alternating layers of inward- and outward- moving fluid. The amplitude of this solution grows exponentially until it becomes unstable to three- dimensional "parasitic modes" that feed off the gradients of velocity and magnetic field provided by the channel flow. The flow rapidly reaches a state of MRI turbulence. This instability can be self-sustaining through a non-linear dynamo process - non-linear because the motion that sustains or amplifies the magnetic field is driven by the field itself through the MRI (Brandenburg et al., 1995). The system is fed by free energy from keplerian shear flow, and the dynamo action implies an amplification of the magnetic field.

THE MAXWELL STRESS TENSOR: THE NUMERICAL VALUE FOR α In a non-vertical magnetic field configuration, the Maxwell-Reynolds stress tensor reads

$$\mathcal{T}_{xy} \equiv \frac{\langle \rho u_x u_y - B_x B_y \rangle}{\langle \rho \rangle} = \alpha. \tag{2.127}$$

In my numerical simulations, I found that both Maxwell and Reynolds (turbulent) stresses are positive, as expected. But, the Maxwell stresses are around four times larger than the Reynolds stresses. This means that the angular momentum is transported outwards while the mass is transported inwards. The turbulence seeded by the MRI provides the stresses responsible for accretion. Typical values of α estimated from MHD simulations are in an interval $[0.01 \div 0.1]$, while observations suggest a value closer to 0.1.

3 COSMIC RAYS AND THEIR GALACTIC ENVIRONMENT

«[...] There are more things in
heaven and earth, Horatio,
Than are dreamt of in your
philosophy [...]»
Hamlet, Act I, Scene V

by William Shakespeare
(Stratford-upon-Avon, 1564 - 1616)

For centuries, man has looked up to the sky, and directed his gaze towards the light coming from distant celestial objects, to gather as much as possible information about the surrounding Universe. When observing the sky on clear nights, to the naked eyes of a terrestrial observer the Milky Way appeared, and *appears*, like a faint luminous band across the sky. Nowadays, we know that the light in this band originates from the accumulation of unresolved stars, and other material when viewed in the direction of the Galactic plane. And dark regions within the band, such as the *Great Rift* and the *Coalsack*, correspond to areas where the light from distant stars is blocked by "clouds" of obscuring matter and interstellar dust.

Nevertheless, besides stars and dust, the Milky Way's interstellar material is filled with radiation made of relativistic particles, which unrelentingly hit the Earth's atmosphere: this is a remarkable fact!

As a sort of high-energy *charged bullets* circulating in the cosmos, Cosmic Rays (Crs) have been intensively studied since their discovery at the beginning of the twentieth century. They constitute an essential part of the Universe. Their origin is interrelated with the main processes and the dynamics of star formation, stellar evolution, supernova explosions and to the state and conditions of the Ism in the Galaxy. Despite extensive efforts we still do not have a coherent theory which can explain a great variety of the features seen in the Crs.

The present chapter aims to give an overview of the main constituents of the interstellar environment of the Milky Way. Particular emphasis will be placed on the Crs, conceived as an active part of a larger galactic ecosystem. A more comprehensive review on the current status of the knowledge of the Ism has been given e.g. by Ferrière (2001) (see also the monograph by Draine, 2011).

3.1 A HITCHHIKER'S GUIDE TO THE GALAXY

This section outlines the main important features and structures of our Galaxy as a conception of enormous mass, energy, dynamics and scale.[a]

a As evident, the section title wants to be a humorous tribute to the comedy science fiction series *The Hitchhiker's Guide to the Galaxy*, created by Douglas Adams, originally a radio comedy broadcast on BBC Radio 4 in 1978, and then published in 1979.

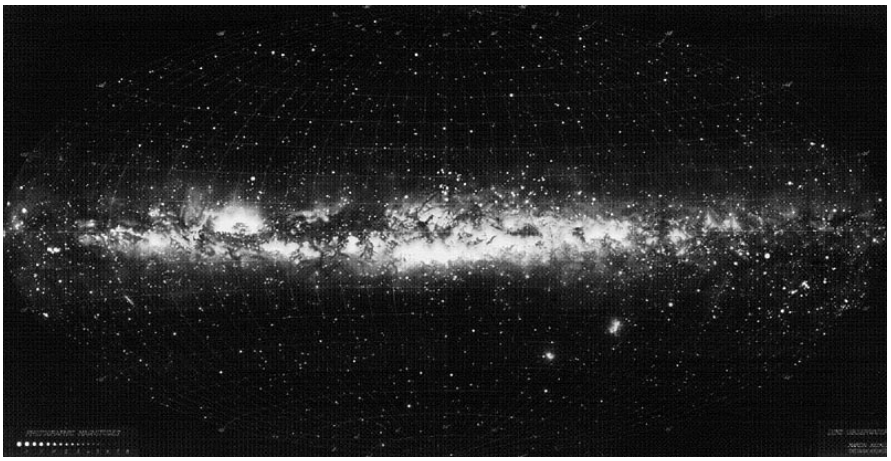

Figure 3.1: *The Lund Panorama of the Milky Way. In the beginning of the 1950's, professor Knut Lundmark at Lund Observatory suggested a stylish Milky Way panorama in an Aitoff projection of the sky. The computation of coordinates, the drawing of the coordinate grid and the marking of the star positions have been carried out by Martin Kesküla, while the drawing of the Milky Way clouds themselves has been made by Tatjana Kesküla. The work took almost two years, and was completed in 1955. The final beautiful piece of art (measures 1x2 meters), still belonging to Lund Observatory, has become well-known to astronomers all over the world from countless reproductions. Credit: by Bo Nilsson/Eva Jurlander, Lund Observatory (http://www.astro.lu.se/Resources/Vintergatan/vintergatane.html).*

3.1.1 Overall Picture of the Galaxy

FROM NAKED EYES, TO THE IMAGING ERA Our understanding begins with the naked eye appearance of the Milky Way. The earliest and one of the finest naked eye descriptions of the Milky Way, in Chapter 2, Book VIII of Ptolemy's Almagest (c.150 CE), begins this way: «*It is easily seen that the Milky Way is not simply a circle but a zone having quite the colour of milk, whence its name; and that it is not regular and ordered, but different in width, colour, density, and position; and that in one part it is double. These particulars we find in need of careful observation.*»

Probably the last scientifically guided artistic representation of the Milky Way is the *Lund panorama* (see Figure 3.1), a 2 meter long painting completed in 1955, currently held at the Lund Observatory, Sweden, that is based on isophote maps completed by Anton Pannekoek[b] and colleagues in 1949.

In 1610 Galileo's *Siderius Nuncius* announced four dramatic telescopic discoveries: the cratered and mountainous surface of the Moon, the four revolving moons of Jupiter, the resolution of nebulae into clusters of stars, and the discovery of many new stars in the Milky Way too faint to be seen by the naked eye: «*For the Milky Way is nothing else than a congeries of innumerable stars distributed in clusters. To whatever region of it you direct your spyglass, ... the multitude of small stars is truly unfathomable.*» This was the first indication that the universe was not identical to the apparent dome of the night sky but contained far more objects, and possibly extended to a greater distance, than the naked eye could see.

b Antonie (Anton) Pannekoek (2 January 1873 - 28 April 1960) was a Dutch astronomer, Marxist theorist, and social revolutionary. He was one of the main theorists of council communism. Credit: http://en.wikipedia.org/wiki/Antonie_Pannekoek.

Much later, toward the end of the 18th century, William Herschel manufactured telescopes of sufficient aperture and optical quality to compile 698 "star gauges" or methodical counts of the number of stars within a standard telescopic field of view in different parts of the sky. Assuming that stars were approximately equally bright and evenly distributed in space, so that a greater density implied a longer view through the cloud, he was able to deduce the Sun's position near the centre of an extended mass of stars (On the Construction of the Heavens, 1785).

Confusion about the actual dimensions and nature of the Galaxy appeared as late as the *Great Debate* between Harlow Shapley and Herber Curtis in April, 1920. This event was held at a time when information about many aspects of the Milky Way (globular clusters, *H II regions*, stellar magnitudes and proper motions) was rapidly increasing. For example, Harlow Shapley (1918) had recently used the period/luminosity relation of RR Lyrae variable stars found in globular clusters to estimate the distance of the clusters; their three dimensional distribution suggested the centre of the Galaxy was in the direction of the constellation Scorpius at a distance of between 13,000 to 20,000 parsecs.

In the same decade, proper motion and radial velocity surveys provided data that allowed Lindblad (1927) to outline the *spiral* kinematics of the Galaxy and the formation of *spiral arms*, and Oort (1927) to estimate the rotational velocity of the Sun and to locate the centre of the Galaxy in the direction of the constellation Sagittarius at a distance of approximately 6300 parsecs (which he later revised to 9000 parsecs, only 8% greater than the current value). Thus, by 1930 the "disc" structure, rotational speed, centre of rotation, and dimensions of the Galaxy, and the relative size and distances of the galaxies around it, were finally established.*

Finally, by the mid 20th century the spiral structure of the Galaxy was clarified using two methods. Following the demonstration by Baade (1951) that dark clouds and star forming regions in the *Andromeda* galaxy were confined to the visible spiral arms, Morgan et al. (1953) applied the method of spectroscopic parallax to determine the distance of 27 OB associations, H II regions and K giant stars. These appeared to identify the local sections of three spiral arms closest to the Sun. The second method followed a suggestion by Hendrick van den Hulst that the 21-cm emission line of atomic hydrogen could be used in radio astronomy.

Subsequent studies improved on these results by combining data from both methods and improving the estimated distances to spiral arm markers. Becker and Fenkart (1970) augmented Morgan's method with a larger sample of young open star clusters and H II regions, and Humphreys (1976) combined data on super giant stars, OB associations, galactic star clusters, H II regions, stellar proper motions and radio observations to produce a more detailed map of the local region of the Galaxy and trace a large arc

* Originally, astronomers had the idea that the arms of a spiral galaxy were material. However, if this were the case, then the arms would become more and more tightly wound, since the matter nearer to the centre of the galaxy rotates faster than the matter at the edge of the galaxy. The arms would become indistinguishable from the rest of the galaxy after only a few orbits. This is called the *winding problem*. Lin and Shu proposed in 1964 (Lin and Shu, 1964) that the arms were not material in nature, but instead made up of areas of greater density, similar to a "traffic jam" on a highway. *Density wave theory* or the Lin-Shu density wave theory is a theory proposed by C.C. Lin and Frank Shu in the mid-1960s to explain the spiral arm structure of spiral galaxies. Their theory introduces the idea of long-lived quasi static density waves (also called heavy sound), which are sections of the galactic disk that have greater mass density (about 10–20% greater). Credit: http://en.wikipedia.org/wiki/Density_wave_theory. (Lin, Yuan, et al., 1969)

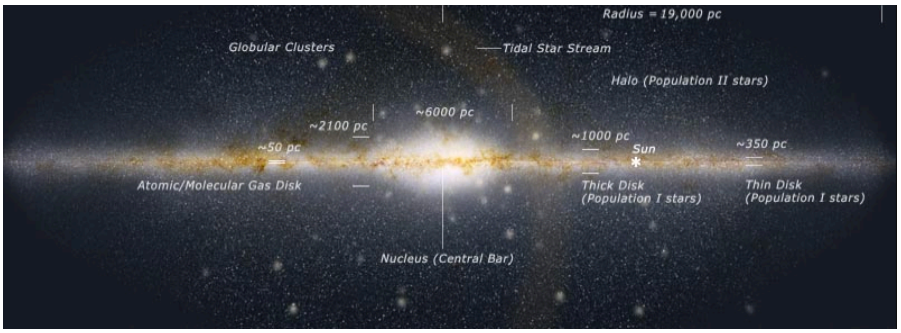

Figure 3.2: *Anatomy of the Galaxy: structure & dimensions. Credit:* http://www.handprint.com/ASTRO/galaxy.html.

of the *Sagittarius-Carina* spiral arm; this led her to conclude that our Galaxy had two prominent spiral arms and, in overall structure, most resembled an Sc or "M 101 type" spiral galaxy such as M 74 or NGC 1232.

3.1.2 Anatomy of the Galaxy

The Galaxy is a *turbulent* system of many distinct components (see e.g., Mac Low, 2004; Robin et al., 2003). The main attribute of a galaxy is its *galaxy type* in the Hubble original or revised (de Vaucouleurs) systems. Our Milky Way is currently believed to be a Hubble type Sb (Vaucouleurs type SB(rs)bc II) galaxy: in other words, it has a pronounced *spiral structure*, that includes a prominent *central bar* (Churchwell and Glimpse Team, 2005) and a *ring structure*. Any component of the galaxy has a characteristic thickness, the *scale height* $\mathcal{H}$[c], and radius measured from the Galaxy barycentre.

The *thin*, galactic disc has a radius $R \sim 15 \div 20$ kpc, and a height varying locally in function of the spectral class of the stars there contained,[d] assuming, on average, a value equal to $2\mathcal{H} \sim 400 \div 600$ pc. The Galaxy is also provided with a central spheroidal structure, called *bulge*, which extends out of the galactic disc plane with a radius of about 2 kpc, enclosing the densest concentration of the stars, of the entire galactic system. Finally, it is present a stellar halo, consisting of *globular clusters* and field stars, extended to even more than 30 kpc far from the centre of the Galaxy (Binney and Merrifield, 1998, see also Figure 3.2).

The typical Milky Way's spiral structure - with relatively loosely wound arms - has been revealed by radio observations of the neutral hydrogen present in the ISM, and it is similar to that seen in several external galaxies, revealed in the optical band (van Woerden et al., 1957. See also Dame and Thaddeus, 2008). Galaxies of this type exhibit, typically, two arms arranged in a spiral way, departing both from the central bulge and from the extremes of the bar which crosses, diametrically, the bulge itself. Recent images in the infra-red (IR), collected by the SPITZER SPACE TELESCOPE, showed the Galaxy's central bar to be larger than previously suspected.

---

c The scale height ($\mathcal{H}$) is the distance within which the density of a feature decreases a factor of $1/e$ (to 37%). If the density gradient is approximately Gaussian, the scale height comprises 63% of the feature mass. Alternatively, one may define the *half-thickness* Δz of a planar distribution of matter as one half the ratio of the total surface density to the volume density at the mid-plane.

d Observations referred to objects sited in the proximities of the Solar System, within ~ 0.5 kpc, indicate that O- B-type stars have a typical half-height of $\mathcal{O}(100)$ pc, instead G-type stars, like our Sun, can be located even to 350 pc far from the galactic plane.

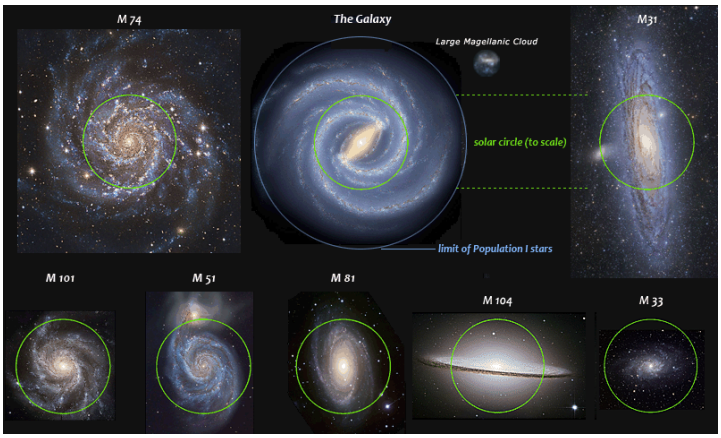

Figure 3.3: *Comparing the size of the Galaxy to other galaxies. Credit:* `http://www.handprint.com/ASTRO/galaxy.html`

Since the bulk of Galactic mass is found in *Dark Matter*, this acts as a frictionless gravitational medium. The primary consequence is that the Galaxy is an *encounter-less* medium with respect to stars, which are spaced about one parsec apart. Recent parallax[e] measurements of water or methane maser sources distant star forming regions with the Very Long Baseline Array[f] put the Sun at about 8.3 kpc from the Galactic barycentre, and at about 15 pc above the disc mid-plane. Using plate scales and best estimates of distance, we can project the radius of the Solar orbit onto other, familiar spiral galaxies (Figure 3.3). This illustrates the astonishing grandeur of both the Galaxy and the Andromeda system. We can compare the size of the Galaxy to other galaxies by projecting the solar radius of 8.3 kpc onto their image, given the current best estimates of their distance and their angular size as seen from Earth (Figure 3.3). This shows that the Galaxy exceeds or rivals the size of the commonly reproduced galaxies in the Messier catalogue, and is only slightly smaller than the Andromeda galaxy, our companion galaxy in the Local Group.[g] Although not the largest galaxy we know of, the Galaxy is one of the larger and more massive galaxies in the catalogue.

I conclude this section with a couple of final remarks about our Milky Way. The Galactic Centre is marked by an intense radio source named Sagittarius A* (SgrA*). The motion of material around the centre indicates that SgrA* harbours a massive, compact object. This concentration of mass is best explained as a super massive black hole with an estimated mass of $4.1 \div 4.5$ million times the solar mass (see e.g. Gillessen et al., 2009). Not so long time ago, in 2010, two gigantic spherical bubbles of high energy emission were detected to the north and the south of the Milky Way core, using data of the *Fermi*-LAT. The diameter of each of the bubbles is about 25,000 light-years

e Parallax in astronomy arises due to change in viewpoint occurring due to motion of the observer, of the observed, or of both. What is essential is relative motion. By observing parallax, measuring angles, and using geometry, one can determine distance. Assuming the angle is small, the distance to an object (measured in parsecs) is the reciprocal of the parallax (measured in arcseconds): $\mathrm{d(pc)} = 1/\mathrm{p(arcsec)}$.

f A group of large radio telescopes interconnected from Hawaii to the Virgin Islands with an angular resolution in the IR of less than one millionth of an arc second

g The Local Group is the group of galaxies that includes the Milky Way, among others (Karachentsev and Kashibadze, 2006). Its gravitational centre is located somewhere between the Milky Way and the Andromeda galaxies. The group is estimated to have a total mass of $1.29 \pm 0.14 \times 10^{12}$ $M_\odot$ and has a velocity dispersion of 61 ± 8 km/s (van den Bergh, 1999). The group itself is part of the Virgo Supercluster (i.e. the Local Supercluster. Tully, 1982).

(7.7 kpc). These observations are best interpreted as a magnetized outflow driven by star formation in the central 640 ly (200 pc) of the Galaxy (Carretti et al., 2013).

In the below diagram (3.11), I summarize the most important aspect of Galactic ecology, which is probably the cycle of matter from the ISM to stars and back to the Ism. In the first step of this cycle, new stars form out of a reservoir of interstellar material. This material, far from being uniformly spread throughout interstellar space, displays dramatic density and temperature contrasts, such that only the densest, coldest molecular regions can offer an environment favourable to star formation. In absence of magnetic support, those regions tend to become gravitationally unstable and collapse into new stars. Afterwards, the Galactic matter goes through a succession of thermonuclear reactions, which enrich it in heavy elements. A fraction of this material eventually returns to the Ism, either via powerful stellar winds, or upon supernova explosions. In both cases, the injection of stellar mass into the Ism is accompanied by a strong release of energy, generating turbulent motions in the Ism and maintaining heterogeneous the structure, closing thus the loop of self-induced Ism-star cycle (Draine, 2011; Ferrière, 2001). The table 3.1 summarizes the physical parameters of the distinct parts of the Galaxy.

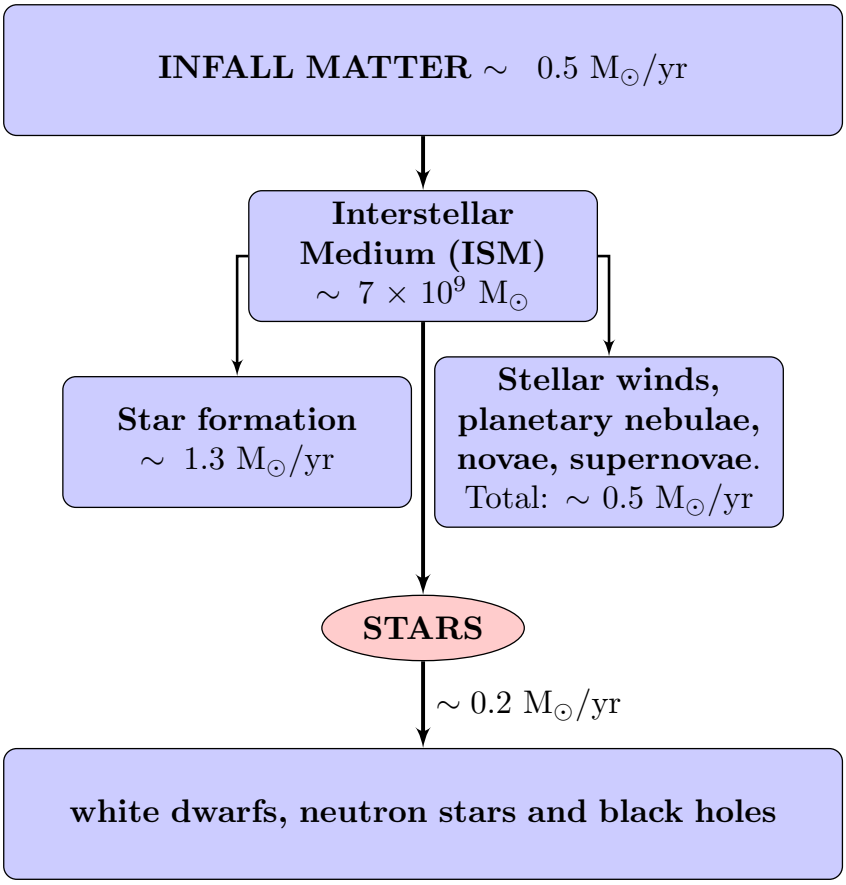

Figure 3.4: *Flow of baryons in the Milky Way. The* Ism *is responsible for forming the stars that are the dominant sources of energy. After Draine (2011).*

Table 3.1: *Summary of the main physical parameters of the distinct parts of the Galaxy (McMillan (2011) and reference therein).*

Feature	$\mathcal{H}$ [kpc]	Radius [kpc]	Z[a] [Fe/H]	$\sigma_U, \sigma_V, \sigma_W$ [km/s]	V_{lag} [km/s]	Age [Gyr]	Mass $[10^6 M_\odot]$	Density $[\rho/\rho_{tot}]$
Central bar	1	4.5	$-1.5/+0.3$	-	-	-	-	-
Thin disc	0.325	15	-0.3	$30, 20, 15$	15	$\leqslant 10$	10	$0.95 \div 0.98$
Thick disc	0.750	15	-0.6	$66, 55, 40$	40	$12 \div 15$	10	$0.02 \div 0.05$
Oblate halo	.	16.5	-1.6	$130, 100, 90$	270	~ 12	10	0.0002
Globular cluster halo	.	.	-1.6	.	.	.	.	.
Dark matter halo	.	85	.	.	.	~ 12.5	$1.9 \cdot 10^6$	.

[a] Metallicity is a measure of the proportion of higher elements to hydrogen: hydrogen is the primal cosmic element, while iron is the exclusive product of supernovae. A negative metallicity is a "metal poor" star, associated with increased stellar age.

3.2 THE ISM AND ITS TYPICAL PHASES

The space between the stars of the Milky Way is populated of diffuse matter and radiation fields, commonly referred to as the *Interstellar Medium* (ISM). To the current knowledge, the interstellar matter accounts for about $10 \div 15\%$ of the total mass of the galactic disc, and it is made mostly of *gas* and *dusts*, with an average mass-ratio of 100 : 1. Generally, the matter tends to concentrate on the galactic plane, and along the spiral arms, getting so a highly inhomogeneous distribution on small scales. Roughly half of the ISM mass is confined in discrete clouds, which occupy only a small fraction ($\sim 1 \div 2\%$) of the total interstellar volume. Conversely to the typical terrestrial values, the ISM is exceedingly tenuous: in the Solar System's neighbourhood, its density changes from $\sim 1.5 \times 10^{-26}$ g cm^{-3}, in the hot ambient, to $\sim 0.02 \div 2 \times 10^{-18}$ g cm^{-3} in the densest molecular regions, with an average value of about $\sim 2.7 \times 10^{-24}$ g cm^{-3} (Ferrière, 2001). The total mass of the Milky Way within 15 kpc of the centre is approximately $10^{11} M_\odot$; according to current estimates, this includes $\sim 5 \times 10^{10} M_\odot$ of stars, $\sim 5 \times 10^{10} M_\odot$ of Dark Matter, and $\sim 7 \times 10^{9} M_\odot$ of interstellar gas, mostly hydrogen and helium (Draine, 2011).

The gas distribution in the Galaxy accounts for three main components: (*i*) about 60% of the interstellar hydrogen is in the form of H atoms (H I), (*ii*) $\sim 20\%$ is in the form of H_2 molecules and (*iii*) $\sim 20\%$ is ionized (H II). Going further into the details, we may note that the baryons of the ISM of the Milky Way are found with a wide range of temperatures and densities; because the ISM is dynamic, all densities and temperatures within these ranges can be found somewhere in the Milky Way. However, it is observed that most of the baryons have temperatures falling close to various characteristic states, namely *phases*. As pointed out in Draine (2011), here we identify seven distinct phases that, between them, account for most of the mass and most of the volume of the ISM. These phases consist of the following:

CORONAL GAS : Gas that has been shock-heated to temperature $T \gtrsim 10^{5.5}$ K (McCammon and Sanders, 1990, York, 1974) by blast waves racing outward from supernova explosions and, to a lesser extent, by powerful star winds (McKee and Ostriker, 1977). The existence of a hot interstellar gas was suggested by the observations of broad ultraviolet (UV) absorption lines of ions formed only at high temperatures by the *Copernicus* satellite (Jenkins and Meloy, 1974), and a soft X-ray[h] background supposed to be the *free-free* emission from hot interstellar plasma (Williamson et al. 1974). The gas is collisionally ionized, with high-ions such as O VI ($\equiv O^{5+}$) and N V present.[i] Most of the coronal gas has low density, filling an appreciable fraction - approximately half - of the volume of the galactic disc. The coronal gas regions may have characteristic dimensions of ~ 20 pc, and may be connected to other coronal gas volumes. The coronal gas cools on $\sim$ Myr time scales. Observations by the X-ray satellite on the *Röntgen Satellite* (ROSAT) highlighted a significant contribution from the Local Bubble, plus an absorbed contribution from the Galactic halo and an absorbed isotropic contribution possibly of extragalactic origin (Snowden et al., 1998). Much of the volume above and below the disc is thought to be pervaded by the coronal gas. It is often referred to as the "hot ionized medium", or HIM.

h 0.25 keV.

i The high ionization potential of these ions makes them difficult to produce by photo ionization

Table 3.2: *Phases of Interstellar Medium. After Draine, 2011 (Chapter 1, §1.1)*

Phase	T(K)	$n_H(cm^{-3})$	Description
Coronal gas (HIM)	$\gtrsim 10^{5.5}$	~ 0.004	Shock-heated; Collisionally ionized; Either expanding or in pressure equilibrium; Cooling by: Adiabatic expansion X-ray emission; Observed by: UV and X-ray emission, Radio synchrotron emission
H II gas	10^4	$0.3 \div 10^4$	Heating by photoelectrons from H, He; Photo ionized; Either expanding or in pressure equilibrium; Cooling by: Optical line emission, Free-free emission, Fine-structure line emission; Observed by: Optical line emission, Thermal radio continuum
Warm H I (WNM)	$\sim 5 \times 10^3$	0.6	Heating by photoelectrons from dust; Ionization by starlight, CRs; Pressure equilibrium; Cooling by: Optical line emission, Fine-structure line emission; Observed by: HI 21-cm emission, absorption, Optical, UV absorption lines
Cool H I (CNM)	~ 100	30	Heating by photoelectrons from dust; Ionization by starlight, CRs; Cooling by: Fine structure line emission; Observed by: HI 21-cm emission, absorption; Optical, UV absorption lines
Diffuse H_2	~ 50	~ 100	Heating by photoelectrons from dust; Ionization by starlight, CRs; Cooling by: Fine structure line emission; Observed by: HI 21-cm emission, absorption; CO 2.6-mm emission, Optical, UV absorption lines
Dense H_2	$10 \div 50$	$10^3 \div 10^6$	Heating by photoelectrons from dust; Ionization and heating by CRs; Cooling by: CO line emission, CI fine structure line emission; Observed by: CO 2.6-mm emission, dust FIR emission
Cool stellar outflows	$50 \div 10^3$	$1 \div 10^6$	Observed by: Optical, UV absorption lines; Dust IR emission; HI, CO, OH radio emission

H II GAS : Gas where the hydrogen has been photo-ionized by UV photons from hot stars.[j] Most of this photo-ionized gas is maintained by radiation from recently formed hot massive O- and B-type stars. The photo-ionized gas may be dense material from a nearby cloud - in which case the ionized gas is called as H II *region* - or low density "inter cloud" medium - referred to as *diffuse* H II).

Bright H II regions, such as the *Orion Nebula*, have dimensions of a few pc; their lifetimes are essentially those of the ionizing stars, $[\sim 3 \div 10]$ Myr. The equilibrium temperature of such regions has a typical value of $\sim$ 8000 K (Osterbrock, 1989). The extended low-density photo-ionized regions - often referred to as the *warm ionized medium* or WIM - contain much more of the total mass than the more visually conspicuous high-density H II regions. According to current estimates, the Galaxy contains $\sim 1.1 \times 10^9$ $M_\odot$ of the ionized hydrogen; about 50% of this is within 500 pc of the disc mid-plane.

In addition to the H II regions, photo-ionized gas is also found in distinctive structures called planetary nebulae[k] - these are created when rapid mass loss during the late stages of the evolution of stars with the initial mass $[0.8 \div 6]$ $M_\odot$ exposes the hot stellar core; the radiation from this core photo-ionizes the out-flowing gas, creating a luminous (and often very beautiful) planetary nebula. Individual planetary nebulae fade away on $\sim 10^4$ yr time scales.

In H II regions, free electrons are accelerated in the field of ions (H^+, He^+, He^{++}), giving rise to radio or microwave continuum radiation through thermal *Bremsstrahlung*, known as *free-free emission*. Emission lines, seen at optical, infrared and radio wavelengths are primarily due to radiative recombination of hydrogen and helium ions with free electrons. In particular, the Hα Balmer line at 6563 Å arises from the transition between the electronic energy level $n = 3$ and $n = 2$. Since the rate per unit volume of recombinations into an excited hydrogen atom is proportional to $n_H n_e \propto n_e^2$, the integrated intensity of the Balmer line is proportional to the *emission measure*

$$EM = \int_0^L n_e^2 dL, \tag{3.1}$$

where dL is the length element along the line of sight through the H II regions.

The presence of warm ionized gas outside well-defined H II regions was first reported by Struve and Elvey (1938), who detected Hα and [O II] 3727Å lines from extended regions in *Cygnus* and *Cepheus*. Because of the obscuration by interstellar dust, Hα and other optical lines can probe only a limited region around the solar system ($\sim 2 \div 3$ kpc). A much better tracer of the warm ionized gas are the signals from *pulsars*. It is a well established result the fact that electromagnetic waves propagating through a plasma interact with the plasma particles, free electrons in this context so that, as a result, the velocity of propagation of the wave, namely the group velocity, differs from the speed of light in vacua: in particular, it decreases with increasing wavelength. The

j Strong UV radiation, above an energy of 13.6 eV.

k They are called planetary nebulae because of their visual resemblance to planets when viewed through a small telescope.

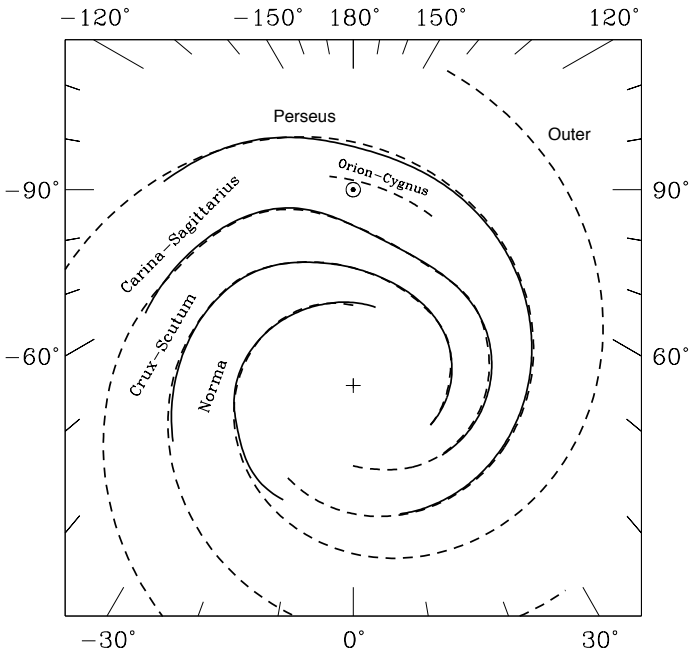

Figure 3.5: *The spiral patter of the Milky Way as estimated from pulsar DM, where spiral arms are assumed to coincide with regions of enhanced electron density n_e. Dashed line: pattern favored by Cordes and Lazio, 2003. Solid line: pattern obtained by Taylor & Cordes (1993). Credit: Cordes and Lazio (2003)*

periodic radio pulses emitted by pulsars show a spread in arrival time[l] between low-energy and high-energy emission, which is directly proportional to the column density of free electrons between the source and the observer, i.e. the *dispersion measure* (DM)

$$DM = \int_0^L n_e \, dL. \tag{3.2}$$

This method has been used to determine the dispersion to many hundreds of pulsars, deriving a three-dimensional model for the enhanced electron density in a four-arm logarithmic spiral pattern. The large-scale structure of ionized gas derived from pulsar DM (Cordes and Lazio, 2003) shows a thin-disc component arising from localized H II regions (roughly consistent with the stellar disc), plus a thick disc associated with the diffuse WIM, with a height > 1 kpc (the Reynolds layer). The spiral arm pattern is visible in the distribution of H II regions (see Figure 3.5).

WARM HI : Predominantly atomic gas heated to temperatures $T \approx 10^{3.7}$ K; in the local ISM, this gas is found at densities $n_H \approx 0.6$ cm^{-3}. It fills a significant fraction of the volume of the disc - perhaps 40%. Often referred to as the *warm neutral medium*, or WIM. Neutral atomic hydrogen present in the Galaxy is not directly observable at optical wavelengths. Indeed, for the typical conditions of the ISM, the collisions are so infrequent to leave the H I to the fundamental state $n = 1$. The possible lines - corresponding to the electronic transitions between the ground

[l] The time of arrival of energy at frequency $\nu = \omega/2\pi$ is $t_{arrival} = L/c + 4.146 \times 10^{-3} (\nu/\text{GHz})^{-2} (\text{DM}/\text{cm}^{-3}\text{pc})$s. From Draine (2011).

state and excited states - lie in the UV, with the Lyman α line (Lα, from $n = 2$ to $n = 1$) at a wavelength of 1216Å, for the which the Earth's atmosphere turns out to be opaque. The H I can be surveyed, in emission or absorption, using the 21-cm radio line (1420 MHz) - due to the hyperfine structure of the hydrogen - by measuring absorption lines in the spectra of stars, and by observing infra-red emission from dust that is mixed with the H I. If a background radio source is available, observations of the 21-cm line in absorption can be used to determine the H I spin temperature T_{spin}, which is normally close to the kinetic temperature. The spin temperature is a function of the position, and therefore the radial velocity of the gas. Differential rotation of gas in the Galactic disc means that - except for the directions $l = 0°$or $l = 180°$- regions at different distances from the Sun will have different radial velocities (see, e.g., Binney and Merrifield, 1998). Therefore, for an assumed Galactic rotation curve, the measured 21-cm intensity vs. radial velocity can be used to map out the 3-dimensional distribution of H I in the Galaxy. Radially, the H I gas extends to > 60 kpc from the Galactic centre. It lies in a roughly flat layer with a characteristic height of 230 pc. The thickness of the H I layer drops to $\lesssim 100$ pc within 3.5 kpc from the Galactic centre, and it expands to almost 3 kpc in the outer Galaxy. This flaring, plausibly due to the steep decrease in the vertical gravitational field, is accompanied by a warping, such as in the first ($0° < l < 90°$) and second ($90° < l < 180°$) Galactic quadrants the mid plane of the H I disk is above the Galactic plane, with a maximum displacement of 4 kpc, and below the Galactic plane in the third ($-180° < l < -90°$) and fourth ($-90° < l < 0°$) quadrant, with a maximum displacement of 1.5 kpc (Kalberla and Dedes, 2008).

COOL HI GAS : Mostly atomic gas at temperatures $T \approx 10^2$ K, with densities $n_H \approx 30$ cm^{-3} filling 1% of the volume of the local ISM. Often referred to as the *cold neutral medium*, or CNM.

DIFFUSE MOLECULAR GAS : Similar to the cool H I clouds, but with sufficiently large densities and column densities so that H_2 self-shielding[m] allows H_2 molecules to be abundant in the cloud interior.

DENSE MOLECULAR GAS : In the Milky Way, about 22% of the interstellar gas is in molecular clouds, where the bulk of the hydrogen is in H_2 molecules. Gravitationally bound clouds that have achieved $n_H \gtrsim 10^3$ cm^{-3}, they are sometimes called stellar nurseries since that star formation process takes place exclusively in these molecular clouds. It should be noted that the gas pressures in these "dense" clouds would qualify as ultra-high vacuum in terrestrial laboratories.

In these clouds, the dust grains are often coated with mantles composed of H_2O and other molecular ices. Interstellar molecules (CH, CH^+, and CN) were discovered in the late 1930s through their optical absorption lines. In the 1970s, UV observations revealed the most abundant interstellar molecule, H_2 (Carruthers, 1970), and the next most abundant molecule, CO (Smith and Stecher, 1971). However, given a visual extinction $A_V \gtrsim 3$ mag through their central regions, these clouds turn out to be often *dark*. Indeed, observations of optical

m Self-shielding refers to the phenomenon where the photo-excitation transitions become optically thick, so that the molecule in question is shielded from starlight by other molecules. Draine (2011).

and UV absorption lines do not allow astronomers to probe the interior of dense clouds, because bright sources beyond them are obscured by the interstellar dust. When two free H atoms, both in the ground electronic state, approach one another, by symmetry there is no electric dipole moment. As a consequence, there is no electric dipole radiation: therefore, the H_2 molecule cannot be directly observed, even in the radio band, since the absence of a permanent dipole moment, so that the low-energy excited levels correspond to quadrupole transitions, with small probabilities and relatively high excitation energies that these reactions can be ignored in astrochemistry. Therefore, we are pushed to resort to the observations of the so-called "tracer" species, namely other molecules of which it is possible to observe electromagnetic transitions, and the presence of which is correlated to that of the H_2.

A primarily used molecule is the carbon monoxide, ^{12}CO, which is observed in its $J = 1 \mapsto 0$ transition at a wavelength of 2.6 mm, that is in the microwave range. In the limit of high densities the CO-line emission is dominated by collisional excitation and de-excitation. Early surveys (Scoville and Solomon, 1975; Burton et al., 1975) showed that most of the molecular gas is located in a ring at 4 kpc from the Galactic centre, and they unveiled a strong molecular concentration in the inner region of the Galaxy, within 0.4 kpc. The first large-scale survey by Dame et al. (1987) brought to light the spiral arm pattern of CO emission. Beyond the solar circle, CO emission drops off rapidly. In the vertical direction CO emission has a characteristic height scale of 90 pc. As said, the CO $J = 1 \mapsto 0$ transition is used as a tracer of molecular cloud mass, and the CO luminosity $L_C = d^2 \int W_{CO} d\Omega$, is proportional to the virial mass of the cloud, where W_{CO} is the antenna temperature integrated over the $J = 1 \mapsto 0$ line,

$$W_{CO} \equiv \int T_A (1 \mapsto 0) \equiv \left(\frac{\lambda^3}{2k}\right) \int I_\nu d\nu, \tag{3.3}$$

and d the distance to the cloud. For a self-gravitating cloud, we then can relate the velocity integrated temperature W_{CO} to the total H_2 column density (averaged over the beam solid angle), by a conversion factor defined as

$$X_{CO} \equiv \frac{N(H_2)}{W_{CO}}. \tag{3.4}$$

A new large scale CO surveys of the entire Milky Way was performed by Dame, Hartmann, et al. (2001): high-resolution observations indicated that the molecular gas is contained in discrete clouds organized hierarchically from giant complexes (size of a few tens of pc and mass up to 106 $M_\odot$) down to small cores (size of a few pc and mass up to 103 $M_\odot$). An approximate power-law relation holds between cloud velocity dispersion and size (Larson, 1981). Recent observational determinations of X_{CO} find a value of

$$X_{CO} = (1.8 \pm 0.3) \times 10^{20} \quad \frac{H_2 \text{ cm}^{-2}}{(\text{K km s}^{-1})}. \tag{3.5}$$

The theoretical value for X_{CO} factor is explicitly sensitive to the values adopted for the cloud density n_{H_2} and the CO excitation temperature T_{exc}: the above value suggests that $n_{H_2} \approx 10^3$ cm^{-3} and $T_{exc} = 8$ K

may be representative of self-gravitating molecular clouds in the local ISM. It would, therefore, not be at all surprising if the value of X_{CO} in other galaxies were to differ appreciably form the value fond for the Milky Way, or if the value of X_{CO} showed cloud-to-cloud or regional variations within the Milky Way.

The dominant process for H_2 molecules formation in the Milky Way, and other galaxies as well, is via *grain catalysis*, namely a recombination of hydrogen atoms on the surface of dust grains, a process first discussed by Gould and Salpeter 2001, Hollenbach and Salpeter, 1971 (Draine, 2011). They can survive in vast numbers only in the interior of *dark* and *translucent* clouds, where they self-shield from photodissociation by external UV photons, and cold enough to avoid collisional dissociation. The thermal state of molecular clouds results from the balance between heating by CRs and cooling by molecular line emission.

STELLAR OUTFLOW : Evolved cool stars can have mass loss rates as high as $10^{-4} M_\odot$ yr^{-1} and low outflow velocities $\lesssim 30$ km s^{-1}, leading to relatively high density outflows. Hot stars can have winds that are much faster, although far less dense.

For many other details on the chemistry of the Galaxy, and the several physical process occurring in the complex structure of the Milky Way, the reader is referred to e.g., Draine (2011).

3.3 COSMIC RAYS: THE STANDARD PICTURE

The discovery of cosmic rays is a milestone in science, and the studies of those now span an epoch of almost exactly 100 years!

After dedicated studies by Faraday around 1835, Crookes observed in 1879 that the speed of discharge of an electroscope decreased when pressure was reduced. Following the uncovering of spontaneous radioactivity by Henri Becquerel in 1896, it was generally believed that only radiation from radioactive elements in the ground, or the radioactive gases or isotopes of radon they produce, were responsible of causing the atmospheric electricity or, in other words, the *ionization of the air*. At the close of the nineteenth century, scientists using gold-leaf electroscopes to study the conductivity of gases discovered that no matter how carefully they isolated their electroscopes from possible sources of radiation they still discharged at a slow rate.

The explanation of such a phenomenon came in the beginning of the 20^{th} century and paved the way to one of mankind's revolutionary scientific discoveries: Cosmic Rays.

3.3.1 The Early Years

In 1901, two research groups investigated the aforementioned phenomenon, J. Elster and H. Geitel in Germany, and C.T.R. Wilson in England. Both groups concluded that some unknown source of ionizing radiation existed. Wilson even suggested that the ionization might be «*due to radiation from sources outside our atmosphere, possibly radiation like Roentgen rays or like cathode rays, but of enormously greater penetrating power*». A year later two groups in

Canada, Ernst Rutherford and H. Lester Cooke at McGill University, and J. C. McLennan and E.F. Burton, at the University of Toronto showed that 5 cm of lead reduced this mysterious radiation by 30%. An additional 5 tonnes of pig lead failed to reduce the radiation further.

In 1907 Father Theodore Wulf of the Institute of Physics of Ignatus College in Valkenburg, Holland, invented a new electroscope. Wulf's electroscope enabled scientists to carry the search for the origin of the mysterious radiation out of the laboratory, into the mountains, atop the Eiffel Tower and, ultimately, aloft in balloons. Assuming that the radiation came from the Earth, they expected to find a rapid decrease in the radiation as they moved away from the surface. They did not find the decrease they expected and in some cases there seemed to be evidence that the radiation actually increased.

Intrigued by the conflicting results obtained by Wulf and his colleagues a young Austrian nuclear physicist, Viktor Hess, obtained support from the Austrian Imperial Academy of Sciences and the Royal Austrian Aero Club to conduct a series of balloon flights to study the radiation. Hess got a license to pilot balloons in order to reduce the size of the crew and thereby increase the altitude to which he could carry his electroscopes. On 12 August 1912, using the hydrogen-filled Böhmen, Hess reached an altitude of 5,350 m. Carrying two hermetically sealed ion chambers, he found that the ionization rate initially decreased, but that at about 1500 m it began to rise, until at 5,000 m it was over twice the surface rate. Hess concluded that the results of these observations can best be explained by the assumption that radiation of a very high penetrating power from above enters into the atmosphere and partially causes, even at the lower atmospheric layers, ionization in the enclosed instruments.†

On a voyage from Amsterdam to Java, Clay observed in 1927 a variation in cosmic ray intensity with latitude with a lower intensity near the equator, thus establishing that before entering the Earth's magnetic field, the bulk of the primary CRs were charged particles. In 1930 Bruno Rossi showed that if the CRs were predominantly of one charge or the other there should be an east-west effect. In the spring of 1933 two American groups, Thomas H. Johnson of the Bartol Research Foundation and Luis Alvarez and Arthur H. Compton of the University of Chicago, simultaneously and independently measured the *east-west effect*. It showed the cosmic radiation to be predominantly charged. In a series of balloon flights in the late 1930s, M. Schein and his co-workers used *Geiger* counter telescopes interspersed with lead absorbers to determine that most of the primary particles were not electrons, and hence protons were most plausibly the dominant constituent.

† The discovery of cosmic rays is, usually, attributed to the Austrian physicist Victor Hess, who in 1936 won the *Nobel Prize for Physics* for his own studies on this type of particles. Actually it came to their discovery, and the explanation of their origin through the studies, contemporary and complementary to one another, carried out by both the Italian physicist Domenico Leone Pacini and Hess. The first by means of experiments carried out between 1906 and 1911, and described in a memoir published in *Nuovo Cimento* in 1912; the Austrian by means of experiments carried out between 1911 and 1912 and also published in 1912. Pacini could exclude the origin of terrestrial radiation by recording them in the marine waters in front of Livorno and in those ones of the Bracciano's lake; Hess by recording the increase of the intensity by means of a flight-balloon. Below it follows an excerpt (translated from the Italian) of what Pacini himself wrote about his own studies on cosmic radiation: «*Observations from the sea in 1910 led me to conclude that a significant proportion of penetrating radiation that is found in the air originated from independent direct action of the active substances in the upper layers of the Earth's crust.*» Taken from: The penetrating radiation from the surface and within the water, Il Nuovo Cimento Series VI , Volume 3: 93-100 (1912).

In 1948, research groups from the University of Minnesota and the University of Rochester flew nuclear emulsions and cloud chambers on the same high-altitude Skyhook balloon flight and discovered the presence of heavy nuclei in the primary cosmic radiation. Further studies by many other groups soon established that essentially all of the elements between H and Fe were present in the cosmic radiation near the top of the atmosphere, including an over abundance of the light elements Li, Be, and B. Then in 1950 it was found that a significant fraction of the cosmic radio emission was synchrotron radiation, being evidence of the presence of highly relativistic electrons throughout our Galaxy including some discrete sources as well as extragalactic sources. However, because of their small abundance (1% of the intensity of cosmic ray nuclei) electrons were not directly detected in the primary cosmic radiation until 1962. These discoveries made it possible to begin constructing realistic models of the origin and interstellar transport of galactic cosmic rays.

As early as 1934, Baade and Zwicky linked the appearance of supernovae with neutron star formation and cosmic ray generation. Fermi in 1949 regarded cosmic rays as a gas of relativistic charged particles moving in interstellar magnetic fields (Fermi, 1949). His paper laid the groundwork for the modern theory of cosmic ray acceleration and transport. The close link between radio astronomy and cosmic rays was conclusively established at the time of the Paris Symposium on Radioastronomy in 1958. This marked the birth of *Cosmic Ray Astrophysics*. The basic model of the origin of galactic cosmic rays was developed by Ginzburg and Syrovatskii (1964).

3.3.2 Cosmic Rays: Energy Spectrum and Composition

The ISM is, as seen before, pervaded by CRs, a population of very energetic nuclei and electrons of extraterrestrial origin. Most of the energy density in CRs comes from trans-relativistic particles with kinetic energies per nucleon $E \approx \mathcal{O}(1)$ GeV. However, since their discovery up to the present days, we have seen the cosmic ray energy spectrum to extend to extraordinarily high energies, between 10^9 and $> 10^{20}$ eV.

The flux of CRs with energy less than 10^{14} eV is intense enough to have made possible the study of each nucleus, through detectors mounted on balloons and satellites: from such *direct* experiments, we have collected considerable details about the energy spectrum and the relative abundances of a great variety of atomic nuclei, protons, electrons, positrons, and also about the intensity, the energy, and the spatial distributions of X- and γ-rays. Beyond 10^{14} eV, the flux gets so low that only ground based experiments - due to their large field of view (FOV) and long exposure time - could gather a relevant, statistically significant number of events. These experiments take advantage of the atmosphere acting like an enormous calorimeter: the impacting cosmic radiation interacts with the molecules and the atoms of the atmosphere itself, and produces *Extensive Air Showers* (EASS) which spread

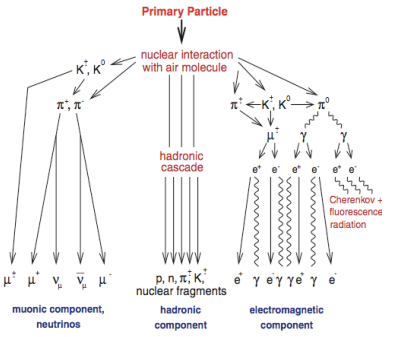

Figure 3.6: *Sketch of an Extensive air Shower. From Haungs et al. (2003)*

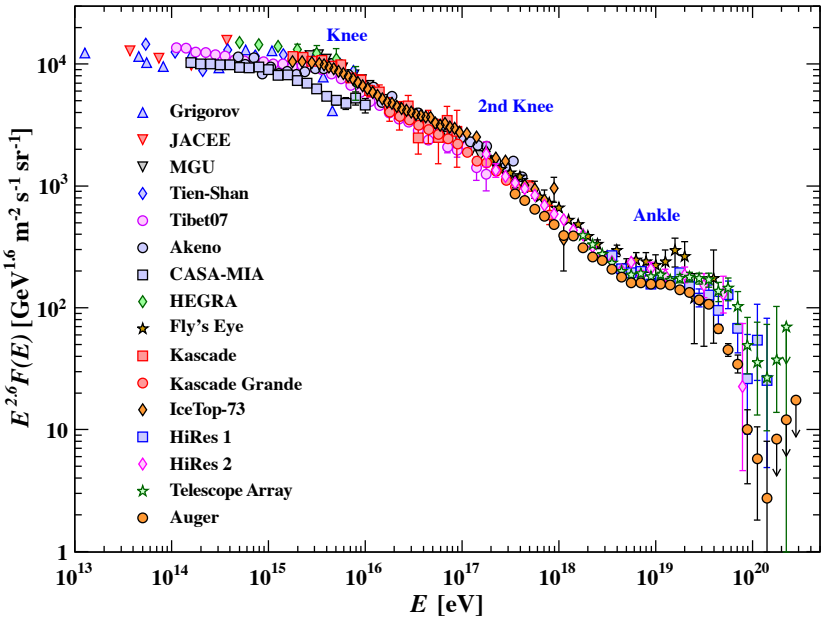

Figure 3.7: *Summary of the measurements of the high energy cosmic ray spectrum. Credit:* http://pdg.lbl.gov/2013/reviews/rpp2013-rev-cosmic-rays.pdf. *See also reference therein contained. Revised October 2013 by J.J. Beatty (Ohio State Univ.), J. Matthews (Louisiana State Univ.), and S.P. Wakely (Univ. of Chicago).*

over a wide area. It was 1938 when Pierre Auger, looking at the extensions of the EAss detected at that time, concluded that the energy spectrum of CRs could extend up to 10^{15} eV, and possibly further than that. Currently, the advances in the field of the experimental techniques have made possible to see extraordinarily low fluxes (order of 1 event km^{-2} yr^{-1}), with energy of the primaries of $\mathcal{O}(10^{20})$ eV.

The most remarkable feature of CRs is their energy spectrum. At energies below a few GeV the influence of *solar modulation* becomes important with significant temporal variations at 1 AU related to the 11- and 22-year solar and helio-magnetic cycles. Between 10^9 eV and 10^{20} eV, over some 10 orders of magnitude, the observed particle flux Φ_{CR} is well-described by a relatively featureless power law distribution, $d\Phi_{cr}/dE \propto E^{-2.65}$. There is a slight steepening at $E \approx 10^{6.5}$ GeV, referred to as the *knee*, with the $d\Phi_{cr}/dE$ changing from $\sim E^{-2.65}$ to $\sim E^{-3}$.

In spite of the bulk of the primary radiation is, as known, of galactic origin, the extended spectrum up to ultra-high energies (above 10^{20} eV) suggests that some of CRs could be of extragalactic origin, since that the galactic magnetic field could not trap such particles within our galaxy. Indeed, there appear to also be further changes in slope at higher energies, at almost 4×10^{18} eV, the so-called *ankle*, most likely indicative of extragalactic sources (see e.g., Ave et al., 2008; Draine, 2011; T. Gaisser and Stanev, 2006; Hillas, 2006; Hoerandel, 2012; Stanev, 2004 and reference therein contained).

To summarize, with reference to the Figure 3.7, the differential spectrum of CRs, above a few GeV, can be so partitioned

$$N(E)dE = \text{const.} \times E^{-2.65}dE \qquad E < E_{knee} = 10^{16} \text{ eV}. \tag{3.6}$$

Exceeding the *knee*, the spectrum gets steeper, with an index close approximately to -3.0,

$$N(E)dE = \text{const.} \times E^{-3.0} dE \qquad E_{\text{ankle}} > E > E_{\text{knee}}, \tag{3.7}$$

before to become again "harder" beyond the *ankle*, at $E_{\text{ankle}} \approx 4 \times 10^{18}$ eV,

$$N(E)dE = \text{const.} \times E^{-2.69} dE \qquad E_{\text{GZK}} > E > E_{\text{ankle}}. \tag{3.8}$$

At energies of $10^{12} \div 10^{14}$ eV there are small anisotropies of $\approx 0.1\%$, which are thought to be due to local effects. At this time there are no meaningful anisotropies observed at higher energies except the ultra-high energies $\sim 10^{18}$ eV. Above $E_{\text{GZK}} = 4 \times 10^{19}$ eV, even if the detections are quite challenging in this range of energies[‡], thanks to EASS experiments, like for example the AUGER experiment sited in Argentina, and the HIRES detector ('Fly's Eye') in Utah, it seems that the CRs spectrum turns out to be strongly suppressed, presumably due to the Greisen-Zatsepin-Kuzmjn effect (the GZK *cut-off*), related to the photo-production of pions, $p + \gamma_{\text{CMB}} \rightarrow N + \pi$ in collisions with photons of the cosmic radiation background (Greisen, 1966; Zatsepin and Kuz'min, 1966). In the corresponding energy interval, the spectrum is parametrized as

$$N(E)dE = \text{const.} \times E^{-4.2} dE \qquad E > E_{\text{GZK}} = 4 \times 10^{19} \text{eV}. \tag{3.9}$$

A simple argument we may use to figure out the transition from galactic CRs to extra-galactic ones is based on the concept of *Larmor* radius for such particles in the interval of energy around 10^{18} eV. By definition, the *Larmor* radius identifies the orbit a charged particle would make in an uniform magnetic field, and it is given by (Rybicki and Lightman, 1979)

$$r_L = \frac{m\gamma v}{Z|e|B} \approx \left(\frac{1}{Z|e|c}\right)\left(\frac{E}{1\ \text{eV}}\right)\left(\frac{\mu G}{B}\right) \text{kpc}, \tag{3.10}$$

$Z|e|$ being the charge of the particle, and B the galactic magnetic field. For make the things as simple as possible, for the moment we neglect effects of diffusion of CRs within the Galaxy (see §§ 2 & 4). From Eq. (3.10), it follows that CRs of energies $> 10^{18}$ eV could not be confined inside the galactic magnetic field. Comprehensive reviews on the origins and transport of ultra-high energy CRs could be found e.g. in Blasi (2013b); Torres and Anchordoqui (2004)

Concerning the cosmic ray composition, it can be directly measured in the low energy region ($< 10^{13}$ eV), since that the flux is high enough to make spectroscopy on satellites and balloons. At higher energies, only indirect measurements of composition are possible, through the analysis of the profile and of the content of the particles in the shower generated by the pass of a cosmic ray in the atmosphere.

Cosmic ray *primary* particles consist mainly of protons (86%), α-particles (11%), heavier nuclei up to uranium (1%), with diminishing amounts. All are fully ionized. Electrons account for approximately 2% of the CRs. In addition to the primary species, which come directly from the astrophysical sources, there is also a small amount of positrons and anti-protons, believed of *secondary* origin and created by the interactions of the primary particles with the interstellar gas, and partly with the thermal plasma inside the accelerators. The percentages above mentioned refer to particles with a given

‡ The HI-RES group reported only 7 events above 10^{20} eV. (Jui, 2000, see also the Figure 3.8)

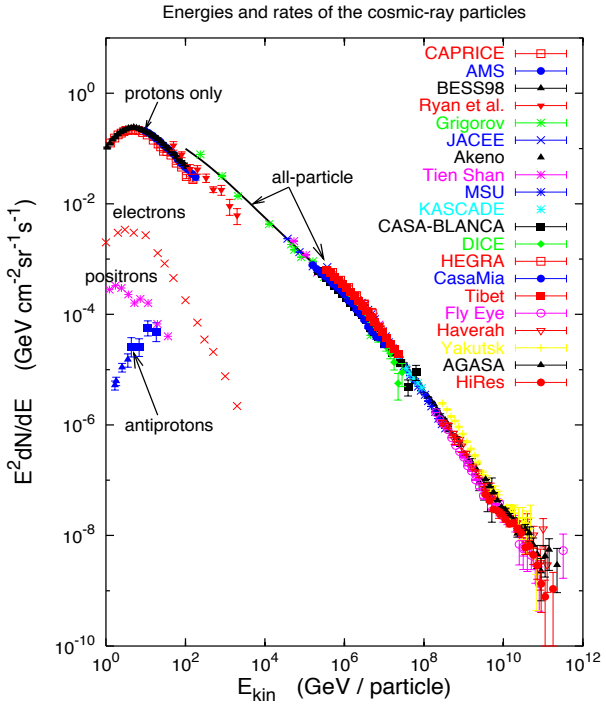

Figure 3.8: *All-particle spectrum of the* CRs *over and very broad range of energy. (Hillas, 2006 and references therein contained).*

magnetic rigidity, $\mathcal{R} \equiv cp/Z|e|$, p being the momentum and $Z|e|$ the particle charge; in other words, particles having the same probability of penetrating the atmosphere across the geomagnetic field. Detected neutral particles consist of γ-rays, neutrinos and anti-neutrinos. Some of them can be identified as they are coming from point-like sources in the sky; e.g., neutrinos coming from the Sun and from Supernovae, and γ-rays from sources like the *Crab Nebula* and active galactic nuclei (AGNs).

The energy density in CRs, if referred to the conditions of the ISM not affected by the magnetic field inside the Solar System, is almost 1 eV cm^{-3}, perfectly comparable then to the energy density of stellar light of 0.6 eVcm^{-3}, of the background cosmic radiation 0.26 eV cm^{-3}, and of the galactic magnetic field of 3μG, or 0.25 eV cm^{-3}.

With a few exceptions, the chemical composition of the hadron CRs exhibits significant similarities to the elemental abundances in our Solar System, the latter ones being derived from the absorption lines in the solar photosphere and from the meteorites; however there are some non negligible differences, as it is possible to appreciate in the Figure 3.9. Both the cosmic abundances and solar ones show the even-odd effects, associated with the fact that nuclei with even atomic number Z, and mass number A, are tightly bound with respect to those with either A odd or Z odd, or both; the first type of nuclei represent then the most frequent products of the thermonuclear reactions in the interiors of stars. The peaks in the normalized abundances for C, N and O, as well as for the Fe are pretty much the same, and this suggests that most of the nucleonic CRs must be of stellar origins, and thus all (heavy) nuclear species have a composition similar to the abundance distribution at their sources.

The main exceptions between the cosmic abundances and the solar ones regard whereas H and He, which are under abundant, and the light ele-

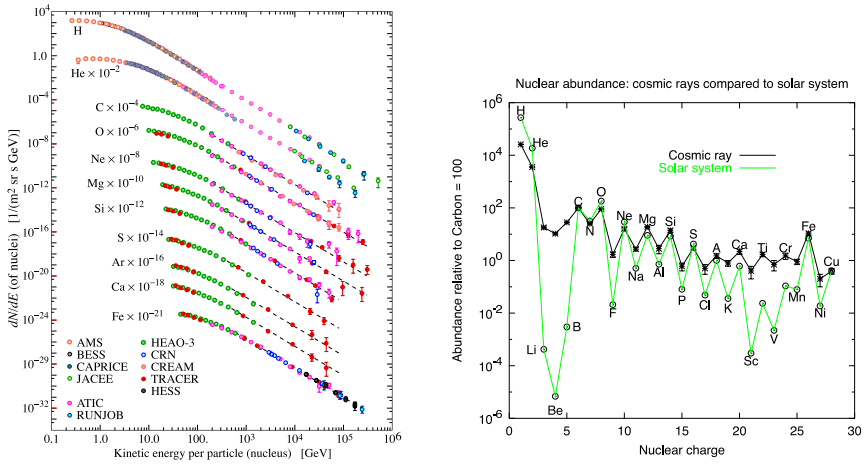

(a) Primary fluxes

(b) Elemental Composition

Figure 3.9: *Panel (**a**): Fluxes of nuclei of the primary cosmic radiation in particles per energy-per-nucleus are plotted vs energy-per-nucleus. Credit:* `http://pdg.lbl.gov/2013/reviews/rpp2013-rev-cosmic-rays.pdf`. *See also reference therein contained. Panel (**b**): typical nuclear abundances of* CRs *compared with the ones own of the Solar System. The composition is normalized to Si. T. Gaisser and Stanev, 2006 and references therein contained.*

ments Li, Be e B ($Z = 3, 4, 5$), which are over abundant, in CRs. The latter elements, since their low Coulomb's barrier, are weekly bound and rapidly burned in the nuclear reactions occurring in the interiors of the stars. Instead, it is inferred that the relative abundances of these nuclei in CRs are due to the *spallation* of the Carbon and Oxygen nuclei with the interstellar hydrogen. The amount of such light elements sets the average thickness of the interstellar material crossed by the cosmic radiation or, in other words, the typical amount of mass passed through, the column density, which must be not less than 3 g/cm^2. Moreover, it determines the mean lifetime of CRs, in the galactic disc, that is pretty much equal to 3 millions of years. Regarding this latter issue, the true lifetime of the cosmic rays observed on Earth, i.e. the interval of time between the initial acceleration of the CRs and the time when they hit the earth's upper atmosphere, can be longer than the spallation estimate, because a cosmic ray after birth may leave the disc and reside in the much lower gas density halo for some time, where it would suffer very little spallation. It could return to the disc and strike the Earth. This true lifetime has been determined by the radioactive decay of the isotropic ^{10}Be (M. Shapiro and Silberberg, 1970). Its true lifetime is found to be about 20 million of years.

Thus, CRs really have "two lifetimes", 3 million years in the disc and 20 million years in the Galaxy. Because the cosmic ray lifetime is so much shorter than the age of the Galaxy it must be the case that the CRs are constantly being produced in the Galaxy perhaps by supernovae, rather than outside in the intergalactic space. Also, it is important to note that all the CRs that we see have been accelerated (or created) in recent times, a time much shorter than the age of the Universe. It is found that the energy spectrum of Li, Be and B are a bit steeper than Carbon and Oxygen ones, suggesting that at higher energies the nuclei suffer of many processes of fragmentation, presumably because those nuclei escape out of the Galaxy

more rapidly than ones at lower energies. At the same way, the abundances of Sc, Ti, V e Mn in CRs are due to the *spallation* of the Fe and Ni nuclei.

3.3.3 Cosmic Rays: Energy and Pressure

Nowadays, among the Astroparticle community it is widely accepted the idea of supernova remnants (SNRs) as the most plausible *loci* for the production and acceleration of galactic cosmic rays we detect on Earth. With no doubts, the main argument in support of a such picture is a phenomenological one, and it has been recognized since the beginning when the cosmic ray issue has raised the interest of the astronomers and physicists (Baade and Zwicky, 1934; Ginzburg and Syrovatskii, 1964).

Indeed, it has been estimated that only a small percentage of the kinetic energy, released by the SNe explosions in our Galaxy, would be enough to provide the required power for giving life to the galactic population of CRs. Naturally, that is a strong argument, but not exclusive, since that other potential source populations like as *pulsars*, extremely powerful winds from young hot O/B stars, *microquasars*, and *gamma-ray bursts* (see e.g., Gaisser, 2001; Ginzburg, 1975; Hillas, 1984) can fulfil, at least formally, a such energetic requirement. The acceleration mechanisms at the sources, and the following propagation in galactic magnetic fields, combine to bring about the so-called *sea* of Galactic Cosmic Rays (GCRs), density of which is, inside the galactic disc, determined by the activity of the sources there present, over a relatively long time, comparable with the cosmic ray escape time, that is order of $\tau_{esc} \sim 10^7$ yr.

As a simple and instructive exercise, we now estimate the average energy density of CRs contained in the galactic disc, when assuming the sea level of GCRs not so far from the fluxes of particles locally measured. As discussed in the previous sections, nucleons and leptons present in CRs are distributed over an extended interval of kinetic energy, with a typical power-law spectrum. Then, it is possible to integrate over all the involved energies, adding the single contribution of each cosmic species i, to obtain the values of the total energy density

$$w_{CR} = \sum_i \int_0^\infty E_k N_i(E_k) dE_k, \tag{3.11}$$

and pressure

$$P_{CR} = \frac{1}{3} \times \sum_i \int_0^\infty E_k v N_i(E_k) dE_k, \tag{3.12}$$

of the CRs, hadrons and electrons, in the local galactic ambient. Here, $N_i(E_k)$, in Eqs. (3.11) and (3.12), indicates the particle spectral density, i.e. dN_i/dE_k, per unit of volume and in the interval of kinetic energy dE_k.

Given that the solar modulation exercises influence on the particles at energies especially below ~ 1 GeV/nuc, we estimate the energy density and the pressure of CRs limiting ourselves just to data observed for $E_k \gtrsim 1$ GeV/nuc. In particular, for what concerns the nucleonic component, it is sufficient to consider the local interstellar spectrum (LIS) of the primary protons, these latter being the dominant component of CRs, as it is possible to appreciate in Figure 3.8. The BESS experiment (Sanuki et al., 2000), during a balloon flight in 1998, has reported the following measurement

$$I_p^{\odot}(E_k) = 1.6 \times 10^4 \left(\frac{E_k}{1\ \text{GeV}} \right)^{-2.73} \quad \text{m}^{-2}\text{s}^{-1}\text{sr}^{-1}\text{GeV}^{-1}, \tag{3.13}$$

about the flux of the protons, where $I_p^{\odot}(E_k)$ is the local spectral intensity of the protons which, in the case the isotropy hypothesis still holds, is connected to the spectral density $N_p^{\odot}$ trough the simple relationship

$$N_p^{\odot}(E_k) = \frac{4\pi}{v} I_p^{\odot}(E_k), \tag{3.14}$$

v being the velocity of the protons (generally relativistic, $v \simeq c$). The Eq. (3.11), referred to only protons observed by Bess experiment, becomes then

$$\begin{aligned} w_p &= \int_0^{\infty} E_k N_p^{\odot}(E_k) dE_k \sim 4\pi \times \int_{1\ GeV/nuc}^{\infty} \frac{E_k I_p^{\odot}(E_k)}{v} dE_k \\ &\simeq \frac{4\pi}{c} \times \int_{1\ GeV/nuc}^{\infty} E_k I_p^{\odot}(E_k) dE_k \sim 0.9\ eV cm^{-3} \sim 10^{-12}\ erg\ cm^{-3}. \end{aligned} \tag{3.15}$$

The simple estimate inferred in this paragraph is in good agreement with what generally reported in literature, about the energy density of hadron classes of Crs, $w_N \simeq 0.5$ eV cm $^{-3} \approx 10^{-12}$ erg cm $^{-3}$ (Berezinskii et al., 1984; Schlickeiser, 2002). Analogously, we may repeat the same computation for the pressure, getting $P_N \simeq 3 \times 10^{-13}$ dyne cm^{-3}. For what concerns the electrons, the experimental evidences show that the intensity of those latter is $\sim 1\%$ of that of the protons, for energies $E_k \sim 1 \div 3$ GeV; it follows that the energy density of the lepton component is $w_e \approx 10^{-2} w_N \approx 10^{-14}$ erg cm $^{-3}$ (see also the Figure 3.8).

Although the value for the energy density written in Eq. (3.15) is intended as representative of the conditions of the local environment in the interstellar medium, in any event it is instructive to refer to it even to estimate the total luminosity of Crs, L_{CR}. In a model assuming the disc as homogeneous, the power required to accelerate Crs within our Galaxy is given by

$$L_{CR} = \frac{w_{CR} V_{disc}}{\tau_{esc}} = 3 \times 10^{40} \qquad erg\ s^{-1}, \tag{3.16}$$

where $V_{disc} = \pi(15\ kpc)^2(500\ pc) \sim 10^{67}$ cm ^{3} is the volume of the disc, of radius ~ 15 kpc ed height ~ 500 pc, inside of which Crs are effectively confined, and $\tau_{esc} \sim 10^7$ yr is the mean time spent by a ~ 1 GeV/nuc cosmic ray in the Galaxy; I remind that a such value has been estimated from the relative abundances of radioactive nuclei (e.g., the unstable isotope ^{10}Be) measured at energies $E_k \sim 1$ GeV/nuc (Gaisser, 2001).

The cosmogony of the heavy nuclei present in Crs has established that the flux of such particles has to hold to be true, within a factor two, constant over the past 10^9 yr (Schlickeiser, 2002). That means that the power computed in (3.16), over a time $\sim 10^9$ yr, held pretty much the same value. Moreover, since the confinement time of Crs inside the Galaxy is two orders of magnitude shorter, we infer that the probable sources of Crs have steadily injected in the Ism a power in Crs similar to that one we got few lines above. Currently, it is believed that Crs of energies up to the *knee* (10^{15} eV), are accelerated in the wave fronts propagating at supersonic speeds in the galactic Snrs. Such a hypothesis is motivated not only by the regular trend and the slope of the spectrum across several energy decades, but also by the good match between the energy of the Supernovae ejecta in the Galaxy, and the energy of galactic Crs.

The kinetic energy released during the explosion of a Supernova is typically $E_{SN} \sim \mathcal{O}(10^{51})$ erg, as indicated by numerical simulations of the collapse of a star with a mass of 10 $M_\odot$ (e.g. Janka, 2012). If only Supernovae contribute to the production of CRs, we expect that the power released in the Galaxy is

$$Q_{SN} = \mathcal{R}_{SN} E_{SN} \sim 10^{42} \qquad \text{erg s}^{-1}, \tag{3.17}$$

where $\mathcal{R}_{SN} \sim 0.03 \div 0.05$ yr^{-1} indicates the rate at which supernova explosion events occur. From the comparison with Eq. (3.16), we infer that only a acceleration efficiency ξ_{CR} of the order of $\sim 1\%$ would be requested to sustain the energetic need of CRs in the galactic disc. The total cosmic ray acceleration efficiency is somewhat higher than the estimate in Eq. (3.17) because of the contribution of nuclei heavier than hydrogen. More refined calculations provide a better estimate of the total acceleration efficiency that is between 5% and 10% for the bulk of SNRs, while it can be higher or smaller for individual objects, depending upon the environment in which the supernova event takes place (see e.g., Blasi, 2013a; McKee and Ostriker, 1975, 1977).

3.4 TRANSPORT OF CRS AT ASTROPHYSICAL SHOCKS

The origin of high-energy CRs has been a long-standing problem, and certainly represents one of the most fascinating problems in the modern Astrophysics. A deep understanding of the details of such an issue requires to establish a mechanism of acceleration - for nuclei, protons, and electrons - able (*i*) to illustrate the high energies ($E \leqslant 10^{15}$ eV, for GCRs) characterizing those particles, and (*ii*) at the same time their energy distribution according to a power-law $(dN/dE)_{obs} \sim E^{-\Gamma_{obs}}$. Last but not least, a fundamental tile to compose the intricate puzzle of the acceleration of CRs is that one nowadays known as the *injection problem*: because very low energy particles can be quickly thermalized by Coulomb scattering, how is it possible to separate a group of particles destined to become non-thermal from the group of thermal particles? Beyond purely phenomenological arguments presented in the previous paragraph, there are certainly also the theoretical explanations, important as well and complementary to the first ones, which highlight the status of SNRs as accelerators of CRs.

So far, the most successful particle acceleration model able to make correct quantitative predictions is the so-called *diffusive shock acceleration* model, referred to as *first order Fermi mechanism* too, when it is applied to the case of strong SNR shocks (the reader may refer e.g., to the pioneering works by Axford et al., 1978; Blandford and Ostriker, 1978, 1980; Krimsky and Petukhov, 1983; see also Jones and Ellison, 1991; Berezhko and Völk, 2007; Berezhko, 2008). The distinctive feature of this model is the "hard" energy spectrum, of type of power law (in particle momentum), with a differential spectral index Γ_{inj} close to 2 (see e.g., Drury et al., 2001).

The combination of a theory of the acceleration which predicts approximatively the exact spectral shape, and the existence of a real astrophysical source "equipped" with the right power, makes the acceleration by shock in Supernovae a serious favorite candidate for the origin of CRs in the Galaxy. Such a scenario has recently found support from the observations too. In Figure 3.10 we see the γ-ray emission from the Supernova Remnant (SNR) RX1713.7 − 3946 as measured by the H.E.S.S. telescope (Aharonian et al., 2007). In the γ-window, the spectrum is a power law with index ≈ 2, and it

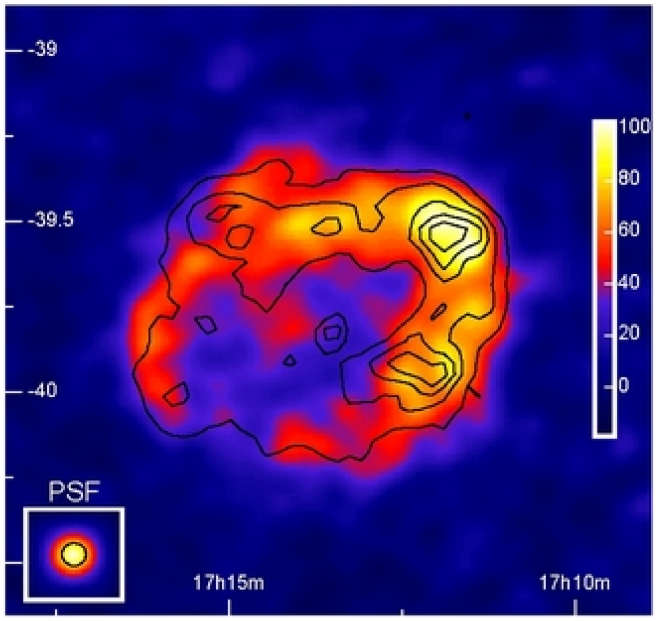

Figure 3.10: *γ-Emission of the Supernova Remnant* RX1713.7 − 3946 *as measured by the* H.E.S.S. *experiment Aharonian et al., 2007. The contour lines trace the emission in the X-band, and the the insert on the left at bottom shows the* H.E.S.S. *point spread function.*

extends up to ∼ 10 TeV, perfectly compatible with the presence of protons accelerated at energies even higher than that. Lately, a new study confirms what scientists have long suspected: CRs are born in the violent aftermath of supernovas, exploding stars throughout the galaxy. A research team led by scientists at the *Kavli Institute for Particle Astrophysics and Cosmology* at the Department of Energy's (DOE) SLAC National Accelerator Laboratory sifted through four years of data from NASA's *Fermi*-LAT to find the first unambiguous evidence of how cosmic rays are born. The team identified two ancient supernovae whose shock waves accelerated protons to nearly the speed of light, turning them into what we call cosmic rays. When these energetic protons collided with static protons in gas or dust they gave rise to gamma rays with distinctive signatures, giving scientists the smoking-gun evidence they needed to finally verify the cosmic ray *nurseries* (Ackermann et al., 2013).

An other independent proof of the shock acceleration theory might be represented by the production of the secondary component of CRs produced by the interaction of primary CRs with the interstellar gas. In the next chapter we have time to realize that the transport in the galactic medium implies a variation of the spectral index with respect to that one at the source, for CRs of energies below the ankle. For the purpose of the present discussion, it is enough saying that the injection spectrum, $Q_{source}(E) \propto E^{-\Gamma_{inj}}$, and the detected one can be related each other by a relationship of type

$$\tau_{esc}(E)\, Q_{source}(E) \propto \left(\frac{dN}{dE}\right)_{obs} \propto E^{-\Gamma_{obs}}. \tag{3.18}$$

Here $\tau_{esc}(E)$ indicates the confinement time of the particles within the Galaxy. That one, in general, depends on the energy as $E^{-\delta}$, with $0.3 \lesssim \delta \lesssim 0.7$ (in this regard, see the discussion proposed in §§ 2 & 4). To produce galactic

CRs with a spectrum $\sim E^{-2.7}$, as seen over a very broad energy range, it is reliable then to suppose that the sources are in charge of an index of the injected particles $2 \lesssim \Gamma_{inj} \lesssim 2.4$. The question relative to the acceleration of charged particles is of such importance and extent in the physics of CRs that I limit myself to a brief introduction of that.

3.4.1 The Fermi Picture

In 1949 Enrico Fermi developed an original conjecture for the origin of CRs that involved a new theory of acceleration of high-energy particles (Fermi, 1949). He envisioned that CRs in interstellar space would collide with moving, magnetized clouds and in the collision the energy of the clouds would be gradually transferred to the CRs. Currently, this mechanism is widely referred to as *second order Fermi acceleration*. I will outline the salient features following the derivation provided in the textbook by Longair (1994b).

The cloud has a velocity v_{cl}, which we assume constant during a typical collision with the particle. To make everything as simple possible, we may assume that the particle is already relativistic, $E_0 \simeq cp_0$, where E_0 is the initial energy. In the frame of the cloud, the cosmic ray energy is

$$E_0^\star = \gamma_{cl}(E_0 + \beta_{cl} p_0 \cos\theta), \tag{3.19}$$

with $\beta_{cl} = v_{cl}/c$, $\gamma_{cl} = (1-\beta_{cl}^2)^{-1/2}$, $\cos\theta$ being the *pitch angle*, i.e. the angle between the trajectory of the particle and the normal to the cloud. Inside this latter, the interactions between the particle and the turbulent magnetic field there present are completely elastic, so that both the energy and the momentum are to be considered unchanged. The energy of the particle, when this one emerges out of the cloud, is, in the observer's frame,

$$E_1 = \gamma_{cl}(E_0^\star + \beta_{cl} p_0^\star \cos\theta) = E_0 \times \gamma_{cl}^2 (1 + \beta_{cl}\cos\theta)^2. \tag{3.20}$$

After a single collision, the cosmic ray gets its own energy increased of ΔE. If we define $\eta \equiv \Delta E/E$ as the relative energy gained in each collision, we have that

$$\eta \equiv \frac{\Delta E}{E} = \frac{E_1 - E_0}{E_0} = \gamma_{cl}^2 (1 + \beta_{cl}\cos\theta)^2 - 1, \tag{3.21}$$

and therefore proportional to the square of the velocity of the magnetic cloud. Expanding the Eq. (3.21) up to the second order in β_{cl} ($v_{cl} \ll c$), we find that

$$\eta \simeq 2\beta_{cl}\cos\theta + 2\beta_{cl}^2. \tag{3.22}$$

Following the interactions with the irregularities of the magnetic field, it is probable that the trajectory of the particle, between two close encounters, gets stochastically deviated: it is suitable to average the Eq. (3.22) on the θ angle. The probability of a collision between the particle and the cloud, at a certain angle θ, is proportional to $\gamma_{cl}(1 + \beta_{cl}\cos\theta)$[§]. Therefore, for the first term in Eq. (3.22), we have

$$\langle 2\beta_{cl}\cos\theta \rangle = 2\beta_{cl} \frac{\int_\Omega \cos\theta\ [1 + \beta_{cl}\cos\theta]\ d\Omega}{\int_\Omega [1 + \beta_{cl}\cos\theta]\ d\Omega} = \frac{2}{3}\beta_{cl}^2, . \tag{3.23}$$

§ It is easy to infer that head-on collisions ($\cos\theta = 1$) are favored respect with tail-on collisions ($\cos\theta = -1$)

where $d\Omega/4\pi = \sin\theta\cos\theta d\theta d\phi/4\pi$, with $0 \leqslant \theta \leqslant \pi$ and $0 \leqslant \phi \leqslant 2\pi$, is the element of solid angle. The relative gain in energy for each collision gets then

$$\left\langle \frac{\Delta E}{E} \right\rangle = \frac{8}{3}\beta_{cl}^2. \tag{3.24}$$

The result just derived describes the original version of the theory proposed by Fermi, according to which the increment in energy of the particle is, on average, only of second order in β_{cl}: that is why we refer to it as the *second order Fermi acceleration*. It is worthy to remind that in the above-mentioned stochastic acceleration process, the relative energy gain is constant. After n collisions, the energy of a cosmic ray is then

$$E = E_0(1+\eta)^n, \tag{3.25}$$

and the number of collisions necessary to get such a value for the energy is

$$n = \frac{\ln(E/E_0)}{\ln(1+\eta)}. \tag{3.26}$$

Let T_c be the characteristic time between two consecutive collisions, and T_{esc} the characteristic time of the particle to reside in the acceleration region: the escape probability for each collision is then $P_{esc} = T_c/T_{esc}$. The density of the particles accelerated up to energies equal to E, or even larger than that, is:

$$N(\geqslant E) = N_0 \sum_{m=n}^{\infty} (1-P_{esc})^m \propto N_0\,(1-P_{esc})^n\,. \tag{3.27}$$

Such a process naturally leads to a (integral) power law spectrum

$$N(E) \propto E^{-S}, \tag{3.28}$$

with $S = [\ln(1-P_{esc})/\ln(1+\eta)]$. Actually, we are mostly interested in the differential distribution of particles, which is simply given by

$$N(E)dE \propto E^{-\Gamma}dE, \tag{3.29}$$

with $\Gamma \equiv 1 - [\ln(1-P_{esc})/\ln(1+\eta)]$, and $N(E)dE$ is the differential number of CRs in the remnant with energy between E and $E + dE$. In the original paper by Fermi, the astrophysical framework of such a mechanism was to be searched in the reflections of the charged particles on the *magnetic mirrors* associated with "clouds" in the Galaxy. Nowadays, we know that in the ISM the role of the magnetized clouds is played by plasma waves, most notably Alfvén waves, which move at speed $v_A = B/\sqrt{4\pi\rho_i} = 2B[\mu G]n_i[cm^{-3}]$ km s^{-1}, where $\rho_i = n_i m_p$ is the mass density of ionized material.

In spite of the fact that Fermi's idea proves to be quite simple and working to explain the non-thermal spectrum of GCRs, a very little is said about the index Γ, which will depend also on the velocity of the interstellar clouds. Furthermore, the energy gain per unit of time relies upon the rate of the encounters between the cloud and the cosmic ray, $\mathcal{R}_{enc}$, and it is

$$\frac{dE}{dt} = \mathcal{R}_{enc}\Delta E = \frac{c}{\lambda_{enc}}\eta E = \frac{\eta E}{T_{enc}}, \tag{3.30}$$

where λ_{enc} is the mean free path between two consecutive collisions, and T_{enc} is the "duration" of a single collision. From Eq. (3.30), it is inferred that

the energy increase rate is linearly proportional to the energy itself: to get higher and higher energies, longer and longer times are required.

The Fermi mechanism suggests an energy growth rate that is too slow to be efficient, and the final gain of energy is proportional to β_{cl}^2 ($\simeq 10^{-7}$). Given that, such a scenario appears to be a failure to explain the observed energies of CRs. However, the revolutionary concepts that it bears is still of the utmost importance: the electric field induced by the motion of magnetized cloud (or wave) may accelerate charged particles.

Before discussing the shock acceleration scenario, I would like to point out a further point. The exponent Γ involves three parameters: T_c, the time between encounters; T_{esc}, the lifetime of CRs; and η, the relative acceleration per encounter. There seems to be no reason why they should be related. Yet, for $\Gamma \sim 2$ they must satisfy (at first order) $P_{esc}/\eta = T_c/(\eta T_{esc}) \approx 1$. In the shock acceleration theory this relation between the three parameters holds automatically, and leads to $\Gamma \sim 2$ in a natural way. (Bell, 1978a,b)

3.4.2 The Test Particle Shock Acceleration

After Fermi's theory for the origin of CRs was abandoned, people most universally came to the conclusion that the origin was associated with Supernovae. Supernovae seemed to be the only places where a sufficient amount of energy is released to account for the enormous power, 10^{40} erg sec, that is required to resupply the GCRs every few million years. Also, supernovae are violent enough to be responsible for such high particle energies.

After a supernova remnant has expanded, its energy is still around in the form of thermal energy of the background ISM. The hot thermal material drives shocks into the undisturbed ISM. In this way the shock can transfer energy to the CRs, and any energy given to them is resupplied to the shock by the hot medium. At the same time, adiabatic expansion no longer decelerates the CRs, since the further expansion is small.

The driven question of this subsection is: how does a shock actually accelerate CRs? The mechanism in which the particle acceleration occurs in the converging flow of a relativistic shock wave is referred to as *diffusive shock acceleration* (DSA). It is an example of *first-order Fermi acceleration*. Given the importance of this phenomenon, not only for particle acceleration but for the propagation as well, here I outline the theory, highlighting some basic concepts that might turn out to be useful also to comprehend the transport of a charged particle in a background of waves.

How it is known from the literature, and discussed in § 2 also, a quite general kinetic equation for the transport of charged particles, suitable for the purpose of the present discussion, is

$$\frac{\partial f}{\partial t} + \boldsymbol{v}\cdot\boldsymbol{\nabla} f = -\boldsymbol{\nabla}\cdot(D\boldsymbol{nn}\cdot\nabla f) + \frac{1}{3}(\boldsymbol{\nabla}\cdot\boldsymbol{V})p\frac{\partial f}{\partial p} + Q(t,\boldsymbol{x},\boldsymbol{p}), \tag{3.31}$$

where $f(t,\boldsymbol{x},\boldsymbol{p})$ is the density of particles with momentum $\boldsymbol{p} \in [\boldsymbol{p},\boldsymbol{p}+d\boldsymbol{p}]$, the second term on the LHS is the *convection* term, while the first term of the RHS is the spatial *diffusion* term. The second term on the RHS describes the effect of fluid compression on the accelerated particles, $\boldsymbol{n}$ being a unit vector along the background magnetic field, and finally $Q(t,\boldsymbol{x},p)$ is the injection term. The diffusion-convection equation described in (3.31) has been derived analytically for the first time in Skilling (1975): here, I will apply it to particle shock acceleration (for a comprehensive discussion of shock acceleration of CRs see also Blandford and Eichler, 1987).

The supernovae shocks expanding in the ordinary ISM belong to the class of *collisionless shocks*. Many fundamental concepts of the physics of particle acceleration in astrophysical shocks rely on this property; here I limit myself to just saying that collisionless shocks are formed because of the excitation of electromagnetic instabilities, namely collective effects generated by groups of charged particles in the background plasma. After the collisionless shock has been formed, we can write the equations for conservation of mass, momentum, and energy across the shock surface. For the purposes of the present section, it is sufficient to consider the simple case of a plain parallel infinite shock, with the accelerated particles treated as test particles, these latter having no dynamical role. For sake of the simplicity, I also assume that, on the scales we are interested in, the shock can be considered stationary in time. On the other hand, I aware the reader that in a realistic scenario, all these approximations get broken to some extent, and it turns out to be fundamental to always have under control the limitations of the calculations we carry out, depending on their application. A exhaustive and recent review about the fundamental role of the non-linearity in shocks of astrophysical size and lifetime can be found in Malkov and O'C Drury, 2001 (see also e.g., Caprioli et al., 2010; Morlino et al., 2010).

In the frame of reference - where the shock front is stationary - the *upstream* (preshock) fluid velocity is u_1, and the *downstream* (postshock) fluid flows around the shock with a velocity u_2. Let the shock wave be characterized by a Mach number M_s, and a compression factor $r = u_1/u_2$, given by

$$r = \frac{4M_s^2}{M_s^2 + 3}. \tag{3.32}$$

I remind that, in the limit of strong shocks, $u_1 \approx V_\Sigma$, the shock speed, $u_2 \approx V_\Sigma/4$, and $M_s \to \infty$. The subscripts 1 and 2 refer to quantities upstream and downstream respectively. A test particle diffusing in the upstream plasma does not gain or lose energy, although the second order Fermi process discussed above may be at work. Let us suppose that there is a background magnetic field crossing the shock perpendicular to the shock front and such that $v_A[\sim 10\ \mathrm{km\ s^{-1}}] \ll V_\Sigma[\sim 10^4\ \mathrm{km\ s^{-1}}]$; in other words we want to solve the transport of particles for a stationary, supersonic, parallel shock. In a such frame, the compression term vanishes everywhere but at the shock $x = 0$, $(\nabla \cdot V) = (u_2 - u_1)\delta(x)$. In steady state, for a 1D scalar distribution $f \equiv f(x, p)$, the Eq. (3.31), in the shock frame, reads

$$v\frac{\partial f}{\partial x} - \frac{\partial}{\partial x}\left[D\frac{\partial f}{\partial x}\right] = \frac{1}{3}(u_2 - u_1)\delta(x)p\frac{\partial f}{\partial p} + Q(x, p). \tag{3.33}$$

Before moving on, just a couple of comments are worthy of being mentioned about the above equation. (*i*) The shock is treated as just an infinite boundary condition at $x = 0$. This implies that the equation cannot describe properly the thermal particles in the fluid. (*ii*) In a self-consistent treatment one would not need to specify the injection term, but the injection would result from the micro-physics of the particle motions at the shock. However, for the test particle theory the injection term is just an arbitrary normalization of the spectrum, even if it is worth to recall that while these approximations work in the case of the injection of protons, the injection of heavier nuclei would require a more complex picture.

Here, it is adequate to assume the injection only taking place at the shock front, immediately downstream of the shock, and that it only consists of particles with a given momentum p_{inj}:

$$Q(x,p) = \xi \frac{n_1 u_1}{4\pi p_{inj}^2} \delta(p - p_{inj})\delta(x) = q_0 \delta(x), \tag{3.34}$$

where n_1 and u_1 are the fluid density and fluid velocity upstream of the shock, and ξ is the acceleration efficiency, which is defined as the fraction of the incoming number flux across the shock surface that takes part in the acceleration process. We solve this equation in the upstream $(x < 0)$ and downstream $(x > 0)$ regions separately (where the 1^{st} term on the RHS is zero) and then match by taking $f(p)$ as continuous at the origin, $f(x = 0^-) = f(x = 0^+)$, and getting a second condition by integrating the Eq. (3.33) over a very thin region about the shock front $(x = 0)$:

$$-D\left(\frac{\partial f_2}{\partial x} - \frac{\partial f_1}{\partial x}\right) = \frac{1}{3}(u_2 - u_1)p\frac{\partial f_0}{\partial p} + q_0(p) \tag{3.35}$$

The Eq. (3.35) represents the conservation of cosmic ray flux. This discontinuity in flux is balanced by a sudden flux in the momentum direction, plus a source term. $f_0 = f(0,p)$ is now the distribution function of accelerated particles at the shock surface.

Upstream, $(-\infty, 0^-]$, the transport equation reduces to

$$u_1 \frac{\partial f}{\partial x} - \frac{\partial}{\partial x}\left(D\frac{\partial f}{\partial x}\right) = 0. \tag{3.36}$$

We assume $f(x,p) \to 0$ and $\partial f/\partial x \to 0$ as $x \to -\infty$, and $f(x,p) \to f_2(p)$ and $\partial f/\partial x \to 0$ as $x \to +\infty$. The upstream solution of Eq. (3.36) is

$$f(x,p) = f_0 e^{x u_1/D} : \quad x < 0 \tag{3.37}$$

$$D\frac{\partial f_1}{\partial x} = u_1 f_0. \tag{3.38}$$

In the downstream region, $[0^+, +\infty)$, we have

$$u_2 \frac{\partial f}{\partial x} - \frac{\partial}{\partial x}\left(D\frac{\partial f}{\partial x}\right) = 0. \tag{3.39}$$

The solution of this equation is a constant distribution of particles, since the $e^{x u_2/D}$ homogeneous part of the solution blows up as $x \to \infty$,

$$f(x,p) = f_0(p) : \quad x > 0 \tag{3.40}$$

$$D\frac{\partial f_2}{\partial x} = 0 \tag{3.41}$$

Substituting equations (3.37) and (3.40) into Eq. (3.35), and with the aid of the conditions (3.38) and (3.41), we have

$$u_1 f_0 = \frac{u_2 - u_1}{3} p \frac{\partial f_0}{\partial p} + \xi \frac{n_1 u_1}{4\pi p_{inj}^2} \delta(p - p_{inj}). \tag{3.42}$$

$q_0(p)$ is the incoming cosmic ray distribution and is regarded as known, so this equation is a differential equation for the downstream distribution function f_0. Notice that D has dropped out of the equation. (We have treated D as constant in x, but if it varied with x and depended on p we

would still get the same differential equation for f_0). After some trivial algebraic manipulation, we can write the Eq. (3.42) as

$$p\frac{\partial f_0}{\partial p} + \alpha f_0 = \alpha \frac{\xi n_1}{4\pi p_{inj}^2}\delta(p - p_{inj}), \tag{3.43}$$

where $\alpha = 3r/(r-1)$. The above equation is easily solved to give

$$f_0(p) = \frac{\alpha}{p^\alpha}\int_0^p \frac{\xi n_1}{4\pi p_{inj}^2}\delta(p - p_{inj})p'^{(\alpha-1)}dp, \tag{3.44}$$

i.e.,

$$f_0(p) = \alpha \frac{\xi n_1}{4\pi p_{inj}^2}\left(\frac{p}{p_{inj}}\right)^{-\alpha}. \tag{3.45}$$

The spectrum of accelerated particles is a power law distribution in momentum with a slope α that only depends on the compression ratio r. In the limit $M_s \to +\infty$ of an infinitely strong shock front, the slope of the spectrum tends asymptotically to $\alpha = 4$. If we indicate with $N(E)dE = 4\pi p^2 f_0(p)(dp/dE)dE$ the particle density with energy $E \in [E, E + dE]$, therefore the distribution of particles in energy is given by the power law $N(E) \propto E^{2-\alpha}$, in the case the particles are relativistic ($E = cp$). Instead, we get $N(E) \propto E^{(1-\alpha)/2}$ for non-relativistic particles ($E = p^2/2m$). In the limit of strong shocks ($r = 4$), $N(E) \propto E^{-2}$ and $N(E) \propto E^{-3/2}$, in the relativistic and non-relativistic regime, respectively. In agreement with what is predicted by the DSA, a strong non radiative shock injects particles in the ISM with a distribution in energy characterized by a spectral index ≈ 2, which is not far from the observed power law index of 2.7 for $10 \leqslant E/GeV \leqslant 10^7$, lending support to the notion that interstellar shock waves play an important role in acceleration of cosmic rays. CRs can be lost to diffusion out of the Galaxy; since this would be more rapid at increasing energy, this process will steepen the interstellar cosmic ray spectrum.

In any case, some of the approximations made to get the final Eq. (3.45) are too ideal, and there are additional losses that we have not considered, which would steepen the spectrum. For example, in the present discussion we have assumed that the shock is supersonic ($V_\Sigma \gg v_A$) and further that the shock is strong. On the other hand, after all it is extremely gratifying that the shock acceleration, which fits the astrophysical situation so well, leads automatically to the nearly correct power law distribution, which, before the introduction of the idea of shock acceleration, seemed such a mystery.

The concept of *maximum energy* of accelerated particles is not naturally involved in the test particle theory of DSA. According to the Eq. (3.45) the power law spectrum does extend, in principle, up to infinite particle energy. In the strong shock limit, such spectrum contains a divergent energy, thereby implying a failure of the test particle assumption. The absence of a maximum energy clearly derives from the assumption of stationarity of the acceleration process, which is directly connected to the issue of maximum energy achieved in a SNR shock expanding in the ISM. To define a maximum energy, we might require that the time of acceleration be finite and shorter than the age of the SNR; in case the accelerated particles are the electrons, we should replace the age of the SNR by the minimum between the time scale for radiative energy losses due to synchrotron and Inverse Compton (IC) scattering, and the age of the SNR. Here, I repeat the essential physics underlying the elegant argument originally proposed by Bell, 1978a,b, in

order to get more quantitative insights about the acceleration time: the key concept is that the acceleration process proceeds through repeated shock crossings of individual particles (see also Longair, 1994b).

Let us consider a particle crossing the shock front from the upstream to the downstream region. The fluid on the downstream side of the shock approaches the incoming particle at a velocity $\Delta u = (u_1 - u_2) = (3/4)V_\Sigma$. The energy of the particle as seen in the reference frame of the downstream plasma is

$$E_2 = E_1 \times \gamma_{\Delta u}(1 + \beta_{\Delta u}\cos\theta_1), \quad 0 \leqslant \cos\theta_1 \leqslant 1, \tag{3.46}$$

where $\beta_{\Delta u} \equiv \Delta u/c = (u_1 - u_2)/c$ is the relative velocity in units of speed of light, and $\gamma_{\Delta u} \equiv (1 - \beta_{\Delta u}^2)^{-1/2}$ is, as usual, the Lorentz factor. So, in the limit $V_\Sigma \ll c$, after crossing the shock the particle has gained an energy $\Delta E/E_1 = \beta_{\Delta u}\cos\theta_1$, while in the downstream region there is no energy gain to the first order (with exception of second order effects, which are negligible). If the particle returns to the shock it may recross the surface, this time with a negative pitch angle ($-1 \leqslant \cos\theta_2 \leqslant 0$), so that the energy of the particle, as seen by an observer in the upstream fluid, is

$$E_1' = E_2 \times \gamma_{\Delta u}(1 - \beta_{\Delta u}\cos\theta_2) = E_1 \times \gamma_{\Delta u}^2(1 - \beta_{\Delta u}\cos\theta_2)(1 + \beta_{\Delta u}\cos\theta_1). \tag{3.47}$$

After a complete *cycle* upstream-downstream-upstream (or vice versa), the final energy is always $E_1' > E_1$: particles gain energy at each cycle. From the hypothesis of isotropy (by scatterings) of the particle distribution in the upstream, and the downstream region as well, the number of particles within the angles $\in [\theta, \theta + d\theta]$ is proportional to $\sin\theta d\theta$; the flux of particles crossing the shock front is instead proportional to the normal component of their velocities, $c\cos\theta$. The integrated probability distribution over all the particles approaching the shock is equal to unity, and thus $\int_0^{\pi/2} A\sin\theta\cos\theta_1 d\theta_1 = \int_{\pi/2}^{\pi} A\sin\theta_2|\cos\theta_2|d\theta_2 = 1 \rightarrow A = 2$, being A the normalization factor; this means, e.g., that for those particles with θ in the range 0 to $\pi/2$, we find a probability function

$$\mathcal{P}(\theta) = 2\sin\theta\cos\theta, \quad \cos\theta \geqslant 0. \tag{3.48}$$

Therefore, we can now compute the mean gain in energy per cycle

$$\begin{aligned}\left\langle \frac{\Delta E}{E} \right\rangle_{\mu_1,\mu_2} \equiv \left\langle \frac{E_1' - E_1}{E_1} \right\rangle_{\mu_1,\mu_2} &= -\int_{-1}^{0} 2\mu_2 d\mu_2 \int_1^0 2\mu_1 d\mu_1 \\ &\times \left[\gamma_{\Delta u}^2 E_1(1 + \beta_{\Delta u}\cos\theta_1)(1 - \beta_{\Delta u}\cos\theta_2) - 1\right] \\ &= \frac{4}{3}\beta_{\Delta u} = \frac{4}{3}\frac{u_1 - u_2}{c},\end{aligned} \tag{3.49}$$

where for convenience we introduced the pitch angle $\mu \equiv \cos\theta$ in the above expressions. Thus, unlike the Fermi mechanism, in which there are both head-on and tail-on collisions, in the case of the shock front, the collisions are always head-on, implying a linear growth of the energy gain: this is the reason why DSA is often named *first order Fermi mechanism*.

From Eq. (3.37), it follows that the total number N of particles per unit of surface Σ of the shock is

$$N = \int_{-\infty}^{0} dx n_0 e^{u_1 x/D_1} = \frac{n_0 D_1}{u_1}, \quad [cm^{-2}], \tag{3.50}$$

where n_0 is the particle density at shock, $x = 0$, and D_1 is the diffusion coefficient in the upstream region. Given the isotropy hypothesis, the total number of particles in the unit of time coming in the pre-shock region, crossing the shock front surface from the downstream, is

$$J_1 = \int_{\cos\theta \geqslant 0} \frac{d\Omega}{4\pi} \underbrace{n_0 c \cos\theta}_{flux} = \frac{n_0 c}{4}, \quad [cm^{-2}s^{-1}]. \tag{3.51}$$

Therefore, a typical particle resides in the pre-shock region for a (diffusion) time

$$t_1 = \frac{N}{J_1} = \frac{4D_1}{u_1 c}. \tag{3.52}$$

By analogous argument, it is inferred that in the downstream a cosmic ray will stay a time

$$t_2 = \frac{N}{J_2} = \frac{4D_2}{u_2 c}, \tag{3.53}$$

so that the duration of a cycle across the shock will be

$$t_{cycle} = t_1 + t_2 = \frac{4D_1}{u_1 c} + \frac{4D_2}{u_2 c}. \tag{3.54}$$

We know that during such a time interval the particle increases its energy of $\Delta E = (4\Delta u/3c)E$, and then we can introduce an *acceleration time* t_{acc}

$$\frac{dE}{dt} = \frac{4(u_1 - u_2)}{3c} \frac{E}{t_{cycle}} = \frac{E}{t_{acc}}, \tag{3.55}$$

with the acceleration time given by:

$$t_{acc} \equiv \frac{3}{(u_1 - u_2)} \left(\frac{D_1}{u_1} + \frac{D_2}{u_2} \right). \tag{3.56}$$

The Eq. (3.56) illustrates the fact that the acceleration time is dominated by particle diffusion in the region with less scattering (larger diffusion coefficient) which in normal conditions is the region of the upstream fluid.

A possible definition of maximum energy arises from requiring that the acceleration time be smaller than the age of a typical SNR, T_{SNR}: basically, only a finite time there is available to accelerate CRs. For the purpose of the present discussion, we are just interested in getting a reliable order of magnitude, therefore it is perfectly fair to consider a *Bohm-like* diffusion coefficient in the plasma flowing around the shock,

$$D_{Bohm} = \frac{1}{3} r_L c = \frac{E}{3eB}, \tag{3.57}$$

where the particle is assumed to be relativistic ($v \approx c$), with a mean free path is approximated by the its Larmor radius r_L. Additionally, in the approximation of a strong shock, it is $u_1 = 4u_2$, and then:

$$E_{max} \approx \frac{3}{20} \frac{eB_{SNR}}{c} V_\Sigma^2 T_{SNR}, \tag{3.58}$$

which holds for parallel shocks, in other words with the magnetic field parallel to the normal to the shock and $B_1 = B_2 = B_{SNR}$. We know that the velocity of the shock drops with the time during the Sedov-Taylor phase,

$V_\Sigma \propto T_{SNR}^{-3/5}$, and the maximum value for E_{max} is achievable in the last part of the ejecta dominated phase, when $V_\Sigma T^{free} \sim R_{SNR}^{free}$, with $R_{SNR}^{free} = (3M_{ej}/4\pi n m_p)^{1/3}$ being the radius of the SNR shell at the end of its free-expansion phase, when it $T^{free} = T_{SNR}$ (Draine, 2011; Vietri, 2008). For typical values of $n = 1\ cm^{-3}, V_\Sigma = 5000\ kms^{-1}$, and $M_{ej} = 10M_\oplus$, we get $T^{free} = 10^3 yr$. Given those values, the maximum energy achieved by nuclei of charge $Z|e|$, by diffusive shock acceleration, is

$$E_{max} \sim Z \times 3 \times 10^{13} eV. \tag{3.59}$$

Here I discuss two more physical upper limits on the energy of the CRs released in a extremely violent event such a supernova explosion. First, the acceleration time give in Eq. (3.56) is linearly proportional to the energy of the cosmic ray, obeying a relationship of type $t_{acc} = \alpha E$, with α given by

$$\alpha \equiv \frac{c}{e(u_1 - u_2)}\left(\frac{1}{u_1 B_1} + \frac{1}{u_2 B_2}\right). \tag{3.60}$$

Instead, the *cooling time* due to radiative losses, affected by a cosmic ray trapped in the shell of a SNR, is given by

$$t_{cool} = \frac{1}{b_0 E}, \tag{3.61}$$

and is inversely proportional to the energy of the particle, since that the energy losses rate, either by the synchrotron emission or by IC scattering, are instead proportional to the square of the energy, $dE/dt = -b_0 E^2$. Then the maximum energy is determined by the condition

$$t_{acc} = t_{cool} \rightarrow E \leqslant \left(\frac{1}{\alpha\beta}\right)^{1/2}. \tag{3.62}$$

Second, to prevent that the particle easily escape out of the acceleration zone, it is necessary that the typical linear size of the candidate accelerator, R, is larger than the typical length scale over which the cosmic ray will be deflected by the magnetic field inside the accelerator itself. Even in this case we may consider the cosmic ray Larmor radius, or a g-multiple of it, and get

$$E \leqslant E_{max} \equiv \frac{Z|e|cBR}{g}. \tag{3.63}$$

Over the last twenty years, the fundamental properties of such a model have been largely reviewed by many astrophysicists, each one adopting a different, and original mathematical approach. Recently, there have been significant improvements in the theoretical framework, based on the non-linear treatment of the acceleration mechanism. From those studies, came out that the *non-linearity* of the interaction of the particles with the shock structures is essential to account the high efficiency of the acceleration processes (Malkov and O'C Drury, 2001).

3.5 INTERSTELLAR RADIATION FIELDS

The interstellar space in our Galaxy is populated by electromagnetic fields intimately bound with stars, the ISM and CRs. A large-scale magnetic field

is observed through the polarization of starlight, Zeeman splitting of radio lines and Faraday rotation of polarized radio signals. The Milky Way shines from radio to γ-rays. Most of this radiation is given by starlight, partially absorbed and reprocessed by dust grains, but continuum emission at lower and higher energies is dominated by interstellar processes related to CRs propagation giving rise to synchrotron emission observed in the radio domain and diffuse γ-ray emission.

3.5.1 The Magnetic Structure of the Galaxy

The presence of interstellar magnetic fields in our Galaxy was first revealed by the linear polarization of starlight (Hall, 1949), later explained in terms of selective extinction by elongated dust grains partially aligned because of a magnetic field (Davis and Greenstein, 1951).

Stellar polarimetry provides information only on the direction of the magnetic fields, its strength can be estimated thanks to the Zeeman splitting of radio lines (mainly the two circularly polarized components of the 21-cm line of H I) or Faraday rotation of polarized radio signals (either from pulsars or extragalactic continuum sources). Zeeman splitting occurs when the 21-cm radiation travels through regions with a magnetic field, so that we observe two circularly polarized components with an energy spread

$$\Delta E = \mu_B B \Delta m, \tag{3.64}$$

where μ_B is the Bohr magneton and Δm is the difference of magnetic quantum number between the two states ($\Delta m = 2$ since the circularly polarized components are produced by electrons with $m = \pm 1$). In this case Zeeman-splitting measurements are biased towards regions with high H I densities and small line widths, so cold H I clouds.

The Zeeman effect has now been observed also for the OH and H_2O lines in molecular clouds (Crutcher et al., 1987; Fiebig and Guesten, 1989), providing values of $10 \div 100$ μG up to 5×10^4 μG in dense cloud cores ($n \simeq 10^{10}$ cm^{-3}). Faraday rotation occurs when a polarized radio wave passes through a plasma. Counter-clockwise rotation occurs if the magnetic field is oriented toward the observer, clockwise if the field points away from the observer. The rotation angle $\Delta\chi = \lambda^2 RM$ increases with the wavelength λ squared and the "rotation measure"

$$RM = \int n_e B_{\parallel} ds, \tag{3.65}$$

where n_e is the number density of free charges. The rotation measure can be combined with the dispersion measure (Eq. (3.2)), which provides an estimate of the column density of ionized gas, to extract the average intensity of the magnetic field in the direction parallel to the observer,

$$\langle B_{\parallel} \rangle = \frac{\int n_e B_{\parallel} ds}{\int n_e ds} = 1.232 \frac{RM}{DM}. \tag{3.66}$$

Thus, Faraday-rotation measurements sample regions of ionized gas. The strength of the large-scale magnetic field averaged over 1 kpc around the solar system is $\sim 6$$\mu$G from radio synchrotron measurements.

Beyond the small-scale features revealed by Faraday rotation and radio polarization, the overall field structure in the Galaxy is still under debate (e.g. Beck, 2009a). In nearby galaxies random fields are concentrated in

spiral arms, whereas ordered fields are stronger in inter arm regions and follow the orientation of adjacent arms. The interstellar magnetic field is coupled with the matter in the ISM through its ionized component (and as a whole thanks to ion-neutral collisions, Spitzer (1978)).

At large scales the magnetic field helps to support interstellar gas against gravitational collapse and it confines CRs in the Galactic halo. On smaller scales the interstellar magnetic field affects all kind of turbulent motions in the ISM, like SNRs expansion, and it supports dense molecular clouds against gravitational collapse.

The origin of the interstellar magnetic field is still mysterious. The most likely scenario is a hydromagnetic dynamo: the motion of a conducting fluid in a magnetic field generate electric currents which amplify an original magnetic field, provided perhaps by a pre-existing intergalactic field. Parker (1992) proposed that the dynamo mechanism might be CRs-driven. Many other details about observations of the magnetic structure of our Milky Way can be found in a very recent review by Han (2009).

3.5.2 Interstellar Radiation

The space between stars is also populated by photon fields. The Galactic interstellar radiation field (ISRF) spanning the window from IR to UV is the result of emission by stars, and the subsequent scattering, absorption and re-emission by dust in the ISM. The spectrum of the ISRF can be approximately described by the combination of some diluted black body distributions ("gray body" distributions), each characterized by a photon energy density and a temperature.

Beyond thermal emission from dust, peaking in the IR domain, other interstellar processes are also present: lines from atomic or molecular transitions of interstellar gas and radioactive decays (see e.g. Cassé et al., 1999), and continuum emission due to free-free emission from ionized gas and CRs-related processes.

CRs propagation in the Galaxy gives rise to diffuse continuum emission through synchrotron radiation (see § 5.2 and PAPER II), peaking in the radio domain, and in the γ-ray band due to interactions with interstellar matter and low-energy interstellar radiation. In general, the ISRF in the Milky Way is dominated by six components (Draine, 2011):

- Galactic synchrotron radiation from relativistic electrons.
- The cosmic microwave background radiation.
- Far-infrared (FIR) and infrared (IR) emission from dust grains heated by starlight.
- Emission from $\sim 10^4$ K plasma - free-free, free-bound, and bound-bound transitions.
- Starlight - photons from stellar photospheres.
- X-ray emission from hot (10^5 to 10^8 K) plasma.

To the purposes of the discussion inherent to the present THESIS, I will briefly review the contribution of the first of above components.

Synchrotron Radiation

The rapid spiralling motion of CRs electrons about magnetic field lines generate non thermal radiation, termed *synchrotron radiation*, over a broad range of radio frequencies. The synchrotron emissivity depends on both the magnetic field strength and the spectrum of CRE, but unfortunately neither quantity is reliably known.

The only all-sky map available is the well-known compilation by Haslam et al. (1981) at 408 MHz, combining good angular resolution and low contamination by thermal emission. On small scales the map is probably dominated by SNRs. On the large scale we can see the emission from CRs electrons propagating through the Galaxy as well as large features known as radio loops (Berkhuijsen et al., 1971), which are thought to be old nearby SNRs.

The synchrotron spectral index at a frequency ν for a population of electrons with power-law spectrum of index γ is $\beta_\nu = (\gamma - 1)/2$ (e.g. Rybicki and Lightman, 1979), so the observed β_ν ranging from $0.6 \div 1$ increasing with frequency implies $\gamma = 2.4 \div 3$ increasing with energy for CRs electrons in our Galaxy. Radio continuum observations of other galaxies provide a complementary view on CRs electrons. The edge-on galaxies, like NGC891 (Allen et al., 1978; Heald et al., 2006; Beck, 2009b), show a nonthermal halo extending to several kpc, giving credence to the idea of a large propagation halo also for our Galaxy (see § 5.2 and PAPER II).

Interstellar γ-ray Emission

Interstellar γ-radiation is produced by interactions of CRs during their propagation in the interstellar space. There are four principal channels for production of γ-rays by the ISM:

- CRs nucleons inelastically collide with nucleons in the ISM, producing π^0 mesons which then decay into γ-rays (*pion decay*);
- CRs electrons and positrons interact with the gas in the ISM emitting Bremsstrahlung radiation (*bremsstrahlung*);
- CRs electrons and positrons produce γ-rays up scattering on low energy photons of the low-energy Galactic ISRF and the CMB (*inverse Compton*);
- pair e^+e^- annihilation.

Since the Galaxy is transparent to high-energy γ-rays up to hundreds of TeV, the interstellar emission is a tracer of CRs densities throughout the Galaxy and also of the total column densities of the ISM, complementary to gas and dust tracers at other wavelengths.

3.6 CONCLUDING REMARKS

ELEMENTAL COMPOSITION : The chemical composition of interstellar matter is close to the "cosmic composition", persisting from the *Big Bang* and inferred from the abundance measurements in the Sun, in other disc stars, and in meteorites, namely 90.9% by number of hydrogen, 9.1% of helium, and 0.12% of heavier elements, commonly called "metals" in the astrophysical community (Ferrière, 2001; Spitzer, 1978)

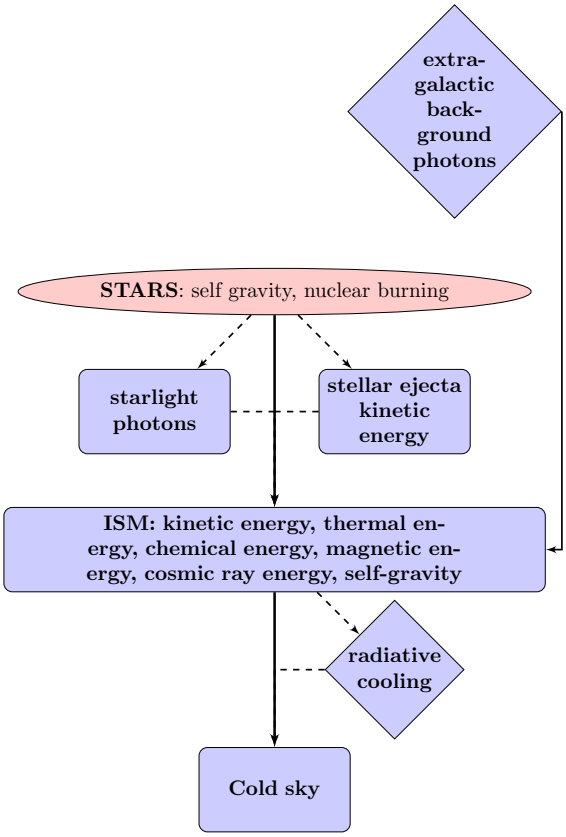

Figure 3.11: *Flow of energy in the Milky Way. After Draine (2011).*

ENERGY DENSITIES : From the arguments have been discussed so far, it clearly appears that the ISM is a dynamic *ecosystem*, and the baryons undergo changes of phase for a number of reasons: ionizing photons from stars can convert cold molecular gas to hot H II regions; radiative cooling can allow hot gas to cool to low temperatures; ions and electrons can recombine to form atoms, and H atoms can recombine to form H_2 molecules. Several forms of energy characterize the ISM: *thermal energy* $u = (3/2)nkT$, *bulk kinetic energy* $(1/2)\rho v^2$, *cosmic ray energy* u_{CR}, *magnetic energy* $B^2/8\pi$, and energy in photons, which can be subdivided into *cosmic microwave background* (CMB) far-infrared (FIR) emission from dust, and starlight. Remarkably, in the local ISM today, these energy densities fall within the range $0.2 \div 2$ eVcm^{-3}. With the exception of the energy density in the CMB, similar to the other energy densities, the near-equipartition among the other six forms of energy is not coincidental at all.

In fact the magnetic energy density $B^2/8\pi$ and the turbulent energy density are comparable in magnitude. Similarly, if the cosmic ray energy density was much larger, it would not be possible for the magnetized ISM to confine the CRs, and they would be able to escape freely from the Galaxy. The cosmic ray energy density approximates equipartition with the sum of the turbulent energy density and thermal pressure in the ISM. If the starlight energy density were much larger (by a factor $\sim 10^2$), radiation pressure acting on dust grains would be able to "levitate" the ISM above and below the Galactic mid-plane, presum-

ably suppressing star formation; this feedback loop may play a role in regulating the starlight energy density in star-forming galaxies.

Finally, the ISM is far from thermodynamic equilibrium, and it only able to maintain this non equilibrium state because of the input of "free energy", primarily in the form of UV radiation emitted by stars, but with a significant contribution of kinetic energy from high-velocity gaseous ejecta from Supernovae (see Figure 3.11).

4 MODELS FOR COSMIC RAY TRANSPORT IN THE INTERSTELLAR MEDIUM

«If my calculations are correct,
when this baby hits 88 miles per hour...
you're gonna see some serious shit.»
Dr. Emmett Brown in
Back to the Future

by Robert Zemeckis (USA, 1985)

The spectrum of GCRs- spanning from tens of MeV/nucleon up to $\gtrsim 10^{18}$ eV- is fundamentally shaped by acceleration and diffusion, at least for energies $\gtrsim 10^2$ MeV. Several other phenomena - for instance convection, reacceleration, nuclear fragmentation, electromagnetic losses, solar modulation - compete at lower energies, where their effect is often degenerate and prevents unambiguous interpretation of the wealth of data collected in the lower tail of the galactic spectrum. Nevertheless, transport models able to reproduce data on a wide energy range can be built (the milestone in the field literature being Berezinskii et al., 1984).

A detailed CRs transport model can help us to understand the physical processes in the CRs acceleration regions, the most energetic regions in our Galaxy. It can be used as a cross check of our models of the local ISM and to smaller extend of the interstellar radiation fields and the magnetic field. For most indirect Dark Matter searches in diffuse γ-rays, synchrotron radiation or charged annihilation or decay products Galactic CRs form the dominant background. Practically all our knowledge of CRs propagation comes via secondary CRs, with additional information from γ-rays and synchrotron radiation. The fact that the primary nuclei are measured (at least locally) means that the secondary production functions can be computed from primary spectra, cross sections and interstellar gas densities with reasonable precision; the secondary particles can then be "propagted" and compared with observations.

In this chapter, starting from recalling the main ideas of a simple phenomenological transport model, I will move on and give an introduction to our numerical package, the `DRAGON` code, which constitutes, with `GalProp`*, the state-of-the-art in CRs transport modelling, presenting comparisons between the model and recent experimental observations. In other words, I will describe in brief how to build a CRs propagation model, under the assumptions on the source term, gas distribution and other astrophysical quantities.

Lastly, I will end with describing the main features of the CRE, necessary for the discussion presented in § 5.

* http://galprop.stanford.edu/

4.1 COSMIC RAY PROPAGATION IN THE LEAKY-BOX APPROXIMATION

The so-called *Leaky-Box* model, originally proposed to explain the local fluxes of extraterrestrial charged particles, has been certainly the simplest model describing the transport of CRs in the galactic environment.

Such a model describes the Galaxy as a finite volume of propagation, inside which CRs are as trapped in a *box* bounded by *semi-permeable walls*, but from which the particles bounce off, with a finite probability of escape (*leak*) in the intergalactic medium. The effects of spatial propagation are, therefore, reduced to a simple loss from the walls of the box. The source distributions, as well as the interstellar matter, are uniform (for a more in-depth knowledge of the Leaky Box model, the reader can consult the excellent *Review* by Cesarsky, 1980).

Indicating with the subscript i the type of nuclear species, and with $1/\tau_{esc}$ the probability per unit time to escape from the galactic boundaries, we can write the CRs density equation, at an energy E, in a way as simple as (Berezinskii et al., 1984)

$$\frac{\partial N^i}{\partial t} + \underbrace{\frac{d}{dE}\left(\frac{dE}{dt}N^i\right)}_{\text{energy loss term}} + \underbrace{\frac{N^i}{\tau_{esc}}}_{\text{escape term}} + \underbrace{\bar{n}_H v \sigma_i N^i}_{\text{catastrophic term}} + \underbrace{\frac{N^i}{\tau_i}}_{\text{decay term}} = \underbrace{Q^i + \sum_{j>i} \bar{n}_H v \sigma_{ij} N^j + \underbrace{\sum_{j>i} \frac{N^j}{\tau_{ij}}}_{\text{decay term}}}_{\text{source term}} . \tag{4.1}$$

Here, $Q^i(E)$ describes the primary CRs spectrum injected by astrophysical sources (e.g., SNe), and $\sum_{j>i}(\bar{n}_H v \sigma_{ij} N^j) + \sum_{j>i} \frac{N^j}{\tau_{ij}}$ characterizes the source terms for secondary nuclei of type i, originated or through nuclear fragmentation processes ($\sigma_{frag}^{j\to i} N^j$), or by radioactive decays ($1/\tau_{dec}^{j\to i} N^j$), or both from the j-th heavier nuclear species. Then, $\bar{n}_H$ and v are the average gas density present in the ISM, and the velocity of primary nuclei, respectively. The energy loss term is dE/dt, and the catastrophic term, $\bar{n}_H v \sigma_i N^i$, determines the annihilation of a nucleus of type i by inelastic scattering with the nuclei of the interstellar gas. Lastly, τ_i is the lifetime of the nucleus i due to the radioactive decay, and $\tau_{esc}(E)$ is, as mentioned above, the characteristic particles time escape, which generally depends on the energies of the particles themselves.

Regardless of the exact nature of the processes responsible for the propagation, it is certain that the CRs, during their galactic journey, cross over significant fractions of interstellar gas, giving rise to nuclear collisions that alter their initial composition, destroying some primaries, and by producing the secondary ones. The nuclear fragmentation process (called *spallation*) accounts for the over abundance of some stable nuclei, such as those belonging to the group of *light elements* (Li, Be and B), or the group of the sub-Fe also, as Sc, Ti, V, Cr and Mn. The ratio of the fluxes of the secondary particles with respect to the primaries provides useful details about the amount of matter passed through by CRs. For stable nuclei, at energies slightly above

few hundreds of MeV/nuc, it is allowed to neglect the energy losses; at the stationary state ($\partial N^i/\partial t = 0$), we can then write

$$\left(\frac{1}{\tau_{esc}} + \bar{n}_H v \sigma_i\right) N^i = Q^i + \sum_{j>i} \bar{n}_H v \sigma_{ij} N^j. \tag{4.2}$$

In the leaky-box model, assuming the cross-sections as known, the relative abundances of the secondary nuclei ($Q^i(E) = 0$) are simply determined by the matter column density, or *grammage*, crossed through by the particles while they are propagating in the ISM, and defined as $X_{CR,l} \equiv \bar{n}_H m_p v \tau_{esc}$, m_p being the proton rest mass. From Eq. (4.2), applied to the relativistic CRs, it is possible to set the relative abundances of the nuclei

$$\left(\frac{1}{X_{CR,l}} + \sigma_i\right) N^i - \sum_{j>i} \sigma_{ij} N^j = 0, \tag{4.3}$$

and then to estimate the ratio of the secondary CRs, N_{sec}, with respect to the primaries, N_{pr},

$$\frac{N_{sec}}{N_{pr}} \simeq \bar{n}_H \sigma_{frag}^{pri\to sec} c\tau_{esc}, \tag{4.4}$$

where $\sigma_{frag}^{pri\to sec}$ is a compact notation indicating the network of the nuclear reactions involved in the production of secondary nuclei. From the ratios N_{sec}/N_{pr} detected on Earth, it was inferred, for the column density, a value of $X_{CR,l} \simeq 10$ gr cm^{-2} (Ferrando et al., 1991).

COSMIC RAY LUMINOSITY After setting the quantity $X_{CR,l}$ and thanks to the measurements of local fluxes, the simple leaky-box model makes it possible to estimate the total luminosity of CRs of the Galaxy, in a way different with respect to what argued in the § 3.3.3. The cosmic ray luminosity is defined as $L_{CR} = W_{CR}/\tau_{esc}$, where $W_{CR} = w_{CR} V_{CR}$ is the total energy of the particles in the Galaxy, w_{CR} and V_{CR} are the mean energy density, per unit of volume, and the confinement volume, respectively. If we assume a cosmic ray density roughly constant over the entire volume of the Galaxy, the total luminosity becomes then

$$L_{CR} = \frac{W_{CR}}{\tau_{esc}} = \frac{c w_{CR} \bar{n}_H V_{CR} m_p}{X_{CR,l}} = \frac{c w_{CR} M_H}{X_{CR,l}} \sim 3 \times 10^{40} \quad \text{erg s}^{-1}, \tag{4.5}$$

where $M_H = \bar{n}_H V_{CR} m_p \simeq 10^{43}$ g is the total mass of the hydrogen in the Galaxy, as it is known from the radio observations, and $w_{CR} \sim 10^{-12}$ erg cm^{-3} (see § 3.3.3). Again, we infer that only small amounts ($\sim 3\%$) of the energy released during the SNe explosions ($\sim 10^{42}$ erg s^{-1}) could be sufficient to provide the fraction of luminosity of the Galaxy due to CRs.

SECONDARY COSMIC RAY CLOCKS Beyond the total luminosity of CRs estimated in the previous paragraph, the leaky-box model allows to determine, in a quite simple manner, the confinement time of the particles in the galactic medium too. Indeed, we know that some isotopes of the group (Li, Be, B) are radioactive. For example, the ^{10}Be isotope decades - by β-decay - in ^{10}B, in a characteristic lifetime $\tau_r = 3.9 \cdot 10^6$ yr†. If the decay time is of the same

† The reader may remind that if the particles are relativistic, the mean lifetime of such particles is defined as $\tau = \gamma\tau_r$, γ being the usual Lorentz factor.

order of the cosmic ray escape time, τ_{esc}, this latter can be estimated by the density of the stable-to-radioactive secondary nuclei ratios, N^s_{sec}/N^r_{sec}.

Beryllium is produced in the fragmentation of the Carbon, Nitrogen and Oxygen nuclei, with the interstellar gas: 10% of the total product is of type ^{10}Be, the rest corresponds to the stable species ^{7}Be and ^{9}Be. From the leaky-box model, we rewrite the transport equation for the stable isotope ^{9}Be as

$$N_9 \left[v\bar{n}_H \sigma_{f,9} + \frac{1}{\tau_{esc}} \right] = \sigma_9 v\bar{n}_H N_{CNO}, \tag{4.6}$$

where $(v\bar{n}_H\sigma_{f,9})^{-1}$ is the catastrophic loss term for the isotope ^{9}Be, and $\sigma_9 v\bar{n}_H N_{CNO}$ is a compact notation expressing the spallation network (CNO)$\rightarrow$ ^{9}Be. Analogously, the transport equation for the unstable isotope ^{10}Be reads

$$N_{10} \left[v\bar{n}_H \sigma_{f,10} + \frac{1}{\tau_{CR,l}} + \frac{1}{\gamma\tau_r} \right] = \sigma_{10} v\bar{n}_H N_{CNO}. \tag{4.7}$$

The ratio between the two isotopes becomes

$$\frac{N_{10}}{N_9} = \frac{\sigma_{10}}{\sigma_9} \frac{v\bar{n}_H \sigma_{f,9} + 1/\tau_{esc}}{v\bar{n}_H \sigma_{f,10} + (1/\gamma\tau_r) + 1/\tau_{esc}}. \tag{4.8}$$

All the cross-sections in Eqs. (4.6), (4.7) and (4.8) are known from measurements made in particle accelerators. The observed value for the abundance of the isotope ^{10}Be, relative to the total product of Be is 0.028 (Simpson, 1983). Therefore, in the leaky-box framework it has been possible to estimate the lifetime of CRs, getting a value of $\tau_{esc} \sim [2 \div 3] \cdot 10^7$ yr (e.g., Ahlen, 2000).

SECONDARY-TO-PRIMARY COSMIC RAY RATIOS The secondary-to-primary ratios allow us also to establish the dependence of the escape probability, of the CRs in the Galaxy or, that is equivalent, of the the matter column density $X_{CR,l}(E)$ upon the energy. With reference to the experimental data about the B/C (boron-to-carbon ratio), we may assign, in an empirical way, to the quantity $X_{CR,l}$ a rigidity dependence of the particle like as

$$x_{CR,l}(\mathcal{R}) = x_{CR,0}\beta \left(\frac{\mathcal{R}}{\mathcal{R}_0} \right)^{-\delta}, \tag{4.9}$$

normalized at the rigidity $\mathcal{R}_0$, and δ being a value in the range $\simeq [0.3 \div 0.7]$ (e.g., Evoli et al., 2008; Garcia-Munoz et al., 1987). For the sake of simplicity, if we assume for the moment a null production of secondary nuclei, and consider only the catastrophic effects of the destruction of the primary nuclei, the leaky-box model, thanks to the Eq. (4.2), provides the spectral shape of the primary nuclei of type i, after the propagation of these latter:

$$N^i(E) = Q^i(E) \times \left(\frac{1}{\tau_{esc}(E)} + \frac{\beta c \bar{n}_H m_p}{x^i_{int}} \right)^{-1}, \tag{4.10}$$

where $\tau_{esc}(E)$ is identical for all nuclei with the same rigidity $\mathcal{R}$, and $x^i_{int} = \beta m_p/\sigma_i$ obviously depends on the mass of the i-th nucleus. For example, in the case of the protons, at low energies it is $x^i_{int} = 50.8$ g cm^{-2}, that is a value much larger than $X_{CR,l} \approx 10$ g cm^{-2}. Recent measurements by experiments like e.g., CREAM (Ahn et al., 2008) and TRACER (Ave et al., 2008),

confirmed that CRs are accelerated at the sources with the same spectral index $E^{-\Gamma_{inj}}$. Therefore, the Eq. (4.10) suggests that the energy spectra, of different nuclei, will differentiate or tend to become asymptotically parallel each other, at low and high energies, respectively. Neglecting the term related to x^i_{int} in the Eq. (4.10), the effect of the propagation then consists uniquely in a steepening of the initial acceleration spectrum by a factor δ:

$$N^i(E) \propto Q^i(E) \times \tau_{esc}(E) \propto \frac{Q^i(E)}{X_{CR,l}(E)} = E^{-(\Gamma_{inj}+\delta)}. \tag{4.11}$$

Yet, thanks to the leaky-box formalism, combining together the Eqs. (4.4) and (4.9), we can write the secondary-to-primary ratios as

$$\frac{N_{sec}}{N_{pr}} \propto \sigma^{pri\to sec}_{frag} \tau_{esc}(E) \propto X_{CR,l}(E) \sim E^{-\delta}. \tag{4.12}$$

Given the values of the column densities $x_{CR,l}$, and the lifetime τ_{esc} of the CRs, determined through this paragraph, we may infer at least two so important conclusions:

- In 10^7 yr, the CRs, if they propagated along a straight line, they would cover a distance of 10^{25} cm, or 3 Mpc. On the other hand, the thickness of the galactic disc is around $300 \div 500$ pc, and its radius nearly $10 \div 15$ kpc. Therefore, the trajectory of the CRs in the Galaxy has to be not rectilinear, but strongly deviated; in other words they move in a *random walk*, due to the many hits with the irregularities of the magnetic field. As we will see later, their propagation can be then described by a simple diffusion-loss equation in the coordinates space;
- Combining the Eqs. (4.4) and (4.8), we might estimate the mean gas density from the values of $X_{CR,l}$ and τ_{esc}, and obtain a value of $\bar{n}_H \simeq 0.25$ cm^{-3} for the mean galactic density of the hydrogen, which is four times smaller than the mean density gas in the galactic disc (~ 1 g cm^{-3}). This means that the CRs spend the majority of their life out of the galactic disc, that is in the galactic halo, where the gas is rarefied. Since the half-height of the disc is roughly 250 pc, the thickness of the halo should be then at least of the order of ~ 1 kpc.

From the discussion so far, we infer that, although the leaky box model permits to get significant predictions in a pretty simple way, it gets inadequate in describing unstable nuclei and mainly the electron CRs, by virtue of, as we will see, strong energy losses which affect the motion of such particles within the Galaxy.

4.2 THE CR FRAMEWORK IN THE DRAGON CODE

In § 2, we have seen that the propagation of charged particles in the ISM is determined, unequivocally, by their interaction with electromagnetic fields of the galactic plasma. To the present days, the concept of *diffusion* constitutes a valid description of the CRs propagation, accounting both for the high isotropy and the confinement properties of CRs in the Galaxy (Dogiel and Breitschwerdt, 2009).

In § 2.2.2 we have seen how the QLT of the plasma turbulence describes, approximately, the diffusion coefficient for $r_g < L$ (V. Ptuskin, 2006),

$$D = \frac{v r_g B^2}{12\pi k_{res} W(k_{res})}, \tag{4.13}$$

where $L \sim 100$ pc is the typical scale for inhomogeneities in the ISM, $k_{res} = 1/r_g$ is the resonant wave number, and $W(k)$ is the spectral (kinetic) energy density of the magnetic fluctuations, normalized as $\int dk W(k) = \delta B^2/4\pi$. The random field, at the resonant scale, is assumed to be weak, $\delta B_{res} \ll B$. Therefore, the diffusion coefficient for the CRs is equal to

$$D = \frac{v r_g^{\delta}}{3(1-\delta) k_L^{1-\delta}} \frac{B^2}{\delta B_L^2}, \tag{4.14}$$

for charged particles with $r_g < k_L^{-1}$, and under the assumption of a spectrum of turbulence of the form $W(k) \propto 1/k^{2-\delta}, k > k_L$. Here, we have introduced the main wave number k_L, and the random field amplitude, δB_L, across the principal turbulent scale L. The diffusion coefficient then scales as $D \propto v(p/Z)^{\delta}$. The momentum diffusion coefficient is instead described by the following equation

$$D_{pp} = p^2 v_A^2/(9D). \tag{4.15}$$

As a first example, we may assume an interstellar turbulence energy spectrum of type $W(k)dk \sim k^{-2+\delta}dk$, $\delta = 1/3$ - over a wide *inertial* range $1/(10^{20}cm) < k < 1/(10^8 cm)$ - and a value $\delta B \approx 5\mu G$ for the intensity of the random field - at the turbulent injection large-scale. Therefore, we estimate the diffusion coefficient as $D \approx 2 \times 10^{27} \beta \mathcal{R}^{1/3} cm^2 s^{-1}$, for all the CRs particles with a magnetic rigidity $\mathcal{R} < 10^8$ GV. The scaling $D \sim \mathcal{R}^{1/3}$ is determined by the exponent $\delta = 1/3$, typical for a *Kolmogorov*'s turbulence spectrum, but in strong tension with the empirical diffusion model ($D \propto \mathcal{R}^{0.6}$).

The observations of random motions in the interstellar gas are consistent with the assumption of a single close-to-Kolmogorov spectrum. However, we notice that a Kolmogorov-like spectrum could, theoretically, refer only to some part of the MHD turbulence, i.e. the *Alfvénic* structures strongly elongated along the large-scale magnetic field (e.g., Goldreich and Sridhar, 1995; Sridhar and Goldreich, 1994; Strong, Moskalenko, and Ptuskin, 2007), and most likely responsible of the typical electron density fluctuation $k^{-5/3}$ (Armstrong et al., 1995). On the other hand, the most isotropic part of the turbulence, with a $\delta = 1/2$ typical of a *Iroshnikov-Kraichnan*'s turbulence - and a smaller value for the random component at the principal scales - could to the same extent exist in the ISM. The IK spectrum has a scaling of type $D \sim \mathcal{R}^{1/2}$, which is close to the asymptotic form of the diffusion coefficient at high energies, as predicted in the *plain-diffusion* empirical propagation model.

As pointed out in § 2, the cascades of Alfvén waves (with the scaling $k^{-5/3}$) and the fast magnetosonic waves ($k^{-3/2}$) are independent and may coexist in the Goldreich and Shridhar model of MHD turbulence. Recent numerical MHD simulations (e.g., Cho et al., 2002; Yan and Lazarian, 2004) support the scenario in which the fast modes are the most efficient in the scattering process of the CRs in the ISM.

To the present days, the approach based on the kinetic theory gives us an estimation of the diffusion coefficient, and predicts, for the diffusion properties, a dependence upon the magnetic rigidity of type power-law. Nevertheless, it must emphasized that the theoretical description of the MHD turbulence, is a complicated and not completely solved problem, even in the case of small amplitude fields.

The CRs in the Galaxy, under the hypothesis of diffusive propagation, obeys the following equation (Berezinskii et al., 1984)

$$\frac{\partial N^i}{\partial t} - \underbrace{\boldsymbol{\nabla}\cdot(D\,\boldsymbol{\nabla} - \boldsymbol{v}_c)\,N^i}_{\text{diffusion}} + \underbrace{\frac{\partial}{\partial p}\left(\dot{p} - \frac{p}{3}\boldsymbol{\nabla}\cdot\boldsymbol{v}_c\right)N^i}_{\text{energy loss}} - \underbrace{\frac{\partial}{\partial p}p^2 D_{pp}\frac{\partial}{\partial p}\frac{N^i}{p^2}}_{\text{reacceleration}} = \\ = \underbrace{Q^i(p,r,z)}_{\text{injection}} + \underbrace{\sum_{j>i} c\beta n_{gas}(r,z)\sigma_{ji}N^j}_{\text{spallation}} - \underbrace{c\beta n_{gas}\sigma_{in}(E_k)N^i}_{\text{catastrophy}}. \quad (4.16)$$

We solve the above equation by running our numerical code DRAGON[‡]. It is a code developed to solve the diffusion equation in the specific case of CRs in the Galaxy environment, taking into account realistic distribution for CRs sources, galactic gas and magnetic field distributions. Now DRAGON is a complete, public code that propagates CRs (by solving the above diffusion-loss equation) and gamma-rays, and performs very quickly. DRAGON is written in C++ and makes full use of the advantages of such a complex language: it features 34 classes and all computations are performed in a highly optimized way, especially from the point of view of memory management (e.g. big bundles of data are always passed in the form of pointers to a structured object).

Being the present first part of the manuscript, just an introduction to the theoretical framework for the research carried out over the time of my Ph.D., I would skip the technical details regarding the structure of the numerical package - the development of which I have given my contribution over the last years - remanding the reader to the seminal paper by Evoli et al. (2008). In the following, I will make clear the meaning of the most relevant terms in Eq. (4.16)

CONVECTION The observation of *galactic winds* as seen in outer galaxies, suggests that the medium, responsible to diffuse CRs in the Milky Way, moves most likely outwards of the galactic disc, with a velocity $\boldsymbol{v}_c$, called *convective* velocity. The motion of CRs in the ISM is therefore affected by the influence of the convective transport that, among the other things, implies a kind of *dilution* of the energy of the particles, initially sited in the disc, and later on flowed into a larger volume. The particles will experience thus an "adiabatic deceleration" (Longair, 1994a). Let us try to derive an analytical expression for this type of energy loss process, influencing the cosmic ray transport in the galactic environment.

I will start from the simplest case of non-relativistic gas, provided with an Maxwell-like energy distribution. The change of internal energy $\mathcal{U}$, when the gas does work in expanding its volume by dV, is given by

$$d\mathcal{U} = -P_g dV, \quad (4.17)$$

where P_g is the pressure of the gas. For an ideal gas, $\mathcal{U} = (3/2)nk_BT$ and $P_g = nk_BT$, n being the number density of the particles and T the temperature. The mean energy particle is $(3/2)k_BT$, so we find that

$$d\mathcal{U} = nV dE = -\frac{2}{3}nE dV. \quad (4.18)$$

If $nV = N$, is the total number of particles, we have

$$\frac{dE}{dt} = -\frac{2}{3}\frac{nE}{N}\frac{dV}{dt}. \quad (4.19)$$

‡ http://www.dragonproject.org/Home.html

Here, dV/dt is the expansion rate of the volume V determined by the velocity field $\boldsymbol{v}(\boldsymbol{r})$. If we consider the volume of a cube of sides dx, dy, dz moving with the flow, then we can get the volume change. Let us sum the changes due to the differential velocities through each of the three pairs of faces of the cube,

$$\frac{dV}{dt} = (v_{x+dx} - v_x)dydz + (v_{y+dy} - v_y)dxdz + (v_{z+dz} - v_z)dxdy. \quad (4.20)$$

By expanding in Taylor series, we get

$$\frac{dV}{dt} = \left(\frac{\partial v_x}{\partial x} + \frac{\partial v_y}{\partial y} + \frac{\partial v_z}{\partial z}\right) = (\boldsymbol{\nabla}\cdot\boldsymbol{v})V. \quad (4.21)$$

Now let us substitute this result in the Eq. (4.18), and we have

$$\begin{aligned}\frac{dE}{dt} &= -\frac{2}{3}\frac{nV}{N}E(\boldsymbol{\nabla}\cdot\boldsymbol{v}) \\ &= -\frac{2}{3}(\boldsymbol{\nabla}\cdot\boldsymbol{v})E.\end{aligned} \quad (4.22)$$

In general, this is the expression for the energy loss rate due to adiabatic losses made of a flow of non-relativistic particles in expansion. In terms of the momentum p of the particle, we can alternatively write

$$\frac{dp}{dt} = -\frac{1}{3}(\boldsymbol{\nabla}\cdot\boldsymbol{v})p. \quad (4.23)$$

It is straightforward to generalize to the ultra-relativistic case, by following the same procedure, but this time applied to the case $\mathcal{U} = 3nkTV$ and $p = (1/3)\mathcal{U}$. Therefore, we infer that the CRs play a *dynamical role* in the galactic halo.

REACCELERATION In addition to the diffusion in the coordinate space, due to the deviation of their trajectories by the fluctuations of the magnetic plasma, relativistic cosmic ray particles of energy $E \gtrsim 1 \div 3$ GeV/nuc may undergo a further weak, distributed *reacceleration* - after they leave their compact sources - as they interact with interstellar MHD turbulence, (Cesarsky, 1980; Seo and V. S. Ptuskin, 1994). There are certain indications that such a stochastic acceleration could play a significant role for low-energy CRs (Ginzburg, 1975; Ginzburg and Syrovatskii, 1964). In fact it has been shown that at energies aforementioned even a comparatively weak reacceleration might distort the measured secondary-to-primary ratios (e.g. Berezinskii et al., 1984). It is almost inevitable that CRs will undergo a certain amount of acceleration in the ISM: if the scattering of relativistic particles by MHD turbulence is responsible of their spatial diffusion, then the scattering should also serve statistically to accelerate the particles (e.g. V. S. Ptuskin et al., 2006b). If we adopt a standard set of ISM parameters, we find that the effective acceleration time for $E \simeq 1$ GeV/nuc particles will be only slightly longer than the time scale for accelerating CRs in the Galaxy. Such statistical acceleration becomes less efficient as the particle energy increases (see e.g. Osborne and Ptuskin, 1988). The reacceleration of the CRs - in the transport equation of CRs - is accounted as a diffusion in the momentum space: thus, such a phenomenon is addressed by introducing a momentum coefficient diffusion D_{pp}. Such a coefficient is related to the propagation velocity of the weak irregularities in the ionized plasma, namely the Alfvén

speed. From the QLT (see e.g. Berezinskii et al. (1984); Schlickeiser (2002)), we know that

$$D_{pp} = \frac{4}{3\delta(4-\delta^2)(4-\delta)} v_A^2 p^2 / D(E), \tag{4.24}$$

where D is simply the spatial diffusion coefficient. The momentum diffusion coefficient reads approximately as $D_{pp} = p^2 v_A^2 / 9D$, where the Alfvèn speed, v_A, has been introduced as the characteristic velocity of the weak irregularities propagating along the magnetic field.

DIFFUSION COEFFICIENT The knowledge of the diffusion coefficient is absolutely essential for understanding the nature of the spectrum of GCRs, determined by the processes of acceleration in the sources (SNRs) and propagation in galactic magnetic fields. CRs diffusion properties are expected to be correlated to the, spatially dependent, properties of the ISM or to the CRs source density injecting turbulence in the ISM. In § 2, according to the picture of QLT, i.e. for small turbulence, the resonant scattering on a weakly turbulent field leads mainly to a diffusion *along* the field; in this theory the perpendicular diffusion coefficient turns out to be very small, and only the component $D_{ii} = D_{\parallel}$ of the diffusion tensor is nonzero.

However, in the typical conditions of interstellar space, the turbulence level is quite high: $\delta B/B_0 \sim 1$, and so the QLT does not provide a satisfactory description of the diffusion in the perpendicular direction: we expect indeed that in such conditions parallel and perpendicular diffusion have comparable strength because the contribution of the regular field, which defines a favourite direction, becomes less important.

In general, the diffusion tensor reads

$$D_{ij} \equiv (D_{\parallel} - D_{\perp}) b_i b_j + D_{\perp} \delta_{ij}. \tag{4.25}$$

In order to clarify the reason of such a decomposition, notice that, if the coordinate system is chosen so that the regular magnetic field lies along one of the axes, e.g. the z axes, the diffusion tensor becomes diagonal and its elements are simply $D_{zz} = D_{\parallel}, D_{yy} = D_{xx} = D_{\perp}$. If we assume a cylindrical symmetry, the only one relevant is the perpendicular diffusion coefficient.

In any case, for the purposes of the present THESIS, being interested in the mean properties of CRs propagation, rather than the details of the Galactic structure, I will follow the isotropic picture, and present here results obtained with a 2-dimensional version of the DRAGON code. A discussion of a more realistic 3D version will be addressed in § 5, where the impact of such a configuration on the propagation of CRs, electrons in particular, will be presented.

The propagation parameters are usually tuned to the secondary-to-primary ratio and the unstable-to-stable ratio of locally observed charged particles, while the injection spectra are chosen to best reproduce the local proton and electron spectra (see PAPER III Gaggero, Maccione, Di Bernardo, et al., 2013, and PAPER IV Gaggero, Maccione, Grasso, et al., 2014). The rigidity dependence is generally taken as $D \propto D_0 \mathcal{R}^{\delta}$. In the following I will refer to three main classes of CRs transport models, in literature (e.g., V. Ptuskin, 2006; Seo and V. S. Ptuskin, 1994) best known as (i) *Reacceleration* Models (KOL), (ii) *Diffusive Reacceleration* Models (KRA), and (iii) *Plain Diffusion* (PD) Models.

REACCELERATION MODEL refers to the diffusion model with distributed reacceleration of CRs by the interstellar MHD turbulence which scatters

particles and provides their spatial diffusion. The K41 spectrum is assumed that leads to the rising with rigidity of the diffusion coefficient $D \propto \mathcal{R}^{1/3}$. For typical value of Alfvén velocity $V_A \sim 30 kms^{-1}$, the reacceleration is not essential for nuclei with energies $E > 40$ GeV/nucleon and the abundance of secondary nuclei is a decreasing function of rigidity. The impact of reacceleration on spectra of primary and secondary nuclei becomes stronger at smaller energies so that the characteristic time of distributed acceleration in the Galaxy becomes equal to the time of diffusion from the Galaxy at about 1 GeV/nucleon. As a consequence the pronounced peak in the secondary-to-primary ratio arises. The asymptotic behaviour of the escape length is $X \propto v(p/Z)^{-1/3}$ at $E > 40$ GeV/nucleon.

DIFFUSIVE REACCELERATION assumes that the IK spectrum describes the interstellar MHD turbulence. It is characterized in particular by a relatively slow non-linear cascade of wave from small to large wave numbers. The resonant wave-particle interaction results in the significant wave damping on cosmic rays and termination of the cascade at $k \sim 10^{-12} cm^{-1}$ (in contrast to the case of Kolmogorov cascade which is fast and not noticeably affected by CRs). The amplitude of short waves is suppressed and the low energy particles rapidly exit the Galaxy without producing many secondary particles. It explains the peaks in secondary-to-primary nuclei ratios at about 1 GeV/nucleon. The asymptotic behaviour of the scape length in this case is $X \propto v(p/Z)^{-1/2}$ at $E > 3$ GeV/nucleon.

PLAIN DIFFUSION the most simple model one can think of, with no diffusive reacceleration and no convection. This model is very similar to a leaky-box approach, except that here we can also take care of the case of slow diffusion, i.e. the steady state CRs distribution is not flat in spatial coordinates.

Low energy effects on the diffusion coefficient may be parametrized in the following way

$$D = D_0 \beta^\eta \mathcal{R}^\delta, \quad \eta \sim -0.4/0.5 \tag{4.26}$$

Such a parametrization can account for an expected low-energy effect such as the dissipation of MHD waves as a consequence of their resonant interaction with CRs: the parametrization above permits an effective modelling of the phenomenon (V. S. Ptuskin et al., 2006b). Further details on the determination of the diffusion coefficient parameters can be e.g., found in the appended PAPER I (Di Bernardo, Evoli, Gaggero, Grasso, Maccione, and Mazziotta, 2011); see also Di Bernardo, Evoli, Gaggero, Grasso, and Maccione (2010).

THE SPATIAL SOURCE DISTRIBUTION AND INJECTION SPECTRUM The source term $Q(\boldsymbol{r}, p)$ included in the transport equation § (4.16), without loss of generality takes the form:

$$Q(R, z, p) = \left(\frac{R}{R_\odot}\right)^\alpha \exp\left(-\beta \frac{R - R_\odot}{R_\odot} - \frac{|z|}{z_0}\right) \times \frac{dQ(\mathcal{R})}{d\mathcal{R}}, \tag{4.27}$$

where α and β are free parameters to fix against the data, R is the galactocentric distance, $R_\odot = 8.5$ kpc is the distance of the Solar System from the

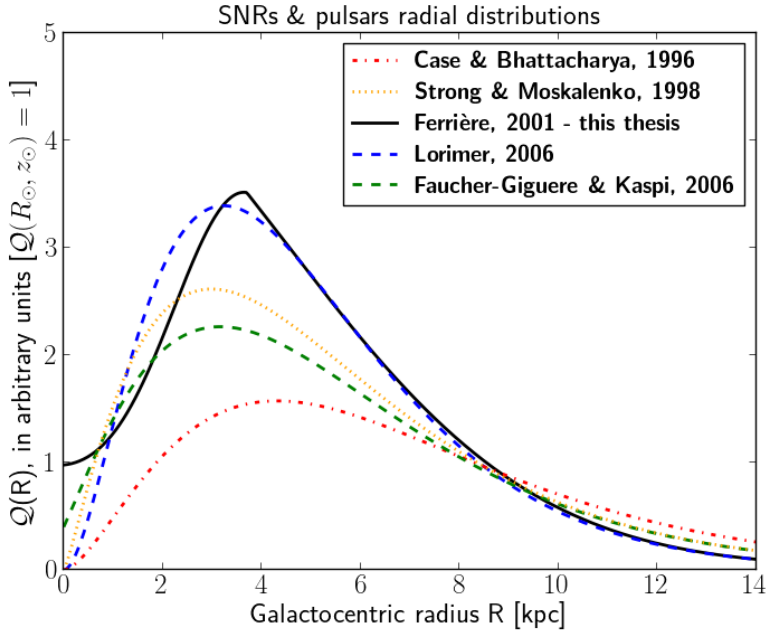

(a) *Radial profile of the distribution functions of the* CRS *sources*

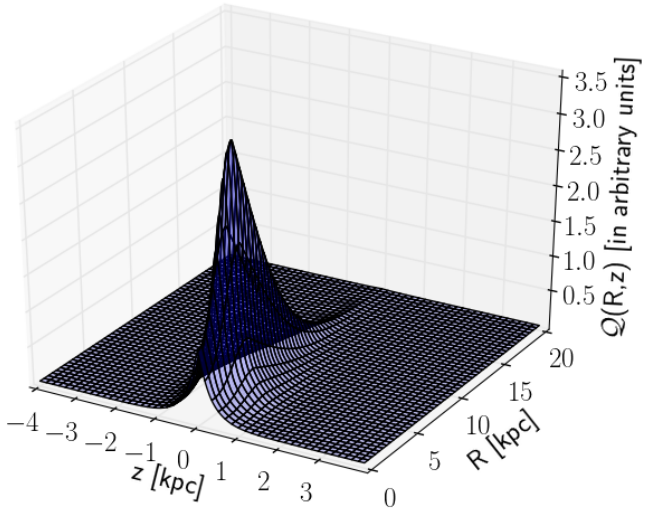

(b) *3-dimensional distribution function of the* CRS *sources*

Figure 4.1: *Models of spatial distribution for* SNRS *and pulsars, believed as the main sources of the* CRS. ***Upper****: Radial distribution of the cosmic ray sources implemented in* DRAGON *and used in the present work of* THESIS *(continuous black line: Ferrière (2001)), compared with other models proposed in Literature: Case and Bhattacharya (1998); Faucher-Giguère and Kaspi (2006); Lorimer (2004); Strong and Moskalenko (1998).* ***Bottom****: 3—D distribution function used in this* THESIS *(Ferrière (2001)).*

galactic centre, and $dQ(\mathcal{R})/d\mathcal{R}$ is the differential injection spectrum in function of the magnetic rigidity of the particles, $\mathcal{R} = pc/Z|e|$. The normalization condition is such that $Q(R_\odot, z_\odot) = 1$, at the position of the Sun.

The radial dependence shown in Eq. (4.27) traces the spatial distribution of SNRs and pulsars, as observed in the Galaxy, for statistically determined values of the parameters α and β. For example, Case and Bhattacharya (1998), relying their studies on the catalogue of SNRs elaborated by Green (1996), provided the following values: $\alpha = 2.00 \pm 0.67$ and $\beta = 3.53 \pm 0.77$. Strong and Moskalenko (1998) instead adopted $\alpha = 0.5$ and $\beta = 1.0$, chosen to reproduce (after propagation) the distribution of CRs in the Galaxy as determined by the analysis of the EGRET γ-data. Throughout in this THESIS we assume $Q(R, z)$ to trace the SNRs distribution as modelled in Ferrière (2001), on the basis of pulsars and progenitor star surveys. This is slightly different from the radial distributions adopted e.g. in Strong and Moskalenko (1998) and Strong, Moskalenko, Reimer, et al. (2004) which are based on pulsar surveys only. We also apply a cut-off in the distribution of the sources at $R_{cut} = 15$ kpc, since that it turns out quite unlikely the presence of significant sources at further distances. The z-dependence in Eq. (4.27) reflects instead the hypothesis of confinement of the sources in the disc.

Mechanisms of acceleration occurring at the shock fronts in the supernova envelopes determine the energy spectrum of the charged particles emitted by the sources in the galactic medium. In this regard, the majority of the theoretical works available in literature centred on the DSA mechanisms (e.g., Berezhko and Völk (2000); Blandford and Ostriker (1978)), suggesting that the injection spectrum of primary CRs follows a typical power-law behaviour, in function of the particle rigidity $\mathcal{R}$. The differential spectrum will be then

$$\frac{dQ(\mathcal{R})}{d\mathcal{R}} \equiv q(\mathcal{R}) = q_0 \left(\frac{\mathcal{R}}{1\,\mathrm{GV}} \right)^{-\Gamma_{inj}}, \tag{4.28}$$

where q_0 is a normalization factor, and the exact value of the index Γ_{inj} is still matter of debate. In what follows, I assume the injection index is identical for all CRs nuclei, and the chosen value is such that primary particles fluxes reproduce, after the propagation, the local spectra.

4.2.1 The Solar Modulation

The low-energy spectra of CRs can be modified by the transport in our Solar system. The sole reason for this modulation is the interaction of the CRs flux from outside the Solar system with the Solar wind which is directed away from the Sun. Depending on the Solar activity this effect can be significant below particle energies of $10 \div 20$ GeV. For these energies the LIS predictions of any transport model have to be corrected for the effect of Solar modulation. Provided, that some specific approximations are taken into account, the propagation theory presented in § 2 can be applied to the Solar system. Gleeson and Axford (1968) showed that the influence of the solar wind on the transport of low-energy CRs approximated as a motion in an effective radial electric field, so CRs modulation is described under this so-called *force-field approximation* by only one parameter: the potential Φ. The modulation of a CRs species is therefore given, with respect to the LIS, by the following formula:

$$J(E_k,\, Z,\, A) = \frac{(E_k + m)^2 - m^2}{(E_k + m + \frac{|Ze|}{A}\Phi)^2 - m^2} \times J_{LIS}(E_k + \frac{|Ze|}{A}\Phi,\, Z,\, A), \tag{4.29}$$

Going beyond the simplified force-field approximation, recently a realistic modulation model has been implemented in the numerical code named HelioProp (Maccione, 2013), in order to take in account the charge-dependent drifts when CRs transport equations are solved in the context of the heliosphere. Helioprop is now perfectly interfaced to the DRAGON code. For the main results achieved by running Helioprop - in order to reproduce low-energy CRs data - I would remand the reader to the Paper III & IV respectively, for further details.

4.3 THE ELECTRON COMPONENT OF COSMIC RAYS

4.3.1 A General Overview

Electrons, characterized by their low mass, constitute a unique, and somewhat enigmatic, constituent of CRs. It is not yet clear why we see so few electrons on Earth ($\sim$ 1% of proton flux, at energies $\sim \mathcal{O}(1)$ GeV), but it is certain that they play a decisive role in the study of the physical properties of the Galaxy.

Conversely to the more massive protons and nuclei, the relativistic electrons effectively lose much of their energy during their galactic journey, as a result of the various electromagnetic interactions with the interstellar environment, mainly bremsstrahlung within the diffuse gas, emission of synchrotron radiation in the galactic magnetic fields, and Inverse Compton scattering with photons in the interstellar radiation fields (ISRF). Indeed, the strong energy losses due to Compton interactions with photons of the cosmic microwave background (CMB) radiation, prevent the electrons from travelling over intergalactic distances. Moreover, the synchrotron radiation, emitted by relativistic electrons, gives a significant addition to the background radio emission of the Galaxy.

Given that, we can exclude any sort of extra-galactic contributions to the electron-kind CRs (about this point the reader can refer, e.g., to the monographs by Berezinskii et al. (1984) and Schlickeiser (2002)).

Regarding their origin, electrons detected in CRs fluxes could be either (*i*) emitted in the interstellar space, directly from astrophysical sources sited in the galactic disc, or (*ii*) the final result of hadron interactions which take place in the interstellar medium. In the first case, electrons are released in the *galactic sea* together with protons and nuclei, and most likely with the same energy injection spectrum; we will call them *primary electrons*, conversely to the opposite case (*secondary electrons*), in which relativistic electrons are produced in decay processes of negative pions, created by collisions of the nuclear component of CRs (especially protons and helium nuclei) with nuclei of gas (mostly hydrogen and helium):

$$\begin{aligned} p + H &\rightarrow \pi^- + X \\ &\hookrightarrow \mu^- + \bar{\nu}_\mu \\ &\hookrightarrow e^- + \bar{\nu}_e + \nu_\mu, \end{aligned} \tag{4.30}$$

where X represents the rest of a bunch of particles produced in a nuclear collision. Besides the scenarios explained above, it is necessary to also consider the eventual contribution of secondary electron fluxes created through annihilations or decays of *exotic matter*.

The intensity of radio emission from the Galaxy, combined with the direct measurements of the ratio of electron and positron fluxes, suggest, however,

that the bulk of electron CRs is mainly of primary nature. As said before, astrophysical sources inject electrons obeying a typical power-law behaviour, $\mathcal{Q}_{e^-}(\boldsymbol{r}, E_{e^-}) \propto E_e^{-\Gamma^e_{inj}}$, where $\mathcal{Q}_{e^-}(\boldsymbol{r}, E_{e^-})$ is the number of electrons, e^-, of kinetic energy E_{e^-}, originated in an unitary volume at position $\boldsymbol{r}$, in the unity of time and energy, whereas Γ^e_{inj} is the spectral index for the injection at the sources, which we take constant. In support of a such assumption, two main arguments are worthy to be mentioned. Firstly, on Earth we observe number density of electrons spread across a wide range of energy ($\lesssim$ few TeV), in a very good agreement with a power-law trend, for several decades. Secondly, the intensity of synchrotron radiation of SNRs is a power-law function of the frequency, $J_\nu \propto \nu^{-\beta}$. The spectral index β of the radio emission emitted from supernova envelopes is $\beta \simeq 0.5$ (e.g., Clark and Caswell, 1976). This value matches with the one provided by the theoretical prediction according the which an electron population, with index Γ^e_{inj}, emits synchrotron radiation with index $\beta = (\Gamma^e_{inj} - 1)/2$, where it is $\Gamma^e_{inj} \simeq 2$ (the reader can refer to the monograph by Longair (1994b)).

As regards the positrons present in CRs, these, at energies of orders of $E_{e^+} \sim 1$ GeV, form about 10% of the total electron density. The standard picture describes such particles as final products of the nuclear spallation reactions, ascribing a secondary nature to them. Indeed, the collision between two nuclei, entails charged pions $\pi^\pm$ and mesons to form, and from those particles positrons take origin as one of the end products of the decay chains. As for the secondary electrons, we have four main possible collisions to produce positrons: either (*i*) protons impinging on hydrogen, or (*ii*) on interstellar helium, or both, (*iii*) α-particles colliding with protons or (*iv*) helium of the interstellar medium (ISM). For the sake of simplicity, here we will briefly review only the chains of processes on the nuclear reactions *proton-proton*. For kinetic energies below 3 GeV, the main channel to generate positrons requires the resonance $\Delta(1232)$ to excite. That has a mass of 1.232 GeV/c^2, and decays chiefly ($> 99\%$) in a nucleon and a pion, according to the following scheme of reactions:

$$\begin{aligned} p + H \rightarrow\ & p + \Delta^+ \\ & \hookrightarrow \begin{cases} p + \pi^0 \\ n + \pi^+. \end{cases} \end{aligned} \tag{4.31}$$

Then, the charged pions decay in muons which, subsequently, decay in positrons:

$$\begin{aligned} \pi^+ \rightarrow\ & \mu^+ + \nu_\mu \\ & \hookrightarrow e^+ + \nu_e + \nu_\mu. \end{aligned} \tag{4.32}$$

For protons with higher energies ($E_p \gtrsim 3$ GeV), a direct pion production takes place, through the process

$$p + H \rightarrow\ p + n + \pi^\pm\text{ 's}. \tag{4.33}$$

Moreover, there exists also the possibility that kaons are produced

$$p + H \rightarrow\ X + K^\pm\text{ 's}, \tag{4.34}$$

the decay of whom yields muons (63.44%) and pions (20.92%). These latter, as we have seen before, decay in positrons as end products of the decay chain (for a review about possible decay channels of the particles explained above, refer to Amsler et al., 2008).

In principle, if we know the spectrum of the proton-nuclear component in the regions where the positrons form, we then can compute the injection spectrum of the latter ones in those regions. Indeed, if with $Q_{e^+}(\mathbf{r}, E_e)$ we express the density number of positrons e^+, of kinetic energies E_e, yielded in the unit of volume at the point $\boldsymbol{r}$, per unit time and energy, then we can write the source term for the positrons as follows

$$\begin{aligned} Q_{e^+}(\mathbf{r},\ E_e) = 4\pi \times \sum_{\text{targ}\ =\ H,He} \ \sum_{\text{proj}\ =\ p,\alpha} n_{\text{targ}}(\mathbf{r}) \\ \times \int J_{\text{proj}}(\mathbf{r},\ E_{\text{proj}}) \times dE_{\text{proj}} \times \frac{d\sigma}{dE_e}(E_{\text{proj}} \to E_e), \end{aligned} \tag{4.35}$$

where $J_{\text{proj}}(\boldsymbol{r}, E_{\text{proj}})$ expresses the nucleonic CRs fluxes at the place $\boldsymbol{r}$, $n_{\text{targ}}(\boldsymbol{r})$ is the number density of the target nuclei, and $d\sigma/dE_e$ the cross-section for the positron production. That makes the positron part a unique observable for analyzing the issue of the origin of CRs, since that conversely to primary CRs, of whom we know only the interstellar spectrum (Is), for positrons we can figure out both the injection spectrum and the interstellar one.

4.3.2 The main features of the transport of relativistic electrons

Given the structure of the Galaxy, and its content of matter, the galactic journey of the electrons, before they reach the Earth, is strongly affected by the following interaction processes (Schlickeiser, 2002):

SYNCHROTRON RADIATION, along the cosmic magnetic fields;

INVERSE COMPTON SCATTERING, with photons of ambient gases;

TRIPLET PAIR PRODUCTION (TPP), that is the pair production $e^{\pm}$ by collisions photon-electron;

NONTHERMAL ELECTRON BREMSSTRAHLUNG, in the ambient matter of the ISM;

IONIZATION AND EXCITATION, of atoms and molecules of the interstellar medium, as well as *Coulomb* interactions with the ionized plasmas.

At energies of interest ($E_e > 100$ MeV) for the research carried out during my PhD time, it turns out that only synchrotron losses and Inverse Compton - on both the stellar and the CMB photons - are crucial, as deeply argued in the next chapters of the present THESIS. A relativistic electron, as well as a positron, have an energy variation rate equal to (Berezinskii et al., 1984)

$$\frac{dE_e}{dt} = -\frac{32\pi c}{9}\left(\frac{e^2}{m_e c^2}\right)\frac{c}{(mc)^2}\left(w_{\text{ph}} + \frac{\mathcal{B}^2}{8\pi}\right)E_e^2, \tag{4.36}$$

which means that the absolute value of the energy-loss rate increases with the square of the energy itself. To apply the Eq. (4.36), it is convenient to rewrite it in the following form:

$$\frac{dE_e}{dt} = b^{\text{loss}}(E_e) = -b_0 E_e^2 - 8\cdot 10^{-17}\left(w_{\text{ph}} + 6\cdot 10^{11}\frac{\mathcal{B}^2}{8\pi}\right)E_e^2, \quad \text{GeV s}^{-1} \tag{4.37}$$

Here, $w_{\text{ph}} = w_{\text{cmb}} + w_{\text{isrf}}$ is the photon energy density, in units of eV cm^{-3}, w_{cmb} e w_{isrf} specify the energy density of the CMB radiation, and of the

interstellar photon fields (ISRF). As argued in more detail hereafter, electrons and positrons detected on Earth, with energies larger than a few hundreds of GeV, are typically of local origin. Therefore, it is reliable the hypothesis of assuming an isotropic radiation field within the diffusive halo, as stated in Eq. (4.36). Also, $\mathcal{B}$ is the average galactic magnetic field strength (G), E_e is the electron (or positron) energy (GeV), and m_e and e are the rest mass and the charge of the electron, respectively §.

From Eqs. (4.36) and (4.37), it follows that as the energy losses of relativistic electrons increase, with increasing energy, in correspondence of that a decrease of the characteristic lifetime happens. An electron (or positron) having an initial energy E_i at time $t_i = 0$, after a time t will be seen with an energy E_e equal to

$$E_e(t) = \frac{E_i}{1 + b_0 E_i t}. \tag{4.38}$$

Hence, it is straightforward to introduce a time scale characterizing the energy losses, $\tau_{e^\pm}$, after that the electron will halve its starting energy:

$$\tau_{e^\pm}(E_i) = \frac{1}{b_0 E_i}. \tag{4.39}$$

For conventional values of the galactic magnetic field, $\mathcal{B} \approx 4\mu$G, and of the energy density of photons, $w_{ph} \approx 1$ eV cm^{-3} (Berezinskii et al., 1984), it turns out $b_0 \approx 10^{-16}$ GeV s^{-1}, and from Eq. (4.39) we get a lifetime (in years) equal to

$$\tau_{e^\pm}(E_e) \sim 3 \times 10^5 \left(\frac{1 \text{ TeV}}{E_e(\text{TeV})} \right) \text{ yr}. \tag{4.40}$$

In a time $\tau_{e^\pm}$, in the case of diffuse propagation, the particle will move on average a distance (in parsecs)

$$\lambda_{e^\pm} \approx (2 D_0 \tau_{e^\pm})^{1/2} \sim 3 \times 10^2 \left(\frac{1 \text{ TeV}}{E_e(\text{TeV})} \right)^{1/2} \text{ pc}, \tag{4.41}$$

where, to get a simple estimate, I choose a typical constant value of the diffusion coefficient $D_0 \approx 10^{29}$ cm^2 s^{-1}, at energies of orders of 1 TeV.

In reality, the resultant electron spectral shape - detected on Earth - turns out to be susceptible to the parameters relevant to the several processes influencing the propagation within the Galaxy: the spatial distribution of the sources, the size of the galactic magnetic halo, the reacceleration in the interstellar space, *etc*. In particular, taking in account the possible energy dependence of the diffusion coefficient, $D \propto (E_e/E_0)^\delta$, the average path length of an electron is properly defined as:

$$\begin{aligned} \lambda_{e^\pm}(E_e, E_i) &\equiv \left(\int_0^{\tau(E_e)} D(E'_e) d\tau' \right)^{1/2} \\ &= \left(\int_{E_i}^{E_e} \frac{D(E'_e)}{b^{\text{loss}}(E'_e)} dE'_{e^\pm} \right)^{1/2} = \left(\frac{D_0 E_e^{(\delta-1)}}{(1-\delta) E_0^\delta b_0} \right)^{1/2}. \end{aligned} \tag{4.42}$$

As an example, we may determine the *mean free path* of an electron across its galactic trip, making reference to the parameters relative to the diffuse

§ **NOTE.** The magnetic energy density, $\mathcal{B}^2/8\pi$, shown in Eq. (4.37), is considered in eV cm^{-3}, and the reason for the numerical factor $6 \cdot 10^{11}$ is connected to the change of units: G $\rightarrow$ eV. Indeed, 1 G = 1 erg$^{1/2}$cm$^{-3/2}$, 1 erg = 10^{-7} J, and 1 eV = $1.60217653(14) \cdot 10^{-19}$ J, so that 1 G$^2 \simeq 6 \cdot 10^{11}$ eV cm^{-3}.

model of type *Kolmogorov* ($\delta = 1/3$) - implemented in the numerical package DRAGON as the **KOL** model. This one adopts a normalization equal to $D_0 = 3.6 \times 10^{28}$ cm^{2}s^{-1} (at 1 GeV), for the diffusion coefficient, and a loss term $b_0 = 1.4 \times 10^{-16}$ GeV^{-1} s^{-1}, referred to the position of the Sun; inserting those values in (4.42) we get

$$\lambda_{e^\pm} \sim 6 \times 10^2 \left(\frac{1 \text{ TeV}}{E_e(\text{TeV})} \right)^{2/3} \text{pc}. \tag{4.43}$$

The Eqs. (4.40) and (4.43) imply that electrons and positrons, with energies around few TeV, have to be produced, in a point of the Galaxy, within a distance equal to $d_{\odot\ \text{source}}^{\pm} \sim 300 \div 600$ pc from the Earth, and injected into the galactic material no longer than 10^5 years ago.

4.3.3 The diffuse propagation of electrons in the Galaxy. The transport equation

We describe the electron component of CRs by introducing the function $N_{e^\pm}(\boldsymbol{r},\ t,\ E_e)$, which states the density of particles (electrons or positrons) with energy E_e, at a point $\boldsymbol{r}$ in the Galaxy, at a time t. In the diffusion approximation, the electron density $N_{e^\pm}(\boldsymbol{r},\ t,\ E_e)$ obeys the transport equation

$$\frac{\partial N_{e^\pm}}{\partial t} - \boldsymbol{\nabla} \cdot (D\ \boldsymbol{\nabla} N_{e^\pm} - \boldsymbol{v}_c N_{e^\pm}) + \frac{\partial}{\partial E_e}\ (b^{\text{loss}}(E_e) N_{e^\pm}) = Q_{e^\pm}(\boldsymbol{r},\ t,\ E_e). \tag{4.44}$$

Here, $\boldsymbol{v}_c$ is the velocity of the galactic wind, in charge of the convective transport within the Galaxy, $b^{\text{loss}}(E_e) \equiv dE_e/dt$ is, as antecedently argued, the average rate at which electrons lose energy, and $Q_{e^\pm}(\boldsymbol{r},\ t,\ E_e)$ is the particles source density, per unit of volume and time[¶].

For the sake of simplicity, we shall limit ourselves to the case in which the diffusion scenario dominates the total transport of particles, i.e. in which the inequality $D/(v_c z_h) \gg 1$ is fulfilled, z_h being the characteristic propagation length scale of CRs in the Galaxy.

For an isotropic spatial diffusion in an infinite volume, with $\boldsymbol{v}_c = 0$, and for homogeneous energy losses, the Green function corresponding to the Eq. (4.44) gets the following expression

$$\mathcal{G}(\boldsymbol{r},\ t,\ E_e | \boldsymbol{r}_s,\ t_s,\ E_s) = \frac{\exp\left[-(\boldsymbol{r} - \boldsymbol{r}_s)^2 / 4\lambda_{e^\pm}\right]}{|b(E_e)|(4\pi\lambda_{e^\pm})^{3/2}} \delta(t - t_s - \tau), \tag{4.45}$$

where the subscript s refers to the sources ($E_s \geqslant E$), $\lambda_{e^\pm}(E_e,\ E_s)$ represents the diffusion length scale, as stated in Eq. (4.42), and

$$\tau(E_e,\ E_s) = \int_{E_s}^{E_e} \frac{dE'_e}{b^{\text{loss}}(E'_e)}, \tag{4.46}$$

defines the typical time scale characterizing the energy radiative losses. By definition, the expression (4.45) solves the Eq. (4.44) with a source term of the type $Q_{e^\pm}(r_s,\ t_s,\ E_s) = \delta(\boldsymbol{r} - r_s)\delta(t - t_s)\delta(E_e - E_s)$. The electron

¶ For a complete derivation of Eq. (4.44), the reader shall refer, e.g., to the monographs by Ginzburg and Syrovatskii (1964), and Berezinskii et al. (1984)

density, for a given sources distribution, can then be expressed in terms of $\mathcal{G}$ and $Q_{e^\pm}$ in the following way:

$$N_{e^\pm}(\boldsymbol{r},\, t,\, E_e) = \int\int_{-\infty}^{t}\int_{0}^{\infty} Q_{e^\pm}(\boldsymbol{r}_s,\, t_s,\, E_s)\mathcal{G}(\boldsymbol{r},\, t,\, E_e|\boldsymbol{r}_s,\, t_s,\, E_s)d\boldsymbol{r}_s\, dt_s\, dE_s. \tag{4.47}$$

Analytic solution of the diffusion equation with boundaries

We shall assume that the galactic disc, where we believe the CRs sources are sited, is surrounded by a magnetic halo in which the particles could be confined for long time before they could escape into the interstellar space.

We can imagine the diffusion region simply as a cylinder of radius R and height $2z_h$; for what concerns the condition at the boundary of the halo, Σ, we consider the free escape of particles into the intergalactic space:

$$N_{e^\pm}(E_e,\, \boldsymbol{r})|_\Sigma = 0. \tag{4.48}$$

Finally, the sources of the electrons - injected with a differential energy spectrum in the ISM - uniformly fill up a disc of height $2z_d$ and radius R:

$$Q_{e^\pm}(E_e,\, r,\, z) = \mathcal{Q}_0\left(\frac{E_e}{E_0}\right)^{-\Gamma^e_{inj}}\Theta(z_d - |z|)\Theta(R - r). \tag{4.49}$$

Given that, the Eq.(4.44) admits as solution an expansion in Bessel series (Bulanov and Dogel, 1974):

$$\begin{aligned} N_{e^\pm}(E_e, r, z) = {} & \frac{4\mathcal{Q}_0 E_e^{-(\Gamma^e_{inj}+1)}}{\pi R^2 z_d(\Gamma^e_{inj}-1)b_0}\sum_{n=0}^{\infty}\frac{\sin\left[\pi\frac{z_d}{z_h}(n+1/2)\right]}{(n+1/2)} \\ & \times\cos\left[\pi\frac{z}{z_h}(n+1/2)\right]\sum_{m=1}^{\infty}\frac{J_0(\nu_m\frac{r}{R})}{\nu_m J_1(\nu_m)} \\ & \times {}_1F_1\left(1, \frac{\Gamma^e_{inj}-\delta}{1-\delta}, -\left[\pi^2(n+1/2)^2 + \nu_m^2\frac{z_h^2}{R^2}\right]\frac{D_0 E_e^{\delta-1}}{z_h^2(1-\delta)b_0 E_0^\delta}\right) \end{aligned} \tag{4.50}$$

Here r and z are the cylindrical coordinates, $J_0(x)$ and $J_1(x)$ are the Bessel functions, $\nu_m (m = 1, 2, 3, ...)$ are the zeros of the Bessel function, $J_0(\nu_m) = 0$, ${}_1F_1(\alpha,\, \beta,\, x)$ is a confluent hypergeometric function, and $R \geqslant z_h > z_d$. It turns out interesting to evaluate the solution (4.50) at the position of the solar system $(r_\odot = 0.67R, z_\odot = 0)$, arguing about the asymptotic expressions of $N_{e^\pm}(\boldsymbol{r},\, E_e)$ in various energy ranges.

For low-energy electrons, $(\lambda_{e^\pm}(E_e) \gg z_h)$, the energy dependence of the electron density becomes

$$\begin{aligned} N_{e^\pm}(E_e) \approx {} & E_e^{-\Gamma^e_{inj}}\,\frac{4\mathcal{Q}_0 z_h^2 E_0^\delta}{R^2 z_d D}\sum_{n=0}^{\infty}\frac{\sin[(\pi z_d/z_h)(n+1/2)]}{n+1/2} \\ & \times\sum_n \frac{J_0(0.67\nu_m)}{\nu_m J_1(\nu_m)[\pi^2(n+1/2)^2 + z_h^2\nu_m^2/R^2]}. \end{aligned} \tag{4.51}$$

In the region of intermediate energies, $(z_h \gg \lambda_{e^\pm}(E_e) \gg z_d)$, we write the electron density as

$$N_{e^\pm}(E_e) \approx\; E_e^{-(\Gamma^e_{inj}+1/2)}\,\frac{4\mathcal{Q}_0}{\pi R^2(\Gamma^e_{inj}-1)}\sqrt{\frac{1}{b_0 D}}\sum_m \frac{J_0(0.67\nu_m)}{\nu_m J_1(\nu_m)}. \tag{4.52}$$

Table 4.1: *Qualitative behaviour of the energy spectrum of the electrons in the various energy intervals, in agreement with Eq. (4.54). Coherently with the text, with $\lambda_{e^\pm}(E_e)$ we express the mean free path of* CRE*, that is the average distance an electron of energy E_e covers; $V_{occ}(E_e)$ is the fraction of Galaxy's volume occupied by the electrons of energy E_e; $\tau^{life}_{e^\pm}(E_e)$ states the lifetime, within the Galaxy, of the particles of energy E_e; and $N_{e^\pm}(E_e)$ is the electron plus positron density per interval of energy.*

Energy range	Mean free path	V_{occ}	$\tau^{life}_{e^\pm}$	$N_{e^\pm}$
$E_e \ll E_1$	$\lambda_{e^\pm} \gg z_h$ [a]	$\approx 2\pi R^2 z_h$	$\sim z_h^2/D$	$\sim E_e^{-(\Gamma^e_{inj}+\delta)}$
$E_1 \ll E_e \ll E_2$	$z_h \gg \lambda_{e^\pm} > z_d$ [b]	$\approx 2\pi R^2 \lambda_{e^\pm}$	$\sim 1/(b_0 E_e)$	$\sim E_e^{-(\Gamma^e_{inj}+(\delta+1)/2)}$
$E_e \gg E_2$	$\lambda_{e^\pm} \ll z_d$	$\approx V_{source}$ [c]	$\sim 1/(b_0 E_e)$	$\sim E_e^{-(\Gamma^e_{inj}+1)}$

[a] z_h is the height of the galactic magnetic halo.
[b] z_d is the galactic disc height.
[c] $V_{source} = 2\pi R^2 z_d$, is the volume occupied by the sources.

Lastly, in the interval of high energies, ($\lambda(E_e) \ll z_d$), we get

$$N_{e^\pm}(E_e) \approx E_e^{-(\Gamma^e_{inj}+1)} \frac{4Q_0}{\pi R^2 z_d (\Gamma^e_{inj}-1) b_0} \left[\frac{\pi}{2} - Si\left(\frac{\pi z_d}{2R}\right)\right] \sum_m \frac{J_0(0.67\nu_m)}{\nu_m J_1(\nu_m)}, \tag{4.53}$$

with Si(x) being the integral function.

It is clearly manifest that the energy spectrum of the electrons will turn out to be different as we take in exam various regions of the Galaxy. The above reported asymptotic expressions tell us about the nature of the changes in the electron spectra, which depend upon the scale of propagation of CRs, the distribution of the sources in such region, the diffusion coefficient, and the time variation of energy losses in that specific region of the galactic space.

It is even more instructive to study the qualitative behaviour of the function $N_{e^\pm}$, comparing the length $\lambda_{e^\pm}$ with the physical sizes of the diffuse galactic region of CRs, i.e. the length scale of the magnetic halo z_h, and the disc thickness z_d: constrained by their radiative losses, the average distance covered by the cosmic charged leptons increases as the energy decreases (see Eq. (4.42)). Hence it is straightforward to identify three regions for the energy spectrum $dN_{e^\pm}/dE_e$ - as we see it on Earth - corresponding to the relationship between the three different length scales involved in the problem, $\lambda_{e^\pm}, z_h$ and z_d. In this regard, we may express the electron density like as

$$N_{e^\pm}(E_e) \approx Q_{e^\pm}(E_e) \frac{V_{source}}{V_{occ}(E_e)} \tau^{life}_{e^\pm}(E_e), \tag{4.54}$$

where V_{source} is the volume the sources take up, $V_{source} = 2\pi R^2 z_d$, and $V_{occ}(E_e)$ is the fraction of the Galaxy volume electrons fill up while they are diffusing with energy E_e, whereas particles of energy E_e have, in the Galaxy, a lifetime $\tau^{life}_{e^\pm}$, not strictly connected with the time scale due to the radiative losses (see Eq. (4.39)). Therefore we have:

HIGH ENERGIES , $\lambda_{e^\pm}(E_e) \ll z_d$ or, which is the same, $E_e \gg E_2$. The propagation of electrons is, in this case, strongly dominated by the energy

losses: in this region of the spectrum, the electrons cannot escape from the galactic disc without first losing the major part of their energy budget. In this scenario, the occupation volume is $V_{occ}(E_e) = V_{source}(E_e)$ (case **(a)** in Figure 4.2). The lifetime of the particles is established by their energy losses, and the detected spectrum will be (Figure 4.3)

$$N_{e^\pm}(E_e) \sim \frac{Q_0}{b_0} E_e^{-(\Gamma^e_{inj}+1)}. \tag{4.55}$$

At very high energies, the discreteness of the sources in the disc is a constrictive factor to keep in account. We expect to see an abrupt steepness of the electron intensity when $\lambda_{e^\pm} < l$, this latter being the mean distance between the sources (see the discussion in § 5)

INTERMEDIATE ENERGIES , $z_h \gg \lambda_{e^\pm}(E_e) \gg z_d$, that will translate into the energy condition:

$$E_1 \ll E_e \ll E_2 = \left[\frac{D_0}{z_d^2 E_0^\delta (1-\delta) b_0}\right]^{1/(1-\delta)} \sim 50 \text{ TeV}. \tag{4.56}$$

The estimated value for the energy E_2 has to be put in relation with the parameters of the diffuse **KOL** Model.

The occupation volume, V_{occ}, this time depends on the energy: the electrons of energy E_e will fill up only a volume characterized by a length scale $\lambda_{e^\pm}(E_e)$, $V_{occ}(E_e) \simeq 2\pi R^2 \lambda_{e^\pm}(E_e)$ (case **(b)** in Figure 4.2). Their lifetime in V_{occ} is, in this case, fixed by the radiative losses ($\tau^{life}_{e^\pm} \sim 1/b_0 E_e$), and the resultant spectrum will then assume the form (see Figure 4.3)

$$N_{e^\pm}(E_e) \sim Q_0 z_d \sqrt{\frac{E_0^\delta}{b_0 D_0}} E_e^{-(\Gamma^e_{inj}+1/2+\delta/2)}. \tag{4.57}$$

LOW ENERGIES , $\lambda_{e^\pm}(E_e) \gg z_h$, that is:

$$E_e \ll E_1 = \left[\frac{D_0}{z_h^2 E_0^\delta (1-\delta) b_0}\right]^{1/(1-\delta)} \tag{4.58}$$

The low-energy electrons will diffuse in almost the entire galactic magnetic halo (case **(c)** in Figure 4.2). The observed spectrum is determined unequivocally by the diffuse escape from the halo, and the energy radiative losses will be not influential. Their lifetime in V_{occ} is instead entirely connected to the time particle takes to diffuse from the the sources up to the boundaries of the halo,

$$\tau^{life}_{e^\pm} \approx \frac{z_h^2}{2D_0}\left(\frac{E_0}{E_e}\right)^\delta. \tag{4.59}$$

For example, with reference to the values of the **KOL** model, typical of the diffusion of the type *Kolmogorov*, the behaviour at low energies will arise at energies $E_e \ll E_1 \sim 6$ GeV, where the observed spectrum will be (see also the Figure 4.3)

$$N_{e^\pm}(E_e) \approx \frac{Q_0 z_d z_h E_0^\delta}{2D_0} E_e^{-(\Gamma^e_{inj}+\delta)}. \tag{4.60}$$

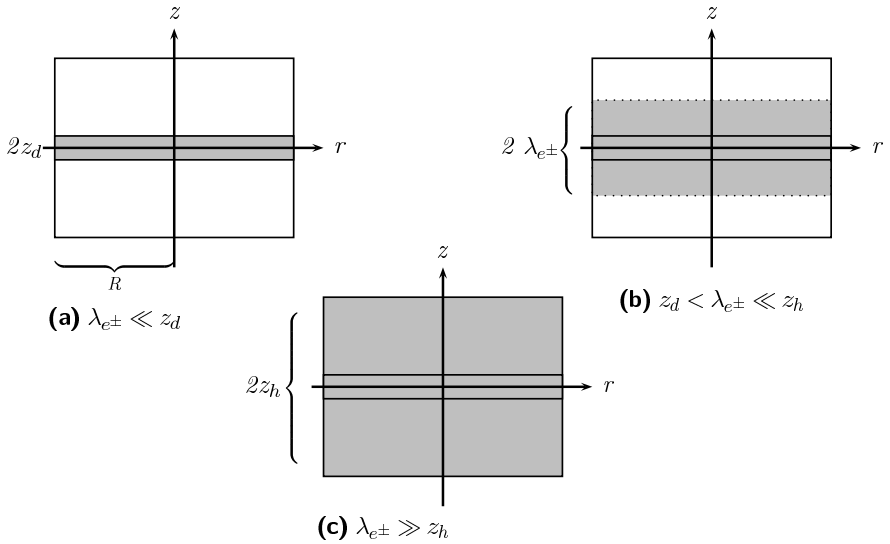

Figure 4.2: *Occupation regions (in gray) for the three possible energy ranges of the electrons, as discussed in the text. After Berezinskii et al., 1984*

From the argument so far discussed, it is evident that the distribution of the electrons (and positrons) is not uniform in the Galaxy, but rather dependent on the energy. From the Figures 4.2 and 4.3, it comes out that more is the energy of the particles, and less is the typical scale of the galactic regions occupied by the particles themselves.

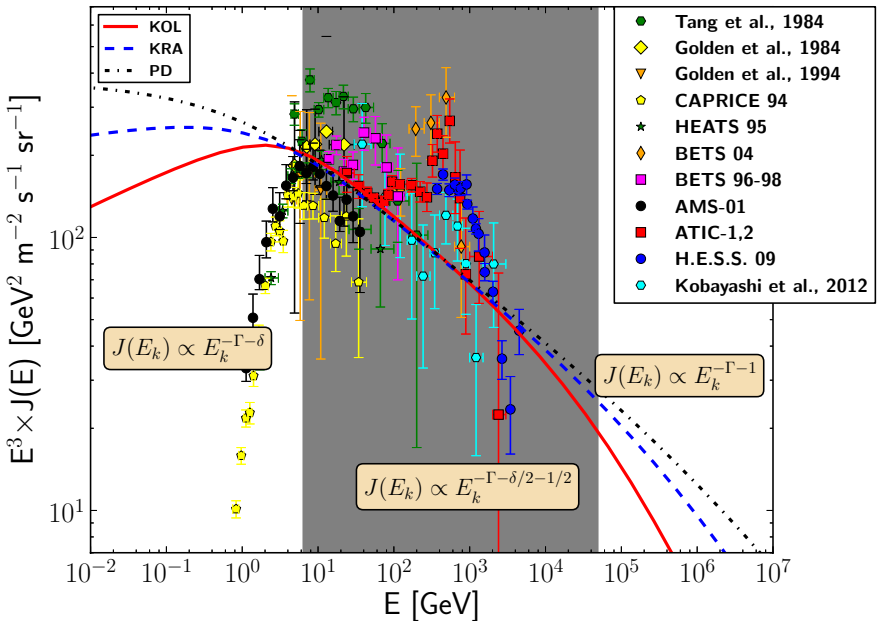

Figure 4.3: *Spectrum of the electrons as predicted by the analytic solution (4.50). The plot clearly points out the three intervals of energy in which a significant change of the behavior of the electron spectrum occurs. For reasons that will be clear in the following sections we report, in comparison, the experimental data concerning the electron plus positron energy spectrum measured, by several experiments (incomplete list), only before 2009 (Tang, 1984; Golden et al., 1984; Golden et al., 1994; CAPRICE 94: Boezio et al., 2000; HEAT 95: DuVernois et al., 2001; BETS 04: Yoshida et al., 2008; BETS 96-98: Torii et al., 2001; AMS-01: Aguilar et al., 2002; ATIC-1,2: Chang and et al., 2005, H.E.S.S.: Aharonian et al., 2009; Kobayashi, Komori, Yoshida, Yanagisawa, et al., 2012). In other words, results got before the Fermi-LAT experiment, Abdo et al., 2009b*

5 ASTROPHYSICAL MODELS FOR GCRE AND THE SYNCHROTRON EMISSION

«Everyday I spend my time
Drinkin' wine, Feelin' Fine
Waitin' here to find the sign,
That I can understand,
Yes I am [...]»
In a broken dream

by Python Lee Jackson
(ft. Rod Stewart; UK, 1972)

In the present chapter, I will present and discuss several astrophysical models aimed to interpret the spectra of electrons and positrons crowding the Galactic Cosmic Rays (GCRs), as they recently have been measured by e.g., the *Fermi*-LAT, PAMELA and AMS-02 experiments. It will serve to the reader as an overview of the current research status, and a general introduction to the papers included in the manuscript.

I will start with tackling the so-called *conventional scenario*, which describes the primary component of Cosmic Ray Electrons (CRE) as accelerated and injected in the Interstellar Medium (ISM) by means of astrophysical galactic sources, as it has been amply discussed in literature, so far (e.g., Berezinskii et al., 1984; Moskalenko and Strong, 1998; Strong, Moskalenko, and Reimer, 2004; Strong, Moskalenko, and Ptuskin, 2007). Secondary electrons, as positrons as well, are instead attributed to byproducts of collisions of CRs nuclei with the rarefied gas of the ISM. In general, the standard cosmic ray propagation picture identifies the SNRs as the most natural candidates to accelerate CRs, electrons in this particular context, and accounts these sources as distributed on large-scale, inside the galactic disc, with a continuous profile. Within such a theoretical framework, we will then talk of interpretation of the observational data based on the *Galactic Cosmic Ray Electrons* (GCRE) *scenario*.

We will see how a model with such attributes is able to reproduce the experimental data published by the *Fermi*-LAT collaboration, about the total flux of electrons and positrons, with a moderate success. At the same time, that specific model turns out to be strongly in tension with those data collected in the region oh high energies ($E_{e^\pm} \gtrsim 1$ TeV). Furthermore, we will then check the inadequacy of a GCRE model when you try to explain the increase of the positron fraction as energy goes up above $E_{e^\pm} \simeq 10$ GeV, a spectral feature already detected by the past experiments (HEAT: Barwick et al., 1997; CAPRICE: Boezio et al., 2000; AMS-01: Aguilar et al., 2002), and confirmed later in 2008 by the spatial observatory PAMELA (Adriani et al., 2009).

Therefore, I will discuss of the prospect to interpret the spectral characteristics revealed by the *Fermi*-LAT satellite, and the *anomaly* of positrons measured by PAMELA, all together, consistently, taking in account the potential contribution to the local flux added by sources either of astrophysical

nature, discretely distributed and possibly "close", in the space and time, to our planet (e.g., Büsching, de Jager, et al., 2008; Büsching, Venter, et al., 2008), or of exotic nature (e.g., Bergström et al., 2009; Delahaye, Lineros, F. Donato, Fornengo, and P. Salati, 2008).

The work presented in this THESIS has been dealing mainly with the astrophysical origins of either primary positrons, e.g. in the magnetosphere enveloping *pulsars* (see e.g. PAPER I), bright celestial objects known to be natural sites of acceleration of pairs of electrons and positrons (e^+, e^-) (e.g., Chi et al., 1996; Harding and Ramaty, 1987; Zhang and Cheng, 2001) - and for that reason destined to be taken naturally in account for the interpretation of the spectrum locally observed - or secondary production (Blasi, 2009) near the SNRs (e.g., PAPER III & IV).

Referring us to an idea proposed for the first time in literature by Shen in the *'70* (Shen, 1970), and evoked later again by Atoyan et al. (1995), in this chapter we will see how it is possible to get an explanation, elegant and simple at the same time, of the features detected in the spectrum of electron CRs locally observed, in particular by the *Fermi*-LAT and by H.E.S.S., in an interval of energy which extends from a few GeVs to above a few TeVs. Indeed, I will show that it is possible to separate the contribution of few local sources (e.g., in our case *pulsars*) from that one of further sources (which are thought to be continuously distributed in the galactic disc) and, conversely to the models GCRE before mentioned, this time I will talk of the *Local Cosmic Ray Electron (*LCRE*) scenario*. Moreover, if we assume that these sources are accelerators of primary positrons and electrons, in equal amounts, the models discussed in this chapter will allow us even to reproduce with success the trend registered by PAMELA, regarding the positron ratio at energies above 10 GeV (Grasso et al., 2009). A similar double component scenario applies even in the case of secondary production of positrons in SNRs.

On the other hand, the annihilation of DM in the galactic halo, represents itself a picture likewise valid and fascinating for the interpretation of the current experimental results, as it has been largely addressed in literature (e.g., M. Cirelli, 2012; Delahaye, Lineros, F. Donato, Fornengo, and P. Salati, 2008; P. Serpico, 2012).

5.1 FERMI-LAT SPECTRUM

5.1.1 The case of the mean distribution of Galactic Cosmic Ray Electrons

Throughout the present subsection, I will present a first possible interpretation of the electron cosmic ray spectrum, both at high energies - as measured in the recent past by the *Fermi*-LAT satellite and H.E.S.S. telescope - and at the lower part of the energy spectrum - as observed by the previous experiments (e.g., AMS-01: Aguilar et al., 2002; and CAPRICE: Boezio et al., 2000). Here, in particular, we will perform our analysis within the conventional scenario of propagation of CRs, and adopting, in this regard, an (almost) exclusively numerical approach.

Unless otherwise specified, the results shown in this subsection, as well as in the next ones, are to be thought achieved by using the `DRAGON` numerical package. I also verified that our results are correctly reproduced by the `GalProp` code, under the same physical conditions. Instead, to model the flux of CRE coming from nearby sources (e.g., pulsars or SNRs), I will fol-

Table 5.1: *Injection and propagation parameters of the electron cosmic rays, relative to the models* GCRE *taken in account in this work*[a]. D_0 *is the coefficient diffusion normalized at* 3 *GV*, δ *is the spectral index of the diffusion coefficient* $D(\mathcal{R})$, *which depends upon the particles rigidity as* $D(\mathcal{R}) \propto \mathcal{R}^{-\delta}$. Γ^{e}_{inj} *is the index of injection power law for primary electrons, and* Γ^{nuc}_{inj} *is the injection index of nucleons. The models* ***S&M***, ***KOL*** *and* ***KRA*** *are based on the diffusive reacceleration picture of* CRS *in the* ISM. *The* ***PD*** *instead is the purely, phenomenological diffusive model, with null Alfvén speed* v_A. *The models* ***S&M***, *and* ***KOL*** *are pretty similar, but they differ each other mostly for the spectral index adopted for the injection of electrons, as specified in the text.*

	Injection index[b]			Diffusion coefficient [c] at 3 GV		
Model	Nucleons Γ^{nuc}_{inj}	Electrons Γ^{e}_{inj}	Break (GV)	D_0 ($cm^2 s^{-1}$)	δ	*Alfvén* speed (km s^{-1})
S&M	1.98/2.42	1.60/2.54	9 4	3.6×10^{28}	0.33	30
KOL	1.60/2.40	1.60/2.50	4 4	5.6×10^{28}	0.33	30
KRA	2.25/2.25	2.00/2.43	4 2	3.0×10^{28}	0.50	15
PD	2.15/2.15	2.00/2.40	4 2	2.4×10^{28}	0.60	-

[a] The height-scale of the magnetic halo for the confinement of CRS is $z_h = 4$ kpc.
[b] Below/above the *break* rigidity, for both nucleons and electrons, respectively.
[c] $D = D_0 \beta^{\eta} (\mathcal{R}/\mathcal{R}_0)^{\delta}$, with $\mathcal{R}_0 = 3$ GV being the reference rigidity. Please note that in the *pre-Fermi* model, in the table labeled as **S&M**, it was custom to choose $\mathcal{R}_0 = 1$ GV (Strong, Moskalenko, and Reimer, 2004).

low a semi-analytical strategy, having developed codes complementary to DRAGON, and interfaced with it: we will have the opportunity to appreciate the potential of those routines in the later on sections of the present chapter.

METHOD In the following, I will refer to the three classes of transport models presented in the § 4.2 which, I remind it, are based on a reacceleration-diffusive scenario of type (*i*) *Kolmogorov*, corresponding - according to the QLT - to a Kolmogorov-like level of ISM turbulence, and typically characterized by fast Alfvén speed (strong reacceleration), $v_A = 30$ km s^{-1}, and a diffusive spectral index $\delta = 1/3$, (*ii*) *Kraichnan*, analogously categorized as a diffusive-reacceleration transport scenario, but with values of the Alfvén speed pretty moderate with respect to the precedent case (weak reacceleration), with index $\delta = 1/2$ and $v_A = 15$ km s^{-1}, and lastly (*iii*) *plain-diffusion*, with $\delta = 0.6$ and Alfvén speed null. The transport parameters have been chosen in order to coherently reproduce as many as observables nowadays available, like for example the secondary-to-primary ratios (e.g., B/C), the ratios of radioactive nuclei fluxes (e.g., $^{10}Be/^{9}Be$), the absolute fluxes of antiprotons, $\bar{p}$, protons, p, and their ratio, $\bar{p}/p$. The propagation models discussed in § 4.2 have been then applied to the case of the electron data set - as released by the *Fermi*-LAT - and numerically implemented in DRAGON. The most important physical inputs each given model assumes are: (*i*) the injection spectrum of the primary CRS, (*ii*) the spatial distribution of the sources (SNRS on galactic scale), (*iii*) the size of the confinement volume of CRS, and (*iv*) the diffusion coefficient; in principle, this latter is allowed to have a physical dependence upon the space coordinates as well as the particle rigidity.

Strong, Moskalenko, and Reimer (2004) proposed a *Kolmogorov*-like conventional model - numerically implemented in GalProp code - in discrete

agreement with the spectrum measured, at that time, up to $\sim \mathcal{O}(1)$ TeV, only by *pre-Fermi* experiments. In literature the name *conventional* was introduced to indicate all those classes of models that assumed the local interstellar spectrum (LIS) as representative of entire galactic environment, in contrast with those models, known as *optimal*, born from the exigency to explain possible fluctuations in the galactic density of CRs. These latter, driven by the EGRET data about the diffuse galactic γ-emission, introduced *ad hoc* diversities between the mean interstellar spectrum and that one measured in the solar neighbourhood. Comparing with the *pre-Fermi* experimental data, the authors assumed, for the primary electrons, an injection spectrum rather "soft", $J_e(E) = E^{-\Gamma^e_{inj}}$, with $\Gamma^e_{inj} \sim 2.5$.

Such a model predicted a CRE spectrum quite at odd predicted with that revealed by *Fermi*-LAT, especially at the very high energies ($E_e \sim \mathcal{O}(1)$ TeV), where it is manifest that the electron flux results instead *harder*.

RESULTS If we want to keep following a conventional approach, with the intent of interpreting the new experimental data, the first step has to be done is, as it is foreseeable, tuning again the spectral index - of the primary electrons - against the new data.

In Table 5.1 I report the most relevant parameters used for the conventional models, namely the GCRE - as they are representative of the *Galactic Cosmic Ray Electrons scenario*. For a standard *Kolmogorov*-like diffusive model, a fair agreement with the *Fermi*-LAT CRE above 20 GeV it was possible by taking up a value equal to 2.50 for the injection spectral index Γ^e_{inj} (model **KRA**, *Diffusive Reacceleration* in Table 5.1, in spite of the "old" *pre-Fermi* index $\Gamma^e_{inj} = 2.54$ (model **S&M** in Table 5.1). Likewise, for a *Kraichnan*-based transport model, with a moderate value of reacceleration, a reliable spectral index for the primary electrons turned out to be $\Gamma^e_{inj} = 2.43$ (model **KRA**, *Diffusive Reacceleration* in Table 5.1). Then, for a purely diffusive model, with $\delta = 0.6$, the optimal injection index has been $\Gamma^e_{inj} = 2.40$ (model **PD**, *Plain Diffusion* in Table 5.1). The flux of the primary electrons, for each model, has been normalized to the reference energy $E_{norm} = 100$ GeV such that

$$J^{norm}_{e^-}(E_{norm}) = \quad 1.3 \times 10^{-4} \quad \text{GeV}^{-1}\ \text{m}^{-2}\ \text{s}^{-1}\ \text{sr}^{-1}. \tag{5.1}$$

Before moving on, it is worthy to remind that the **S&M** model has been officially adopted by the FERMI Collaboration to reproduce the diffuse γ-emission spectrum of the Galaxy, measured by the *Fermi*-LAT at intermediate latitudes (Abdo et al., 2009a). For this reason, we first checked that the γ emissions, via IC and synchrotron predicted by our models were compatible with what shown by the authors in Abdo et al., 2009a. Here, it is sufficient to say that, changing the parameters of the injection, for example $\Gamma^e_{inj} = 2.54 \mapsto 2.50$, between the "old" conventional model *pre-Fermi* **S&M**, and the "new" model **KOL** , implies a variation of only ~ 0.04 in the injection index of the IC, such that the predictions about the diffuse γ at intermediate latitudes are not significantly affected.

The effects of the solar modulation, on the low-energy ($\leqslant 10$ GeV) simulated spectra, were accounted within the force-free field framework, by using a potential equal to $\Phi = 550$ MV; this one tuns out to be very appropriate for the periods of data-taken corresponding to the experiments AMS-01 and HEAT.

Concerning the excess of the electron + positron flux - as predicted by the models taken in account in this subsection - with respect to the H.E.S.S. data

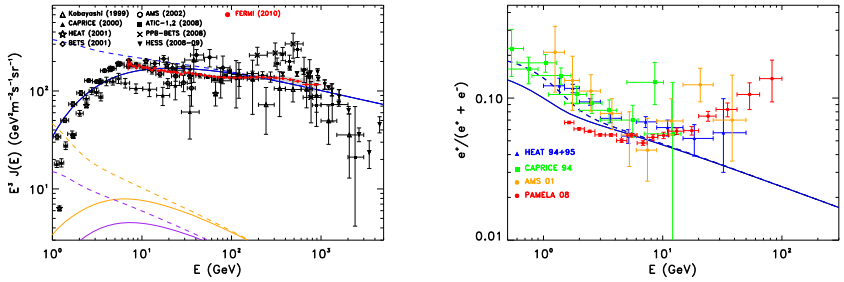

(a) e^+, e^- *spectrum due to the contribution of the galactic background* (GCRE)*, as described in the text.*

(b) *Positron ratio according to the* GCRE *scenario.*

Figure 5.1: ***Left panel****: Theoretical predictions for the flux of* e^+ e^-*, based on the model* GCRE*, discussed in the text. The total electron-plus-positron spectrum is indicated with the blue continuous line.* ***Right panel****: Positron ratio predicted under the same conditions. The chosen model for the* GCRE *component is based on the* KRA *diffusive framework, and strongly ruled out by the* PF *measured by* PAMELA *experiment. Dashed lines are the corresponding* LIS*. The potential modulation applied to our model is* $\Phi = 550$ MV*, in free-force field approximation (Credit:* PAPER I*, Di Bernardo, Evoli, Gaggero, Grasso, Maccione, and Mazziotta (2011)).*

at $E_{e^\pm} \gtrsim 1$ TeV, a viable explanation could be to admit a *cutoff* in the spectrum of the primary electrons at the high energies. Or, even more likely, to give up to the hypothesis of continuous and stationary source distributions in the galactic disc, especially when one enters in the domain of the very high energies ($E_{e^\pm} \gtrsim 1$ TeV), i.e. when the typical diffusion length of such relativistic particles becomes comparable to the average distances between the discrete sources. Indeed, as pointed out in the § 4.3, the radiative losses via IC and synchrotron are, in correspondence of those energies, so efficient to make the lifetime of an electron (e.g., $E \simeq 1$ TeV) drastically shorter (3×10^5 yr), *de facto* forcing the particle to diffuse in the ISM only within few hundreds pc away from its own source. Such a length is comparable with the mean distance between the active SNRs and thus, unless we are in the vicinity of a source of relativistic electrons, the spectrum of the electrons really observed will be inevitably affected by an stronger steepening with respect to that predicted by simple, homogeneous, models considered so far.

To address these effects, it is possible to follow either a *statistical* approach, attempting to estimate the stochastic effects due to the sources, or a *discrete* one which, in spite of the GCRE models, foresees and models also the contribution coming from nearby sources, really existing in nature. In what follows, I will briefly discuss about the first approach, leaving room for a more detailed analysis on the second one.

Stochastic effects of the sources

Quick energy losses, combined with the stochastic nature of the astrophysical sources, imply fluctuations in the spectrum of relativistic electrons: such deviations have to be taken in account if one is going to attempt to give a correct interpretation of the data on CRE detected by the *Fermi*-LAT, and in general data corresponding to the realm of high energies.

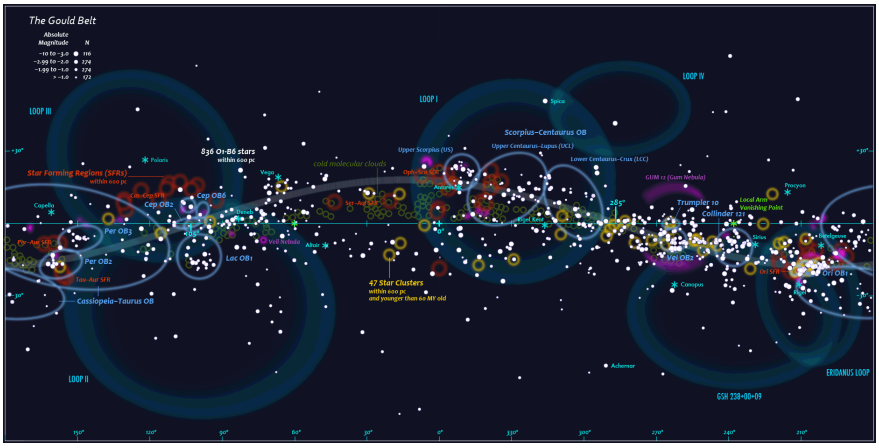

Figure 5.2: *The Belt was first noticed by John Herschel in 1847 while observing in South Africa, then was described and measured by Benjamin Gould during observations for his Uranometria Argentina (1879, the "Flamsteed catalogue" of southern skies). Jacob Halm (1910) identified peculiar proper motions among these stars, and Edwin Hubble (1922) added nearby H II regions and molecular clouds. Viewing the Gould Belt as a large, active star forming region is consistent with the theory that the assembly resulted from a series of about 20 supernova explosions over the past 60 million years - a rate that is about 5 times the Galactic average. It accounts for the many radio loops, nova remnants and neutron stars of varying ages within the region. And it can attribute the "disc" tilt to the remarkable contrast between the Scorpius–Centaurus OB association and the Orion star forming complex (Image credit:* `http://www.handprint.com/ASTRO/galaxy.html`*).*

The idea of considering the local electron-plus-positron spectrum as the result of stochastic fluctuations - in the time and in the space - of the sources distribution, was exploited for the first time by Pohl and Esposito (1998). Actually, a method of this kind was adopted in precedence by Nishmura et al. (1995), but with the remarkable difference that Pohl & Esposito, aiming to reproduce the local spectrum, did not based their computations only on particular, explicitly identified, sources.

Here, I will follow the approach of these latter, presenting what was argued by the authors Grasso et al. (2009), about the interpretation of the *Fermi*-LAT data (Abdo et al., 2009b) and H.E.S.S. (Aharonian et al., 2008, 2009). The main involved parameters concern the source-events rate, as function of the position in the Galaxy, and the injection time of the primary electrons, released in the galactic sea by each source. Other possible effects could be the distribution of the spectral shapes on the population of the sources (as traced by the spectral indexes of the SNRs observed in the radio, and the very likely influence of the spiral arms structure of the Galaxy on the distribution of the sources themselves. For what concerns the injection time, Grasso et al. (2009) chose a value equal to 20 kyr for each source. As for the SNe, they assumed an uniform source distribution, overall in the galactic disc, this latter modelled with a semi-thickness of 80 pc. A time-dependent source distribution was instead taken in account in the *Gould Belt*, the largest feature in the Solar neighbourhood.* The results achieved

* The *Gould Belt* is a ring-like assembly of molecular clouds, star forming regions, and recently formed stars, star clusters and OB associations, about 3000 light years across, tilted toward the galactic plane by about 16-20 degrees. It contains a great number of O- and B-type stars, and may represent the local spiral arm to which the Sun belongs, at about 325 light years away

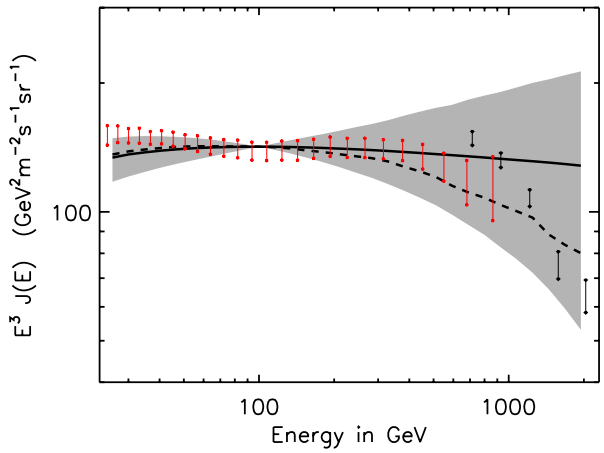

Figure 5.3: *Results of the analytical calculations regarding the stochastic nature of the* CRE *sources, comprised those in the Gould Belts (Grasso et al., 2009). The propagation parameters, here adopted, refer to the Model* **S&M**, *as reported in Table 5.1, and all the spectra are normalized to the fiducial flux at* $E_{norm} = 100$ *GeV. The continuous black line represents the mean spectrum got under the hypothesis that the sources are homogeneously distributed in the galactic disc. The grey region indicates the* $1 - \sigma$ *fluctuation range of the electron flux, at each value of the energy. The dashed line represents instead only a possible random realization of the electron spectrum. The* Fermi-LAT *(Abdo et al., 2009b), and* H.E.S.S. *(Aharonian et al., 2008) data are indicated as black and red lines, respectively.*

suggested that the *Gould Belt* could increase the rate of local SNRs, implying therefore a slightly harder electron spectrum.

The analytical results discussed in the present subsection are shown in Figure 5.3, only for illustrative purposes. There can be seen the fluctuations of the electron flux within $1 - \sigma$ apart from the mean value. In the 32% of the cases, it is found that the electron flux lies outside the grey band. The corresponding uncertainty in the spectral index can be therefore estimated from the aperture angle of the grey band, with a value of $\Delta\alpha = 0.2$ in a range $[10^2 \div 10^3]$ GeV. In other words, the spectral index measured by the *Fermi*-LAT experiment could differ of 0.2 from the mean galactic value, in virtue of such fluctuations. The remaining details of such fluctuating configuration are reported in the caption of Figure 5.3. It is worthy to remind that the authors used the same conditions of the conventional model (model **S&M**) about the propagation of electrons in the galactic medium. This implied a distribution $E^3_{e^\pm} \times J(E_{e^\pm})$ relatively flat. Pohl and Esposito (1998) instead assumed a stronger dependence upon the energy for the diffusion coefficient ($\delta = 0.6$), getting in this way some excesses in the resultant spectrum.

from the arm's centre. The belt is thought to have an age between 30 and 50 million years, and its origins is stil unknown. Among the stars belonging to the Gould Belt, there are many close blue stars belonging to the *Cassiopeia, Perseus, Taurus, Orion, Canis Major* (except the *Sirius* star), ex *Argo Navis (Puppis, Carina and Vela), Crux, Centaurus, Lupus* and *Scorpius* constellations. The Gould Belt has roughly an elliptical shape, with a semi-axis between 354 ± 5 and 232 ± 5 pc (1154 and 756 light years), an height of 60 pc (about 200 hundreds light years) and an inclination between 16 and 20 degrees with respect to the plane of the *Milky Way*. The centre of the belt is made of the *Perseus OB3* association, a member of the association *Taurus-Cassiopeia*. The Sun position is at about half-way between *Per OB3* and *Sco OB2*, a part of the association *Scorpius-Centaurus*. The belt is in expansion and rotates around its centre in a bit different way with respect to the galactic rotation, so that its eccentricity increases not homogeneously: the major axis grows quicker than the minor one.

5.1.2 Modelling the Fermi-LAT spectrum by Local astrophysical sources of Cosmic Ray Electrons (LCRE)

The pulsars (and Pulsar Wind Nebulae) scenario

The idea put forward for the first time in the *1968*, independently each other by Thomas Gold and Franco Pacini, in regard to the *pulsars*, constitutes even nowadays, *43* years since their discovery (Pilkington et al., 1968), the main environmental theory for all the models proposed in literature so far.

Pulsars are described like as neutron stars, rapidly rotating (with a period $P \in [0.001 \div 1]$ s), embedded in an extremely strong magnetic field ($10^9 \div 10^{14}$ G), and produced most likely during the explosions of Supernovae type II (S. L. Shapiro and Teukolsky (1986)). Remarkably, Pacini argued that the neutron stars, in rapid rotation and with intense magnetic fields, could provide for the energy budget necessary to a supernova remnant, like the CRAB NEBULA, to shine for so quite long time; he thus predicted that those spinning magnetized stars might be observable at radio frequencies. In this regard, it is worthy to highlight that the ages of the two young radio pulsars lying in the CRAB and VELA SNRS, as derived from their periods P and time derivative periods $\dot{P}$, are in fairly good agreement with the ages of the two remnants. Moreover, it has been established that the synchrotron radiation emitted from the nebulae are powered by pulsars, most likely through relativistic winds terminated at standing reverse shock waves (Rees and Gunn, 1974). Currently, the number of the sources catalogued as radio pulsars are more than 1000. Only six of them have been classified by the EGRET mission like as high energy gamma ray emitters.

The bulk of the radiation released by the pulsars has to be really imputed to their fast rotation. The rate to which the kinetic rotational energy is getting dissipated, and then converted in luminosity, is defined as the *spin-down luminosity* of a pulsar - an observable which will turn be out very important for our interpretative analysis. Despite pulsars irradiate in the radio band a small fraction ($\lesssim \mathcal{O}(10^{-6})$) of their rotational energy, the γ-luminosity of some pulsars exceeds, above 100 MeV, 1% of their *spin-down luminosity*.

Celestial objects extraordinarily luminous, the pulsars constitute, without any doubts, suitable sites for the production and acceleration of relativistic charged particles, such electrons and positrons, originated in pairs inside the magnetosphere enveloping the central neutron star (in this regard, see the excellent works by Arons (1996a,b,c,d); Blasi and Amato (2011); Chi et al. (1996); Harding and Ramaty (1987); Shen (1970); Zhang and Cheng (2001)). The total γ-luminosity is believed as due mostly to the ultra-relativistic motion of such particles, *stripped off* from the stellar surface by intense, quasi-static, electric fields, themselves induced by the rapid rotation of the magnetized neutron star.

Presently, for what concerns the pulsar γ-ray emission, only two families of models have been exhaustively addressed in literature, and classified as: (*i*) the *polar cap model* (or *inner gap model*), and (*ii*) the *outer gap model*, according to the regions of the magnetosphere candidate to produce and accelerate electrons (see Aharonian, 2004). The grass roots idea, for both the models, is the production of γ-rays through radiative processes occurring in the pulsars magnetosphere, like for example the curvature radiation, IC and the synchrotron radiation.

THE ASTROPHYSICAL PICTURE Discussing the details about the pair $e^{\pm}$ production mechanisms, and the subsequent emission of γ-rays inside the pulsar magnetosphere, goes beyond the goals of the present chapter. Here, I limit myself to emphasize those general aspects that make pulsars ideal astrophysical sources of high energy electron-plus-positron CRs, relevant for the rest of this chapter too (**Serpico**; P. Serpico, 2012).

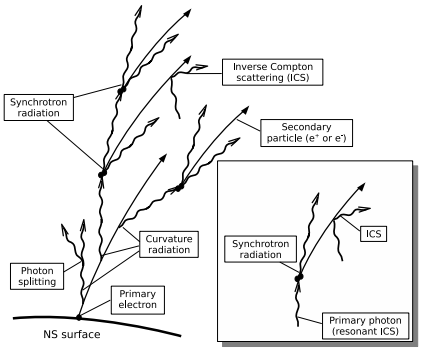

Figure 5.4: *Diagram showing the pair cascades (e^+, e^-), in the magnetosphere of a highly magnetized neutron star, since the beginning of the process, triggered by an high energy electron, until the end of it. The box shows a cascade activated by a photon experiencing a collision of type* IC *(Image credit: Medin and Lai, 2010).*

In the polar cap picture, one can envisages the particle acceleration to occur in the proximities of the stellar surface, namely in connection with the magnetic poles. A decisive role for the emission of the γ-spectrum is played by the radiative cascade processes, triggered by pairs $e^{\pm}$ created via IC and curvature radiation in presence of intense magnetic fields. The γ-spectrum, predicted by such models, shows a super-exponential *cutoff* in energy, typically below 10 GeV.

On the other hand, the outer gap models describe the production of γ-rays as to take place at further distances from the central star, in regions where the local magnetic field gets reduced of several orders of magnitude, compared with the value in correspondence of the neutron star surface: for this reason, the magnetic field is not so enough to absorb γ-rays required for the trigger of the "IC or curvature radiation initiated cascades" $e^{\pm}$, that instead occur only in presence of intense magnetic fields by IC and curvature radiation. Conversely to the polar cap models, that predict γ-spectra with super-exponential cutoffs, in the outer-gap picture the cutoff is due to the maximum energy accelerated electrons can achieve, and for that reason not uniquely determined. In any case, the γ spectrum provided by the outer gap models drops down more slowly than in the polar cap ones.

After their birth, electrons created inside the magnetosphere will start flowing outwards, as a consequence of the rapid pulsars rotation, making a coherent wind of relativistic plasma, and transporting with them the bulk of the rotational energy of the pulsars. Such a wind will end with the formation of a *reverse shock*, which separates the proper wind zone from the *Pulsar Wind Nebula (*PWN*)*, a bubble of relativistic particles crossed by the shock and produced as a consequence of the interaction between the pulsar wind and the ambient medium. The particles originated in the magnetosphere, from now on will remain trapped in the magnetic field of the PWN, having thus many chances of being furthermore accelerated by the shock, up to the moment they may reach so high maximum energies ($\mathcal{O}(10^{15})$ eV), like as the case of young and bright pulsars (Aharonian, 2004). Positron and electron pairs, confined within the nebulae, or in the remnants wrapping the pulsars themselves, will keep being accelerated inside the PWNE, to an extent those bubbles, made of relativistic plasmas, will definitely dissolve

and breaking up in the ISM (for a review on the PWNe, the reader may refer, e.g., to Gaensler and Slane (2006)).

After about $10^4 \div 10^5$ years since the birth of a neutron star, the ambient gas pressure of the ISM will result larger than the magnetic pressure - $B^2_{pwn}/(8\pi)$ - of the PWN. This latter therefore will lose its structure, releasing pairs of electrons and positrons in the ISM, thenceforth free to randomly diffuse in the turbulent magnetic field of the Galaxy. To this day, we do not have experimental evidences of PWNe associated to pulsars older than 100 kyr: this confirm what argued so far in the present subsection. For example, Becker *et al.* 1999, studying the pulsars GEMINGA, PSR B1055-52 and B0656+14 in the X-part of the electromagnetic spectrum gathered by the satellites ROSAT and ASCA, pointed out that those pulsars, of age $\geqslant 10^5$ yr, were devoid of nebulae (Zhang and Cheng, 2001).

Our task will be therefore to compute the amount of charged leptons - irradiated in the galactic sea by the pulsars - giving a substantial contribution to the local electron-plus-positron spectrum. As I pointed out several times in the previous sections, for energies comprised between 100 GeV and 1 TeV, it is logical, and natural as well, to think of the total electron flux reaching the Earth as the sum of a stationary, and homogeneous component (GCRE), accelerated in the SNRs distributed on galactic scales, and the contribution - dominant as the energy goes up - of a few local (LCRE) sources (e.g., pulsars or SNRs).

Assuming that pairs of $e^\pm$ - accelerated in the pulsar magnetosphere - are first confined within PWNe, and then released in the ISM only when the nebulae "melt" in the surrounding ambient, we will focus on a particular class of pulsars, the so-called *mature* pulsars, namely astronomical objects of middle age, with $10^4 \lesssim T_{age} \lesssim 10^6$ yr†. Chi et al. (1996) proposed that pulsars of age $> 10^5$ yr could still represent valid candidate sources of electrons and positrons - diffusing then in the bulk of GCRE- showing that the flux they estimated could reproduce the measurements - available at that time - about the positron fraction. Moreover, even the maximum energy of an electron released by a pulsar is expected to decrease in time, proportionally to the spin-down luminosity of the pulsar itself, Büsching, Venter, et al. (2008) found that middle-aged pulsars actually were still able to accelerate electrons with energies up to a few TeV.

As it is easy to guess, the mechanism of emission of pairs $e^\pm$ up to relativistic energies will depend, for each pulsar, on the possible combination of the several parameters, some of them affected by uncertainties not minimal at all. Yet, not having a solid, and especially unique theory on the injection spectrum, and how to normalize the electron-plus-positron fluxes, we have chosen to follow, in the course of our work, a phenomenological approach, which aimed to show convincingly how it could be possible to get an excellent interpretation of the new experimental data by the *Fermi*-LAT and PAMELA, by just exploiting a reliable set of free parameters involved in this kind of study.

THE ENERGY BUDGET A pivotal parameter to our purposes is, surely, the amount of energy each middle-aged pulsar will set free in the form of pairs $e^\pm$, which then will diffuse in the ISM. To estimate such a quantity, I will adopt the classic scheme that describe the pulsars as "magnetic spinning top", whom dipole axis is not aligned with respect to the spin vector. Let

† A lower cut on age is introduced for discarding sources where (presumably) leptons are still confined in the source.

E_0 and $L_{sd,0}$ be the rotational energy and the spin-down luminosity, respectively, of the pulsar at the time of its birth, and we find out that (S. L. Shapiro and Teukolsky, 1986)

$$E_0 = \frac{1}{2} I \Omega_0^2, \tag{5.2}$$

$$L_{sd,0} = \frac{B_p^2 R^6 \sin^2 \alpha}{6c^3} \Omega_0^4. \tag{5.3}$$

Here, Ω_0 is the initial spin frequency, R the pulsar radius, I the momentum of inertia, B_p the superficial magnetic field, and α is the angle between the spin and magnetic axes. Typically, the energy budget amounts to a value

$$E_0 \approx 2.2 \times 10^{46} \left(\frac{M_{ns}}{1.4 M_\odot} \right) \left(\frac{R_{ns}}{10 km} \right)^2 \left(\frac{\Omega_0}{Hz} \right)^2 \simeq 10^{49} \quad erg, \tag{5.4}$$

or more, mostly converted into a magnetized, relativistic wind in a time τ_0 (see later on for its definition). The reader may notice that the Eq. (5.3) is nothing else but the electromagnetic radiation emitted by a magnetic rotating dipole.‡ The rotational kinetic energy is therefore dissipated by emission of magnetic dipole radiation:

$$I \Omega \dot{\Omega} = -\frac{B_p^2 R^6 \sin^2 \alpha}{6c^3} \Omega^4. \tag{5.5}$$

If we define the "characteristic decay time" of a pulsar like

$$\tau_0 \equiv \frac{E_0}{L_{sd,0}} = \frac{3c^3 I}{B_p^2 R^6 \sin^2 \alpha}, \tag{5.6}$$

we then can integrate over the time the energy-loss equation getting, under the hypothesis of dipole emission,

$$\Omega(t) = \Omega_0 \left(1 + \frac{t}{\tau_0} \right)^{-\frac{1}{2}}, \tag{5.7}$$

$$L_{sd}(t) = L_{sd,0} \frac{1}{\tau_0} \left(1 + \frac{t}{\tau_0} \right)^{-2}. \tag{5.8}$$

As for the decay time τ_0, for the typical parameters of the middle-aged pulsars, it is generally assumed a value of $\tau_0 = 10^4$ yr; since we are interested in the diffusion times typically of the order of $t \geqslant 10^5$ yr, we might simplify the Eq. (5.7), and rewrite it as

$$\Omega_0^2 \simeq \Omega^2(t) \frac{t}{\tau_0}. \tag{5.9}$$

We are now able to determine the energy released in the form of pairs $e^\pm$, from each pulsar taken in account in our future calculations :

$$\begin{aligned} E_{e^\pm}^{pair} &= -f_{e^\pm} \times \int L_{sd}(t)\, dt = f_{e^\pm} \times I \times \int \Omega(t) \dot{\Omega}(t)\, dt \\ &= -f_{e^\pm} \frac{L_{sd,0}}{\tau_0} \times \int \left(1 + \frac{t}{\tau_0} \right)^{-2} dt \approx f_{e^\pm} L_{sd} \frac{t^2}{\tau_0}, \end{aligned} \tag{5.10}$$

‡ In absolutely general form, the slowdown frequency rate is given by $\dot{\Omega} = -K\Omega^n$ - where n is called the *braking* index - yielding a spin-down luminosity $L \equiv \dot{E} = I\Omega|\dot{\Omega}| = KI\Omega^{n+1}$. For simplicity, in the text I referred just to the special case of magnetic dipole, corresponding to $n = 3$.

which at the time $t = T_{age}$ - i.e. the pulsar age - and after Eq. (5.9), becomes

$$E_{e^\pm}^{pair} \approx f_{e^\pm} L_{sd} \frac{T_{age}^2}{\tau_0}, \qquad \text{Energy converted in pairs } e^\pm \tag{5.11}$$

where L_{sd} is the spin-down luminosity at the present time, determined observationally for each pulsar, $T_{age} = P/2\dot{P}$ (where P is the pulsar period) is, as already mentioned, the pulsar age, and $f_{e^\pm}$ represents the efficiency conversion factor of the electromagnetic energy in pairs $e^\pm$.

VERY HIGH ENERGY ELECTRON FLUXES IN THE ISM NEAR THE ACCELERATORS

In the following, I will determine the electron-plus-positron flux released, in the ISM, from all the nearby pulsars currently known, computing semi-analytically the $e^\pm$ spectrum for each one of these objects. Later on, I will sum up the several contributions (LCRE) to the diffuse galactic component (GCRE), computed instead by running the DRAGON code, accordingly to the standard diffusion models argued in the § 5.1. Here, the approach I followed is similar to that one implemented in several works by the authors Atoyan et al. (1995), Aharonian et al. (1997), and Kobayashi, Komori, Yoshida, and Nishimura (2004).

In § 4.3, I pointed out that the evolution of the electron number density ($e^\pm$), diffusing along the magnetic field lines in the Galaxy, can be described through the transport equation

$$\begin{aligned} \frac{\partial}{\partial t} N_{e^\pm}(E_{e^\pm},\, t,\, \boldsymbol{r}) - D(E_{e^\pm}) \boldsymbol{\nabla}^2 N_{e^\pm} = \\ - \frac{\partial}{\partial E_{e^\pm}} (b^{loss}(E_{e^\pm}) N_{e^\pm}) + Q(E_{e^\pm},\, t,\, \boldsymbol{r}), \end{aligned} \tag{5.12}$$

where, as usual, $N_{e^\pm}(E_{e^\pm},\, t,\, \boldsymbol{r})$ is the $e^\pm$ number density per unit of energy, $D(E_{e^\pm})$ is the diffusion coefficient, here assumed spatially uniform, $b^{loss}(E_{e^\pm})$ is the energy-loss rate, and $Q(E_{e^\pm}, t, \mathbf{r}) = dN_{e^\pm}/(dE_{e^\pm} dt\, d\mathbf{r})$ is the sources term, per unit of energy and time. In principle, it is possible to include the effects due to the reacceleration, convection and decays too, but for electrons with $E_{e^\pm} \gtrsim 10$ GeV, and specially on distances of $\simeq \mathcal{O}(100)$ pc, we can serenely neglect such contributions.

As for the diffusion coefficient, I assume an energy dependence of type power-law

$$D(E_{e^\pm}) = D_0 \left(\frac{E_{e^\pm}}{E_0} \right)^{\delta}. \tag{5.13}$$

In order to get a perfect coherence between the sources continuously, and uniformly, distributed in the galactic disc, and those discrete, the normalization and the diffusion index of Eq. (5.13) have been chosen identical to the values implemented in DRAGON, set up to simulate the GCRE models (refer to the Table 5.1). Concerning the energy-loss term, $b^{loss}(E_{e^\pm})$, I will take in account just the effects due to the synchrotron emission and IC scattering, being those processes dominant at the energies of interest ($E_{e^\pm} \gtrsim 10$ GeV),

$$\dot{E}_{e^\pm} \equiv b^{loss}(E_{e^\pm}) = -b_0 E_{e^\pm}^2, \tag{5.14}$$

where $b_0 = 1.4 \times 10^{-16}$ GeV $^{-1}$s $^{-1}$ matches consistently the value inserted in DRAGON at the position of the Sun.

The pulsars considered in our studies are sited at a distances sufficiently large ($d_{\odot\ psr} \gtrsim 100$ pc) so that one can envisages them as point-like sources.

Also, supposing that the bulk of the rotational energy of a pulsar is dissipated by radiation of magnetic dipole - a fraction of this will be then later on converted in pair energy $e^{\pm}$ - it is right to assume a source term like

$$Q_{psr}(E_{e^{\pm}},\, t,\, \mathbf{r}) = Q_{psr}(E_{e^{\pm}})\, \frac{1}{\tau_0} \left(1 + \frac{1}{\tau_0}\right)^{-2} \delta(\boldsymbol{r}), \tag{5.15}$$

in agreement with what written in Eq. (5.8), where one can notice how the pulsar spin-down luminosity changes in time like $L_{sd} \propto t^{-2}$. It follows that a pulsar will radiate the majority of its spinning energy on time-scales of the order of $t \sim \tau_0 \lesssim 10$ kyr, that is over times much less than those typical of the electron propagation, $t \gtrsim 100$ kyr. As a consequence, we can formally take the limit $\tau_0 \to 0$

$$\frac{1}{\tau_0} \left(1 + \frac{t}{\tau_0}\right)^{-2} \Bigg|_{\tau_0 \to 0} \to \delta(t), \tag{5.16}$$

and modelling then the pulsars not only like point-like, but also impulsive (or *bursting*) sources, provided with a spectrum that, without loss of generality, reads

$$Q_{psr}(E_{e^{\pm}},\, t,\, \boldsymbol{r}) = Q_{psr}(E_{e^{\pm}})\delta(t - t_0)\delta(\boldsymbol{r}). \tag{5.17}$$

Here, the reader can recognize in t_0 the injection time, namely the instant in which the charged particles confined inside the PWNe will be set free in the ISM, and $\boldsymbol{r}$ the distance from the source. Such a burst-injection model seems appropriate to the mature pulsars considered in our analysis.

For an impulsive and point-like source, with an energy spectrum given by the Eq. (5.17), the solution to the transport equation will be (Atoyan et al., 1995)

$$N^{psr}_{e^{\pm}}(E_{e^{\pm}},\, t,\, \boldsymbol{r}) = \frac{Q_{psr}(E_0)\; b^{loss}(E_0)}{\pi^{3/2}\; b^{loss}(E_{e^{\pm}})\; r^3_{diff}} \exp\left\{-\left(\frac{r}{r_{diff}}\right)^2\right\}, \tag{5.18}$$

where E_0 corresponds to the initial energy of the particles that, in a time $(t - t_0)$, will be *cooling down* to an energy $E_{e^{\pm}}$, i.e., from Eq. (5.14),

$$E_0 = \frac{E_{e^{\pm}}}{1 - E_{e^{\pm}} \cdot\; b_0(t - t_0)}, \tag{5.19}$$

and $r_{diff} \equiv r_{diff}(E_{e^{\pm}}, t)$ is the "diffusion horizon", namely the distance of propagation over the which an electron will lose half of its energy budget. It only remains to specify the energy dependence of the source term.

In our computations we assumed that the energy spectrum of the particles injected in the ISM, $Q(E_{e^{\pm}},\, t,\, \boldsymbol{r})$, has the following form

$$Q_{psr}(E_{e^{\pm}},\, t,\, \boldsymbol{r}) = Q_0 \left(\frac{E_{e^{\pm}}}{1\ \mathrm{GeV}}\right)^{-\Gamma_{e^{\pm}}} \exp\left(-\frac{E_{e^{\pm}}}{E_{cut}}\right) \delta(t - t_0)\delta(\boldsymbol{r}), \tag{5.20}$$

where $\Gamma_{e^{\pm}}$ is the injection spectral index, and E_{cut} is the exponential-cutoff energy. These latter parameters are, to the present day, quite affected by uncertainties(cit.): from the radio observations of the synchrotron radiation, and the IC photons emitted from the PWNe, we realize that we can only set a reliable range of values for those parameters. The Q_0 coefficient is instead a normalization factor, determined by the condition

$$\int Q_{psr}(E_{e^{\pm}}) E_{e^{\pm}}\, dE_{e^{\pm}} = E^{pair}_{e^{\pm}} = f_{e^{\pm}} L_{sd} \frac{T^2_{age}}{\tau_0}. \tag{5.21}$$

In this particular case, the solution to the transport equation becomes then

$$N^{psr}_{e^\pm}(E_{e^\pm}, t, \boldsymbol{r}) = \frac{Q_0}{\pi^{3/2}\, r^3}\left(1-\frac{E_{e^\pm}}{E_{max}}\right)^{\Gamma_{e^\pm}-2}\left(\frac{E_{e^\pm}}{1GeV}\right)^{-\Gamma_{e^\pm}}\left(\frac{r}{r_{diff}}\right)^3 \times \exp\left\{-\frac{E_{e^\pm}}{(1-E_{e^\pm}/E_{max})E_{cut}}\right\}\exp\left\{-\left(\frac{r}{r_{diff}}\right)^2\right\}, \tag{5.22}$$

in an interval of energy $E_{e^\pm} < E_{max}$ (0 elsewhere), in correspondence of the which the diffusion distance becomes

$$r_{diff}(E_{e^\pm}, t) \simeq 2\sqrt{D(E_{e^\pm})(t-t_0)\,\frac{1-(1-E_{e^\pm}/E_{max}(t))^{1-\delta}}{(1-\delta)E_{e^\pm}/E_{max}(t)}} \tag{5.23}$$

with E_{max} defined as the maximum energy an electron can achieve while it is diffusing within the Galaxy in an interval of time $(t-t_0)$,

$$E_{max}(t) = \frac{1}{b_0\,(t-t_0)}. \tag{5.24}$$

We may notice that the sources throwing in electrons at an instant t_0, such that $(t-t_0) \ll \tau_{diff} \simeq r^2/D(E_{e^\pm})$, definitely cannot contribute to the total flux reaching the observer at a later time t, and for that reason I will not consider those sources in the following analysis.

A relevant parameter in determining the electron spectral shape, in the domain of very high energies, is the ratio $\varepsilon \equiv E_{cut}/E_{max}$, between the energy cutoff at the injection, and the maximum arrival energy: the value of this latter is influenced by the heavy energy losses affecting the journey of the lepton pairs before they reach the Earth. If $\varepsilon > 1$, then the exponential-cutoff at the source will not play any role, at all, and the spectrum of the electrons, due to a single nearby source, could be strongly suppressed above the energy E_{max}. In the opposite case, ($\varepsilon \ll 1$), instead one may expect a cutoff significantly smoother. The above considerations may be determinant when one attempts to distinguish between a pulsar- and a *Dark Matter*-based interpretative scenario of the CRE recently measured, as we will see later on.

Since the extra-component does not affect the low-energy tail of the CRE, and the secondary positron spectrum too, the method to fix the GCRE- as previously explained - holds in the present discussion as well. Therefore, in the following of our computations, to model the spectrum - on the large-scale - due to the galactic component (GCRE), we will adopt the propagation parameters relative to the **KRA** set up, (see Table 5.1), but an injection with $\Gamma^e_{inj} = 2.65$, in order to leave room for the extra-component. Such strategy is similar to the approach in Grasso et al. (2009), with the difference that a **KOL** set up was used in that work[§]. Relevant propagation parameters have been fixed against nuclear cosmic ray experimental data set. Similar results can be obtained with a **PD** set up too (see PAPER I).

The contribution of local pulsars: results from Paper I

In order to account the possible contribution, to the total CRE spectrum, due to the pulsars, we first considered the case in which a few, *nearby* and *mature* pulsars - and for a representative choice of the relevant parameters - could

§ I actively took part to the realization of that work, while I was completing my undergraduate studies at the Department of Physics in Pisa, Italy

give their significant contribution to the high-energy electron flux arriving on the Earth.

We selected the candidate sources by consulting the radio-pulsars ATNF[¶] catalogue, taking care of choosing only those pulsars relatively close to the Earth, at distances $d_{\oplus psr} \lesssim 2$ kpc, and of middle age, i.e. older than $T_{age} \gtrsim 5 \times 10^4$ yr. This latter request derives from the arguments presented in § 5.1.2, where I pointed out the fact that younger pulsars, e.g., VELA ($d_{\oplus\ Vela} = 290$ pc, $T_{age}^{Vela} = 1.1 \times 10^4$yr), do not presumably play any role, since that the pairs of electrons and positrons produced in their magnetosphere would be still confined in the PWNe, or in the SNRs wrapping the internal star. In any case, their contribution would regard energies higher than those we are dealing with.

I implemented the analytical solution described in Eq. (5.22) in numerical codes, written in both the programming languages `IDL` and `PYTHON`, with the aim to compute, and diffuse in the ISM, the flux of primary $e^{\pm}$, injected by each one of the pulsars here considered. From our computations we fond out that, in the set of the candidate sources, most likely MONOGEM (PSR B0656+14), at distance $d_{\oplus\ mon} = 290$ pc and with age $T_{age}^{mon} = 1.1 \times 10^5$ yr, and GEMINGA (PSR J0633+1746), with $d_{\oplus\ gem} = 160$ pc and age $T_{age}^{gem} = 3.7 \times 10^5$ yr, pulsars could give a significant contribution to the total flux of electrons and positrons, in the high energy part of the spectrum. The spin-down luminosities seen in correspondence of these two pulsars are $L_{sd}^{mon} \simeq 3.8 \times 10^{34}$ erg s^{-1} and $L_{sd}^{gem} \simeq 3.2 \times 10^{34}$ erg s^{-1}, respectively.

Hooper et al. (2009) showed that, as for the data relative to only the positron fraction measured by PAMELA, this latter could be reproduced under the hypothesis that MONOGEM and GEMINGA injected lepton pairs with a spectrum of the form shown in Eq. (5.20), and with a value for the spectral equal to $\Gamma_{e^{\pm}} = 1.5$[‖]. Our computations have allowed us to find a similar result, extending the validity of such an approach to energies higher than those considered in Hooper et al. (2009).

In Figures 5.6a and 5.6b, I show the spectrum $E_{e^{\pm}}^3 \times J_{e^{\pm}}$, and the ratio of positrons respectively, as predicted by our model, in comparison with the entire experimental dataset at that time available, in particular those published recently by the PAMELA and *Fermi*-LAT collaborations. In our computations, we adopted a value $\Gamma_{e^{\pm}} = 1.4$ for the spectral index of the source. I recall attention to the fact that such a value is compatible with the current *multi-wavelength* observations of the pulsars. Synchrotron emission spectra, seen at radio frequencies, or γ-spectra measured by the EGRET satellite in a range of energy $[0.1 \div 10]$ GeV, have constrained the injection spectral index lying in an interval $1.4 < \Gamma_{e^{\pm}} < 2.2$ (see e.g., Blasi and Amato (2011); Hooper et al. (2009); Profumo (2008), and references therein). In the case of the CRAB PWN, it has been demonstrated that the detected γ-spectrum can be explained in terms of IC emissions by a population of pairs $e^{\pm}$, with a spectrum reproducible by a broken power-law, of index $\Gamma_{e^{\pm}} \simeq 1.5$ up to an energy-break, $E_{break} \sim 200$ GeV, and then, at higher energies, a softer spectrum getting a value much closer to that one found in our interpreta-

¶ http://www.atnf.csiro.au/research/pulsar/psrcat/

‖ The authors Hooper et al. (2009) used, in their own work, a simplified version of the Eq. (5.22), more appropriate for an injection spectrum of type power-law. Although such a simplification does not influence the interpretation of the PAMELA data, as it has been argued in that article, it turns out to be necessary to accomplish the own computations making use of the expression given by the Eq. (5.22), in order to get a correct model of the electron spectrum at energies above a few hundreds of GeV

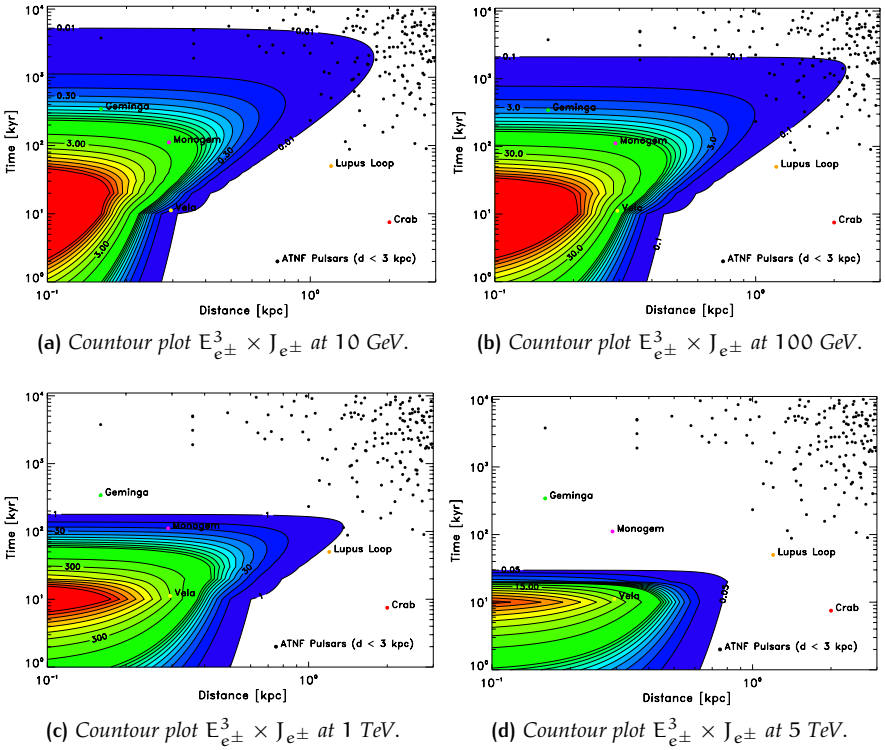

(a) *Countour plot* $E^3_{e^\pm} \times J_{e^\pm}$ *at* 10 *GeV*.

(b) *Countour plot* $E^3_{e^\pm} \times J_{e^\pm}$ *at* 100 *GeV*.

(c) *Countour plot* $E^3_{e^\pm} \times J_{e^\pm}$ *at* 1 *TeV*.

(d) *Countour plot* $E^3_{e^\pm} \times J_{e^\pm}$ *at* 5 *TeV*.

Figure 5.5: *Contour plot of the electron-plus-positron fluxes at different energies, as function of typical distances and ages of the nearby* ($d_{\delta psr} < 3$ *kpc*)*, and middle-aged pulsars* ($10^4 yr \lesssim T_{age} \lesssim 10^6 yr$)*, computed in the case of immediate release of the pairs (bursting sources). The lines show contours of the same value* $E^3_{e^\pm} \times J_{e^\pm}$ $[GeV^2 m^{-2} s^{-1} sr^{-1}]$*, where* $J_{e^\pm}$ *is the flux of electrons and positrons at that energy of interest. Here, for illustrative purposes, I have considered an injection spectrum of* (e^+, e^-) *of type power-law with an exponential-cutoff, with index* $\Gamma_{e^\pm} = 1.7$ *and cutoff* $E_{cut} = 1.1$ *TeV. Moreover, it has been applied a delay at the sources equal to* $\Delta t = 6.5 \times 10^4$ *yr. The propagation parameters refer to a Kraichnan diffusive scenario (Model* **KRA** *in Table 5.1).*

tive analysis (Malyshev et al., 2009). Moreover, since the magnetic field of a PWN, and then the energy losses associated with it via synchrotron, decreases with the age of the pulsars, we expect that the energy-break itself shifts towards higher energies, for pulsars older than the CRAB pulsar, just as the mature pulsars considered in the present work (see e.g., Aharonian et al., 1997).

As for the cutoff in energy, E_{cut}, currently it is a parameter not well known for the mature pulsars, unfortunately. The γ-spectrum emitted by the PWNe of young pulsars - as it has been observed by *Cerenkóv* telescopes (ACTS) like as H.E.S.S. - has been interpreted in terms of the synchrotron emission by electrons with $E_{cut} \approx 10^3$ TeV (Aharonian, 2004). This upper limit represents the maximum energy achievable by the electrons confined in the PWNe and crossed over by the termination shock. Nevertheless, since this quantity decreases as the spin-down luminosity drops down, it is acceptable to expect, in correspondence of older pulsars, a value considerably smaller (see Büsching, de Jager, et al., 2008; Büsching, Venter, et al., 2008).

From the Figures 5.6a and 5.6b, it clearly comes into sight how the data about CRE of PAMELA and *Fermi*-LAT can be reproduced in an optimal way under the same working conditions. In lack of a complete, and consistent

theory able to predict both the energy cutoff E_{cut} and the conversion efficiency $f_{e^\pm}$ of rotational energy in production of pairs $e^\pm$ - as function of the age of the pulsars and their luminosity - we envisaged to attribute the same set of parameters to each pulsar taken in account, taking care of re-normalizing the different parameters involved aiming to get an optimal agreement with the experimental result**.

Furthermore, for all the pulsars we considered the same delay Δt, between the pulsar "birth date" and the time when the PWN merges in the ISM, releasing then electrons and positrons. We found out that our predictions are in remarkable agreement with the entire dataset, and for several different combinations of those parameters. In particular, the models shown in Figures 5.6a and 5.6b have been obtained by using the following parameters: $E_{cut} = 2.0$ TeV, $f_{e^\pm} = 35\%$ and $\Delta t = 75$ kyr. It is worthy to remind that our parameters choice represents only a particular realization of the scenario discussed so far in the present subsection.

Table 5.2: *Physical properties of the pulsars drawn from the ATNF catalogue. B indicates the magnetic field on the star surface, in Gauss [G], and L_{sd} is the spin-down luminosity of each pulsar. For sake of the simplicity, here I report only those pulsar that, according our model described in the text, contribute to the local flux $e^+ + e^-$ within a distance of 1 kpc far from the Earth. Precisely, the complete sample of pulsars within 2 kpc contributing to the flux, as discussed in the text, counts $\approx$ 70 celestial objects.*

Pulsar	Distance [kpc]	Age [yr]	B [G]	L_{sd} [erg/s]
J0633+1746 (Geminga)	0.16	3.42×10^5	1.63×10^{12}	3.2×10^{34}
J1856-3754	0.16	3.76×10^6	1.47×10^{13}	3.3×10^{30}
B0656+14 (Monogem)	0.29	1.11×10^5	4.66×10^{12}	3.8×10^{34}
J0720-3125	0.36	1.90×10^6	2.45×10^{13}	4.7×10^{30}
B0823+26	0.36	4.92×10^6	9.64×10^{11}	4.5×10^{32}
B1133+16	0.36	5.04×10^6	2.13×10^{12}	8.8×10^{31}
B1929+10	0.36	3.10×10^6	5.18×10^{11}	3.9×10^{33}
B2327-20	0.49	5.62×10^6	2.79×10^{12}	4.1×10^{31}
J1908+0734	0.58	4.08×10^6	4.23×10^{11}	3.4×10^{33}
B0906-17	0.63	9.50×10^6	5.25×10^{11}	4.1×10^{32}
B2045-16	0.64	2.84×10^6	4.69×10^{12}	5.7×10^{31}
J1918+1541	0.68	2.31×10^6	9.83×10^{11}	2.0×10^{33}
J0006+1834	0.70	5.24×10^6	1.22×10^{12}	2.5×10^{32}
B0834+06	0.72	2.97×10^6	2.98×10^{12}	1.3×10^{32}
B0450+55	0.79	2.28×10^6	9.10×10^{11}	2.4×10^{33}
B0917+63	0.79	6.89×10^6	2.41×10^{12}	3.7×10^{31}
B2151-56	0.86	5.15×10^6	2.44×10^{12}	6.4×10^{31}
B0203-40	0.88	8.33×10^6	8.80×10^{11}	1.9×10^{32}
B1845-19	0.95	2.93×10^6	1.01×10^{13}	1.1×10^{31}
J0636-4549	0.98	9.91×10^6	2.54×10^{12}	1.6×10^{31}
B0943+10	0.98	4.98×10^6	1.98×10^{12}	1.0×10^{32}
B0053+47	1.00	2.25×10^5	1.27×10^{12}	1.2×10^{33}
B1822-09	1.00	2.33×10^5	6.42×10^{12}	4.5×10^{33}

** The reader may notice that, in any event, such a choice is not critical to reproduce the data.

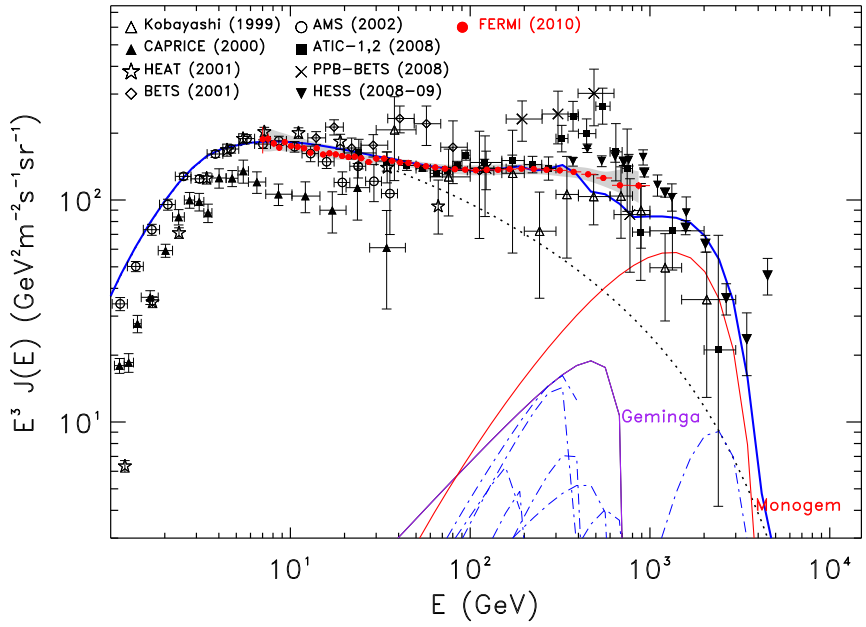

(a) *Electron-plus-positron spectrum computed in the case in which, to the galactic background* (GCRE)*, we add the relevant contribution from local pulsars selected from the* ATNF *catalogue, with distances* $d_{\pm psr} < 2$ *kpc* (LCRE).

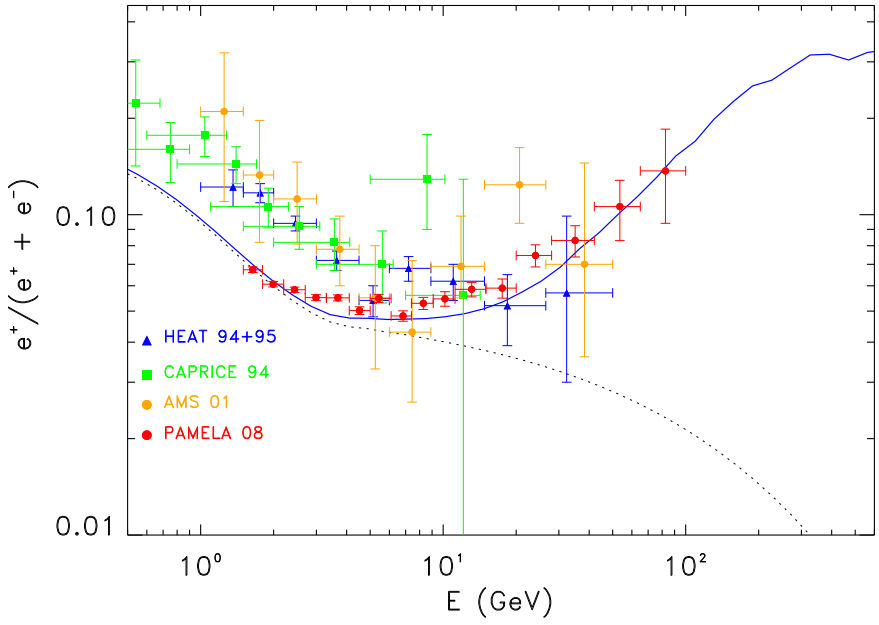

(b) *Positron ratio according to the* GCRE + LCRE *scenario, as shown also in Figure 5.6a.*

Figure 5.6: ***Upper panel****: Theoretical predictions - numerical plus analytical - for the flux of* $e^+ + e^-$*, based on the model* GCRE + LCRE*, discussed in the § 5.1.2, and compared to the entire experimental dataset - at that time available - (Ackermann et al., 2010a; Aguilar et al., 2002; Aharonian et al., 2008, 2009; Chang et al., 2008; Golden et al., 1984, 1994; Kobayashi, Komori, Yoshida, and Nishimura, 2004; Torii et al., 2008). The electron-plus-positron spectrum is indicated in figure with the blue continuous line. The dominant contribution of the pulsars* MONOGEM *e* GEMINGA*, analytically computed, is shown with dot-dashed lines (red and purple, respectively), whereas the* GCRE *component has been computed with* **DRAGON**, *and is shown with a black dotted line.* ***Bottom panel****: Positron ratio predicted under the same conditions of Figure 5.6a. The chosen model for the* GCRE *component is based on the* **KRA** *set up, with an exponential cutoff at 3 TeV. The potential modulation applied to our model is* $\Phi = 550$ MV*, in free-force field approximation (Credit:* ***Paper I****, Di Bernardo, Evoli, Gaggero, Grasso, Maccione, and Mazziotta, 2011).*

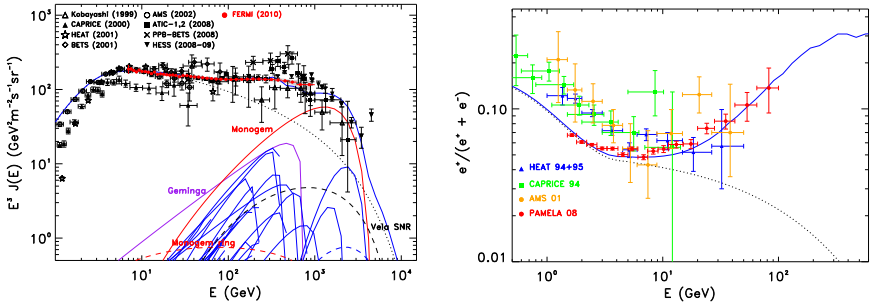

(a) e^+, e^- *spectrum due to the contribution of both nearby pulsars and* SNRs *(*LCRE*), to the galactic background (*GCRE*), as described in the text.*

(b) *Positron ratio according to the* GCRE + LCRE *scenario, as shown in Figure 5.7a too.*

Figure 5.7: ***Upper panel**: Theoretical predictions - numerical plus analytical - for the flux of e^+ e^-, based on the model* GCRE + LCRE*, discussed in the text. The total electron-plus-positron spectrum is indicated with the blue continuous line. **Bottom panel**: Positron ratio predicted under the same conditions of Figure 5.7a. The chosen model for the* GCRE *component is based on the* KRA *diffusive framework, with an exponential cutoff at 3 TeV. The potential modulation applied to our model is $\Phi = 550$ MV, in free-force field approximation (Credit:* PAPER I*, Di Bernardo, Evoli, Gaggero, Grasso, Maccione, and Mazziotta (2011)).*

Adding the contribution from local supernova remnants: results form Paper I

The hypothesis of continuous and stationary source distributions in the galactic disc is clearly not realistic, for the reasons motivated in the § 5.1. On the other hand, if we keep thinking of SNRs as the main sites for the acceleration of CRE - as it is widely accepted among the Astroparticle community - then we are driven to admit that, in the domain of the (very) high energies, $E_{e^\pm} \geqslant 100$ GeV, only few of those objects will give a contribution to the total CRE observed spectrum: in that window of energy, spectral features are potentially observable.

In the PAPER I (Di Bernardo, Evoli, Gaggero, Grasso, Maccione, and Mazziotta, 2011), my colleagues and I addressed such a phenomenon, by treating the propagation of CRE from nearby SNRs, with the same formalism of § 5.1.2, where we addressed the only-pulsars scenario. Here, I limit myself to just reporting the main results achieved, and I refer the reader to the aforementioned paper - attached to the THESIS- for further details. From the GREEN catalogue (Green, 1996), we selected all the SNRs observable within 2 kpc, and looked upon them as point-like sources, of only primary electrons e^- injected on level of the galactic sea with a spectrum of type (5.20). Since the typical lifetime of a supernova remnant is shorter ($\sim 10^4$ yr) than the diffusion propagation time ($\simeq 10^7$ yr), it turns out straightforward to regard those sources as bursting ones. In Figures 5.7a and 5.7b, the results based on the arguments of the present subsection are shown for a suitable choice of the free parameters: $f_{e^\pm} \simeq 30\%$, $\Gamma^{snr}_{e^-} = 2.4$, $E^{snr}_{cut} = 2$ TeV and $E^{snr}_{e^-} = 2 \times 10^{47}$ erg. Under those conditions, from Figure 5.7a it is evident that MONOGEM pulsar plays still the role of favourite candidate source, dominating the scene in the region of $\mathcal{O}$(TeV).

Upper limits on anisotropy: comparison with our CRE model

The distribution of the arrival directions, or *anisotropy*, of the CRs, together with the chemical composition and the energy spectrum of the different components, account for the essential evidences in the exploration of the origins of the CRs, and their propagation between the sources to the observer. In particular, the study of the anisotropy is clearly of great interest to clarify the nature of the motion of the charged relativistic particles, and to localize their candidate sources. Given the peculiar position of the Solar System in the galactic disc, we eventually would expect an anisotropic signal in the direction of the galactic centre ($l \simeq 0, b \simeq 0$), if the CRs sources were distributed uniformly on large-scale, inside the Galaxy.

In the past, researchers have been involving in remarkable experimental efforts, aimed to establish a possible anisotropy in the nucleon component of the CRs. At the present day, unfortunately, there have not been obtained positive results in this regard, but only upper limits of $\simeq 1\%$, at energies of the order $E_{cr} \sim 10^{14}$ eV (Ambrosio et al., 2003). The high degree of isotropy observed in the CRs has to be put in relationship with the disordered motion these particles make when travelling from the sources to the edge of the Solar System: the trajectories are constantly tangled along the irregularities of the galactic magnetic fields, giving rise to a *random walk*. Given the escape time - namely the time CRs take to get out of the galactic edges - of hadron CRs shorter than the characteristic time scale of any other relevant interactions, we can envisage the cosmic ray propagation in the interstellar space as a diffusion, during that the particles loose memory of their initial direction (e.g., see V. S. Ptuskin et al., 2006a).

However, the propagation of CRE differs from that of the hadron-type component in virtue of the heavy radiative energy losses, which drastically limit the motion of the lepton-type species. Charged lepton CRs, although get rapidly isotropic in the ISM magnetic field, they would give rise to a dipole anisotropy - potentially observable in the flux of CRE in the spectrum region around the TeV- if they are produced in the Earth's neighbourhoods, and provided of very high energies (Yoshida, 2008). Several authors have, in the past, pointed out that the emission of electrons and positrons by nearby sources, distant from us a few hundreds of pc, such as pulsars or SNRs, could cause a not negligible anisotropy in direction of those specific sources (e.g., the reader may refer to the works by Büsching, Venter, et al. (2008); Hooper et al. (2009); Kobayashi, Komori, Yoshida, and Nishimura (2004); Mao and Shen (1972)).

In the model described in the subsection 5.1.2, we have speculated about the possibility that MONOGEM and GEMINGA could be, potentially, sources of pairs (e^-, e^+), thus giving a significant contribution to both the total CRE spectrum, at the high energies (100 GeV $\div$ 5 TeV) as measured by *Fermi*-LAT and H.E.S.S., and the raise of the positron fraction above 10 GeV, as observed by the PAMELA satellite. The relatively short angular distance between GEMINGA and MONOGEM, joint to the fact that both the pulsars are sited in the opposite direction with respect to the galactic centre, could cause, at the energies aforementioned, an anisotropy in the flux of CRE locally observed, to be attributed eventually to those sources. Conversely, a possible anisotropy signal due to a *Dark Matter* scenario, should point in direction of the galactic centre, or at most towards local clumps of DM, unlikely in case they were on the same direction of the nearby pulsars. In this subsection I aim to estimate the degree of anisotropy connected to the high

energy electron flux ($E_{e^\pm} \sim TeV$) from local and discrete sources, on the basis of the arguments presented in the previous subsection.

The computation of the anisotropy expected in the flux of electron and positrons, propagating along the directions of the local astrophysical sources, such as pulsars and SNRs considered in the present subsection, requires the use of the notations I have introduced in CHAPTER 3. For an isotropic emission, the particle density N_i (per cm^3) of type i with velocity v is, I remind it, equal to

$$N_i = 4\pi \times \frac{I_i}{v}, \tag{5.25}$$

where I_i is the intensity of the particles. The cosmic ray anisotropy is generally defined as

$$|\zeta| \equiv \frac{I_{max} - I_{min}}{I_{max} + I_{min}}, \tag{5.26}$$

where I_{max} and I_{min} are the maximum and the minimum intensity, respectively, in function of the direction (Berezinskii et al., 1984 and Shen, 1970). In general, the dependence on the direction can be expressed in series of spherical harmonics, $Y_l^m(\theta, \phi)$:

$$I(\theta, \phi) = \sum_{l,m} A_{l,m} Y_l^m(\theta, \phi). \tag{5.27}$$

For our purposes, it is enough to consider the case in which the anisotropy is 1-directional (e.g., a contribution of a single sources is dominant), and therefore we will have all the terms $A_{l,m}$, except the first two, identically null. In other words, we are assuming an angular dependence of the type $I(\theta) = I_0 + I_1 \cos\theta$, with

$$I_0 \equiv \langle I(\theta) \rangle = \frac{1}{2}(I_{max} + I_{min}), \tag{5.28}$$

such that we get

$$\zeta = I_1 / I_0, \tag{5.29}$$

whereas the direction of the vector ζ coincides with the maximum intensity, that is with the direction $\theta = 0$.

As it has often been pointed out throughout the present THESIS, the motion of CRs in the galactic medium is of diffusive nature. Within the theoretical framework of the diffusion approximation, the anisotropy is attributable to the non uniform distribution of the cosmic ray densities. Let $I = I_0 + I_1 \cos\theta$ be the angular dependence of the CRs intensity at the observation point, with $I_1 \ll I_0$[††]. For sake of simplicity, I choose the direction of maximum intensity coincident with the z-axis, in a Cartesian coordinate system. Given that, the net flux of the particles, pointing along the z-axis, is equal to

$$J_z(E) = \int_\Omega I(E, \theta)\, d\Omega = \int I_1(E) \cos^2\theta \sin\theta d\theta d\phi = \frac{4}{3}\pi I_1(E). \tag{5.30}$$

In the diffusion approximation, the cosmic ray flux, along the maximum intensity direction, becomes

$$J_z(E) = -D_{zz} \frac{\partial N(E)}{\partial z}, \tag{5.31}$$

†† **NOTE**. The applicability of the diffusion approximation does not exclude a more complicated angular dependence of I_θ (Berezinskii et al., 1984).

(D_{zz} is a component of the diffusion tensor). From Eqs. (5.30) and (5.31), we get

$$I_1(E) = -\frac{3}{4\pi} D_{zz} \frac{\partial N(E)}{\partial z}. \tag{5.32}$$

As a consequence, the cosmic ray anisotropy is equal to

$$\zeta_z = \frac{I_1}{I_0} = -\frac{3D_z}{\nu N} \frac{\partial N}{\partial z}. \tag{5.33}$$

Assuming the diffusion as isotropic and describable in terms of a diffusion coefficient $D \equiv D(E)$, only energy-dependent, the anisotropy of CRE propagating from a few local sources, can be inferred by the simple relationship (Berezinskii et al., 1984)

$$|\zeta| \equiv \frac{I_{max} - I_{min}}{I_{max} + I_{min}} = \frac{3D}{c} \times \frac{|\nabla N_{e^\pm}|}{N_{e^\pm}}, \tag{5.34}$$

which connect the anisotropy ζ, to the density gradient of electrons and positrons $\nabla N_{e^\pm}$ present in the flux of CRs [n]. The quantities I_{max} and I_{min} represent the total number of the events coming from the hemisphere centred on the direction of the source under investigation, and from the opposite hemisphere, respectively.

In the present thesis, I will present the anisotropy expected in the total flux of CRE due to local accelerators of lepton pairs - among them, MONOGEM and GEMINGA stand out - according to the two scenarios presented so far. Splitting the contribution of the pulsars from the galactic component of the electrons, (GCRE), the total electron-plus-positron density reads

$$N^{tot}_{e^\pm} \equiv N^{lcre}_{e^\pm} + N^{gcre}_{e^\pm}, \tag{5.35}$$

where $N^{lcre}_{e^\pm}$ is the CRE density propagating from the pulsars, or nearby SNRs, as computed in Eq.(5.22), and $N^{gcre}_{e^\pm}$ is the CRE density on galactic scale, numerically computed with the `DRAGON` code. Explicitly, the Eq.(5.34), as referred to few pulsars and SNRs, becomes

$$\zeta = \frac{3}{2c} \frac{r}{t - t_0} \frac{N^{lcre}_{e^\pm}}{N^{tot}_{e^\pm}} \times \left[\frac{1 - (1 - E_{e^\pm}/E_{max}(t))^{1-\delta}}{(1-\delta) E_{e^\pm}/E_{max}(t)} \right]^{-1}, \tag{5.36}$$

in virtue of that, the contribution of GEMINGA, due to its old age, gets negligible, leaving MONOGEM playing the lead role on the stage, in a scenario compatible with what described in 5.1.2, as it is evident also in Figure 5.8.

Remanding to the attached PAPER I (Di Bernardo, Evoli, Gaggero, Grasso, Maccione, and Mazziotta, 2011) for further details, here I briefly summarize the results achieved in this regard:

- the *pure pulsar* model - in which the only emission of extra positrons and electrons from nearby pulsars is added to the GCRE model - is compatible with the upper limits reported by the *Fermi*-LAT Collaboration (Ackermann et al., 2010b). A positive detection could be expected in the near future towards the middle-aged pulsar MONOGEM;

n In literature, quite often the value for the anisotropy is indicated with the symbol δ: in the computations shown in this subsection, I prefer to indicate it differently, to avoid confusion with the diffusion index, also that usually indicated with δ.

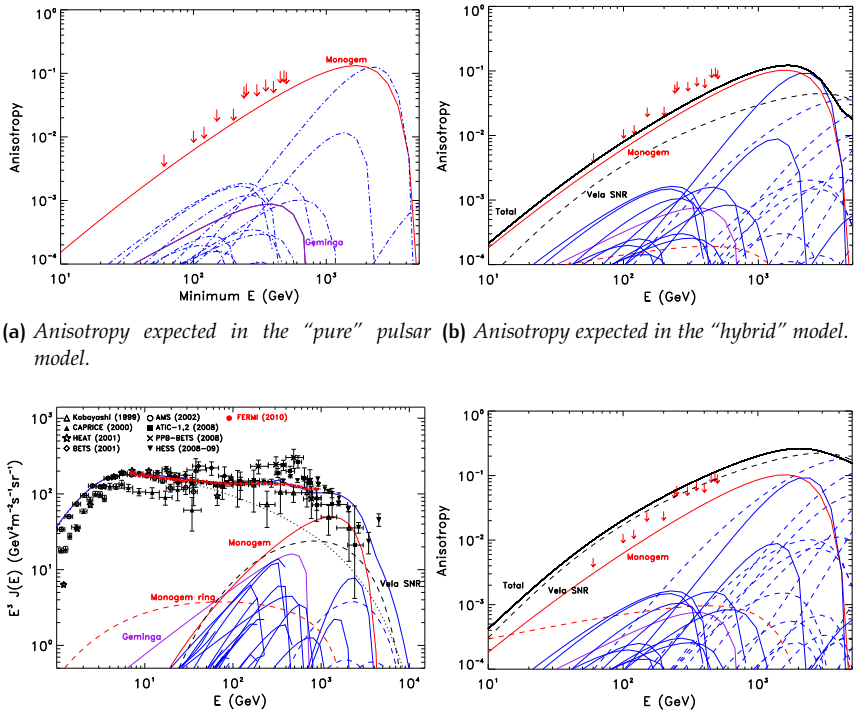

(a) *Anisotropy expected in the "pure" pulsar model.*

(b) *Anisotropy expected in the "hybrid" model.*

(c) *Modified version of the hybrid model.*

(d) *Anisotropy expected in the modified version of the hybrid model.*

Figure 5.8: ***Upper left****: Integrated anisotropy computed in the* GCRE + LCRE *pure pulsar model, compared with the* 95% *C.L.* Fermi-LAT *upper limits;* ***Upper right****: Same comparison, but in the* GCRE + LCRE *hybrid scenario;* ***Bottom left****: Modified version of the hybrid model in which the energy output of* SNRS *is augmented to* 1×10^{48} *erg. Still compatible with the* Fermi-LAT *and* H.E.S.S. *electron data;* ***Bottom right****: A strong contribution from nearby* SNRS *is in clear tension with the* Fermi-LAT CRE *upper limits. (Credit:* ***Paper I****, Di Bernardo, Evoli, Gaggero, Grasso, Maccione, and Mazziotta, 2011).*

- analogously, the *hybrid model* - where it has taken in account also a contribution of only electrons injected by nearby SNRS - is not excluded by the *Fermi*-LAT anisotropy measurements. The total anisotropy (black solid line in Figure 5.8b) is computed as the sum of each anisotropy weighted by the cosine of the angle of the corresponding source with respect to the direction of the maximum flux.

- a scenario in which a larger contribution of electrons emitted by nearby SNRS ($E_{e^-}^{snr} : 2 \times 10^{47} \mapsto 1 \times 10^{48}$ erg) is still able to reproduce the data by *Fermi*-LAT and H.E.S.S. at high energies; nevertheless, it implies an expected anisotropy in evident contrast with the upper limits published by the *Fermi*-LAT collaboration, especially for the large contribution by VELA supernova remnant in the TeV region.

The results found in our work are, in this regard, in good agreement with what published in precedence by several authors, whom works were rather aimed to the only interpretation of PAMELA data (see e.g. Büsching, Venter, et al., 2008; Hooper et al., 2009).

I conclude the present subsection by summarizing, in the next paragraph, the main achievements accomplished in PAPER I

CONCLUDING REMARKS

- The most straightforward evidence that the electron acceleration takes place in SNRs is represented by synchrotron emission observed from those objects. If on the one hand the source spectral index, chosen to reproduce the spectral shape at energies below few GeV, is clearly in agreement with the synchrotron observations, on the other hand requiring an index $\Gamma_{e^-}^{gcré} \approx -2.6$ turns out marginally at odds with the observational constraints, and with the 1^{st} order Fermi acceleration theory. In this regard, we might note that the results achieved in PAPER I are based on the approximation of a large-scale sources distribution of primary electrons (GCRE), uniform and cylindrically symmetric inside the Galaxy. That is not really appropriate for low-mass charged leptons in the energy interval $\approx [0.1 \div 1]$ TeV. A more realistic sources distribution, which takes in account the complex spiral arm structure of the Galaxy, and, as a consequence, of the SNRs distribution as well, is demanded: I will focus more on this aspect in the coming sections (see § 5.3);

- Nearby pulsars are, beyond doubts, realistic source candidates of the $e^{\pm}$ extra-component. To the present day, we still need to give solid, theoretical grounds to the acceleration mechanism, in charge of the electron-plus-positron spectrum emitted by PWNe. However, I want to stress that the values adopted by my colleagues and myself - for the extra-component spectrum - in the aim to well reproduce the raise of PAMELA positron ratio, and the high-energy $e^{\pm}$ *Fermi*-LAT and H.E.S.S. data too, are well suited with the broken power-law spectrum of radiation observed from several PWNe. Those sources can accelerate both electrons and positrons, with a hard spectrum $[E_e^{-1} \div E_e^{-1.8}]$ up to several hundreds of GeV, as it is well discussed e.g. in Blasi and Amato (2011). The main issue about such a scenario (pulsars as $e^{\pm}$ extra-component) might concerns instead the energy converted in pairs: we showed that under reliable conditions, a fraction of the rotational energy is enough to account for the lepton experimental data;

- It is certainly unrealistic to consider all pulsars share the same values of the injection parameters; however such an assumption turned out to be not critical for our results since that, being interested mostly in the high energy tail of the spectrum, this latter is always dominated by a bright single object, namely MONOGEM pulsar, as it is evident from Figure 5.6a. The MONOGEM energy budget, considering an eventual delay equal to ≈ 70 kyr, is $E^{mon} = L_{sd}^{mon}(T_{age} - \Delta t)^2/\tau_0 \simeq 5 \times 10^{47}$ erg (note the spin-down power in Table 5.2);

- Significantly larger spin-down luminosity, hence smaller values for the conversion efficiencies $f_{e^{\pm}}$, are obtained for values of the braking index smaller than $n = 3$, as observed for several pulsars (note e.g. that for the CRAB pulsar $n = 2.5$), which make the *pulsar scenario* even more palatable. The absence of pronounced bumps in the CRE spectrum, around and above the TeV, as predicted in several other papers (see e.g. Kobayashi, Komori, Yoshida, and Nishimura, 2004; Profumo, 2008) and not confirmed in our work (Di Bernardo, Evoli, Gaggero, Grasso, Maccione, and Mazziotta, 2011), it explained by the fact that young, bright - in the GeV and TeV γ-ray sky - sources, e.g. VELA and CRAB, do not contribute to the final spectrum,

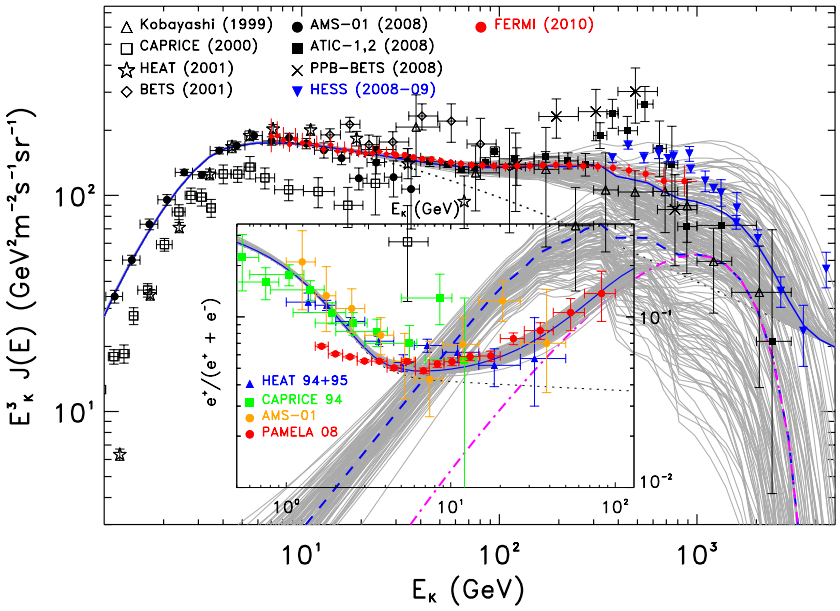

Figure 5.9: *(e^+, e^-) spectrum from multiple pulsars (grey lines, at the bottom in the figure) added to the Galactic diffuse component (dotted black line), compared with the experimental data. Each grey line - top of the figure - represents the total flux for a particular combination of parameters. It is assumed the contribution of all nearby pulsars in the ATNF catalogue with $d_{\odot\ psr} < 3$ kpc and age $5 \times 10^4 < T_{age} < 10^7$ yr, by randomly varying the other relevant parameters: $E_{cut} \in [800 \div 1400]$ GeV, $f_{e^\pm} \in [10 \div 30]\%$, $\Delta t/10^4 yr \in [5 \div 10]$, and $\Gamma_{e^\pm} \in [1.5 \div 1.9]$. The blue dot-dashed (pulsars only) and the blue solid (pulsars + GCRE) lines correspond to a representative choice among the set of possible realizations. The magenta dot-dashed line represents the contribution of the MONOGEM pulsar in that particular configuration. The solar potential modulation is accounted as done in previous figure, that is $\Phi = 550$ MV. Credit: image adapted from Grasso et al. (2009), where a* **KOL** *diffusive set up was used, updating the Fermi-LAT spectrum with data down to 7 GeV (Ackermann et al., 2010a).*

- As shown by in Grasso et al. (2009), it is possible to reproduce the CRE spectrum, and the positron ratio, even allowing combinations of randomly varied pulsar parameters (see Figure 5.9);

- Finally, we believe that an eventual anisotropy observed in the arrival direction of high-energy cosmic-ray electrons and positrons, can constitute a suggestive scientific evidence (a *smoking gun*) in favour of the interpretative scenario centred on the leading role of astrophysical nearby sources, thus so the dark matter annihilation is ruled out as an explanation to the positron excess. In this regard, the detection of such an anisotropy represents a sufficient (but not necessary) condition to discard a Dark Matter origin for the anomalous positron fraction, as it has been pointed out by Profumo (2014). At the same time, it is worthy to outline that the absence of a signal of an anisotropy would not represent a experimental constraint that rejects the idea of an astrophysical origin for the excess $e^\pm$, that has nothing to do with Dark Matter.

5.2 THE SYNCHROTRON EMISSION OF THE GALAXY

Relativistic cosmic ray electrons and positrons, propagating around interstellar magnetic fields lines on spiral trajectories, are at the origin of the diffuse radio emission from the Milky Way.

Synchrotron emission is one of the major Galactic components, from several hundred MHz to several hundred GHz. Its intensity is a measure of the number density of CRE in the relevant energy range, and of the strength of the *total magnetic field* component in the sky plane. As I pointed out since the beginning in § 1 - and throughout the rest of the manuscript - transport and magnetic fields models should be studied simultaneously, because both have influence on the synchrotron modelling. A parallel study of radio emission, and γ-rays as well, together with CRs measurements, can put better constraints on all the ISM components involved. Indeed, the γ-ray and the synchrotron diffuse emissions of the Galaxy offer valuable complementary checks of the low energy spectrum and of the spatial distribution of CRs in the Galaxy. The interpretation of those measurements requires a proper modelling of injection, propagation and losses in the Galaxy.

However, given the significant "contamination" from $p-p$ interaction in the ISM to the total γ-ray luminosity, we restricted our study to the only synchrotron emission, as it offers a more direct probe of the lepton CRs component. The present section is based on the results obtained by my colleagues and I in this regard, as reported in PAPER II (Di Bernardo, Evoli, Gaggero, Grasso, and Maccione, 2013), to which the reader is welcomed to refer for a complete discussion; here I will just briefly point out the main achievements.

GOALS AND STRATEGY We performed a multichannel analysis of cosmic ray electron and positron spectra, and of the diffuse synchrotron emission of the Galaxy by running the DRAGON code[‡‡] with:

- the aim to determine the CRE LIS below ~ 7 GeV, under the condition that the *Fermi*-LAT, PAMELA and H.E.S.S. lepton data were reproduced above that energy.
- The second main goal was to constrain the vertical scale height of the diffusion region in the Galaxy, by reproducing the radio spectrum, the latitude profile of the synchrotron emission and the positron fraction at energies below ~ 5 GeV;
- in order to get a realistic description of the synchrotron emission angular distribution, two main components for the galactic magnetic field (GMF) were taken in account. The ordered component, based on a wide and updated compilation of Faraday rotation measurements, and that random, the main responsible for the CRs diffusion: we assumed it to fill a thick disk with a vertical profile and an effective scale-height z_h;
- for the above purposes, we run DRAGON accounting for a possible spatial dependence of the diffusion coefficient

$$D(\rho, R, z) = D_0 \beta^\eta f(z) \left(\frac{\rho}{\rho_0}\right)^\delta , \tag{5.37}$$

‡‡ In its 2-dimensional version, i.e. with a CRs distribution invariant for rotations about the Galactic disk axis. This is well suited to model the CRE propagation below 10 GeV where energy losses can be neglected. At larger energies the spiral arm distribution of astrophysical sources cannot be neglected since the energy loss length become comparable, or smaller, than the solar system distance from the closest arms.

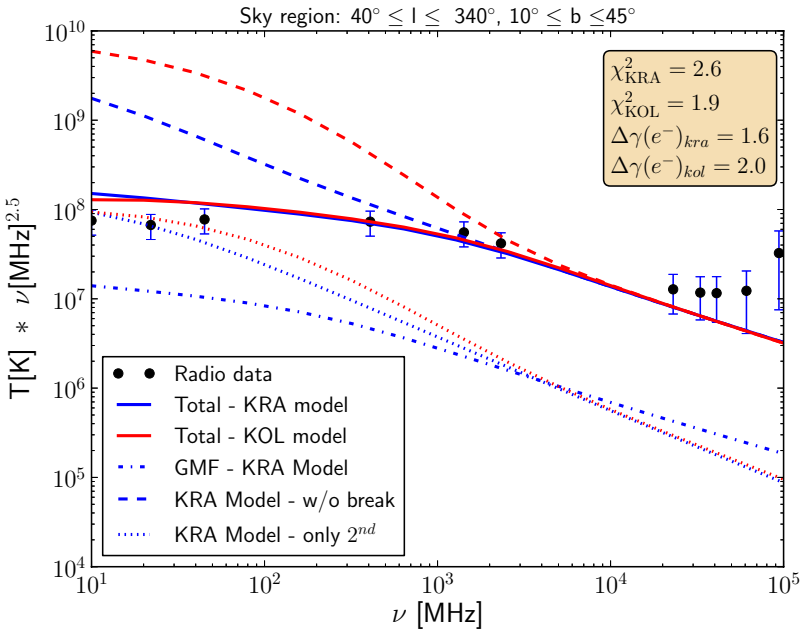

Figure 5.10: *The average synchrotron spectra, computed for the reference propagation set up KRA (blue line) and KOL (red line) - as defined in the text and in the* Paper II *- and compared with experimental data. The magnetic halo-height is* $z_h = 4$ *kpc. For each set up we show the spectra obtained with (solid lines) and without (dashed lines) the spectral break in the* e^- *source spectra. Dotted lines represent the corresponding contribution of secondary* e^- *source spectra. In this figure, as an example, the same spectral break has been adopted. The contribution to the synchrotron flux of the regular GMF with* $B_{halo} = 4\mu G$ *computed for the KRA set up is shown as the dot-dashed line. The random component field strength is tuned to reproduce the spectrum normalization at* 408 MHz. The required normalization is $B_{ran}(0) = 7.6\mu G$. More details are reported in Paper II

ρ being the rigidity of the particle, and $f(z)$ indicates the spatial dependence of the diffusion coefficient. As predicted by the QLT, it should be related to the fluctuating magnetic field as $D(z)^{-1} \propto B_{ran}(z) \propto \exp(-z/z_h)$.

- Four representative classes of propagation regimes were taken in consideration: PD (plain diffusion), KRA (Kraichnan), KOL (Kolmogorov) and CON (convective);
- for each of them, we varied the scale-height of the diffusive halo in the range $z_h = [1 \div 16]$ kpc, and the main diffusive parameters were determined in order to to minimize the combined χ^2 against the boron-to-carbon ratio and the proton observed spectra;
- the spectral index and the normalization of the injection spectrum of the primary electrons and of the extra-component were fixed by fitting the $e^+ + e^-$ spectrum and the positron fraction measured by *Fermi*-LAT, for data above 7 GeV. Below that energy, we modelled the LIS of the $e^+ + e^-$ on the basis of the observed synchrotron spectrum of the Galaxy, which is unaffected by propagation in the heliosphere.

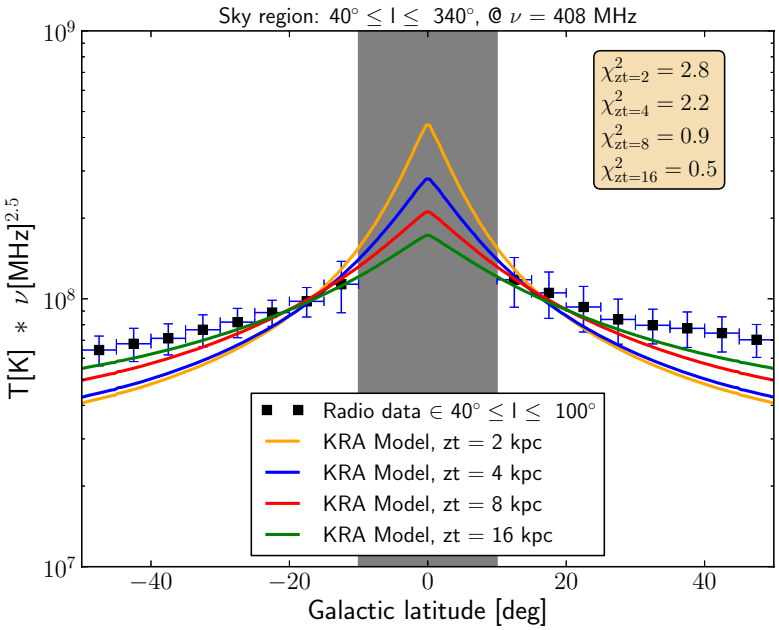

Figure 5.11: *The latitude profile for the synchrotron emission at* 408 MHz, computed for the KRA propagation set up at different magnetic halo height. The grey shadowed region is not considered when placing the constraint. Refer to PAPER II for further explanations.

SYNCHROTRON SPECTRUM We computed the synchrotron spectrum of the Galaxy for the representative models aforementioned, normalizing time to time the value of random component of the GMF in order to fit the observed synchrotron spectrum at 408 MHz. We integrated the Galactic emission along the line of sight and averaged the resulting flux over the sky regions $40° < l < 340°, 10° < b < 45°, -45° < b < -10°$, where l and b are Galactic longitude and latitude respectively. This is the region where the contamination from point-like and local extended sources is expected to be the smallest. In this region we compare the simulated spectra with the ones measured by a wide set of radio surveys at 22, 45, 408, 1420, 2326 MHz as well as WMAP foregrounds at 23, 33, 41, 61 and 94 GHz.

- One of the main implications of this work has been that the radio data are clearly incompatible with a single power-law electron spectrum, suitable to fit the *Fermi*-LAT CRE data. Rather, we find that introducing either a break or an exponential IR cut-off in the primary e^- source spectrum, below a few GeV provides a very good description of the radio data;

- as a consequence, below a few GeV the total electron flux, and hence the radio spectrum below 100 MHz, are dominated by secondary particles, offering thus a probe of the interstellar proton spectrum. In this regard, we found that once the low energy e^- source spectrum is tuned to reproduce the observed e^+ spectrum, only models featuring low re-acceleration can reproduce the observed e^+ spectrum and fraction.

- For the first time in this framework, our modelling of the synchrotron emission of the Galaxy accounts for the presence of the $e^{\pm}$ *charge-symmetric extra-component*, with the form

$$J_0^{e^{\pm}} \propto E^{-\Gamma_{e^{\pm}}} \times \exp(-E/E_{cut}), \quad E_{cut} \approx 1\ TeV. \tag{5.38}$$

  This is required not only to consistently model PAMELA and *Fermi*-LAT high energy data, but also to correctly estimate the e^- source spectrum from CRs and radio data. With our method we exploited the galactic diffuse synchrotron emission as a way to measure the low energy LIS spectrum of CRs, electrons and positrons.

THE MAGNETIC HALO HEIGHT To determine the vertical (perpendicular to the Galactic plane) extension of the CRs diffusion region is one of the main goals of the modern Astro-particle physics. This quantity is crucial not only for conventional CRs physics but also for Dark Matter indirect search, since the local flux of Dark Matter decay and annihilation products is expected to depend significantly on it. So far, this quantity has been constrained on the basis of CRs radionuclide, $^{10}Be/^{9}Be$ ratio most commonly. This method, however, is seriously affected by the uncertainties related to the local distribution of sources, gas, and by solar modulation.

On the other hand, the synchrotron emission of the Galaxy offers instead a much more direct probe of the scale height z_h. Firstly, we may notice that, when a realistic vertical distribution is adopted for the radiation interstellar field and for the GMF, energy losses in the $\mathcal{O}$(GeV) energy range - hence in the radio energy band - do not affect significantly the CRE vertical distribution, determined predominantly by the diffusion and therefore coincident with that of CRs nuclei.

Two main independent arguments to constrain z_h have been adopted:

- for a given propagation set up, the synchrotron flux depends only on the random field normalization $B_{ran}(z=0)$ and on z_h, the scale-height of the diffusion region. The radio data imply a tight relation $B_{ran}^{rms}(z=0) \propto z_h^{-1}$
- we compared the observed latitude profile of the synchrotron emission at 408 MHz to that calculated for the KRA set up, choosing different values for z_h. For each z_h we tune the value of $B(z=0)$ so that the average spectrum in these regions is reproduced. Low values of z_h are disfavoured: a χ^2 analysis showed that $z_h \leqslant 2$ kpc are excluded at 3σ level.
- For the first time, we have placed a constraint on the CRs diffusive halo scale height based on the comparison of the computed synchrotron emission intensity with observations.

5.3 THE IMPACT OF A 3D DISTRIBUTION

The present section serves as a brief introduction to the results presented in the following papers: PAPER III (Gaggero, Maccione, Di Bernardo, et al., 2013) and PAPER IV (Gaggero, Maccione, Grasso, et al., 2014).

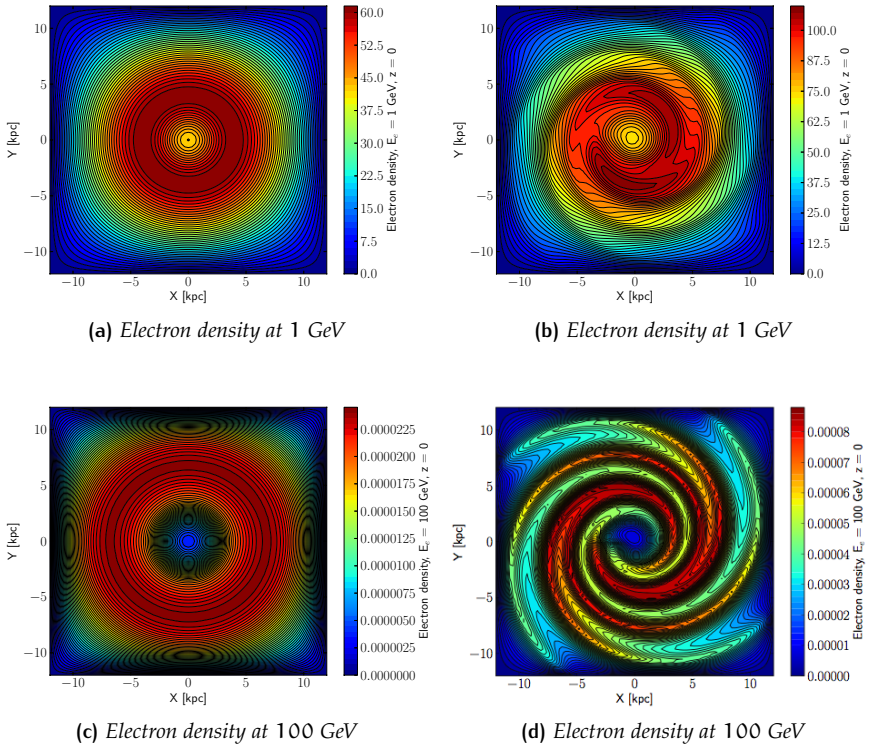

(a) *Electron density at* 1 *GeV*

(b) *Electron density at* 1 *GeV*

(c) *Electron density at* 100 *GeV*

(d) *Electron density at* 100 *GeV*

Figure 5.12: *The face-on view of the primary electron density at different energies, without (left) and with (right) accounting for a spiral arm source distribution.*

For the first time, we used a full 3D version of DRAGON with position-dependent diffusion[o]. In this version, the propagation is calculated within a 3D Cartesian grid and the user is able to implement realistic and structured three dimensional source, gas and regular magnetic field distributions. Moreover, it is possible to specify an arbitrary function of position and rigidity for the diffusion coefficients in the parallel and perpendicular direction to the regular magnetic field of the Galaxy. The code opens many new possibilities in the study of CR physics. In particular, we studied in PAPER III & IV for the first time the impact of the spiral arm structure on the lepton spectra: taking into account the fact that we live in an inter arm region, far from most sources, we obtained - due to increased energy losses - a steeper electron spectrum compared to the assumption of a smooth source term.

Indeed, it is well known that, in order to reproduce the CRE spectra, it is necessary to consider - beyond a conventional component of primary electrons and secondary electrons and positrons - some extra contribution of unclear origin. In this class of models a very steep injection for the primary component is required to match the data: the injection slope is $-2.65 \div -2.70$ depending on the diffusion set up and appears to be in strong tension with

- that inferred from radio observations of SNRS, $\langle \Gamma \rangle = -(2.0 \pm 0.3)$;
- the values $-2.2 \div -2.4$ required to reproduce the CRS nuclei spectra;
- the shock acceleration theory which generally predicts the same spectral index, close to $-2 \div -2.3$.

o A fully anisotropic (this feature is not used in this work) is going to be used in a forthcoming paper released by the DRAGON collaboration

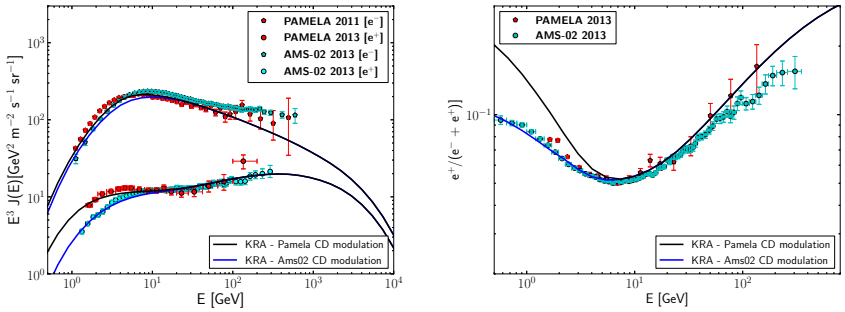

(a) *Electron spectrum* **(b)** *Positron fraction*

Figure 5.13: *Electron spectrum and positron fraction computed assuming for a spiral arm source distribution. See details in the text (refer also to* Paper III & IV*).*

Here instead I present, as an important application of our 3D code, a realistic model in which this serious problem is naturally solved. The idea is to consider the fact that we live in an inter arm region and the bulk of the CRs sources are expected to lay in the arms: the energy losses suffered by the $e^{\pm}$ are highly enhanced with respect to the simple model in which CRs sources are smoothly distributed in the Galaxy, because of the greater average distance that $e^{\pm}$ have to cross to arrive on Earth.

This effect allowed us to fit the observed CRE spectra and the PF, including the new data recently provided by AMS-02, by adopting a CRE injection index very close to the one needed for CRs protons and other nuclear elements. In our model, both the conventional CRs sources and the extra electron-plus-positron source term are located in the arms.

Concerning low energies, we considered the effect of solar modulation using the recently developed HELIOPROP numerical code. Remanding to the aforementioned papers, here I will conclude the present chapter briefly summarizing the main results achieved in this context:

- if the sources are located mainly in the spiral arms, and given that the Sun is located in an inter arm region, the enhanced energy losses permit to reproduce the current electron and positron data with a primary injection spectrum compatible with shock acceleration theory;
- our model allows us to reproduce the AMS-02 PF accounting for an extra-component located in the Galactic arms with a high energy cut-off (10 TeV) and an harder spectrum;
- we also considered the possibility of different values of the cut-off, and we found that values down to 1 TeV yield a good fit the AMS-02 PF;
- the physical interpretation of the extra component, according to the value of the cut-off, may be compatible either with an enhanced secondary production near the accelerator, or or with a pulsar population located in the arms;
- the energetic of the extra component - required in order to fit the data - is compatible with a pulsar or SNRs origin;
- strong reacceleration propagation models are severely disfavoured.

6 EPILOGUE

«Quanta strade che portano a niente
è quanta strada ca ancora amma fà
ciorta ca puorte chistu turmiento
nuje nun' 'nce stancamme maje [...]»
Assaje

by Pino Daniele
(Napoli, 19/03/1955 -)

In a deep cave some people have been caught since their early childhood. They are chained down in a way that they even cannot turn their heads around. They can only see shadows on the walls of their inconvenient shelter, which are cast by a fire blazing in the background. The shadows stem from objects of unknown form and material carried by some servants.

During the years they have given the shadows names and they interpret them as the reality. One of these cave dwellers is able to shake-off his chains and leave the cave. His eyes get dazzled by the light of the Sun at first, but after a while he becomes able to see all the wonderful objects that cast the shadows. And again he names them all and calls them the reality. But, upon his return to his pitiable colleagues, he is far from being welcome: his view of reality has been revolutionised by his stunning experience outside and has nothing more to do with the prisoners' view of reality.

So far Plato' cave parable. It tells us about the relation between our ideas and the objects behind them. We are in a similar situation like the cave dwellers when it comes to exploring the universe. What we can see with the best of our sophisticated technical means are nothing more than shadows of the reality out there and, like the prisoners in the cave, we have to content ourselves with the images on the wall.

But - in contrast to Plato's parable - an unexpected second fire lights up in the background casting additional shadows from the unknown objects onto the wall of our cave. This second fire are the cosmic ray particles that reach us from the depth of the Universe. Apart from the electromagnetic spectrum, where astronomical observations have taken place since mankind started looking at the stars, the CRs are independent and complementary messengers from violent processes in the Universe. That is why CRs are such a fascinating topic, which is still in our days rich of mysteries.

CRs are a major component of the ISM. They share an equivalent energy density with the magnetic field and the interstellar gas. At low energies CRs possibly take an active part in the dynamics of the structures of the ISM. They generate plasma waves and magnetic turbulence. This turbulence has in turn an important role in the evolution of molecular gas and in the star formation cycle. At high energies, CRs are identified by their interaction with the molecular gas and produce neutral and charged pions and secondary particles (γ rays, electron-positron and neutrinos). CRs are also responsible for the spallation nucleosynthesis of light and stable and radioactive elements. They are likely associated with the remnants of su-

pernovae. A large fraction of these supernovae explode as a result of the collapse of the core of massive stars. Massive stars, their evolution and the way they shape their environment appear also to have a central role in the cosmic ray production. CRs turn out to be a key ingredient in the local and global dynamics of the ISM. But this is only very recently since this component started to be integrated in the modelling of the ISM evolution.

The study of CRs has a special role in physics, not only in its own right, but because of the pioneering role that cosmic ray research has played, and is still playing, in the study of elementary particles and their interactions. An extraordinary discovery has recently shaken the foundations of Cosmology and Particle Physics, sparking a scientific revolution that has profoundly modified our understanding of our Universe and that is still far from over. Pioneering astronomers in the 1920s and 1930s had already noticed suspicious anomalies in the motion of celestial bodies in distant galaxies and clusters of galaxies, but it was not until the late 20th century that the scientific community was confronted with an astonishing conclusion: the Universe is filled with an unknown, elusive substance that is fundamentally different from anything we have ever seen with our telescopes or measured in our laboratories. It is called *Dark Matter*, and it constitutes one of the most pressing challenges of modern science.

We are living in the golden age of Dark Matter, where thousands of scientists around the globe are furiously competing to see who will discover the secret of Dark Matter first. It has led to a worldwide race to identify the nature of this mysterious form of matter. We may be about to witness a pivotal paradigm shift in Physics, as we set out to test the existence of Dark Matter particles with a wide array of experiments, including the Large Hadron Collider at CERN, as well as with a new generation of Astroparticle experiments underground and in space.

Studies of high-energy phenomena in the broad area of Cosmoparticle Physics have fundamental importance and are at the frontiers of today's physics and astrophysics. They demand most qualified manpower, and are successfully conducted only at the best universities in the world were they are adequately financially supported. My research at Göteborg University has a significant and visible international impact and enjoys the world-class status. I have been most fortunate in my graduate student career to have had ample opportunity to visit and collaborate with most of the world's leading experts in the subject.

In the next coming years, I plan to concentrate my research in Astroparticle physics around two main problems: (i) supercomputer simulations of time dependent, three dimensional, fully realistic propagation of CRs in our Galaxy aimed, among the other things, to identify the nature of Dark Matter particles through a combined analysis of the experimental results of the Large Hadron Collider at CERN, and of the upcoming generation of Astroparticle experiments, (2) and analytical and numerical studies of nonlinear mode trapping, mode coupling, and parametric resonances in the plasma inhomogeneities, with the aim to revisit the propagation of GCRs in light of recent advances in the non-linear cosmic ray diffusion theory in realistic interstellar turbulence.

Secondary particles production can be cosmic ray antiparticles, searched for by PAMELA, or neutrinos searched for in ICECUBE, emitted from mass concentrations such as the centre of the Earth, the Sun, or the Milky Way. A flux of high energy neutrinos from weakly interacting massive particles (WIMPS) annihilations may be detected in large neutrino telescopes such as

Super-Kamiokande, Antares and IceCube. In fact, the cubic-kilometre sized IceCube neutrino observatory, constructed in the glacial ice of South Pole, searches indirectly for dark matter via neutrinos from dark matter self-annihilations. It has a high discovery potential through striking signatures. IceCube has put constraints on self-annihilating or decaying dark matter in the galactic halo (Abbasi and et al., 2011) and Galactic Center (The IceCube collaboration et al., 2012). Neutrino telescopes may also search for neutrino annihilation from large celestial bodies, such as the Sun (Sivertsson and Edsjö, 2010).

Many Dark Matter models predict the emission of γ-rays, the highest energy photons, as annihilation products, detectable by *Fermi*-Lat (see e.g., M. Cirelli et al., 2013; Tavakoli et al., 2013). Researchers are using γ-ray data from the *Fermi*-Lat to search for the annihilation products. In order to search for these products, the astrophysical foreground have to be well understood before detections or limits on these particles can be derived. In the future the ground-based *Cerenkov Telescope Array* (CTA) will search for Dark Matter annihilation products at even higher masses. We expect that a better understanding of the energy deposition by Dark Matter annihilation will be relevant in particular with the upcoming Planck data, with their better sensitivity, which allow a better constraint of this additional source of ionization.

Therefore, improving our knowledge on cosmic ray transport models represents an essential tool for searching for *Dark Matter signatures*. Without a better understanding of phenomena occurring in the field of High Energy Astrophysics, blind searches for Dark Matter will become more and more challenging. Indirect Detection of Dark Matter is essential to us in order to confirm for example that the properties observed in laboratories are the same responsible for astrophysical and cosmological observations, and to infer cosmological properties of Dark Matter not easily accessible otherwise.

In this context, the aim of my proposed research program is to exploit the experimental results of the Large Hadron Collider at CERN, and of the upcoming generation of Astroparticle experiments, to identify the nature of Dark Matter particles. At the same time, I will devote part of my scientific activity to theoretical aspects of acceleration and escape of Crs from astrophysical sources. A combined analysis of all the different channels together with improved modelling of known astrophysical sources and the propagation of Crs may actually help to discriminate among various scenarios.

In addition to the above research guidelines, the improved knowledge on the Galactic magnetic fields in a propagation modelling context, and the effect of different cosmic ray electron propagation parameters, represent a significance advance in the understanding of these subjects. My approach will be useful for the interpretation of Galactic emission at synchrotron frequencies (< 30 GHz) observed by Planck mission. It helps in components separation, and for multi-wavelength studies including gamma rays observed by Fermi-Lat, and Integral. By combining high precision cosmic ray electrons data from Ams-02 as well as forthcoming radio observations by Planck mission, it can become possible to detect the contribution to the synchrotron spectrum of the extra-component invoked in order to explain the so called *positron excess*.

So, why computational astrophysics? Astrophysics is an observational science. As astrophysicists, we generally do not have the option of making direct measurements, or performing experiments on the objects we wish to study. In such a discipline, quantitatively generating and testing models

to compare to observations is critical, as such models are often the only window available into the science underlying the objects that define our field.

Astrophysics is also an integrative science, taking knowledge from many other disciplines and applying them to the objects we study. In some phenomenon, one or two pieces of physics dominate and fairly simple models can capture its behaviour. But as the field advances - observations become richer in detail and broader in scope, and theoretical understanding improves - interesting astrophysics usually results from the interactions between many different physical mechanisms.

That astrophysics is an observational science makes accurate models crucial; that astrophysics studies objects driven by a wide range of physics makes accurate models very complex. The richness of the interactions involved, however maddening, is essential to the phenomena we'd like to understand. The only way to adequately explore such complex models is often through high-performance computation.

Numerical supercomputer simulations of magneto hydrodynamics interstellar turbulence already belong to the very few top and most challenging subjects in the whole high-energy astrophysics, and will continue to grow in importance for many years to come. In my opinion, in a near future researchers working on these simulations will concentrate on three most crucial issues: making present numerical codes fully 3D, directly introducing relevant radiation processes into the codes, implementing physically more realistic astrophysical turbulence properties. I *plan to be very actively working* on these three issues.

On the other side, understanding of accretion discs progresses through a multidisciplinary union of observational, theoretical and computational methods. Today's numerical simulations of black holes and their environment span an enormous range of scales, from cosmological volumes to isolated galaxies, to accretion disks to a few *Schwarzschild* radii black hole merger simulations in general relativity. These simulations, however, are not interconnected, and it is crucial to assume different approaches when working on black holes physics on different scales, in order to explore the relevant physical processes and their interplay. That astrophysics is an observational science makes accurate models crucial; the only way to adequately explore such complex models is often through high- performance computation.

Numerical supercomputer simulations of MHD of black hole accretion flows already belong to the very few top and most challenging subjects in the whole black hole astrophysics, and will continue to grow in importance for many years to come. In my opinion, in a near future researchers working on these simulations will concentrate on three most crucial issues: making present numerical codes fully relativistic, directly introducing relevant radiation processes into the codes, implementing physically more realistic outer and inner boundary conditions. Again, as before, I *plan to be very actively work* on these three issues. Jets and outflows are a particular example of an outstandingly important, but yet unexplained, astrophysical phenomenon that could be, and will be, seriously studied with the new generation codes.

Today, there are many numerical codes available that include relativistic hydrodynamics or even general relativistic magnetohydrodynamics (GRMHD) that are, or can be, used to simulate black holes, accretion discs, AGNs and galaxy formation. A partial list includes: COSMOS++ (Anninos et al., 2005), ENZO (The Enzo Collaboration et al., 2013), AREPO (Springel, 2010), RAM-

SES (Teyssier, 2002), etc. Over my graduate student career, I acquainted a large experience about large scale numerical simulations with some of the existing numerical MHD codes, such as the PLUTO CODE (Mignone et al., 2012) and the ATHENA CODE (Stone et al., 2008). Future progress requires a combination of numerical simulations and semi-analytic studies to extract physical insights.

I propose to perform and analyse a suite of *state-of-the-art numerical* simulations of some key processes in MBH evolution, fuelling, binary merging, and AGN feedback. The numerical codes nowadays available will allow me to run both non-relativistic and fully general relativistic simulations of the relevant astrophysical processes, including MHD.

We now observe the spectacular and powerful interactions of the super massive black hole, residing at the centre of the AGN, with the surrounding medium, in the form of buoyant bubbles, shock cocoons, metals dredge-up, turbulence, jets and nuclear outflows. Numerous questions are far to be settled. What is the dominant engine of heating? How can the AGN energy couple to the interstellar/intracluster plasma? How can the galaxy, group or cluster maintain a state of quasi thermal equilibrium for several Gyr? What is the original feedback process that generates the wealth of observational features? Why do we observe extended (filamentary) and nuclear cold gas, even in the presence of strong heating? My intention will be running many (magneto)-hydrodynamic simulations of galaxy formation and mergers, including gas heating and cooling, star formation, feedback, and the crucial role of dust, resolving the galaxy nuclei and studying the detailed physics of MBH binary formation, gas fuelling, and radiation and mechanical feedback.

Possible projects I plan to begin involve are the interaction of cooling, shock-heating, and accretion in proto-planetary and AGN discs; and the formation of a turbulent boundary layer at the surface of a disc interacting with a *wind*. A direct aim of this project is to revisit numerically the model which employs a standard accretion disk description and fast magnetic reconnection theory, and discuss the role of magnetic reconnection and associated heating and particle acceleration in different jet/disc accretion systems, namely young stellar objects (YSOs), micro quasars, and active galactic nuclei (AGNS).

Fragmentation is another important issue in disks, both for angular momentum transport and for planet or star formation. Fragmentation is largely controlled by the balance between shock heating and local cooling process, meaning that getting the cooling rates, shock physics, and dimensionality correct is essential to properly determine limits for the creation of structures.

I am planning projects to perform 3D global simulations of proto-planetary and AGN discs, paying close attention to the cooling physics. I will perform one set of simulations using both a grid code (e.g., ENZO) and an SPH code (e.g., GADGET-2), to examine carefully the difference in fragmentation - caused both directly and indirectly (through shock physics) - due to different numerical methods. The next step will be to refine the thermal physics and the relation between fragmentation and accretion.

Another project involves wind-disc interactions. If the central object emits a wind, then on the surface of a disk a turbulent boundary layer will be set up, determined by the incoming hot wind and the cooling rate in the disc material. The turbulent boundary layer mediates the ablation of the disc by the wind, and determines the vertical boundary conditions of the disc. I am going to perform a study of such disc-wind interactions to understand the

interplay of cooling, *Kelvin-Helmholtz*, and rotation in the formation of the turbulent boundary layer.

The strongest evidence for black hole feedback is in galaxy clusters, but we still lack a sufficient understanding of the processes that transfer energy from AGN to the surrounding gas and thermalize the hydrodynamic disturbances excited by expanding jets and raising bubbles. Standard viscosity, turbulent viscosity, the stretching and tearing of magnetic field lines, and CRs could all contribute to heat and, or lift the intra cluster medium (ICM). In brief, with the help of massively parallel, multi-dimensional, fully covariant, modern object-oriented (C++) radiation-magneto-hydrodynamics codes, written to support structured and unstructured adaptively refined meshes, and for both Newtonian and general relativistic astrophysical applications, I plan to investigate the open issues in the role of black holes in galaxy formation and evolution.

BIBLIOGRAPHY

Abbasi, R. and et al.

2011 "Search for dark matter from the Galactic halo with the IceCube Neutrino Telescope", *Physical Review D*, vol. 84, 2, 022004 (July 2011), p. 022004, DOI: 10.1103/PhysRevD.84.022004, arXiv: 1101.3349 [astro-ph.HE].

Abdo, A. A. et al.

2009a "Fermi Large Area Telescope Measurements of the Diffuse Gamma-Ray Emission at Intermediate Galactic Latitudes", *Physical Review Letters*, vol. 103, 25 (Dec. 2009), pp. 251101-+, DOI: 10.1103/PhysRevLett.103.251101, %5Curl%7Bhttp://adsabs.harvard.edu/abs/2009PhRvL.103y1101A%7D.

2009b "Measurement of the Cosmic Ray $e^+ + e^-$ Spectrum from 20 GeV to 1 TeV with the Fermi Large Area Telescope", *Physical Review Letters*, vol. 102, 18 (May 2009), pp. 181101-+, DOI: 10.1103/PhysRevLett.102.181101, arXiv: 0905.0025, %5Curl%7Bhttp://cdsads.u-strasbg.fr/abs/2009PhRvL.102r1101A%7D.

Abramowicz, M. A. and P. C. Fragile

2013 "Foundations of Black Hole Accretion Disk Theory", *Living Reviews in Relativity*, vol. 16 (Jan. 2013), p. 1, DOI: 10.12942/lrr-2013-1, arXiv: 1104.5499 [astro-ph.HE], http://www.livingreviews.org/lrr-2013-1.

Ackermann, M. et al.

2010a "Fermi LAT observations of cosmic-ray electrons from 7 GeV to 1 TeV", *Phys. Rev. D*, vol. 82, 9, 092004 (Nov. 2010), p. 092004, DOI: 10.1103/PhysRevD.82.092004, arXiv: 1008.3999 [astro-ph.HE].

2010b "Searches for cosmic-ray electron anisotropies with the Fermi Large Area Telescope", *Phy. Rev. D*, vol. 82, 9, 092003 (Nov. 2010), p. 092003, DOI: 10.1103/PhysRevD.82.092003, arXiv: 1008.5119 [astro-ph.HE].

2013 "Detection of the Characteristic Pion-Decay Signature in Supernova Remnants", *Science*, vol. 339, 6121, pp. 807-811, DOI: 10.1126/science.1231160, eprint: http://www.sciencemag.org/content/339/6121/807.full.pdf, http://www.sciencemag.org/content/339/6121/807.abstract.

Adriani, O. et al.

2009 "An anomalous positron abundance in cosmic rays with energies 1.5-100GeV", *Nature*, vol. 458 (Apr. 2009), pp. 607-609, DOI: 10.1038/nature07942, arXiv: 0810.4995.

Aguilar, M. et al.

2002 "The Alpha Magnetic Spectrometer (AMS) on the International Space Station. I: Results from the test flight on the space shuttle", *Phys. Reports*, vol. 366 (Aug. 2002), pp. 331-405, DOI: 10.1016/S0370-1573(02)00013-3.

Aharonian, F.

2004 *Very high energy cosmic gamma radiation : a crucial window on the extreme Universe*, World Scientific, River Edge, New York.

Aharonian, F. et al.

2007 "Primary particle acceleration above 100 TeV in the shell-type supernova remnant RX J1713.7-3946 with deep HESS observations", *Astron. & Astrophys.*, vol. 464 (Mar. 2007), pp. 235-243, DOI: 10.1051/0004-6361:20066381, eprint: arXiv:astro-ph/0611813.

2008 "Energy Spectrum of Cosmic-Ray Electrons at TeV Energies", *Physical Review Letters*, vol. 101, 26 (Dec. 2008), pp. 261104-+, DOI: 10.1103/PhysRevLett.101.261104, arXiv: 0811.3894.

2009 "Probing the ATIC peak in the cosmic-ray electron spectrum with HESS", *arXiv:0905.0105 [astro-ph.HE]* (May 2009), arXiv: 0905.0105.

Aharonian, F., A. M. Atoyan, and T. Kifune

1997 "Inverse Compton gamma radiation of faint synchrotron X-ray nebulae around pulsars", *Mon.Not.R.Astron.Soc.*, vol. 291 (Oct. 1997), pp. 162-176.

Ahlen, and others

2000 "Measurement of the Isotopic Composition of Cosmic-Ray Helium, Lithium, Beryllium, and Boron up to 1700 MEV per Atomic Mass Unit", *Astrophys. J.*, vol. 534 (May 2000), pp. 757-769, DOI: 10.1086/308762.

Ahn, H. S. et al.

2008 "Measurements of cosmic-ray secondary nuclei at high energies with the first flight of the CREAM balloon-borne experiment", *Astroparticle Physics*, vol. 30 (Oct. 2008), pp. 133-141, DOI: 10.1016/j.astropartphys.2008.07.010, arXiv: 0808.1718.

Akhiezer, A. I.

1975 *Plasma electrodynamics - Vol.1: Linear theory; Vol.2: Non-linear theory and fluctuations*.

Ambrosio, M. et al.

2003 "Search for the sidereal and solar diurnal modulations in the total MACRO muon data set", *Physical Review D*, vol. 67, 4 (Feb. 2003), pp. 042002-+, DOI: 10.1103/PhysRevD.67.042002, eprint: arXiv:astro-ph/0211119.

Amsler, C. et al.

2008 "Review of particle physics", *Physics Letters*, vol. B667, p. 1, DOI: 10.1016/j.physletb.2008.07.018.

Anninos, P., P. C. Fragile, and J. D. Salmonson

2005 "Cosmos++: Relativistic Magnetohydrodynamics on Unstructured Grids with Local Adaptive Refinement", *Astrophysical Journal*, vol. 635 (Dec. 2005), pp. 723-740, DOI: 10.1086/497294, eprint: astro-ph/0509254, http://adsabs.harvard.edu/abs/2005ApJ...635..723A.

Armstrong, J. W., B. J. Rickett, and S. R. Spangler

1995 "Electron density power spectrum in the local interstellar medium", *Astrophys. J.*, vol. 443 (Apr. 1995), pp. 209-221, DOI: 10.1086/175515.

Arons, J.

1996a "Pulsar Death at an Advanced Age", in *IAU Colloq. 160: Pulsars: Problems and Progress*, ed. by S. Johnston, M. A. Walker, & M. Bailes, Astronomical Society of the Pacific Conference Series, vol. 105, pp. 177-+.

1996b "Pulsar Winds", in *IAU Colloq. 160: Pulsars: Problems and Progress*, ed. by S. Johnston, M. A. Walker, & M. Bailes, Astronomical Society of the Pacific Conference Series, vol. 105, pp. 401-+.

1996c "Pulsars as gamma ray sources." *A&AS*, vol. 120 (Nov. 1996), pp. C49+.

1996d "Pulsars as Gamma-Rays Sources: Nebular Shocks and Magnetospheric Gaps", *Space Science Reviews*, vol. 75 (Jan. 1996), pp. 235-255, DOI: 10.1007/BF00195037.

Atoyan, A. M., F. A. Aharonian, and H. J. Völk

1995 "Electrons and positrons in the galactic cosmic rays", *Physical Review D*, vol. 52, 6 (Sept. 1995), pp. 3265-3275, DOI: 10.1103/PhysRevD.52.3265.

Ave, M., P. J. Boyle, F. Gahbauer, C. Hoppner, J. R. Horandel, M. Ichimura, D. Muller, and A. Romero-Wolf

2008 "Composition of Primary Cosmic-Ray Nuclei at High Energies", *Astrophys. J.*, vol. 678, p. 262, doi:10.1086/529424.

Axford, W. I., E. Leer, and G. Skadron

1978 "The acceleration of cosmic rays by shock waves", in *International Cosmic Ray Conference*, pp. 132-137.

Baade, W.

1951 "Galaxies - Present Day Problems", *Publications of Michigan Observatory*, vol. 10, p. 7.

Baade, W. and F. Zwicky

1934 "Remarks on Super-Novae and Cosmic Rays", *Physical Review*, vol. 46 (July 1934), pp. 76-77, DOI: 10.1103/PhysRev.46.76.2.

Balbus, S. A. and J. F. Hawley

1991 "A powerful local shear instability in weakly magnetized disks. I - Linear analysis. II - Nonlinear evolution", *Astrophys. J.*, vol. 376 (July 1991), pp. 214-233, DOI: 10.1086/170270.

Barwick, S. W. et al.

1997 "Measurements of the Cosmic-Ray Positron Fraction from 1 to 50 GeV", *Astrophys. J.*, vol. 482 (June 1997), pp. L191+, DOI: 10.1086/310706, eprint: arXiv:astro-ph/9703192.

Becker, W. and R. B. Fenkart

1970 "Galactic Clusters and H II Regions", in *The Spiral Structure of our Galaxy*, ed. by W. Becker and G. I. Kontopoulos, IAU Symposium, vol. 38, p. 205.

Bell, A. R.

1978a "The acceleration of cosmic rays in shock fronts. I", *Mon. Not. R. Astron. Soc.*, vol. 182 (Jan. 1978), pp. 147-156.

1978b "The acceleration of cosmic rays in shock fronts. II", *Mon. Not. R. Astron. Soc.*, vol. 182 (Feb. 1978), pp. 443-455.

Berezhko, E.

2008 "Acceleration of cosmic rays", *Journal of Physics Conference Series*, vol. 120, 6 (July 2008), pp. 062003-+, DOI: 10.1088/1742-6596/120/6/062003.

Berezhko, E. and H. J. Völk

2000 "Kinetic theory of cosmic ray and gamma-ray production in supernova remnants expanding into wind bubbles", *Astron. & Astrophys.*, vol. 357 (May 2000), pp. 283-300, eprint: arXiv:astro-ph/0002411.

2007 "Spectrum of Cosmic Rays Produced in Supernova Remnants", *Astrophys. J. Letters*, vol. 661 (June 2007), pp. L175-L178, DOI: 10.1086/518737, arXiv: 0704.1715.

Berezinskii, V. S., S. V. Bulanov, V. L. Ginzburg, V. A. Dogel, and V. S. Ptuskin

1984 *The astrophysics of cosmic rays*, North-Holland Elsevier Science Publishers B. V.

Bergström, L., J. Edsjö, and G. Zaharijas

2009 "Dark Matter Interpretation of Recent Electron and Positron Data", *Physical Review Letters*, vol. 103, 3, 031103 (July 2009), p. 031103, DOI: 10.1103/PhysRevLett.103.031103, arXiv: 0905.0333 [astro-ph.HE].

Bertone, Gianfranco

2010 "The moment of truth for WIMP dark matter", *Nature*, vol. 468, pp. 389-393, DOI: M3-10.1038/nature09509, http://dx.doi.org/10.1038/nature09509.

Bertone, Gianfranco, Dan Hooper, and Joseph Silk

2005 "Particle dark matter: Evidence, candidates and constraints", *Phys.Rept.*, vol. 405, pp. 279-390, DOI: 10.1016/j.physrep.2004.08.031, arXiv: hep-ph/0404175 [hep-ph].

Binney, J. and M. Merrifield

1998 *Galactic astronomy*, ed. by Binney, J. & Merrifield, M., Princeton University Press, Princeton, NJ.

Biskamp, D.

2003 *Magnetohydrodynamic Turbulence*.

Blandford, R. and D. Eichler

1987 "Particle acceleration at astrophysical shocks: A theory of cosmic ray origin", *Physics Reports*, vol. 154 (Oct. 1987), pp. 1-75, DOI: 10.1016/0370-1573(87)90134-7.

Blandford, R. and J. P. Ostriker

1978 "Particle acceleration by astrophysical shocks", *Astrophys. J.*, vol. 221 (Apr. 1978), pp. L29-L32, DOI: 10.1086/182658.

1980 "Supernova shock acceleration of cosmic rays in the Galaxy", *Astrophys. J.*, vol. 237 (May 1980), pp. 793-808, DOI: 10.1086/157926.

Blasi, P.

2009 "Origin of the Positron Excess in Cosmic Rays", *Physical Review Letters*, vol. 103, 5, 051104 (July 2009), p. 051104, DOI: 10.1103/PhysRevLett.103.051104, arXiv: 0903.2794 [astro-ph.HE].

2013a "The origin of galactic cosmic rays", *The Astron. & Astrophys. Review*, vol. 21, 70 (Nov. 2013), p. 70, DOI: 10.1007/s00159-013-0070-7, arXiv: 1311.7346 [astro-ph.HE].

2013b "Theoretical challenges in acceleration and transport of ultra high energy cosmic rays: A review", in *European Physical Journal Web of Conferences*, European Physical Journal Web of Conferences, vol. 53, p. 1002, DOI: 10.1051/epjconf/20135301002, arXiv: 1208.1682 [astro-ph.HE].

Blasi, P. and E. Amato

2011 "Positrons from pulsar winds", in *High-Energy Emission from Pulsars and their Systems*, ed. by D. F. Torres and N. Rea, p. 624, arXiv: 1007.4745 [astro-ph.HE].

Boezio, M. et al.

2000 "The Cosmic-Ray Electron and Positron Spectra Measured at 1 AU during Solar Minimum Activity", *Astrophys. J.*, vol. 532 (Mar. 2000), pp. 653-669, DOI: 10.1086/308545.

Brandenburg, A., A. Nordlund, R. F. Stein, and U. Torkelsson

1995 "Dynamo-generated Turbulence and Large-Scale Magnetic Fields in a Keplerian Shear Flow", *Astrophysical Journal*, vol. 446 (June 1995), p. 741, DOI: 10.1086/175831, http://adsabs.harvard.edu/abs/1995ApJ...446..741B.

Bulanov, S. V. and V. A. Dogel

1974 "The Influence of the Energy Dependence of the Diffusion Coefficient on the Spectrum of the Electron Component of Cosmic Rays and the Radio Background Radiation of the Galaxy", *Astrophys. Space. Sci.*, vol. 29 (Aug. 1974), pp. 305-318, DOI: 10.1007/BF02639066.

Büsching, I., O. C. de Jager, M. S. Potgieter, and C. Venter

2008 "A Cosmic-Ray Positron Anisotropy due to Two Middle-Aged, Nearby Pulsars?", *Astrophys. J.*, vol. 678 (May 2008), pp. L39-L42, DOI: 10.1086/588465, arXiv: 0804.0220.

Büsching, I., C. Venter, and O. C. de Jager

2008 "Contributions from nearby pulsars to the local cosmic ray electron spectrum", *Advances in Space Research*, vol. 42 (Aug. 2008), pp. 497-503, DOI: 10.1016/j.asr.2007.08.005.

Caprioli, D., E. Amato, and P. Blasi

2010 "Non-linear diffusive shock acceleration with free-escape boundary", *Astroparticle Physics*, vol. 33 (June 2010), pp. 307-311, DOI: 10.1016/j.astropartphys.2010.03.001, arXiv: 0912.2714 [astro-ph.HE].

Carretti, E., R. M. Crocker, L. Staveley-Smith, M. Haverkorn, C. Purcell, B. M. Gaensler, G. Bernardi, M. J. Kesteven, and S. Poppi

2013 "Giant magnetized outflows from the centre of the Milky Way", *Nature*, vol. 493 (Jan. 2013), pp. 66-69, DOI: 10.1038/nature11734, arXiv: 1301.0512 [astro-ph.GA].

Case, G. L. and D. Bhattacharya

1998 "A New Sigma -D Relation and Its Application to the Galactic Supernova Remnant Distribution", *Astrophys. J.*, vol. 504 (Sept. 1998), pp. 761-+, DOI: 10.1086/306089, eprint: arXiv:astro-ph/9807162.

Cattaneo, A., S. M. Faber, J. Binney, A. Dekel, J. Kormendy, R. Mushotzky, A. Babul, P. N. Best, M. Brüggen, A. C. Fabian, C. S. Frenk, A. Khalatyan, H. Netzer, A. Mahdavi, J. Silk, M. Steinmetz, and L. Wisotzki

2009 "The role of black holes in galaxy formation and evolution", *Nature*, vol. 460 (July 2009), pp. 213-219, DOI: 10.1038/nature08135, arXiv: 0907.1608 [astro-ph.CO], http://adsabs.harvard.edu/abs/2009Natur.460..213C.

Cesarsky, C. J.

1980 "Cosmic-ray confinement in the galaxy", *Ann.Rev.Astron.Astrophy.*, vol. 18, pp. 289-319, DOI: 10.1146/annurev.aa.18.090180.001445.

Chang, J. et al.

2008 "An excess of cosmic ray electrons at energies of 300-800GeV", *Nature*, vol. 456 (Nov. 2008), pp. 362-365, DOI: 10.1038/nature07477.

Chang, J. and et al.

2005 "The Electron Spectrum above 20 GeV Measured by ATIC-2", in *International Cosmic Ray Conference*, International Cosmic Ray Conference, vol. 3, pp. 1-+.

Chi, X., K. S. Cheng, and E. C. M. Young

1996 "Pulsar Wind Origin of Cosmic Ray Positrons", *Astrophys. J.*, vol. 459 (Mar. 1996), pp. L83+, DOI: 10.1086/309943.

Cho, J., A. Lazarian, and E. T. Vishniac

2002 "Simulations of Magnetohydrodynamic Turbulence in a Strongly Magnetized Medium", *Astrophys. J.*, vol. 564 (Jan. 2002), pp. 291-301, DOI: 10.1086/324186, eprint: astro-ph/0105235.

Cholis, I., L. Goodenough, D. Hooper, M. Simet, and N. Weiner

2009 "High energy positrons from annihilating dark matter", *Physical Review D*, vol. 80, 12, 123511 (Dec. 2009), p. 123511, DOI: 10.1103/PhysRevD.80.123511, arXiv: 0809.1683 [hep-ph].

Churchwell, E. and Glimpse Team

2005 "Selected First Results from the GLIMPSE Survey", in *Revista Mexicana de Astronomia y Astrofisica Conference Series*, ed. by S. Torres-Peimbert and G. MacAlpine, Revista Mexicana de Astronomia y Astrofisica, vol. 27, vol. 23, pp. 53-59.

Cirelli, M.

2012 "Indirect searches for dark matter", *Pramana*, vol. 79 (Nov. 2012), pp. 1021-1043, DOI: 10.1007/s12043-012-0419-x, arXiv: 1202.1454 [hep-ph].

Cirelli, Marco, Pasquale D. Serpico, and Gabrijela Zaharijas

2013 "Bremsstrahlung gamma rays from light Dark Matter", *JCAP*, vol. 1311, p. 035, DOI: 10.1088/1475-7516/2013/11/035, arXiv: 1307.7152 [astro-ph.HE].

Clark, D. H. and J. L. Caswell

1976 "A study of galactic supernova remnants, based on Molonglo-Parkes observational data", *Mon. Not. R. Astron. Soc.*, vol. 174 (Feb. 1976), pp. 267-305.

Cordes, J. M. and T. J. W. Lazio

2003 "NE2001. II. Using Radio Propagation Data to Construct a Model for the Galactic Distribution of Free Electrons", *ArXiv Astrophysics e-prints* (Jan. 2003), eprint: astro-ph/0301598.

Dame, T. M., D. Hartmann, and P. Thaddeus

2001 "The Milky Way in Molecular Clouds: A New Complete CO Survey", *Astrophy. J.*, vol. 547 (Feb. 2001), pp. 792-813, DOI: 10.1086/318388, eprint: astro-ph/0009217.

Dame, T. M. and P. Thaddeus

2008 "A New Spiral Arm of the Galaxy: The Far 3 kpc Arm", *Astrophys. J. Lett.*, vol. 683 (Aug. 2008), pp. L143-L146, DOI: 10.1086/591669, arXiv: 0807.1752.

Davis, A. J. et al.

2000 "On the low energy decrease in galactic cosmic ray secondary/primary ratios", in *Acceleration and Transport of Energetic Particles Observed in the Heliosphere*, ed. by R. A. Mewaldt, J. R. Jokipii, M. A. Lee, E. Möbius, & T. H. Zurbuchen, American Institute of Physics Conference Series, vol. 528, pp. 421-424, DOI: 10.1063/1.1324351.

Delahaye, T., R. Lineros, F. Donato, N. Fornengo, J. Lavalle, P. Salati, and R. Taillet

2009 "Galactic secondary positron flux at the Earth", *Astron. & Astrophys.*, vol. 501 (July 2009), pp. 821-833, DOI: 10.1051/0004-6361/200811130, arXiv: 0809.5268.

Delahaye, T., R. Lineros, F. Donato, N. Fornengo, and P. Salati

2008 "Positrons from dark matter annihilation in the galactic halo: Theoretical uncertainties", *Physical Review D*, vol. 77, 6 (Mar. 2008), pp. 063527-+, DOI: 10.1103/PhysRevD.77.063527, arXiv: 0712.2312.

Di Bernardo, G., C. Evoli, D. Gaggero, D. Grasso, and L. Maccione

2010 "Unified interpretation of cosmic ray nuclei and antiproton recent measurements", *Astroparticle Physics*, vol. 34 (Dec. 2010), pp. 274-283, DOI: 10.1016/j.astropartphys.2010.08.006, arXiv: 0909.4548 [astro-ph.HE].

2013 "Cosmic ray electrons, positrons and the synchrotron emission of the Galaxy: consistent analysis and implications", *JCAP*, vol. 3, 036 (Mar. 2013), p. 36, DOI: 10.1088/1475-7516/2013/03/036, arXiv: 1210.4546 [astro-ph.HE].

Di Bernardo, G., C. Evoli, D. Gaggero, D. Grasso, L. Maccione, and M. N. Mazziotta

2011 "Implications of the cosmic ray electron spectrum and anisotropy measured with Fermi-LAT", *Astroparticle Physics*, vol. 34 (Feb. 2011), pp. 528-538, DOI: 10.1016/j.astropartphys.2010.11.005, arXiv: 1010.0174 [astro-ph.HE].

Di Bernardo, G. and U. Torkelsson

2013 "Wave modes from the magnetorotational instability in accretion discs", in *IAU Symposium*, ed. by C. M. Zhang, T. Belloni, M. Méndez, and S. N. Zhang, IAU Symposium, vol. 290, pp. 201-202, DOI: 10.1017/S1743921312019618.

Dogiel, V. and D. Breitschwerdt

2009 "Cosmic Rays in the Disk and Halo of Galaxies", *ArXiv e-prints* (May 2009), arXiv: 0905.3071.

Draine, B. T.

2011 *Physics of the Interstellar and Intergalactic Medium*, Princeton University Press, 2011. ISBN: 978-0-691-12214-4.

Drury, L. O. et al.

2001 "Test of galactic cosmic-ray source models - Working Group Report", *Space Science Reviews*, vol. 99 (Oct. 2001), pp. 329-352.

DuVernois, M. A. et al.

2001 "Cosmic-Ray Electrons and Positrons from 1 to 100 GeV: Measurements with HEAT and Their Interpretation", *Astrophys. J.*, vol. 559 (Sept. 2001), pp. 296-303, DOI: 10.1086/322324.

Elmegreen, B. G. and J. Scalo

2004 "Interstellar Turbulence I: Observations and Processes", *Ann. Rev. Astron. Astrophy.*, vol. 42 (Sept. 2004), pp. 211-273, DOI: 10.1146/annurev.astro.41.011802.094859, eprint: astro-ph/0404451.

Evoli, C., D. Gaggero, D. Grasso, and L. Maccione

2008 "Cosmic ray nuclei, antiprotons and gamma rays in the galaxy: a new diffusion model", *Journal of Cosmology and Astroparticle Physics*, vol. 10, 018 (Oct. 2008), p. 18, DOI: 10.1088/1475-7516/2008/10/018, arXiv: 0807.4730.

Fabian, A. C., E. Churazov, M. Donahue, W. R. Forman, M. R. Garcia, S. Heinz, B. R. McNamara, K. Nandra, P. Nulsen, P. Ogle, E. S. Perlman, D. Proga, M. J. Rees, C. L. Sarazin, R. A. Sunyaev, G. B. Taylor, S. D. M. White, A. Vikhlinin, and D. M. Worrall

2009 "Cosmic Feedback from Supermassive Black Holes", in *astro2010: The Astronomy and Astrophysics Decadal Survey*, Astronomy, vol. 2010, p. 73, arXiv: 0903.4424 [astro-ph.CO], http://adsabs.harvard.edu/abs/2009astro2010S..73F.

Faucher-Giguère, C.-A. and V. M. Kaspi

2006 "Birth and Evolution of Isolated Radio Pulsars", *Astrophys. J.*, vol. 643 (May 2006), pp. 332-355, DOI: 10.1086/501516, eprint: astro-ph/0512585.

Fermi, ENRICO

1949 "On the Origin of the Cosmic Radiation", *Physical Review*, vol. 75, 8 (Apr. 1949), pp. 1169-1174, DOI: 10.1103/PhysRev.75.1169.

Ferrando, P., N. Lal, F. B. McDonald, and W. R. Webber

1991 "Studies of low-energy Galactic cosmic-ray composition at 22 AU. I - Secondary/primary ratios", *Astron. & Astrophys.*, vol. 247 (July 1991), pp. 163-172.

Ferrière, K. M.

2001 "The interstellar environment of our galaxy", *Reviews of Modern Physics*, vol. 73 (Oct. 2001), pp. 1031-1066, DOI: 10.1103/RevModPhys.73.1031, eprint: arXiv:astro-ph/0106359.

Forman, M. A. and L. J. Gleeson

1975 "Cosmic-ray streaming and anisotropies", *Astrophysics and Space Science*, vol. 32 (Jan. 1975), pp. 77-94, DOI: 10.1007/BF00646218.

Gaensler, B. M. and P. O. Slane

2006 "The Evolution and Structure of Pulsar Wind Nebulae", *Ann. Rev. Astron. Astrophys.*, vol. 44 (Sept. 2006), pp. 17-47, DOI: 10.1146/annurev.astro.44.051905.092528, eprint: arXiv:astro-ph/0601081.

Gaggero, D., L. Maccione, G. Di Bernardo, C. Evoli, and D. Grasso

2013 "Three-Dimensional Model of Cosmic-Ray Lepton Propagation Reproduces Data from the Alpha Magnetic Spectrometer on the International Space Station", *Physical Review Letters*, vol. 111, 2, 021102 (July 2013), p. 021102, DOI: 10.1103/PhysRevLett.111.021102, arXiv: 1304.6718 [astro-ph.HE].

Gaggero, D., L. Maccione, D. Grasso, G. Di Bernardo, and C. Evoli

2014 "PAMELA and AMS-02 e^+ and e^- spectra are reproduced by three-dimensional cosmic-ray modeling", *Physical Review D*, vol. 89, 8, 083007 (Apr. 2014), p. 083007, DOI: 10.1103/PhysRevD.89.083007, arXiv: 1311.5575 [astro-ph.HE].

Gaisser

2001 "Origin of cosmic radiation", in *American Institute of Physics Conference Series*, ed. by F. A. Aharonian & H. J. Völk, American Institute of Physics Conference Series, vol. 558, pp. 27-42, DOI: 10.1063/1.1370778.

Gaisser, T. and T. Stanev

2006 "High-energy cosmic rays", *Nuclear Physics A*, vol. 777 (Oct. 2006), pp. 98-110, DOI: 10.1016/j.nuclphysa.2005.01.024, eprint: arXiv:astro-ph/0510321.

Garcia-Munoz, M., J. A. Simpson, T. G. Guzik, J. P. Wefel, and S. H. Margolis

1987 "Cosmic-ray propagation in the Galaxy and in the heliosphere - The path-length distribution at low energy", *Astrophys. J. Supp.*, vol. 64 (May 1987), pp. 269-304, DOI: 10.1086/191197.

Gillessen, S., F. Eisenhauer, S. Trippe, T. Alexander, R. Genzel, F. Martins, and T. Ott

2009 "Monitoring Stellar Orbits Around the Massive Black Hole in the Galactic Center", *Astrophys. J.*, vol. 692 (Feb. 2009), pp. 1075-1109, DOI: 10.1088/0004-637X/692/2/1075, arXiv: 0810.4674.

Ginzburg, V. L.

1975 "On the Origin of Cosmic Rays", *Philosophical Transactions of the Royal Society of London. Series A, Mathematical and Physical Sciences*, vol. 277, 1270, pp. 463-479, ISSN: 00804614, http://www.jstor.org/stable/74494.

Ginzburg, V. L. and S. I. Syrovatskii

1964 *The Origin of Cosmic Rays*, Pergamon Press, Oxford.

Gleeson, L. J. and W. I. Axford

1968 "Solar Modulation of Galactic Cosmic Rays", *Astrophys. J.*, vol. 154 (Dec. 1968), pp. 1011-+, DOI: 10.1086/149822.

Golden, R. L. et al.

1984 "A measurement of the absolute flux of cosmic-ray electrons", *Astrophys. J.*, vol. 287 (Dec. 1984), pp. 622-632, DOI: 10.1086/162720.

1994 "Observations of cosmic-ray electrons and positrons using an imaging calorimeter", *Astrophys. J.*, vol. 436 (Dec. 1994), pp. 769-775, DOI: 10.1086/174951.

Goldreich, P. and S. Sridhar

1995 "Toward a theory of interstellar turbulence. 2: Strong alfvenic turbulence", *Astrophys. J.*, vol. 438 (Jan. 1995), pp. 763-775, DOI: 10.1086/175121.

Grasso, D., S. Profumo, A. W. Strong, et al.

2009 "On possible interpretations of the high energy electron-positron spectrum measured by the Fermi Large Area Telescope", *Astroparticle Physics*, vol. 32 (Sept. 2009), pp. 140-151, DOI: 10.1016/j.astropartphys.2009.07.003, arXiv: 0905.0636, %5Curl%7Bhttp://cdsads.u-strasbg.fr/abs/2009APh....32..140G%7D.

Green, D. A.

1996 "A Catalogue of Galactic Supernova Remnants (Green 1995)", *VizieR Online Data Catalog*, vol. 7187 (July 1996), pp. -+.

Greisen, K.

1966 "End to the Cosmic-Ray Spectrum?", *Physical Review Letters*, vol. 16 (Apr. 1966), pp. 748-750, DOI: 10.1103/PhysRevLett.16.748.

Harding, A. K. and R. Ramaty

1987 "The Pulsar Contribution to Galactic Cosmic Ray Positrons", in *International Cosmic Ray Conference*, International Cosmic Ray Conference, vol. 2, pp. 92-+.

Haungs, Andreas, Heinigerd Rebel, and Markus Roth

2003 "Energy spectrum and mass composition of high-energy cosmic rays", *Reports on Progress in Physics*, vol. 66, 7, p. 1145, http://stacks.iop.org/0034-4885/66/i=7/a=202.

Hawley, J. F. and S. A. Balbus

1991 "A Powerful Local Shear Instability in Weakly Magnetized Disks. II. Nonlinear Evolution", *Astrophys. J.*, vol. 376 (July 1991), p. 223, DOI: 10.1086/170271.

Hillas, A. M.

1984 "The Origin of Ultra-High-Energy Cosmic Rays", *Ann. Rev. Astron. Astrophys.*, vol. 22, pp. 425-444, DOI: 10.1146/annurev.aa.22.090184.002233.

2006 "Cosmic Rays: Recent Progress and some Current Questions", *ArXiv Astrophysics e-prints* (July 2006), eprint: arXiv:astro-ph/0607109.

Hoerandel, J.

2012 "On the transition from Galactic to extragalactic cosmic rays", in *APS April Meeting Abstracts*, H3001.

Hooper, D., P. Blasi, and P. Dario Serpico

2009 "Pulsars as the sources of high energy cosmic ray positrons", *Journal of Cosmology and Astro-Particle Physics*, vol. 1 (Jan. 2009), pp. 25-+, DOI: 10.1088/1475-7516/2009/01/025, arXiv: 0810.1527.

Humphreys, R. M.

1976 "A model for the local spiral structure of the Galaxy", *Publications of the Astronomical Society of the Pacific*, vol. 88 (Oct. 1976), pp. 647-655, DOI: 10.1086/130002.

Iroshnikov, P. S.

1963 "Turbulence of a Conducting Fluid in a Strong Magnetic Field", *Astronomicheskii Zhurnal*, vol. 40, p. 742.

Janka, H.-T.

2012 "Explosion Mechanisms of Core-Collapse Supernovae", *Annual Review of Nuclear and Particle Science*, vol. 62 (Nov. 2012), pp. 407-451, DOI: 10.1146/annurev-nucl-102711-094901, arXiv: 1206.2503 [astro-ph.SR].

Jones, F. C. and D. C. Ellison

1991 "The plasma physics of shock acceleration", *Space Science Reviews*, vol. 58 (Dec. 1991), pp. 259-346, DOI: 10.1007/BF01206003.

Jui, C. C. H.

2000 "Results from the High Resolution Fly's Eye Experiment", in *26th International Cosmic Ray Conference, ICRC XXVI*, ed. by B. L. Dingus, D. B. Kieda, & M. H. Salamon, American Institute of Physics Conference Series, vol. 516, pp. 370-+.

Kachelrieß, M. and S. Ostapchenko

2012 "Deriving the cosmic ray spectrum from gamma-ray observations", *Physical Review D*, vol. 86, 4, 043004 (Aug. 2012), p. 043004, DOI: 10.1103/PhysRevD.86.043004, arXiv: 1206.4705 [astro-ph.HE].

Kachelrieß, M., S. Ostapchenko, and R. Tomàs

2012 "Constraints on the intergalactic magnetic field from gamma-ray observations of TeV blazars", *Journal of Physics Conference Series*, vol. 375, 5, 052030 (July 2012), p. 052030, DOI: 10.1088/1742-6596/375/1/052030.

Karachentsev, I. D. and O. G. Kashibadze

2006 "Masses of the local group and of the M81 group estimated from distortions in the local velocity field", *Astrophysics*, vol. 49 (Jan. 2006), pp. 3-18, DOI: 10.1007/s10511-006-0002-6.

Kobayashi, T., Y. Komori, K. Yoshida, and J. Nishimura

2004 "The Most Likely Sources of High-Energy Cosmic-Ray Electrons in Supernova Remnants", *Astrophys. J.*, vol. 601 (Jan. 2004), pp. 340-351, DOI: 10.1086/380431, eprint: arXiv:0308470[astro-ph].

Kobayashi, T., Y. Komori, K. Yoshida, K. Yanagisawa, J. Nishimura, T. Yamagami, Y. Saito, N. Tateyama, T. Yuda, and R. J. Wilkes

2012 "Observations of High-energy Cosmic-Ray Electrons from 30 GeV to 3 TeV with Emulsion Chambers", *The Astrophysical Journal*, vol. 760, 2, p. 146, http://stacks.iop.org/0004-637X/760/i=2/a=146.

Kolmogorov, A.

1941 "The Local Structure of Turbulence in Incompressible Viscous Fluid for Very Large Reynolds' Numbers", *Akademiia Nauk SSSR Doklady*, vol. 30, pp. 301-305.

Kraichnan, R. H. and S. Nagarajan

1967 "Growth of Turbulent Magnetic Fields", *Physics of Fluids*, vol. 10 (Apr. 1967), pp. 859-870, DOI: 10.1063/1.1762201.

Krimsky, G. F. and S. I. Petukhov

1983 "Cosmic Ray Acceleration Efficiency by Supernovae Remnant", *International Cosmic Ray Conference*, vol. 2 (Aug. 1983), p. 301.

Kulsrud, R. M.

2005 *Plasma physics for astrophysics*.

Kulsrud, R. and W. P. Pearce

1969 "The Effect of Wave-Particle Interactions on the Propagation of Cosmic Rays", *Astrophys. J.*, vol. 156 (May 1969), p. 445, DOI: 10.1086/149981.

Lavalle, Julien and Pierre Salati

2012 "Dark Matter Indirect Signatures", *Comptes Rendus Physique*, vol. 13, pp. 740-782, DOI: 10.1016/j.crhy.2012.05.001, arXiv: 1205.1004 [astro-ph.HE].

Lin, C. C. and F. H. Shu

1964 "On the Spiral Structure of Disk Galaxies." *Astrophys. J.*, vol. 140 (Aug. 1964), p. 646, DOI: 10.1086/147955.

Lin, C. C., C. Yuan, and F. H. Shu

1969 "On the Spiral Structure of Disk Galaxies. III. Comparison with Observations", *Astrophys. J.*, vol. 155 (Mar. 1969), p. 721, DOI: 10.1086/149907.

Lindblad, B.

1927 "On the state of motion in the galactic system", *Mon. Not. R. Astron. Soc.*, vol. 87 (May 1927), pp. 553-564.

Longair, M. S.

1994a *High energy astrophysics. Vol.1: Particles, photons and their detection*, Cambridge university Press.

1994b *High energy astrophysics. Vol.2: Stars, the Galaxy and the interstellar medium*, Cambridge university Press.

Lorimer, D. R.

2004 "The Galactic Population and Birth Rate of Radio Pulsars", in *Young Neutron Stars and Their Environments*, ed. by F. Camilo & B. M. Gaensler, IAU Symposium, vol. 218, pp. 105-+.

Mac Low, M.-M.

2004 "Turbulent Structure of the Interstellar Medium", in *The Dense Interstellar Medium in Galaxies*, ed. by S. Pfalzner, C. Kramer, C. Staubmeier, and A. Heithausen, p. 379, eprint: astro-ph/0311032.

Maccione, L.

2013 "Low Energy Cosmic Ray Positron Fraction Explained by Charge-Sign Dependent Solar Modulation", *Physical Review Letters*, vol. 110, 8, 081101 (Feb. 2013), p. 081101, DOI: 10.1103/PhysRevLett.110.081101, arXiv: 1211.6905 [astro-ph.HE].

Malkov, M. A. and L. O'C Drury
2001 "Nonlinear theory of diffusive acceleration of particles by shock waves", *Reports on Progress in Physics*, vol. 64 (Apr. 2001), pp. 429-481, DOI: 10.1088/0034-4885/64/4/201.

Malyshev, D., I. Cholis, and J. Gelfand
2009 "Pulsars versus dark matter interpretation of ATIC/PAMELA", *Physical Review D*, vol. 80, 6 (Sept. 2009), pp. 063005-+, DOI: 10.1103/PhysRevD.80.063005, arXiv: 0903.1310.

Mao, C. Y. and C. S. Shen
1972 "Anisotropy and Diffusion of Cosmic Ray Electrons", *Chinese Journal of Physics*, vol. 10 (Apr. 1972), pp. 16-28, DOI: 10.1086/180650.

Maron, J. and P. Goldreich
2001 "Simulations of Incompressible Magnetohydrodynamic Turbulence", *Astrophys. J.*, vol. 554 (June 2001), pp. 1175-1196, DOI: 10.1086/321413, eprint: astro-ph/0012491.

Matthaeus, W. H. and M. L. Goldstein
1982 "Measurement of the rugged invariants of magnetohydrodynamic turbulence in the solar wind", *Journal of Geophysical Research*, vol. 87 (Aug. 1982), pp. 6011-6028, DOI: 10.1029/JA087iA08p06011.

Maurin, D., Richard Taillet, Fiorenza Donato, Pierre Salati, Aurelien Barrau, et al.
2002 "Galactic cosmic ray nuclei as a tool for astroparticle physics", arXiv: astro-ph/0212111 [astro-ph].

McKee, C. F. and J. P. Ostriker
1975 "Supernova Explosions and the Maintenance of a Hot Component of the Interstellar Medium", in *Bulletin of the American Astronomical Society*, Bulletin of the American Astronomical Society, vol. 7, p. 419.
1977 "A theory of the interstellar medium - Three components regulated by supernova explosions in an inhomogeneous substrate", *Astrophy. J.*, vol. 218 (Nov. 1977), pp. 148-169, DOI: 10.1086/155667.

McMillan, P. J.
2011 "Mass models of the Milky Way", *Mont. N. R. Astron. Soc.*, vol. 414 (July 2011), pp. 2446-2457, DOI: 10.1111/j.1365-2966.2011.18564.x, arXiv: 1102.4340 [astro-ph.GA].

Medin, Z. and D. Lai
2010 "Pair cascades in the magnetospheres of strongly-magnetized neutron stars", *ArXiv e-prints* (Jan. 2010), arXiv: 1001.2365.

Mignone, A., C. Zanni, P. Tzeferacos, B. van Straalen, P. Colella, and G. Bodo
2012 "The PLUTO Code for Adaptive Mesh Computations in Astrophysical Fluid Dynamics", *Astrophysical Journal Supplement Series*, vol. 198, 7 (Jan. 2012), p. 7, DOI: 10.1088/0067-0049/198/1/7, arXiv: 1110.0740 [astro-ph.HE], http://adsabs.harvard.edu/abs/2012ApJS..198....7M.

Morgan, W. W., A. E. Whitford, and A. D. Code
1953 "Studies in Galactic Structure. I. a Preliminary Determination of the Space Distribution of the Blue Giants." *Astrophys. J.*, vol. 118 (Sept. 1953), p. 318, DOI: 10.1086/145754.

Morlino, G., E. Amato, P. Blasi, and D. Caprioli

2010 "Spatial structure of X-ray filaments in SN 1006", *Mon. Not. R. Astron. Soc.*, vol. 405 (June 2010), pp. L21-L25, DOI: 10.1111/j.1745-3933.2010.00851.x, arXiv: 0912.2972 [astro-ph.HE].

Moskalenko, I. V. and A. W. Strong

1998 "Production and Propagation of Cosmic-Ray Positrons and Electrons", *Astrophys. J.*, vol. 493 (Jan. 1998), pp. 694-+, DOI: 10.1086/305152, eprint: arXiv:astro-ph/9710124.

Nishmura, J., T. Kobayashi, and et al.

1995 "Astrophysical Significance of the Confinement Time of Primary Electrons in the Galaxy", in *International Cosmic Ray Conference*, International Cosmic Ray Conference, vol. 3, pp. 29-+.

Oort, J. H.

1927 "Observational evidence confirming Lindblad's hypothesis of a rotation of the galactic system", *Bull. of the Astro. Inst. of the Nether.*, vol. 3 (Apr. 1927), p. 275.

Osborne, J. L. and S. Ptuskin V.

1988 "Cosmic-Ray Reacceleration in the Interstellar Medium", *Soviet Astronomy Letters*, vol. 14 (Mar. 1988), p. 132.

Parker, E. N.

1965 "The passage of energetic charged particles through interplanetary space", *Planetary and Space Science*, vol. 13 (Jan. 1965), pp. 9-49, DOI: 10.1016/0032-0633(65)90131-5.

Pilkington, J. D. H., A. Hewish, S. J. Bell, and T. W. Cole

1968 "Observations of some further Pulsed Radio Sources", *Nature*, vol. 218 (Apr. 1968), pp. 126-129, DOI: 10.1038/218126a0.

Pohl, M. and J. A. Esposito

1998 "Electron Acceleration in Supernova Remnants and Diffuse Gamma Rays above 1 GeV", *Astrophys. J.*, vol. 507 (Nov. 1998), pp. 327-338, DOI: 10.1086/306298, eprint: arXiv:astro-ph/9806160.

Potgieter, M.

2013 "Solar Modulation of Cosmic Rays", *Living Reviews in Solar Physics*, vol. 10 (June 2013), p. 3, DOI: 10.12942/lrsp-2013-3, arXiv: 1306.4421 [physics.space-ph].

Profumo, S.

2008 "Dissecting cosmic-ray electron-positron data with Occam's Razor: the role of known Pulsars", *arXiv:0812.4457 [astro-ph]* (Dec. 2008), arXiv: 0812.4457.

2014 "The detection of a cosmic-ray electron-positron anisotropy is a sufficient (but not necessary) condition to discard a Dark Matter origin for the anomalous positron fraction", *ArXiv e-prints* (May 2014), arXiv: 1405.4884 [astro-ph.HE].

Ptuskin, V.

2006 "Cosmic ray transport in the Galaxy", *Journal of Physics Conference Series*, vol. 47 (Oct. 2006), pp. 113-119, DOI: 10.1088/1742-6596/47/1/014.

Ptuskin, V. S., F. C. Jones, E. S. Seo, and R. Sina

2006a "Effect of random nature of cosmic ray sources Supernova remnants on cosmic ray intensity fluctuations, anisotropy, and electron energy spectrum", *Advances in Space Research*, vol. 37, pp. 1909-1912, DOI: 10.1016/j.asr.2005.08.036.

Ptuskin, V. S., I. V. Moskalenko, F. C. Jones, A. W. Strong, and V. N. Zirakashvili

2006b "Dissipation of Magnetohydrodynamic Waves on Energetic Particles: Impact on Interstellar Turbulence and Cosmic Ray Transport", *arXiv:0510335v2 [astro-ph]* (Jan. 2006), arXiv: 0510335v2, doi:10.1086/501117.

Robin, A. C., C. Reylé, S. Derrière, and S. Picaud

2003 "A synthetic view on structure and evolution of the Milky Way", *A&A*, vol. 409 (Oct. 2003), pp. 523-540, DOI: 10.1051/0004-6361:20031117.

Rybicki, G. B. and A. P. Lightman

1979 *Radiative processes in astrophysics*.

Sanuki, T. et al.

2000 "Precise Measurement of Cosmic-Ray Proton and Helium Spectra with the BESS Spectrometer", *Astrophy. J.*, vol. 545 (Dec. 2000), pp. 1135-1142, DOI: 10.1086/317873, eprint: arXiv:astro-ph/0002481.

Scalo, J. and B. G. Elmegreen

2004 "Interstellar Turbulence II: Implications and Effects", *Ann. Rev. Astron. Astrophy.*, vol. 42 (Sept. 2004), pp. 275-316, DOI: 10.1146/annurev.astro.42.120403.143327, eprint: astro-ph/0404452.

Schlickeiser, R.

2002 *Cosmic Ray Astrophysics*, Springer-Verlag, Berlin, %5Curl%7Bhttp://adsabs.harvard.edu/abs/2002cra..book.....S%7D.

Seo, E. S. and V. S. Ptuskin

1994 "Stochastic reacceleration of cosmic rays in the interstellar medium", *Astrophys. J.*, vol. 431 (Aug. 1994), pp. 705-714, DOI: 10.1086/174520.

Serpico, P.

2012 "Astrophysical models for the origin of the positron 'excess'", *Astropart.Phys.*, vol. 39-40, pp. 2-11, DOI: 10.1016/j.astropartphys.2011.08.007, arXiv: 1108.4827 [astro-ph.HE].

Serpico, P. D.

2012 "Status of indirect dark matter detection", *Journal of Physics Conference Series*, vol. 375, 1, 012029 (July 2012), p. 012029, DOI: 10.1088/1742-6596/375/1/012029.

Shakura, N. I. and R. A. Sunyaev

1973 "Black holes in binary systems. Observational appearance." *Astronomy & Astrophysics*, vol. 24, pp. 337-355, http://adsabs.harvard.edu/abs/1973A&A....24..337S.

Shapiro, M. and R. Silberberg

1970 "Lifetime of cosmic rays", *International Cosmic Ray Conference*, vol. 1, p. 485.

Shapiro, S. L. and S. A. Teukolsky

1986 *Black Holes, White Dwarfs and Neutron Stars: The Physics of Compact Objects*, John Wiley & Sons, New York, Chichester, Brisbane, Toronto, Singapore.

Shaviv, N. J., E. Nakar, and T. Piran

2009 "Inhomogeneity in Cosmic Ray Sources as the Origin of the Electron Spectrum and the PAMELA Anomaly", *Physical Review Letters*, vol. 103, 11, 111302 (Sept. 2009), p. 111302, DOI: 10.1103/PhysRevLett.103.111302, arXiv: 0902.0376 [astro-ph.HE].

Shen, C. S.

1970 "Pulsars and Very High-Energy Cosmic-Ray Electrons", *Astrophys. J.*, vol. 162 (Dec. 1970), pp. L181+, DOI: 10.1086/180650.

Silk, J.

2004 "Dark Matter Theory", *Measuring and Modeling the Universe*, p. 67.

Simpson, J. A.

1983 "Elemental and Isotopic Composition of the Galactic Cosmic Rays", *Annual Review of Nuclear and Particle Science*, vol. 33, pp. 323-382, DOI: 10.1146/annurev.ns.33.120183.001543.

Sivertsson, S. and J. Edsjö

2010 "Accurate calculations of the WIMP halo around the Sun and prospects for its gamma-ray detection", *Physical Review D*, vol. 81, 6, 063502 (Mar. 2010), p. 063502, DOI: 10.1103/PhysRevD.81.063502, arXiv: 0910.0017 [astro-ph.HE].

Skilling, J.

1975 "Cosmic ray streaming. I - Effect of Alfven waves on particles", *Monthly Notices of the Royal Astronomical SOciety (MNRAS)*, vol. 172 (Sept. 1975), pp. 557-566.

Spitzer, L.

1978 *Physical processes in the interstellar medium*.

Springel, V.

2010 "E pur si muove: Galilean-invariant cosmological hydrodynamical simulations on a moving mesh", *Monthly Notices of the Royal Astronomical Society*, vol. 401 (Jan. 2010), pp. 791-851, DOI: 10.1111/j.1365-2966.2009.15715.x, arXiv: 0901.4107 [astro-ph.CO], http://adsabs.harvard.edu/abs/2010MNRAS.401..791S.

Sridhar, S. and P. Goldreich

1994 "Toward a theory of interstellar turbulence. 1: Weak Alfvenic turbulence", *Astrophys. J.*, vol. 432 (Sept. 1994), pp. 612-621, DOI: 10.1086/174600.

Stanev, T.

2004 *High energy cosmic rays*, Springer-Verlag, Berlin, Heidelberg, New York.

Stone, J. M., T. A. Gardiner, P. Teuben, J. F. Hawley, and J. B. Simon

2008 "Athena: A New Code for Astrophysical MHD", *Astrophysical Journal Supplement Series*, vol. 178 (Sept. 2008), pp. 137-177, DOI: 10.1086/588755, arXiv: 0804.0402, http://adsabs.harvard.edu/abs/2008ApJS..178..137S.

Strong, A. W. and I. V. Moskalenko

1998 "Propagation of Cosmic-Ray Nucleons in the Galaxy", *Astrophys. J.*, vol. 509 (Dec. 1998), pp. 212-228, DOI: 10.1086/306470, eprint: arXiv:astro-ph/9807150.

Strong, A. W., I. V. Moskalenko, O. Reimer, S. Digel, and R. Diehl

2004 "The distribution of cosmic-ray sources in the Galaxy, γ-rays and the gradient in the CO-to—H_2 relation", *Astron. & Astrophys.*, vol. 422 (July 2004), pp. L47-L50, DOI: 10.1051/0004-6361:20040172, eprint: arXiv:astro-ph/0405275.

Strong A., W., I. V. Moskalenko, and O. Reimer

2004 "Diffuse Galactic Continuum Gamma Rays: A Model Compatible with EGRET Data and Cosmic-Ray Measurements", *Astrophys. J.*, vol. 613 (Oct. 2004), pp. 962-976, DOI: 10.1086/423193, eprint: arXiv:astro-ph/0406254.

Strong A., W., V. Moskalenko I., and S. Ptuskin V.

2007 "Cosmic-Ray Propagation and Interactions in the Galaxy", *Annual Review of Nuclear and Particle Science*, vol. 57 (Nov. 2007), pp. 285-327, DOI: 10.1146/annurev.nucl.57.090506.123011, eprint: arXiv:astro-ph/0701517.

Swordy, S. P., D. Mueller, P. Meyer, J. L'Heureux, and J. M. Grunsfeld

1990 "Relative abundances of secondary and primary cosmic rays at high energies", *Astrophys. J.*, vol. 349 (Feb. 1990), pp. 625-633, DOI: 10.1086/168349.

Tang, K.-K.

1984 "The energy spectrum of electrons and cosmic-ray confinement A new measurement and its interpretation", *Astrophys. J.*, vol. 278 (Mar. 1984), pp. 881-892, DOI: 10.1086/161857.

Tavakoli, Maryam, Ilias Cholis, Carmelo Evoli, and Piero Ullio

2013 "Constraints on dark matter annihilations from diffuse gamma-ray emission in the Galaxy", arXiv: 1308.4135 [astro-ph.HE].

Teyssier, R.

2002 "Cosmological hydrodynamics with adaptive mesh refinement. A new high resolution code called RAMSES", *Astronomy & Astrophysics*, vol. 385 (Apr. 2002), pp. 337-364, DOI: 10.1051/0004-6361:20011817, eprint: astro-ph/0111367, http://adsabs.harvard.edu/abs/2002A&A...385..337T.

The Enzo Collaboration, G. L. Bryan, M. L. Norman, B. W. O'Shea, T. Abel, J. H. Wise, M. J. Turk, D. R. Reynolds, D. C. Collins, P. Wang, S. W. Skillman, B. Smith, R. P. Harkness, J. Bordner, J.-h. Kim, M. Kuhlen, H. Xu, N. Goldbaum, C. Hummels, A. G. Kritsuk, E. Tasker, S. Skory, C. M. Simpson, O. Hahn, J. S. Oishi, G. C So, F. Zhao, R. Cen, and Y. Li

2013 "Enzo: An Adaptive Mesh Refinement Code for Astrophysics", *ArXiv e-prints* (July 2013), arXiv: 1307.2265 [astro-ph.IM], http://adsabs.harvard.edu/abs/2013arXiv1307.2265T.

The IceCube collaboration, R. Abbasi, Y. Abdou, M. Ackermann, J. Adams, J. A. Aguilar, M. Ahlers, D. Altmann, K. Andeen, J. Auffenberg, and et al.

2012 "Search for Neutrinos from Annihilating Dark Matter in the Direction of the Galactic Center with the 40-String IceCube Neutrino Observatory", *ArXiv e-prints* (Oct. 2012), arXiv: 1210.3557 [hep-ex].

Torii, S. et al.

2001 "The Energy Spectrum of Cosmic-Ray Electrons from 10 to 100 GeV Observed with a Highly Granulated Imaging Calorimeter", *Astrophys. J.*, vol. 559 (Oct. 2001), pp. 973-984, DOI: 10.1086/322274.

2008 "High-energy electron observations by PPB-BETS flight in Antarctica", *arXiv:0809.0760 [astro-ph]* (Sept. 2008), arXiv: 0809.0760.

Torres, Diego F and Luis A Anchordoqui

2004 "Astrophysical origins of ultrahigh energy cosmic rays", *Reports on Progress in Physics*, vol. 67, 9, p. 1663, http://stacks.iop.org/0034-4885/67/i=9/a=R03.

Tully, R. B.

1982 "The Local Supercluster", *ApJ*, vol. 257 (June 1982), pp. 389-422, DOI: 10.1086/159999.

van den Bergh, S.

1999 "The local group of galaxies", *A&A Rev.*, vol. 9, pp. 273-318, DOI: 10.1007/s001590050019.

van Woerden, H., G. W. Rougoor, and J. H. Oort

1957 "Expansion d'une structure spirale dans le noyau du Système Galactique, et position de la radiosource Sagittarius A", *Academie des Sciences Paris Comptes Rendus*, vol. 244, pp. 1691-1695.

Vietri, Mario

2008 *Foundations of High-Energy Astrophysics*, illustrated edition, University Of Chicago Press, ISBN: 0226855694, http://www.amazon.com/exec/obidos/redirect?tag=citeulike07-20%5C&path=ASIN/0226855694.

Waxman, E.

2011 "High energy cosmic ray and neutrino astronomy", arXiv: 1101.1155 [astro-ph.HE].

Yan, H. and A. Lazarian

2004 "Cosmic-Ray Scattering and Streaming in Compressible Magnetohydrodynamic Turbulence", *Astrophys. J.*, vol. 614 (Oct. 2004), pp. 757-769, DOI: 10.1086/423733, eprint: astro-ph/0408172.

Yoshida, K.

2008 "High-energy cosmic-ray electrons in the Galaxy", *Advances in Space Research*, vol. 42 (Aug. 2008), pp. 477-485, DOI: 10.1016/j.asr.2007.03.060.

Yoshida, K., S. Torii, T. Yamagami, T. Tamura, H. Kitamura, J. Chang, I. Iijima, A. Kadokura, K. Kasahara, Y. Katayose, T. Kobayashi, Y. Komori, Y. Matsuzaka, K. Mizutani, H. Murakami, M. Namiki, J. Nishimura, S. Ohta, Y. Saito, M. Shibata, N. Tateyama, H. Yamagishi, and T. Yuda

2008 "Cosmic-ray electron spectrum above 100 GeV from PPB-BETS experiment in Antarctica", *Advances in Space Research*, vol. 42 (Nov. 2008), pp. 1670-1675, DOI: 10.1016/j.asr.2007.04.043.

Zatsepin, G. T. and V. A. Kuz'min

1966 "Upper Limit of the Spectrum of Cosmic Rays", *Soviet Journal of Experimental and Theoretical Physics Letters*, vol. 4 (Aug. 1966), p. 78.

Zhang, L. and K. S. Cheng

2001 "Cosmic-ray positrons from mature gamma-ray pulsars", *Astron. & Astrophys.*, vol. 368 (Mar. 2001), pp. 1063-1070, DOI: 10.1051/0004-6361:20010021.